Stony Brook University

BET Inhibition Releases the Mediator Complex from Specific *cis* Elements in Acute

Myeloid Leukemia Cells

A Dissertation Presented

by

Anand Shripad Bhagwat

to

The Graduate School

in Partial Fulfillment of the

Requirements

for the Degree of

Doctor of Philosophy

in

Molecular Genetics and Microbiology

Stony Brook University

May 2016

Stony Brook University

The Graduate School

Anand Shripad Bhagwat

We, the dissertation committee for the above candidate for the

Doctor of Philosophy degree, hereby recommend

acceptance of this dissertation.

Dr. Christopher Vakoc – Dissertation Advisor
Associate Professor, Cold Spring Harbor Laboratory

Dr. Arne Stenlund - Chairperson of Defense
Associate Professor, Cold Spring Harbor Laboratory

Dr. David Tuveson – Thesis Committee member
Professor, Cold Spring Harbor Laboratory

Dr. Adrian Krainer – Thesis Committee member
Professor, Cold Spring Harbor Laboratory

Dr. Lingbo Zhang – Thesis Committee member
Fellow, Cold Spring Harbor Laboratory

This dissertation is accepted by the Graduate School

Charles Taber
Dean of the Graduate School

ii

Abstract of the Dissertation

BET Inhibition Releases the Mediator Complex from Specific *cis* Elements in Acute

Myeloid Leukemia Cells

by

Anand Shripad Bhagwat

Doctor of Philosophy

in

Molecular Genetics and Microbiology

Stony Brook University

2016

Acute myeloid leukemia (AML) is a hematologic malignancy with a 5-year survival rate of less than 30%. We recently identified the bromodomain and extraterminal (BET) protein Brd4 as a therapeutic target in AML, and several trials are currently evaluating the clinical utility of BET inhibitors for this disease. BET inhibitors displace Brd4 from chromatin and subsequently reduce the expression of key oncogenes, such as Myc, leading to AML blast differentiation and cell death. However, the mechanism by which Brd4 maintains oncogene expression in AML is still unclear. We hypothesized that Brd4 functions by working with other coactivators in AML to promote expression of oncogenes. Brd4 is capable of associating with the Mediator complex, but the relevance of this interaction to the therapeutic effects of BET inhibition has not been explored. Here, we show that the BET inhibitor JQ1 causes the rapid release of Mediator from specific *cis* elements in the genome of AML cells. This effect occurs with greatest severity at a distal Myc super-enhancer, however JQ1 does not alter Mediator occupancy at all super-enhancers in the genome. Nonetheless, the degree of Mediator eviction provides a reliable correlate with JQ1-induced transcriptional suppression, a relationship that may have utility as a mechanism-based biomarker. Genetic knockdown of several Mediator subunits in AML cells, including Med12 and Med23, led to proliferation arrest, myeloid differentiation, and suppression of Brd4, Myb, and Myc target gene signatures. These findings unify Brd4 and Mediator functions within a common gene regulatory pathway that sustains the pathogenesis of AML.

Table of Contents

List of Figures

List of Tables

List of Abbreviations

Abbreviation	Meaning
ALL	Acute Lymphoblastic Leukemia
AML	Acute Myeloid Leukemia
APL	Acute Promyelocytic leukemia
ARC	Activator recruited coactivator
BET	Bromodomain and extraterminal
Cas9	CRISPR associated protein 9
Cdk	Cyclin dependent kinase
CRISPR	Clustered regularly-interspaced short palindromic repeats
CRSP	Coactivator required for Sp1 activation
Cryo-EM	Cryo-electron microscopy
CTD	C-terminal domain
DNA	Deoxyribonucleic acid
DRIP	Vitamin D Receptor interacting proteins
ETS family	E26 transformation specific family
FAB	French-American-British classification system
HSC	Hematopoietic stem cell
ICD	Intracellular domain
IRES	Internal Ribosomal Enry Site
KAT	Lysine acetyltransferase
KIX domain	Kinase inducible domain interacting domain
MDS	Myelodysplastic syndrome
MEF	Mouse embryonic fibroblast
MLL	Mixed Lineage Leukemia
P-TEFb	Positive transcription elongation factor b
PC2	Positive cofactor 2
PIC	Preinitiation complex
Pol II	RNA polymerase II
RNA	Ribonucleic acid
SEC	Super Elongation Complex
SET	Su(var)3-9 and Enhancer of zeste proteins
shRNA	Short hairpin RNA
TF	transcription factor
TRAP	Thyroid Receptor associated proteins
WHO	World Health Organization

Author Contributions

A number of authors contributed to the work presented in Chapter II. Jae Seok Roe completed the Brd4, Med1, H3K27Ac, and TF ChIP-seq experiments in RN2 cells. Furthermore, he performed one of the replicates of the DMSO vs. JQ1 ChIP-seq used for the analyses in that chapter. Beverly Mok performed some of the flow cytometric and morphologic differentiation analyses completed in this chapter. Finally, Anja Hohmann aided in the preparation of some of the RNA-seq libraries from the leukemia cells in which Mediator head subunits were knocked down.

Acknowledgments

Completing a PhD is never a solo feat, and there are innumerable people to whom I owe this accomplishment. I first want to thank my advisor, Dr. Chris Vakoc, for allowing me to work in his lab. Chris was always pushing me to do better. His drive is inspiring, and his mentorship allowed me to accomplish things I never would have thought possible. From the beginning of my rotation in the lab, I had great teachers at the bench. Dr. Shinpei Kawaoka always challenged me to think deeply about things I otherwise would never have given a second thought. Later on, Dr. Jae Seok Roe taught me all the genomics I know and patiently dealt with my millions of questions. Maybe most importantly, being in this lab has given me a strong perspective on scientific problems and approaches. I now see things from a totally new point of view. Going forward, I will always carry with me the techniques, the knowledge, the lessons I learned here.

I have formed a lot of real and great friendships during my time at CSHL. I'd like to thank the members of the Vakoc and Tuveson labs, past and present, for always being there when I needed someone to talk to about protocols, scientific mysteries, or the weather. In particular, I want to thank Joe for putting up with me for three and a half years and for always being willing to put me in my place when I needed it. Also, for being a willing rival on the racetrack. I want to thank Anja for being a close friend and confidante throughout our shared PhD experiences, for commiserating and celebrating the constant ups and downs of lab life, and for rarely eating more than half a sandwich. My roommate and my friend Bobby is full of immense compassion, and he is always

there for everybody. I've called on him so many times the past few years, and he has always answered that call.

I'd especially like to thank my family. My brother Vivek's intelligence and positivity will never cease to fill me with pride as an older brother. It must be all those hard lessons I had to teach him growing up. Now, as the responsible adult between the two of us, he is a source of inspiration for me. My parents turned me into the person I am today. From the start, they fueled my curiosity and my need to keep learning. They also taught me to be honest, dedicated, and good-natured. In doing so, they gave me all the tools I need to succeed. Most importantly, they have supported me at every turn and made sure I knew that support was unconditional.

Last, I want to thank Cara. She has been with me at every step of this long, crazy process, and without her I wouldn't have made it to this point where I'm writing acknowledgements. She was there when I decided to come here for school and she's been there eagerly greeting me every time we get to share the same space for a minute or two. Her dedication, passion, and loyalty are examples anybody would be lucky to have. Her relentless warmth and humor have repeatedly pulled me out of my worst moments of despair. She is my source of joy, my sense of purpose, my constant.

Chapter I – Introduction

1.1 Myeloid development and Acute Myeloid Leukemia

Acute myeloid leukemia (AML) is an aggressive cancer of the blood in which cells that normally give rise to granulocytes, macrophages, red blood cells, mast cells, or platelets are arrested at an early stage of development and proliferate unlimitedly. These immature cells, or blasts, eventually overtake the bone marrow and the peripheral blood at the expense of normal hematopoiesis. This impaired ability to produce red blood cells, platelets, and innate immune cells results in the most frequent causes of death in patients with AML: infection and hemorrhage. The basic treatment for AML involves a regimen of cytotoxic chemotherapy that has changed little in recent decades, and accordingly, our ability to cure patients diagnosed with AML has improved very little in the same time period.

1.1.1 – Normal blood development

To understand the origins of AML, one must first understand the normal development of blood cells. Each day, more than 100 billion new blood cells must be produced in the human body (Boulais and Frenette, 2015). Observations of the profound toxicity on the blood system

conferred by radiation damage, a looming specter in atomic age, spurred intense research into hematopoietic development (Eaves, 2015). Early on, it was discovered that individual cells isolated from the bone marrow had the capacity to self-renew and to develop into multiple blood lineages, establishing the current hierarchical model of normal hematopoiesis with hematopoietic stem cells (HSCs) at the top of the hierarchy (Becker et al., 1963; Jacobson et al., 1951).

To ensure that HSCs are protected from external stressors and insults that may compromise their ability to produce normal blood when necessary, HSCs are generally kept quiescent (Cheshier et al., 1999). One mechanism by which HSCs are prevented from entering the cell cycle is that their location near arterioles in the bone marrow stroma exposes them to a number of secreted factors such as stem cell factor and transforming growth factor-β1, that suppress their cycling (Ding et al., 2012b; Yamazaki et al., 2011). This perivascular niche is composed of the endothelium itself as well as mesenchymal stem cells, sympathetic neuronal fibers, and Schwann cells (Boulais and Frenette, 2015). Another niche factor that appears crucial in maintaining stem cell quiescence is hypoxia (Parmar et al., 2007; Spencer et al., 2014; Suda et al., 2011). As would be expected, hypoxia results in increased expression of the transcription factor (TF) HIF-1α in HSCs (Takubo et al., 2010). When this TF is knocked out, HSC numbers are decreased in mice; when over-stabilized, it causes an impaired ability to transplant the marrow-derived stem cells (Takubo et al., 2010). When a requirement for HSC expansion develops, the cells move toward the endothelial sinusoids in the marrow, which can promote the entry of HSCs into the cell cycle by secreting Notch ligands (Butler et al., 2010). Disruption of mechanisms that suppress HSC cycling or activation of those that promote cycling can directly result in the

2

development of AML. Recently discovered examples of niche-dependent mechanisms of leukemogenesis include constitutive activation of β-catenin in osteoblasts that leads to increased Notch signaling and a sympathetic neuropathy in bone marrow that can support leukemia infiltration and can be reversed with β2 agonists to slow AML progression (Hanoun et al., 2014; Kode et al., 2014).

The tight control of hematopoietic activity in the bone marrow heavily relies on intrinsic transcriptional regulation within the HSC. By way of example, knockout of the critical HSC TF Runx1 results in embryos with entirely absent hematopoiesis (Okuda et al., 1996). Even further on in development, as an HSC's daughter cell commits to a lineage, the repertoire of TFs expressed in the cell change rapidly and control the ultimate outcome of differentiation. For example, maintenance of stemness in HSCs requires Runx1, Gata2 and Evi1, while myeloid lineage specification requires Pu.1 for monocyte commitment and the C/EBP TFs for granulocyte lineage choice (Goyama et al., 2008; Ling et al., 2004; Rosenbauer and Tenen, 2007; Tenen, 2003). However, the transcriptional development of hematopoietic cells is highly complex. Runx1 is known to relocalize other hematopoietic TFs to prime Pu.1 expression in HSCs, and the myeloid factors Pu.1 and C/EBPα are also important for maintaining HSC quiescence and stemness (Hasemann et al., 2014; Lichtinger et al., 2012; Staber et al., 2013).

The timing and dosage of TF expression appears to be tightly regulated and closely interconnected. The erythroid TF Gata1 is known to interact with Pu.1 and can suppress its transcriptional output such that inappropriate overexpression of Gata1 in myeloid cells can block

Pu.1-driven myeloid development (Zhang et al., 1999). Interestingly, the reverse is also true, with Pu.1 suppressing erythroid development via suppression of Gata1 output (Rekhtman et al., 1999). This TF-mediated blockade of normal blood development is an example of why disruption of transcriptional control is, as discussed below, a frequent contributor to development of leukemia. A similar, and physiologically important, mechanism of TF antagonism occurs between Pu.1 and C/EBPα, which directly blocks the DNA-binding domain of Pu.1, leading to a loss of Pu.1 target gene expression in myeloid progenitor cells (Reddy et al., 2002). This appears to drive a switch from the monocyte lineage to the granulocytic lineage (Reddy et al., 2002). Underscoring the complexity in transcriptional regulation of myeloid lineage development, however, C/EBPα also binds to and activates an enhancer element 14kb upstream of Pu.1 in myeloid cells, driving Pu.1 expression and supporting myeloid lineage commitment (Yeamans et al., 2007). It has been suggested that loss of function mutations of C/EBPα, found in AML, may in part contribute to myeloid differentiation blockade by reducing levels of Pu.1 in leukemic cells (Yeamans et al., 2007).

1.1.2 – The genetics of AML

Major advances have been made in understanding the genetics of AML. We now know that, on average, fewer than 13 mutations can be found in each patient's AML, and less than half of these mutations are recurrent (Cancer Genome Atlas Research, 2013). This genetic heterogeneity poses a challenge to design of targeted therapies for AML. Nevertheless, some recurrent mutations do occur and may yet represent good therapeutic targets for many AML patients. The most commonly mutated gene in AML, occurring in about a third of patients, is NPM1, which

encodes nucleophosmin (Grimwade et al., 2015). About 90% of mutations in NPM1 result in a nuclear export signal that relocates the protein to the cytoplasm and results in enhanced self-renewal of hematopoietic progenitor cells via aberrant Hox gene expression (Vassiliou et al., 2011). NPM1 is typically not associated with high-risk disease, but given its mutation in a large fraction of patients, identifying ways to treat NPM1-mutant AML is an urgent need (Burke, 2016). A gene that is frequently mutated in AML and is associated with high-risk disease is Flt3. This gene encodes a receptor tyrosine kinase, and in about a quarter of AML patients, internal duplications in the juxtamembrane domain, resulting in constitutive, ligand-independent activation of Flt3, can be found (Dohner et al., 2015). Several inhibitors of Flt3 have been developed and are now being tested in clinical trials; unfortunately, resistance has already emerged to the first generation of these molecules, suggesting a need for higher-potency inhibitors or combination therapies (Grimwade et al., 2015; Zarrinkar et al., 2009).

In keeping with the importance of transcription in regulation of hematopoiesis, many of the recurrently mutated genes in AML are transcriptional regulators (Cancer Genome Atlas Research, 2013). For example, as described above, mutations in sequence-specific transcription factors are a frequent event in AML. Of particular note are a number of germline mutations in hematopoietic TFs, such as Runx1, Gata2, and CEBP/α, that contribute to inherited forms of AML (Godley, 2014). There are also translocations involving myeloid TFs that dysregulate their function and lead to distinct subtypes of AML. These include the AML1-ETO translocation (Runx1-Runx1T1, t(8;21)), the inv(3) Gata2-Evi1 lesion, which is associated with a poor prognosis (Gröschel Cell 2014, Dohner NEJM 2015), and the CBFB-MYH11 (inv(16))

aberration (Dohner et al., 2015; Groschel et al., 2014; Illendula et al., 2015). Interestingly, inv(16) AML was recently rendered therapeutically tractable by a small molecule that sequesters the oncogenic fusion protein (Smooth Muscle myosin heavy chain-core binding factor b, SMMHC-Cbfb), reinstating the ability of the wild-type Cbfb to bind Runx1 and restoring normal transcription (Illendula et al., 2015).

However, the array of genetic anomalies in AML that affect transcription can be extended beyond TF lesions to include epigenetic regulators. One of the most frequent mutations in AML, in about 30% of patients and almost always in concert with NPM1 mutations, is in the DNA methyltransferase DNMT3A, which leads to focal hypomethylation of CpGs in the genome and changes in gene expression patterns (Grimwade et al., 2015; Ley et al., 2010; Russler-Germain et al., 2014). Because Dnmt3a functions as a tetramer, heterozygous mutations at R882 in DNMT3A appear to be dominant negative, leading to reduced enzymatic activity that leads to the focal hypomethylation pattern observed in patients with these mutations (Russler-Germain et al., 2014). Another group of AML mutations occurs in the genes encoding isocitrate dehydrogenase (IDH1/2) or ten-eleven translocation (TET1/2) proteins in a mutually exclusive manner (Figueroa et al., 2010a). Gain of function mutations in IDH genes lead to aberrant production of the 2-hydroxyglutarate (2HG) oncometabolite instead of the normal α-ketoglutarate. 2HG inhibits the normal 5-methylcytosine hydroxylation function of Tet (Figueroa et al., 2010a). The end result of these IDH or TET mutations is a DNA hypermethylation phenotype and subsequently aberrant gene expression (Figueroa et al., 2010a).

Frequent, mutually exclusive mutations in the cohesin complex have also been described in AML (Kon et al., 2013). Cohesin is central to physical regulation of transcription, particularly in the formation and maintenance of DNA structural elements, including promoter-enhancer looping (Grimwade et al., 2015). The cohesin mutations found in AML are mutually exclusive between subunits and are heterozygous. Recently, the lesions have been shown to result in marked changes in chromatin accessibility and may thereby contribute to leukemogenesis via a shift in gene expression away from lineage commitment (Mullenders et al., 2015; Viny et al., 2015).

One class of acute leuekmia is driven by lesions involving the mixed lineage leukemia (MLL) gene. Similar to Runx1, mice lacking MLL show no hematopoietic development (Ernst et al., 2004). MLL obtained its name because, depending on the lesion, genetic aberrations involving the MLL gene can lead to acute lymphoblastic leukemia (ALL), AML, or a disease in which leukemic cells express markers of both lymphoblasts and myeloblasts (Slany, 2009). The genetic alterations are typically chromosomal translocations involving MLL and another protein partner. While most of these fusions are associated with a dismal prognosis, the t(9;11)(p22;q23) translocation, which fuses MLL to AF9, is associated with an intermediate prognosis (Dohner et al., 2015; Lavallee et al., 2015). Interestingly, MLL-fusion leukemias bear the lowest mutational burden among all AML subtypes but frequently harbor mutations in Ras proteins. (Cancer Genome Atlas Research, 2013; Kampen et al., 2014; Lavallee et al., 2015). These leukemias are thus more sensitive to MEK inhibitors but less sensitive to receptor tyrosine kinase inhibitors, which are upstream of Ras proteins in the signaling cascade (Kampen et al., 2014; Lavallee et al., 2015)`.

The MLL1 gene encodes a histone 3 lysine 4 (H3K4) methyltransferase and is normally associated with gene activation (Chen and Armstrong, 2015). However, the fusion events in leukemia generally truncate the catalytic C-terminal SET domain of MLL and replace it with various fusion partners (Chen and Armstrong, 2015). Many of these partners share the ability to recruit transcription elongation complexes and promote the catalytic activity of the H3K79 methyltransferase Dot1l (Deshpande et al., 2012; Deshpande et al., 2014). This ability to bind Dot1l appears to be essential for MLL fusion leukemias and results in the aberrant activation of characteristic MLL-fusion target genes such as Meis1 and Hoxa9 (Bernt et al., 2011). This appears to be due in part to Dot1l's ability to restrict access of the histone deacetylase SIRT1 and H3K9 methyltransferase SUV39H1 to important MLL target genes including the HoxA cluster (Chen et al., 2015). Importantly, direct pharmacologic inhibition of the Dot1l methyltransferase activity has been successful in preclinical models and has resulted in initiation of clinical trials of Dot1l inhibitors in patients with MLL-fusion AML (Daigle et al., 2011). A recent study, however, used transcriptional signatures of MLL-fusion leukemias to identify cryptic MLL-fusions and partial duplications within the MLL protein itself in AML samples that had not been classified as MLL-driven AML (Lavallee et al., 2015). Despite a lack of a Dot1l-binding partner, non-fusion MLL-driven (i.e. MLL-duplication) AML is still sensitive to inhibitors of Dot1l, suggesting this dependency is maintained across all MLL-driven leukemias regardless of karyotypic status (Lavallee et al., 2015).

The fact that less than half of mutations in a given AML tumor are recurrent suggests that there is a high rate of background mutations in hematopoietic progenitor cells. Indeed, recent sequencing studies have highlighted frequent spontaneous mutations in peripheral blood cells

that did not directly cause malignant transformation (Busque et al., 2012; Welch et al., 2012). Instead, these mutations, most frequently in DNMT3A, ASXL1, and TET2, appear to cause clonal expansion of cells and are associated with an increased risk of subsequent hematologic cancer (Genovese et al., 2014; Jaiswal et al., 2014). Similarly, in therapy-related AML (t-AML), it was recently found that the mutational burden of chemotherapy naïve *de novo* AML and t-AML are similar, undermining the prevailing idea that the prior chemotherapy directly causes the t-AML-driving mutations (Wong et al., 2015). Instead, it was found that age-related spontaneous p53 mutations occur in untransformed hematopoietic cells, and that chemotherapy or radiation therapy preferentially expands these cells, leading to increased rates of spontaneous transformation and, because of the p53 mutation, increased incidence of cytogenetic abnormalities (Wong et al., 2015). Sequencing AML as it responds to therapy and relapses has also revealed important characteristics about the clonality of the disease. It is now believed that between one and 5 clones arise and propagate the disease, and failure to eradicate all of these clones with chemotherapy directly results in relapse (Ding et al., 2012a).

1.1.3 – Classification and Prognosis of AML subtypes

In the clinic, AML often presents as nonspecific, constitutional symptoms, such as bleeding diathesis, infection, fever, weakness, or malaise, that are direct consequences of impaired normal hematopoiesis (Rowe and Tallman, 2010). A diagnosis of AML is made following a blood draw and smear or a bone marrow biopsy. Two methods of classifying AML predominate. For a leukemia diagnosis, the French-American-British (FAB) system requires ≥30% of cells in the peripheral blood or bone marrow to be leukemic blasts. FAB categorization of AML uses light-

microscopic, morphologic, and cytogenetic analysis of AML cells to distinguish eight subtypes of AML (M0-M7) (Bennett et al., 1976). Because it was established prior to knowledge of recurrent genetic abnormalities, the FAB system does not take the genetics of AML, except in the case of cytogenetics, into account (Vardiman et al., 2002).

The newer World Health Organization (WHO) classification of AML requires only 20% of blood or bone marrow cells to be blasts for diagnosis, and integrates genetic abnormalities, immunophenotypes, and clinical features into the categorization (Harris et al., 1999; Vardiman et al., 2002). The WHO classification also distinguishes AML that arises *de novo* from those arising from a pre-existing myelodysplastic syndrome (MDS) because of the different origins and features of the disease as well as its poorer therapeutic responses as compared to *de novo* AML (Vardiman et al., 2002). For similar reasons, AMLs that arise secondary to chemotherapy or radiation therapy for another malignancy, are categorized separately (Vardiman et al., 2002).

Importantly, both systems of AML classification are able to distinguish acute promyelocytic leukemia (APL) from other AML subtypes (Rowe and Tallman, 2010; Vardiman et al., 2002). The FAB system categorizes APL as M3 based on the presence of distinguishing morphologic features, such as Auer Rods, while the WHO system classifies it as "Acute myeloid leukemia with recurrent genetic abnormalities – Acute promyelocytic leukemia with translocations between chromosome 15 and 17" (Bennett et al., 1976; Vardiman et al., 2002). This is a crucial distinction because this subtype of AML, which indeed harbors the t(15;17), PML-Retinoic acid receptor α (RARA) translocation in more than 98% of cases, is now treated very differently from

other AML types in the clinic and can be cured in almost all patients (Rice and de The, 2014; Rowe and Tallman, 2010). Empirical evaluation of drug sensitivities led to the discovery that APL cells are highly sensitive to treatment with all-trans retinoic acid (ATRA), a ligand of RARA. This finding was remarkable, as the therapeutic activity of ATRA was discovered before identification of PML-RARA as the causative oncogene in this disease (Huang et al., 1988; Huang et al., 1987). Combination therapy using ATRA and arsenic trioxide, another chemical that appears to selectively perturb PML-RARA function, has replaced chemotherapy as the standard of care for APL and results in cures in over 90% of patients (Lo-Coco et al., 2013; Rice and de The, 2014). Both agents exert anti-leukemia activity by targeting the PML-RARA fusion protein for degradation and represent the most successful example of targeted therapy used in oncology today (Rice and de The, 2014; Zhang et al., 2010; Zhu et al., 1999).

In addition to subtypes of AML, like APL, that can be treated more effectively, a number of other factors play roles in predicting outcome for patients diagnosed with AML. As mentioned above, AML arising out of MDS or prior therapy is associated with a poorer outcome than *de novo* AML (Dohner et al., 2015). Additionally, older patients and those with pre-existing conditions are often unable to withstand intensive chemotherapy regiments and thus have poorer outcomes, although treatment-related mortality has declined with an improved ability to manage the patient's health (Othus et al., 2014). Characteristics of the disease itself, such as blast counts at diagnosis and disease genetics, are also important prognostic factors (Rowe and Tallman, 2010).

1.1.4 – Clinical management of AML and emerging therapies

Following diagnosis, treatment of AML commences; chemotherapy for AML consists of induction therapy followed by consolidation therapy. The purpose of induction therapy is to induce remissions. The prevailing standard for induction chemotherapy, the "7+3" regimen, was first proposed in 1973 and consists of 7 days of continuous-infusion of the nucleoside analog cytarabine with 3 days of intravenous daunorubicin, an anthracycline (Rowe and Tallman, 2010; Yates et al., 1973). For adults under 60 years old, remission rates are around 70%, however for adults over 60 years old, induction therapy is less successful, with complete responses about 50% of the time in part because of dose-limiting toxicities in frailer patients (Dohner et al., 2015; Rowe and Tallman, 2010). In these frailer patients, addition of decitabine or azacytidine, agents that reduce DNA methylation, has extended median survival as compared to their standard of care, low-dose cytarabine chemotherapy (Dombret and Gardin, 2015).

Following remission, a patient usually undergoes consolidation therapy consisting of a few doses of intravenous cytarabine (Dohner et al., 2015). Patients with a favorable risk profile are cured up to 70% of the time, but patients with intermediate or poor risk profiles are cured less than 15% of the time (Dohner et al., 2015). An alternative to consolidation therapy is allogenic transplantation, which provides the lowest rate of relapse of any post-remission therapy (Rowe and Tallman, 2010). Overall, however, the cure rate for AML remains below one in three patients (Pulte et al., 2010).

Despite a great increase in the depth of our molecular understanding of AML, few discoveries have been successfully translated to clinical advancements (Rowe and Tallman, 2010). However,

a number of new, targeted therapies are making their way through clinical trials and may prove important for subsets of patients with AML. IDH inhibitors have shown promise in phase I clinical trials by releasing the differentiation blockade that is created by gain of function mutant IDH proteins (Stein et al., 2014). As mentioned above, internal tandem duplication of the receptor tyrosine kinase FLT3 is found in approximately 30% of AML patients and is associated with a poor outcome (Cancer Genome Atlas Research, 2013; Dohner et al., 2015). While complete responses have been attained using FLT3 inhibitors, resistance develops rapidly (Wander et al., 2014), and combination therapies are thus being explored. One recent study suggests that attention should be paid to cooperating mutations, as inhibitors targeting the differentiation-blocked state, such as IDH inhibitors, can strongly and positively impact the efficacy of FLT3-targeted therapies (Shih et al., 2015).

1.2 – Brd4 and BET inhibitors in AML

Another class of targeted therapy that is currently being evaluated in clinical trials is the relatively new category of molecules targeting bromodomain and extraterminal (BET) proteins (Dombret et al., 2014). BET proteins are a family of coactivators comprised of Brd2, Brd3, Brd4, and BrdT (Shi and Vakoc, 2014). These proteins utilize their tandem bromodomains to bind acetylated proteins, especially diacetylated histone tails and TFs, and subsequently positively regulate transcription of the associated genes (Shi and Vakoc, 2014).

1.2.1 – Regulation of Polymerase Pausing

Studies of the mechanisms by which BET proteins activate transcription have largely focused on their ability to recruit regulators of transcriptional pause release and elongation. While earlier studies in yeast mainly focused on regulation of the initiation step as the primary barrier to productive transcription, it is now clear that at most active genes in the genome, RNA Polymerase II (Pol II) is paused approximately 50 nucleotides downstream of the transcription start site (TSS) and must be released from this site for a round of transcription to be completed (Adelman and Lis, 2012). This phenomenon was first characterized at the *drosophila* heat shock genes, where it was discovered that Pol II initiates transcription and creates a nascent RNA but cannot continue transcribing through genes without the heat shock stimulus (Adelman and Lis, 2012). Genomewide localization studies of Pol II confirmed that in higher organisms, pausing is a common phenomenon at active genes (Adelman and Lis, 2012). Pol II pausing has been shown to be due in part to the activity of the pausing factors DSIF and NELF, which appear stabilize Pol II in the paused state (Wada et al., 1998; Yamaguchi et al., 1999). Hypotheses as to why Pol II pausing is so pervasive in higher organisms include the need to rapidly and coordinately activate transcription in response to urgent stimuli and the requirement for an additional checkpoint to prevent unwanted transcription of genes (Adelman and Lis, 2012). After the signal or stimulus to productively elongate transcription is received, such as by heat shock, the release of paused Pol II is coordinated by the positive transcription elongation factor b (P-TEFb) complex, which is comprised of Cdk9 and either Cyclin T1, T2, or K (Adelman and Lis, 2012). P-TEFb phosphorylates DSIF and NELF and results in their dissociation from Pol II, thus releasing its pause (Jonkers and Lis, 2015). P-TEFb also directly phosphorylates the Pol II C-terminal domain (CTD) (Jonkers and Lis, 2015).

The recruitment of P-TEFb to paused genes is often facilitated by coactivator proteins such as Brd4 (Jang et al., 2005; Shi and Vakoc, 2014). Brd4's bromodomain 2 recognizes acetylated Cyclin T1, while the Brd4 C-terminal domain interacts directly with both Cdk9 and Cyclin T1 (Bisgrove et al., 2007; Jang et al., 2005). Brd4 competes with an inhibitory RNA/protein complex called 7SK/HEXIM for PTEF-b binding (Jonkers and Lis, 2015). 7SK/HEXIM sequesters PTEF-b in an inactive state while Brd4 releases PTEF-b, thus activating its kinase activity and Pol II elongation function (Shi and Vakoc, 2014).

1.2.2 – Brd4 in cancer

Brd4 is a target of translocations with the NUT protein in a rare squamous cell cancer called NUT midline carcinoma (Filippakopoulos et al., 2010). This Brd4-NUT fusion oncoprotein enforces a differentiation block in squamous cells and appears to cause massive enhancer spreading into up to two Megabase "megadomains" that lead to aberrant gene activation (Alekseyenko et al., 2015). This pathognomonic Brd4-NUT translocation provided the rationale to generate inhibitors of BET bromodomains that could remove Brd4 from chromatin and release the differentiation block in NUT midline carcinoma (Filippakopoulos et al., 2010). This was accomplished via the development of JQ1, a BET inhibitor that competes with acetyl-lysine residues for binding to BET bromodomains (Filippakopoulos et al., 2010). JQ1 was well tolerated in mouse models and this study established Brd4 as a therapeutically tractable target in cancer despite its apparently ubiquitous role in transcription coactivation (Filippakopoulos et al., 2010).

In AML, Brd4 is not mutated, translocated, or amplified (Shi and Vakoc, 2014). Instead, it was first identified as a therapeutic target through an RNA interference screen in a MLL-AF9/Nras^{G12D} primary mouse AML cell line (Zuber et al., 2011c). After knocking down chromatin regulators one-by-one, Brd4 emerged as a strong hypersensitivity in AML relative to other cell types. Knockdown of Brd4 resulted in cell cycle arrest, apoptosis, and myeloid differentiation of AML blasts (Dawson et al., 2011; Zuber et al., 2011c). Furthermore, BET inhibitors were shown to remove Brd4 from chromatin in AML and result in the loss of expression of a number of important proto-oncogenes in this disease (Dawson et al., 2011; Zuber et al., 2011c). Most crucially, transcription of c-Myc is rapidly downregulated following JQ1 treatment or Brd4 knockdown, and exogenous expression of Myc can restore the differentiation blockade that is lifted by JQ1 (Zuber et al., 2011c). These initial preclinical results led to the initiation of clinical trials of BET inhibitors for AML, and have been reported to result in complete responses in some patients enrolled in a Phase I study (Dombret et al., 2014).

The utility of BET inhibitors has been extended to a number of other hematopoietic malignancies, including multiple myeloma, acute lymphoblastic leukemia, and diffuse large B cell lymphoma, that also lack genetic alterations in Brd4 (Chapuy et al., 2013; Delmore et al., 2011; Ott et al., 2012). Thus, a major avenue of research since the development of BET inhibitors has been to understand the mechanisms underlying the surprising therapeutic window of these molecules.

1.2.3 – The super-enhancer concept

One prominent model proposed that regulatory elements known as super-enhancers can explain the activity of BET inhibitors (Loven et al., 2013). Super-enhancers are large domains of chromatin that harbor marks typical of enhancers, including the active chromatin mark H3K27 Acetyl (H3K27Ac) and a lack of transcriptionally-associated H3K4 trimethylation (Loven et al., 2013; Whyte et al., 2013). What separates them from typical enhancers is merely the presence of extra-ordinary levels of H3K27Ac, the Mediator complex subunit Med1, certain TFs, or Brd4 (Loven et al., 2013; Whyte et al., 2013). To formally define super-enhancers, the Rank Ordering of Super-Enhancers (ROSE) algorithm is used to stitch together peaks of interest that are within 12.5kb of each other (under the assumption that proximity implies cooperativity) and to then rank signal of the protein of interest at these stitched loci, and to name the top-ranking peaks as super-enhancers (Loven et al., 2013; Whyte et al., 2013). Several features of super-enhancers are salient, including their loading of excess activators and coactivators, their proximity to key lineage- and cell-state-defining genes, and the fact that they harbor a disproportionate abundance of disease-associated polymorphisms (Hnisz et al., 2013; Loven et al., 2013; Whyte et al., 2013). A modest reduction in the occupancy of Mediator and PTEF-b complexes that occurs only at super-enhancers has been observed after BET inhibitor treatment, but the effects of these events on transcription is unclear (Di Micco et al., 2014; Loven et al., 2013). Consistent with super-enhancers explaining JQ1 response, transcripts of genes proximal to super-enhancers are moderately more sensitive to JQ1 than those adjacent to non-super-enhancers and the empirically identified crucial transcriptional targets of JQ1 treatment, such as *Myc* and *Cdk6*, are associated with super-enhancer elements (Loven et al., 2013; Roe et al., 2015; Shi et al., 2013).

Thus, super-enhancers as a concept seem to encompass the necessary features to predict JQ1 sensitivity among transcribed genes.

However, closer examination of super-enhancers reveals that much remains to be explained. For example, the response of super-enhancer associated transcripts to JQ1 is highly heterogeneous. Many super-enhancer associated genes are not transcriptionally suppressed by JQ1, even though Brd4 appears to be uniformly released from chromatin by JQ1 (Loven et al., 2013). An example of this is *HoxA9* in MLL-driven AML cells. *HoxA9* is a direct target of MLL-fusion proteins, and is essential to mediate transformation and maintenance of the MLL-leukemia state (Bernt et al., 2011). Consistent with super-enhancers marking crucial genes for a cell state, *HoxA9* is associated with a super-enhancer element (Eaton et al., 2015). However, *HoxA9* transcription is unperturbed by JQ1, underscoring the insufficiency of super-enhancers as a concept that can explain JQ1-mediated transcriptional suppression (Zuber et al., 2011c). Additionally, recent studies have demonstrated that THZ-1, an inhibitor of TFIIH's Cdk7, and 5,6-dichloro-1-b-D-ribofuranosylbenzimidazole (DRB), an inhibitor of Pol II elongation, also preferentially suppresses super-enhancer associated genes, raising the possibility that the response of super-enhancers to various chemical perturbations may reflect a more general property of these elements, such as higher rates of turnover, or perhaps a flaw in normalization methods, rather than a Brd4- or JQ1-specific mechanism (Chipumuro et al., 2014; Sigova et al., 2015).

1.2.4 – Brd4 interaction with other proteins

Another approach in the pursuit to understand Brd4 sensitivity has been to define the repertoire of interacting factors that may contribute to the increased dependence on Brd4 in cancers such as AML. Given the importance of the bromodomains' acetyl-lysine binding to Brd4's overall function, our lab hypothesized that a lysine acetyltransferase (KAT) may act upstream of Brd4 to create an acetylated chromatin environment and to recruit Brd4 to its sites of activity (Roe et al., 2015). By genetically screening the KATs in AML, P300 was found to maintain a similar cell state as Brd4 in this disease (Roe et al., 2015). Interestingly, P300 is known to acetylate histone tails as well as TFs, and Brd4 is binds acetylated versions of both of these substrates. Indeed, a number of hematopoietic lineage TFs were identified as being acetylated by P300 in AML and directly bound by Brd4 (Roe et al., 2015). Thus, one layer of specificity may arise from the AML repertoire of TFs, which can direct local acetylation at its target regulatory loci and directly recruit Brd4 to coactivate gene expression (Roe et al., 2015; Shi and Vakoc, 2014). Indeed, JQ1 was found to suppress the transcriptional output of the Brd4-binding TFs in AML cells (Roe et al., 2015).

Interest has also been developed in the downstream effectors of Brd4. As mentioned above, Brd4 is well known to interact with and recruit PTEF-b. Recent mass-spec approaches have identified another protein, the SET domain-containing H3K36 methyltransferase Nsd3, as binding to the extra-terminal (ET) domain of Brd4 (Rahman et al., 2011). Through detailed biochemical and genetic studies, it was discovered that a shorter isoform of Nsd3 that lacks the SET domain and any catalytic activity binds directly to Brd4's ET domain and is recruited to the genome in this manner (Shen et al., 2015). Furthermore, Nsd3 knockdown caused myeloid differentiation of

AML cells that was completely rescued by Myc over expression (Shen et al., 2015). Thus, Nsd3 appears to be crucial for the Brd4's actions to maintain AML. Nsd3 appears to be an adaptor molecule that allows Brd4 to recruit the chromatin remodeler Chd8 to genes, as knockdown of Nsd3 prevented this recruitment from occurring and knockdown of Chd8 also recapitulates the anti-leukemia phenotype observed after Brd4 knockdown (Shen et al., 2015). The full complement of Brd4 effectors has not been defined, but it appears that Brd4 functions as a molecular scaffold at regulatory elements in the genome. Its ability to recruit PTEF-b, Nsd3, Chd8 and other proteins thus suggests that Brd4 assembles a highly complex assortment of regulators to enforce transcription of key target genes. Defining the key components of this effector complex may therefore shed light on the mechanisms by which Brd4 can selectively perturb oncogenic transcription in AML. One Brd4 interaction partner is the Mediator coactivator complex. Mediator has been demonstrated in a number of studies to bind Brd4 (and in a number of other studies to not bind Brd4), yet its relationship to the transcriptional function of Brd4 has not been explored (Dawson et al., 2011; Jang et al., 2005; Jiang et al., 1998; Wang et al., 2013; Wu and Chiang, 2007).

1.3 – The Mediator Complex

1.3.1 – The limiting reagent in transcription

In the late 1980s, it was discovered that overexpression of the yeast transcriptional activator GAL4 had the unexpected effect of suppressing transcription at genes that were not GAL4 targets (Gill and Ptashne, 1988). This was similar to an unexplained repressive effect of the

herpesvirus VP16 activator on transcription from non-VP16-target plasmid (Triezenberg et al., 1988). Subsequently, this finding was extended to the mammalian setting, where it was found that expression of the estrogen receptor could suppress transcription at progesterone receptor targets (Meyer et al., 1989). This effect, termed "activator-interference" or "squelching" was thought to be the result of a factor in the transcription apparatus that is present in limited quantities; overexpression of an exogenous activator thus sequesters that limiting reagent from other transcription sites and reduces expression of other genes. The Kornberg lab confirmed this effect in yeast and demonstrated that the limiting factor was not TFIID or Pol II, as initially expected, because additions of purified TFIID or Pol II failed to relieve squelching *in vitro*. Instead, using a roughly purified yeast nuclear extract, they suggested a novel "mediator" of transcription activation was the limiting reagent (Flanagan et al., 1991; Kelleher et al., 1990). A series of complex purification steps finally yielded the Mediator of Pol II transcriptional activation (Kim et al., 1994). This complex included 20 protein subunits, associated with Pol II and other general transcription factors, stimulated activator-dependent transcription, and appeared to enhance the ability of the TFIIH kinase Cdk7 to catalyze Pol II CTD phosphorylation (Kim et al., 1994). Interestingly, this complex also overlapped previously identified SRB proteins that suppressed the phenotype of Pol II CTD mutants in yeast (Nonet and Young, 1989). The specificity of SRBs in suppressing some CTD mutant phenotypes, but not others, suggested a direct interaction with Pol II.

Subsequently, numerous large protein complexes that shared Mediator's coactivator function were purified, each identified and named by a different lab. The first of these was thyroid hormone receptor associated proteins (TRAP) from the Roeder lab, which was identified in a

ligand-dependent association with the thyroid hormone receptor (Fondell et al., 1996). The TRAP complex, in an *in vitro* system lacking thyroid hormone, could activate transcription, which was a hint at its general, and not thyroid-hormone specific, function (Fondell et al., 1996). Shortly thereafter, the Kornberg lab purified from murine B cells the mammalian version of its previously-isolated yeast Mediator complex, again confirming the presence of SRB homologs (Jiang et al., 1998). A number of activators were then used to purify activator-associated coactivator complexes from HeLa cells that had varying degrees overlap with Mediator, yet were all considered distinct. These include Sp1 to yield the coactivator required for Sp1 activation (CRSP), GAL4-AH to yield positive cofactor 2 (PC2), the vitamin D receptor to yield DRIP, SREBP-1a, VP16, and p65, to yield activator recruited cofactor (ARC), and adenoviral E1A to yield a complex that was not given a unique name (Boyer et al., 1999; Kretzschmar et al., 1994; Malik et al., 2000; Naar et al., 1999; Rachez et al., 1998; Ryu et al., 1999). Surprisingly it took until 2004 before differences were settled and the universal name Mediator was applied to each of these complexes (Bourbon et al., 2004). Some of the confusion arose from the fact that these complexes were often partial, lacking one or more components of the complete Mediator complex, in part due to differences in purification schema and washing conditions (Conaway et al., 2005). Furthermore, in an issue that has yet to be definitively resolved, Mediator complexes may naturally exist in partial forms on chromatin as a result of different activator interactions (Poss et al., 2013). Nonetheless, mass spectrometry approaches have defined the full complement of Mediator subunits in mammalian cells and demonstrated that each subunit can exist in a complex with each other subunit (Sato et al., 2004).

1.3.2 – Architecture of the Mediator complex

At a maximum, Mediator can contain up to 30 subunits (Sato et al., 2004). These subunits can be subdivided into four distinct domains: the head, middle, tail, and kinase modules (Asturias et al., 1999; Malik and Roeder, 2010). The mammalian Mediator head module is comprised of Med6, 8, 11, 17, 18, 20, 22, 27, 28, 29 and 30 (Tsai et al., 2014). Early work demonstrated that subunits in the Mediator head module, especially yeast Med17, were required for transcription in an essentially identical manner to the Pol II subunit RPB1 (Holstege et al., 1998). Furthermore, early cryo-electron microscopy (cryo-EM) structures of Mediator showed at a low resolution that the head module of Mediator appeared to embrace Pol II (Asturias et al., 1999). Importantly, the complex of Mediator and Pol II did not form in the absence of a CTD on Pol II (Asturias et al., 1999), confirming transcriptional results that this domain is crucial for the Mediator-Pol II functional interaction (Myers et al., 1998). A later study demonstrated that amongst 80 pairwise possible interactions between yeast Mediator head or middle subunits and core Pol II subunits, only Med17 and Rpb3 could be validated as interaction partners by a UV-induced crosslinking approach (Soutourina et al., 2011). A direct interaction between Med11 and the TFIIH subunit Rad3 has also been described (Esnault et al., 2008). Crystal structures of the yeast Mediator head module have been determined and confirmed a Med11-TFIIH interaction and the centrality of Med17 to the yeast head module (Imasaki et al., 2011; Lariviere et al., 2012). Further analysis of EM structures of Mediator along with other members of the pre-initiation complex (PIC) demonstrate how the head might bring TFIIH to the CTD to support its phosphorylation activity (Kim et al., 1994; Plaschka et al., 2015).

The yeast and mammalian Mediator complexes, despite limited sequence conservation, appear to adopt similar conformations and are each further partitioned into middle (Med1, 4, 7, 9, 10, 19, 21, 26, 31), tail (Med14, 15, 16, 23, 24, 25), and kinase (Med12/12L, Med13/13L, Cdk8/19, any cyclin C) modules (Asturias et al., 1999; Poss et al., 2013; Tsai et al., 2014). While the remainder of Mediator has not been crystallized in full, key features of the complex architecture are still discernable from the lower resolution studies. For example, cryo-EM of a yeast Mediator complex with Med16 deleted reveals a complex with intact Middle and Head modules but a missing tail, suggesting that the tail of Mediator is not required for complex integrity (Dotson et al., 2000). Consistent with this interpretation, the same deletion results in viable yeast cells (Li et al., 1995). A highly detailed analysis of the cryo-EM structure of Mediator, coupled with biochemical crosslinking and deletion experiments, revealed the most complete understanding of the general layout of the yeast and human versions of the Mediator complex to date (Tsai et al., 2014). This study confirmed that yeast and human Mediator adopts similar baseline configurations, and also defined the network of intra-complex interactions between Mediator subunits, providing a useful platform to understand Mediator subunit biology (Tsai et al., 2014).

A major discovery about Mediator structure was that it is highly dynamic in response to various stimuli (Taatjes et al., 2002). Purification of a Flag-tagged Mediator complex from HeLa cells resulted in a complex that is identical in subunit composition but highly divergent in conformation from a VP16 activator-purified Mediator complex (Taatjes et al., 2002). Furthermore, Mediator purified with the SREBP-1a activator adopted an even more distinct conformation relative to Flag-Mediator (Taatjes et al., 2002). This revealed that, depending on the transcriptional stimulus, Mediator can function in different modes that might have major

impacts on the output at a target gene. For example, varying effects on Pol II activity and differential recruitment of coactivator proteins could result from individual activator-stimulated Mediator conformations.

1.3.3 – Mediator interactions with TFs

TFs have preferences for specific binding partners within the Mediator complex. As an example, nuclear hormone receptors, including the thyroid receptor that was initially used to identify TRAP complexes, preferentially bind Med1's LxxLL motifs (Malik and Roeder, 2010). Deletions of Med2, Med3, or Med16, all of the tail module were also shown to affect a subset of transcriptional activation functions in response to Gal4-VP16, but leave unaffected other transcriptional activities of the remaining Mediator complex (Myers et al., 1999). Similarly, deletion of Med15 led to specific transcriptional deficits while deletion of Med18 led to more complete loss of transcriptional activity in yeast (Han et al., 1999).

While knockout of Mediator subunits in mammals has always led to embryonic lethality (Poss et al., 2013), cells derived from these embryos have allowed study of the contributions of individual subunits to TF stimuli. Knock out of Med1, as expected, led to a deficit in nuclear hormone-dependent transcriptional signaling, such as PPARγ2-induced adipogenesis, but not other transcription pathways, such as Myo-D-induced myogenesis (Ge et al., 2002). Med1 also binds to GATA1 and is required for transactivation at GATA1 target genes, and deficiency in Med1 leads to an inability for the developing embryo to undergo erythropoiesis (Stumpf et al., 2006). Med23 was identified as binding to adenoviral E1a and to the MAP kinase pathway ETS

transcription factor Elk1 (Boyer et al., 1999). Cells from Med23 knockout embryos were unable to activate gene expression in response to these TFs, which can result in phenotypes such as deficient adipogenesis (Stevens et al., 2002; Wang et al., 2009). An example of this with important implications arises from studies of Med15. Originally identified as binding to the master lipid biogenesis regulator SREBP-1a through its KIX domain, deletion of Med15 from *c. elegans* led to impaired lipid homeostasis and an inability to activate SREBP-1a target genes (Yang et al., 2006). The specificity of the KIX domain of Med15 to bind SREBP-1a's activation domain has since been exploited by the development of a boron-containing chemical probe that selectively blocks the interaction of Med15 and SREBP-1a, resulting in a suppression of SREBP-1a target genes in mouse livers and a reduction in serum lipids (Zhao et al., 2014). These results demonstrate how understanding of Mediator-TF interactions can be exploited for therapeutic aims.

1.3.4 – The Mediator kinase module

A four protein module called the kinase module reversibly associates with the core Mediator complex. This module, comprised of Cyclin C and Cdk8, Med12, and Med13 (or their paralogs Cdk19, Med12L, and Med13L), was originally described as repressive because deletion of Cdk8 from yeast led to transcriptional activation of approximately 3% of the genome (Holstege et al., 1998). Association of the kinase module was also shown to block Pol II from binding Mediator (Elmlund et al., 2006). Furthermore, addition of the kinase module to purified transcription systems revealed that the module inhibited the activating function of core Mediator, even in the absence of kinase activity (Knuesel et al., 2009a). This repressive effect was recapitulated with

just Med12/Med13, the two largest subunits of the kinase module and of the entire Mediator complex, supporting a steric inhibitory role for this module (Knuesel et al., 2009a). However, work from the same group also showed that Cdk8 phosphorylates Histone 3 serine 10, a chromatin mark associated with transcriptional activation (Knuesel et al., 2009b). Furthermore, kinase modules were required for activation of gene expression in response to serum stimulation and hypoxia (Donner et al., 2010; Galbraith et al., 2013). This dichotomy persists within the TF targets of Cdk8 kinase activity. Cdk8 can promote TGF-b signaling by phosphorylating the Smads, a modification that both promotes Smad target gene activation and marks the Smad proteins themselves for degradation (Alarcon et al., 2009). Similarly, Cdk8 can phosphorylate the Notch ICD to activate target gene expression and mark the protein for degradation, and STAT1, with both positive and negative effects on target gene activation (Bancerek et al., 2013; Fryer et al., 2004). Thus, even within a single transcriptional system, Cdk8 has bidirectional effects on gene expression. The kinase module as a whole, too, has activating and repressing effects within transcriptional systems. Cdk8 can phosphorylate E2F1 to repress its transcriptional output with the consequence of releasing β-catenin transcription from E2F1's own repressive effects (Morris et al., 2008). Cdk8 is also amplified in colorectal cancer, a malignancy with a well-established dependence on the β-catenin pathway (Firestein et al., 2008). Intriguingly, Med12 has been demonstrated to directly bind β-catenin through its PQL domain and is essential for b-catenin target gene activation (Kim et al., 2006). Despite their close association within the kinase module, Med12/13 and Cdk8/19 have frequently been demonstrated to carry out distinct functions in cells. A genomewide screen of factors necessary for maintenance of ES cell pluripotency identified, among other Mediator subunits, Med12 but not the Mediator

kinases as requirements for this phenotype (Kagey et al., 2010). More strikingly, a separate genomewide shRNA screen for modulators of *drosophila* crystal cell development identified Med12 and 13, but not the other kinase subunits, as crucial coactivator partners of the GATA TF Serpent that regulates this cell type (Gobert et al., 2010). This finding was extended in a recent microarray analysis of Med12, Med13, Cdk8, and Cyclin C knockdown S2 cells, which highlighted a stark contrast in the transcriptional profiles that result from perturbation of Med12/13 vs Cdk8/Cyclin C (Kuuluvainen et al., 2014).

1.3.5 – Mediator regulates multiple steps of Pol II transcription

After being recruited to chromatin by TFs, Mediator regulates transcriptional output in a number of ways. Mass-spectrometry approaches revealed that in response to activators in live cells, Mediator is recruited in a step that is required for subsequent assembly of the pre-initiation complex (PIC) components TFIIB, TFIID, and TFIIH, as well as for the recruitment of Pol II itself and other complexes such as those containing MLL (Chen et al., 2012). This work confirmed the biochemical results on purified DNA templates that suggested a role for Mediator in the assembly of these components of the PIC (Baek et al., 2006; Johnson and Carey, 2003). Mediator can also coordinate the histone modifications that accompany PIC assembly, as shown in a study in which the P300 acetyltransferase bound to VP16-recruited Mediator, acetylated chromatin, and then dissociated from chromatin, allowing TFIID to bind Mediator (Black et al., 2006).

Additionally, Mediator has been shown to bind directly to the super-elongation complex (SEC, including ELL, EAF, and PTEF-b) through the Med26 subunit, thus supporting gene expression both at the pre-initiation stage as well as the elongation step (Takahashi et al., 2011). An additional mechanism of transcriptional regulation that is controlled by Mediator appears to be the chromatin architecture itself. Enhancers often occur long distances from the genes they regulate and subsequently loop back towards their target genes (Sanyal et al., 2012). Furthermore, enforcing enhancer-promoter looping can selectively affect gene transcription in cells (Deng et al., 2012). Mediator was recently shown to be required for the maintenance of enhancer-promoter loops in embryonic stem cells by associating with the cohesin complex and thus providing a molecular bridge through which enhancer bound TFs can assemble and regulate promoter-bound PICs in cells (Kagey et al., 2010). This may additionally be facilitated by production of noncoding RNA species from enhancers, which have been demonstrated to bind directly to some Mediator subunits and drive looping toward target genes (Lai et al., 2013).

1.3.6 – Mediator and disease

Given Mediator's centrality in nearly all aspects of transcription regulation, it is no surprise that Mediator function is altered in a number of human disease states (Malik and Roeder, 2010). While loss of function alleles of Mediator subunits have consistently proven to be embryonic lethal at various stages of development, a number of germline point mutations in Mediator subunits have revealed developmental syndromes, suggesting important roles for Mediator in human development (Poss et al., 2013). After sequencing a single seven year old girl with transposition of the great arteries (TGA), condition in which the aorta arises from the right

ventricle and the pulmonary trunk arises from the left ventricle, a mutation was detected in a novel gene that was named PROSIT240 (protein similar to TRAP240, or Med13) and has since been renamed Med13L, a subunit of the kinase module (Muncke et al., 2003). Subsequent sequencing of 97 further patients with TGA revealed 3 missense mutations in Med13L and none in 400 controls (Muncke et al., 2003). Interestingly, deletion of Med13 from cardiomyocytes also had a phenotype in mice, albeit a metabolic syndrome in which mice were more prone to develop obesity and insulin resistance due to reduced expression of metabolic genes (Grueter et al., 2012).

Also within the kinase module, Med12 harbors mutations that are associated with familial, X-linked mental retardation syndromes. FG syndrome, originally called Opitz-Kaveggia syndrome (R961W), and Lujan syndrome (N1007S) are both intellectual disability syndromes associated with heritable mutations in the LS (leucine-serine-rich) domain of Med12 (Graham and Schwartz, 2013). Mechanistically, Med12 has been shown to recruit the histone methyltransferase G9a and the REST corepressor in a manner that is disrupted by these point mutations, thus leading to aberrant expression of neuronal genes such as Synapsin1 (Ding et al., 2008). However, the same group also later showed that these same mutations disrupt Med12's chromatin association with Cdk8 in cells derived from patients with FG or Lujan syndromes, which leads to a lost ability to constrain activation of Gli3-dependent sonic hedgehog pathway target genes, such as Bmp4 (Zhou et al., 2012). However, this disruption of mutant Med12 association with Cdk8 was not recapitulated in biochemical experiments, suggesting further work is needed to understand the true mechanisms underlying these syndromes (Zhou et al., 2012).

Med12 mutations have also been detected via exome sequencing in approximately 5% of prostate cancer patients, with the LS domain L1224F lesion occurring most often (Barbieri et al., 2012). However, another report identified overexpression of Med12 in castration resistant prostate cancers, raising the possibilities of differential requirements for Med12 activity at different stages of prostate cancer or that a gain of function conferred by the L1224F mutation (Shaikhibrahim et al., 2014).

Most notable, however, are mutations in exon 2, especially at glycine 44, of Med12. The mutations were initially discovered in 70% of uterine leiomyomas from 80 patients, suggesting a major role for these mutations in driving or initiating the disease (Makinen et al., 2011). These same mutations, which were subsequently identified in 5% of chronic lymphocytic leukemias (and are associated with poor prognosis), and 73% of breast fibroepithelial tumors, including 59% of breast fibroadenomas and 80% of phyllodes tumors (Kampjarvi et al., 2015a; Landau et al., 2013; Lim et al., 2014; Tan et al., 2015; Yoshida et al., 2015). Importantly, these mutations have been demonstrated not to be loss of function alleles, because deletion of Med12 in mice does not lead to tumorigenesis (Mittal et al., 2015). Instead, Med12^{G44D} the most common variant observed in uterine leiomyomas, needed to be expressed for tumors to arise and could cause tumorigenesis even on a fully wild-type background (Mittal et al., 2015). Importantly, chromothripsis, or complex and catastrophic chromosomal "shattering," is also observed frequently in leiomyomas, and Med12^{G44D} murine leiomyomas recapitulated this phenotype, suggesting that the Med12 alteration precedes the chromothripsis (Mehine et al., 2013; Mittal et al., 2015). Interestingly, the most upregulated gene in Med12 mutant uterine leiomyoma patient samples is Rad51b, which fits this model (Mehine et al., 2013). These mutations have been

demonstrated to disrupt the interaction of Med12 with Cyclin C and Cdk8 in 293T cells, an association that is required for the catalytic activity of the Cdk8 kinase (Knuesel et al., 2009b; Turunen et al., 2014). However, corresponding mutations in Ccnc that also disrupt this interaction, or mutations in Cdk8's kinase domain, have not been observed in any cancers, suggesting that a simple dissociative effect or loss of kinase activity might not capture the entire gain of function of Med12 exon 2 mutants. Interestingly, Med12 has also been identified in two independent screens for drivers of resistance to targeted kinase inhibitors used in cancer therapy (Huang et al., 2012; Shalem et al., 2014). In a genome-wide shRNA screen of non-small cell lung cancer (NSCLC) cells harboring an EML4-ALK translocation, shRNAs targeting Med12 conferred resistance to the tyrosine kinase inhibitor crizotinib (Huang et al., 2012). These results were extended to show that Med12 knockdown generated NSCLC resistance to the EGFR inhibitors gefinitib and erlotinib, melanoma resistance to the mutant BRAF inhibitor vemurafinib and the MEK inhibitor selumetinib, and hepatocellular carcinoma resistance to the multi-kinase inhibitor sorafenib (Huang et al., 2012). Knockdown of TGFβ receptor 2 reversed this resistance, and it was demonstrated that Med12 had an unexpected, Mediator-independent cytoplasmic role in glycosylating and thus destabilizing this receptor (Huang et al., 2012). Thus, knockdown of Med12 resulted in activation of TGFβ signaling and kinase inhibitor resistance (Huang et al., 2012). Interestingly, the Med12 exon 2 mutations found in CLL and breast and uterine tumors and the prostate cancer Med12[L1224] mutation lead to dissociation of Med12 from Mediator complexes, raising the intriguing possibility that these mutants lead to hyperactivation of TGFβ signaling in this therapy-resistant disease (Kampjarvi et al., 2015b; Turunen et al., 2014).

The kinase module subunit cyclin C was recently found to be a tumor suppressor in T-cell acute lymphoblastic leukemia (T-ALL) (Li et al., 2014). Cyclin C is required for the kinase activity of Cdk8, which has previously been shown to phosphorylate the Notch intracellular domain to promote its degradation, and thus loss of CCNC, which occurs homozygously via chromosome 6q21 deletion in 9% of patients and heterozygously in many more leads to aberrant notch signaling and T-ALL (Fryer et al., 2004; Li et al., 2014). Interestingly, the repressive effects of Cdk8 and Cdk19 were also recently reported to be required for the growth of acute myeloid leukemia cells by selectively restricting the expression of super-enhancer-associated genes (Pelish et al., 2015). However, Cdk8 has also been found to be an oncogene in some solid tumor types. An shRNA screen to uncover modulators of β-catenin signaling in colon cancer identified Cdk8 as a requirement for β-catenin transcriptional activity and as a target of copy number gain in 47% of colon cancer patient samples (Firestein et al., 2008). Cdk8 was shown to be required for even β-catenin-mediated transformation of cells in a kinase-dependent manner (Firestein et al., 2008). Further work suggests that in colon cancer, Cdk8 also cooperates with the TF HIF1a to recruit PTEF-b and promote transcriptional elongation of HIF1a target genes in the disease (Galbraith et al., 2013). Interestingly, the recently reported kinase inhibitor of Cdk8 and Cdk19 showed no growth-inhibitory phenotype in the identical colon cancer cell line used in these studies, although a more recently reported Cdk8/Cdk19 inhibitor does (Dale et al., 2015; Pelish et al., 2015). Cdk8 has also been shown to be transcriptionally upregulated in murine and human melanoma malignant progression cell line series (Kapoor et al., 2010). This upregulation was shown to be mediated by loss of expression of macroH2A (mH2A), a histone variant that is

generally associated with transcriptional suppression, and patient samples show an inverse correlation of mH2A and Cdk8 expression levels (Kapoor et al., 2010). Knocking down Cdk8 slowed the growth of melanoma cells, but this effect could be reversed by exogenous expression of a kinase-dead mutant of Cdk8, suggesting that the kinase activity of the protein is unnecessary in this disease (Kapoor et al., 2010).

The newly-appreciated role for Mediator in human disease and the importance of transcription regulation in AML disease initiation and progression led us to examine the roles of Mediator in maintaining AML. The results presented here shed new light on important mechanisms of leukemogenic transcription and on mechanisms of action of novel therapeutics in this disease and also support the development of new modes of Mediator inhibition to help treat AML.
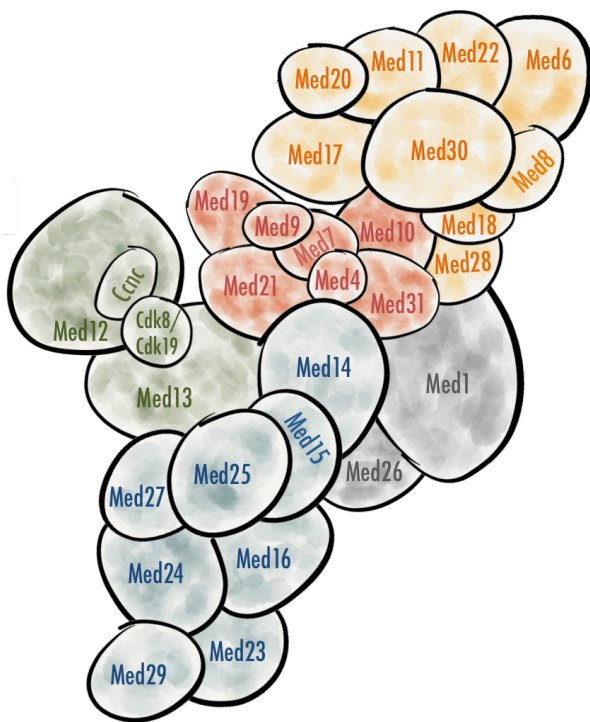
Figure 1-1 The Mediator Complex. The Mediator complex is composed of up to 30 subunits and is divided into head (yellow), middle (red and gray), tail (blue), and kinase (green) modules. Subunit organization is based on Tsai et al, 2014.

Chapter II - BET inhibition releases the Mediator Complex from select *cis* elements in Acute Myeloid Leukemia

2.1 – Brief Introduction

Inhibitors of bromodomain and extra terminal (BET) proteins are an emerging class of therapy for a wide range of hematopoietic malignancies. BET inhibitors have been demonstrated to be well tolerated and effective at delaying disease progression and extending survival in a number of preclinical models of leukemias, lymphomas, and myelomas (Chapuy et al., 2013; Dawson et al., 2011; Delmore et al., 2011; Ott et al., 2012; Zuber et al., 2011c). Furthermore, a phase I clinical trial of a BET inhibitor in acute myeloid leukemia (AML) demonstrated promising therapeutic activity in patients who had failed prior chemotherapy (Dombret et al., 2014). We previously showed that the BET protein Brd4 is required in AML for the expression of key oncogenes such as *Myc* and *Cdk6* and for the maintenance of aberrant self-renewal of AML blasts (Zuber et al., 2011c). However, the underlying molecular mechanism of Brd4 function in supporting cancer progression remains poorly understood. Brd4 utilizes tandem bromodomain modules to

recognize acetyl-lysine side chains on histones and transcription factors, thereby localizing to hyper-acetylated promoter and enhancer regions of the genome (Dey et al., 2003; Roe et al., 2015). Chemical inhibitors of BET bromodomains, such as JQ1 and IBET, cause a global release of Brd4 from the genome. Thus, why certain genes respond to BET inhibition while others do not remains unclear. It has been proposed that genes associated with super-enhancers, defined as regions of extraordinary Mediator occupancy, are selectively affected by BET inhibition (Loven et al., 2013). Other studies have focused on interacting proteins and protein complexes as potential effectors of Brd4 in AML. Proteomic analyses of Brd4 complexes have revealed numerous associated factors, and while a few of these associated factors, such as Nsd3, Chd8, and Cdk9 have been shown to be required for leukemia cell viability, the relevance of most Brd4 interactions to the AML maintenance function of this BET protein is largely unstudied (Dawson et al., 2011; Garcia-Cuellar et al., 2014; Jang et al., 2005; Rahman et al., 2011; Shen et al., 2015).

An association between the Mediator complex and Brd4 has been noted previously, although it is unclear to what extent these two machineries cooperate to regulate transcription (Donner et al., 2010; Jang et al., 2005; Jiang et al., 1998; Wu and Chiang, 2007). Mediator is a ~30-subunit coactivator complex that interacts with the activation domains of DNA binding transcription factors (TFs) and participates in the recruitment and activation of RNA polymerase II (Pol II). The first purification of the mammalian Mediator complex included peptides later shown to be derived from Brd4, and several subsequent studies have also identified a physical interaction between Mediator and Brd4 (Dawson et al., 2011; Donner et al., 2010; Jang et al., 2005; Jiang et al., 1998; Wang et al., 2013). However, many other studies have not observed an interaction

between Mediator and Brd4, including those used for structural examinations of the Mediator complex (Boyer et al., 1999; Naar et al., 1999; Ryu et al., 1999; Taatjes et al., 2002; Takahashi et al., 2011; Tsai et al., 2014). One possible distinction between studies that identify a Mediator-Brd4 interaction and those that do not is that purifications of Mediator involving an activation-domain affinity step do not seem to co-purify with Brd4 (Boyer et al., 1999; Jang et al., 2005; Jiang et al., 1998; Naar et al., 1999; Ryu et al., 1999; Taatjes et al., 2002; Takahashi et al., 2011; Tsai et al., 2014). This may be related to the induction of a rigid structural conformation of Mediator that does not accommodate Brd4 binding, and may also hint at mutually exclusive modes of Mediator recruitment that involve either TFs or Brd4, but not both.

Since TF interactions are thought to tether Mediator to DNA, the role of Brd4 in Mediator recruitment is unclear. Brd4 and Mediator have been found to colocalize at super-enhancers (clusters of highly active enhancers) and BET inhibition can modestly perturb Mediator occupancy at such sites (Di Micco et al., 2014; Loven et al., 2013). In embryonic stem cells, Brd4 and Mediator are each required to maintain Oct4 expression and the pluripotent cell state (Di Micco et al., 2014; Kagey et al., 2010; Wu et al., 2015). However, a recent study has shown that the Cdk8 and Cdk19 kinase subunits of Mediator function in opposition to Brd4 to repress super-enhancer associated genes (Pelish et al., 2015). This series of studies raises two key questions: 1) At what locations of the genome is Mediator released following BET inhibitor treatment? And 2) Does perturbation of Mediator contribute to the observed therapeutic effects of BET inhibition in cancer?

Here, we show that the BET inhibitor JQ1 causes a dramatic loss of Mediator occupancy at select *cis* elements in the genome of AML cells, partially overlapping with super-enhancers. Notably, Mediator eviction tracked closely with the sensitivity of transcription to JQ1-mediated suppression, which suggests that release of Mediator from the genome contributes to the transcriptional effects of BET inhibition. Moreover, a Mediator-focused shRNA screen performed in AML revealed that Brd4 and Mediator coordinate a common gene regulatory network that maintains a blocked state of differentiation in this disease. Since Mediator is preferentially evicted by JQ1 at genes with known roles in supporting leukemogenesis, our findings implicate Mediator antagonism as a contributor to the therapeutic efficacy of BET inhibition in AML.

2.2 - Results

2.2.1 – The Mediator complex is released form the leukemia genome in a variable manner following JQ1 exposure

We tested the hypothesis that BET inhibition with JQ1 elicits anti-leukemia effects by interfering with the function of the Mediator complex. We performed ChIP-seq of Brd4 and Med1 in murine MLL-AF9;Nras^{G12D} AML cells (RN2 cells) (Zuber et al., 2011a). In agreement with prior studies, Brd4 and Med1 colocalize in a pattern that overlaps with H3K27 hyper-acetylated regions across the AML genome (Figure 2-1A) (Loven et al., 2013; Roe et al., 2015; Whyte et al., 2013). Additionally, the levels of occupancy of Med1 and Brd4, as measured by ChIP-seq reads at each peak, were highly correlated (R^2=0.91, Figure 2-1B). The close
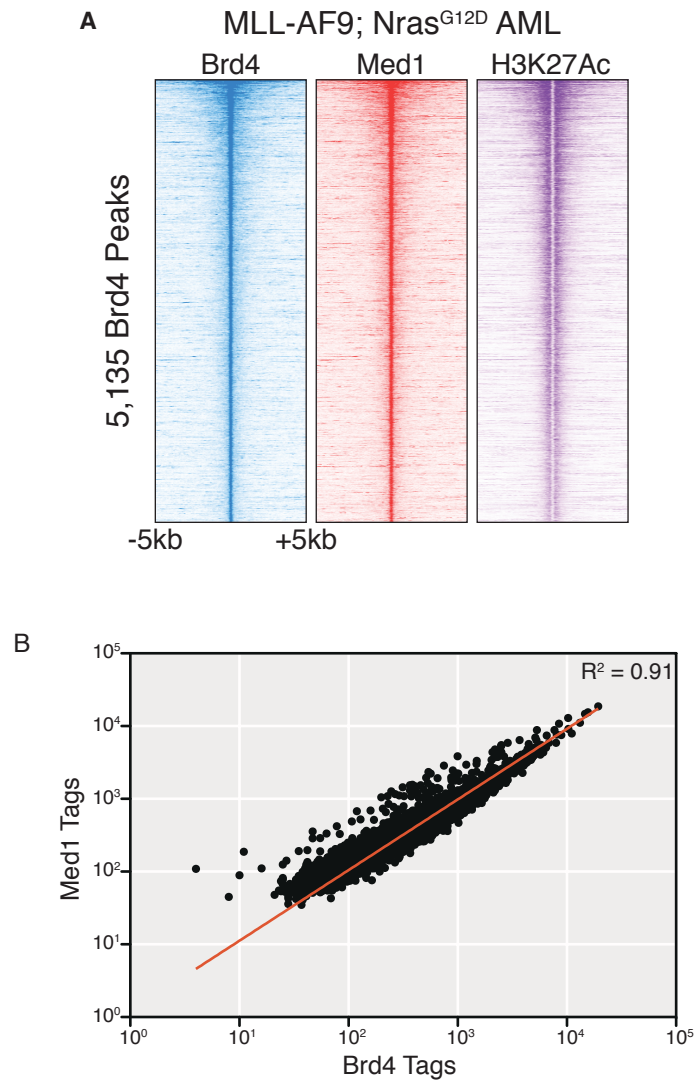
Figure 2-1 Brd4 and Mediator co-localize across the AML genome.
A) Density plot of Brd4, Med1, and H3K27Ac ChIP-seq datasets in murine
MLL-AF9/NRAS[G12D] AML cells.
B) Comparison of tag counts of Brd4 ChIP-seq and Med1 ChIP-seq at 10,604
Med1 peaks in the genome.

correlation of Brd4 and Med1 across the AML genome is consistent with a physical interaction between these factors in this cell type.

We next performed ChIP-seq analysis of Brd4 and Med1 in RN2 cells following 2-hour treatment with 500 nM JQ1 or DMSO as a vehicle control. Transcription of the *Myc* proto-oncogene in RN2 cells is highly sensitive to JQ1 and is regulated by Brd4 via a cluster of super-enhancers (E1-E5) 1.7 Megabases downstream of the *Myc* promoter (Shi et al., 2013; Zuber et al., 2011c). As expected, Brd4 was evicted from the E1-E5 super-enhancers and from the *Myc* promoter by JQ1 (Figure 2-2). We additionally observed an equally dramatic reduction of Med1 occupancy at this region (Figure 2-2). To ensure that the entirety of Mediator was being released from these sites, and not just the Med1 subunit, we performed ChIP-qPCR analysis of Brd4, Med1, Med12, and Med23 at the *Myc* E1-E5 super-enhancers. This revealed parallel reductions of all four factors following JQ1 treatment (Figure 2-3). Since Med1, Med12, and Med23 are present in distinct modules of Mediator (the middle, kinase, and tail modules, respectively), this result suggests that the entire Mediator complex is released from the *Myc* super-enhancers following BET bromodomain inhibition.

The observed loss of Mediator from chromatin was not due to suppression of Mediator subunit protein levels, as 2-hour treatment with JQ1 did not affect steady-state quantities of Med1, Med12, or Med23 protein, nor was RNA of any Mediator subunits affected after 6 hours of treatment (Figures 2-4A and 2-4B). Furthermore, by ChIP-qPCR, 30-minute treatment with JQ1 also had similar effects on Mediator occupancy at the E1-E5 super-enhancers, suggesting
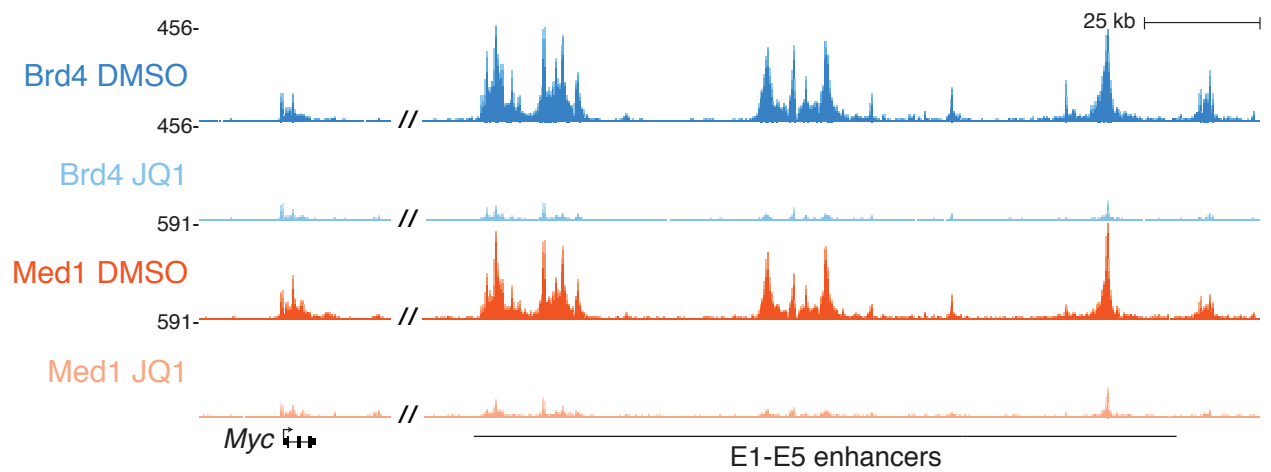
Figure 2-2 JQ1 treatment removes Mediator complexes from the Myc super-enhancers
ChIP-seq occupancy profiles of Brd4 and Med1 following 2hr treatment with either DMSO or 500nM JQ1.
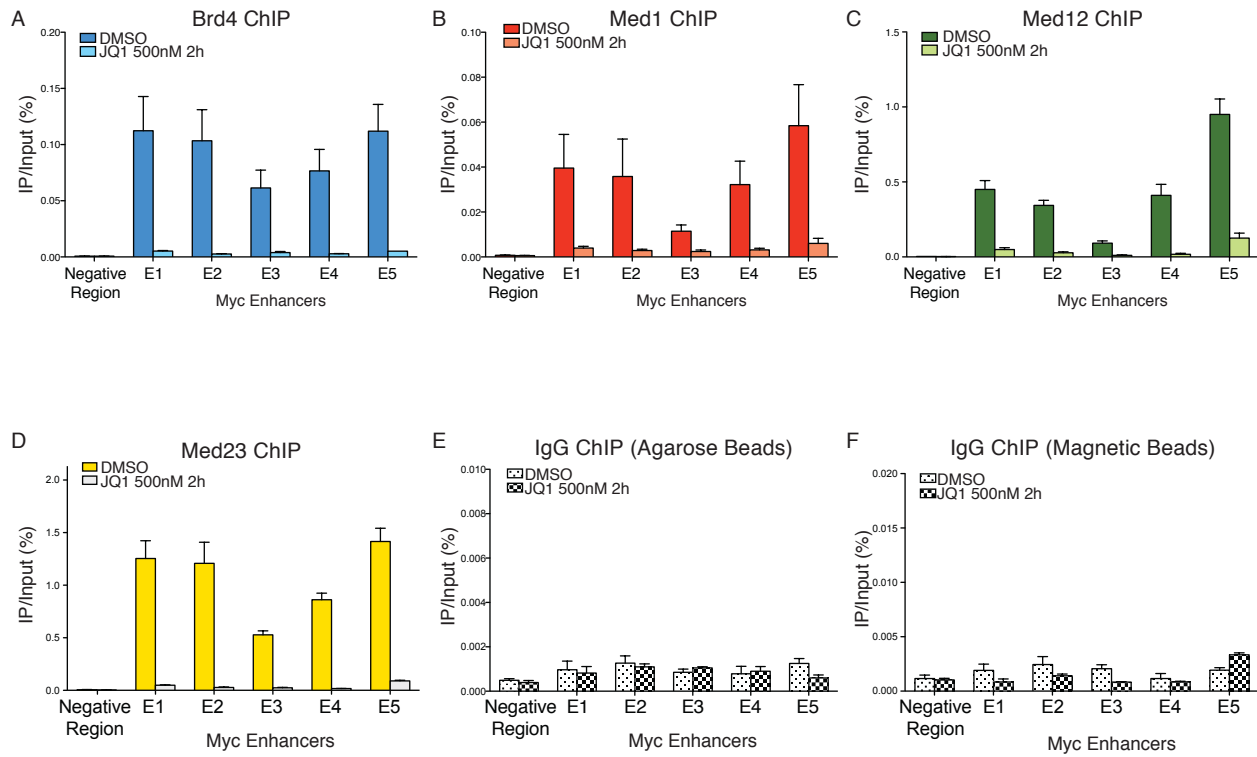
Figure 2-3 JQ1 treatment removes Mediator complexes from the Myc super-enhancers

A-F) ChIP-qPCR analysis with indicated antibodies at the Myc Locus following 2hr treatment with DMSO or 500nM JQ1.
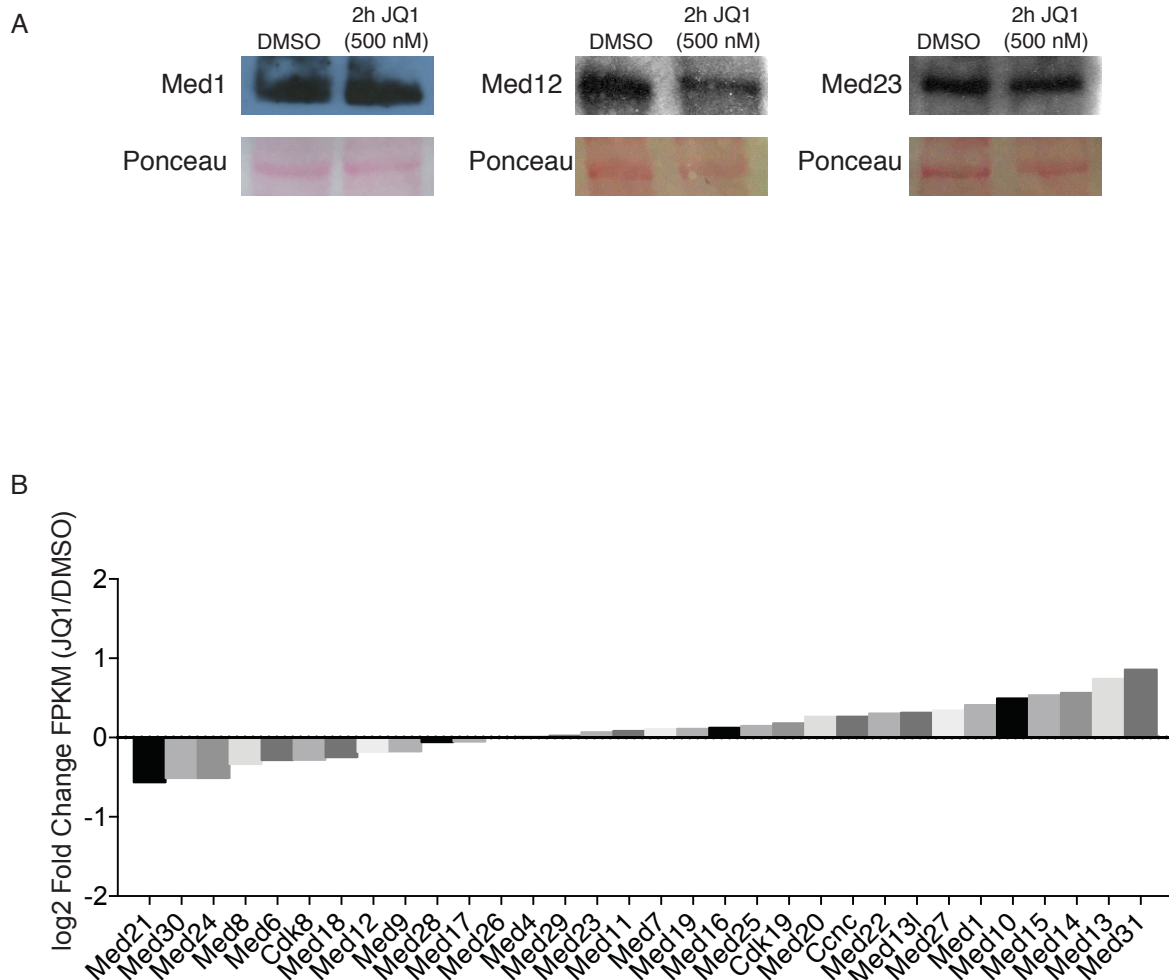
Figure 2-4 JQ1 results in eviction of Mediator without affecting levels of Mediator

A) Western blot analysis of Med1, Med12, and Med23 proteins after 2 hr treatment with DMSO or 500 nM JQ1.

B) Fold change in FPKM values for Mediator subunits from RNA-seq data in RN2 cells after 6h 500nM JQ1 treatment as compared to DMSO control.
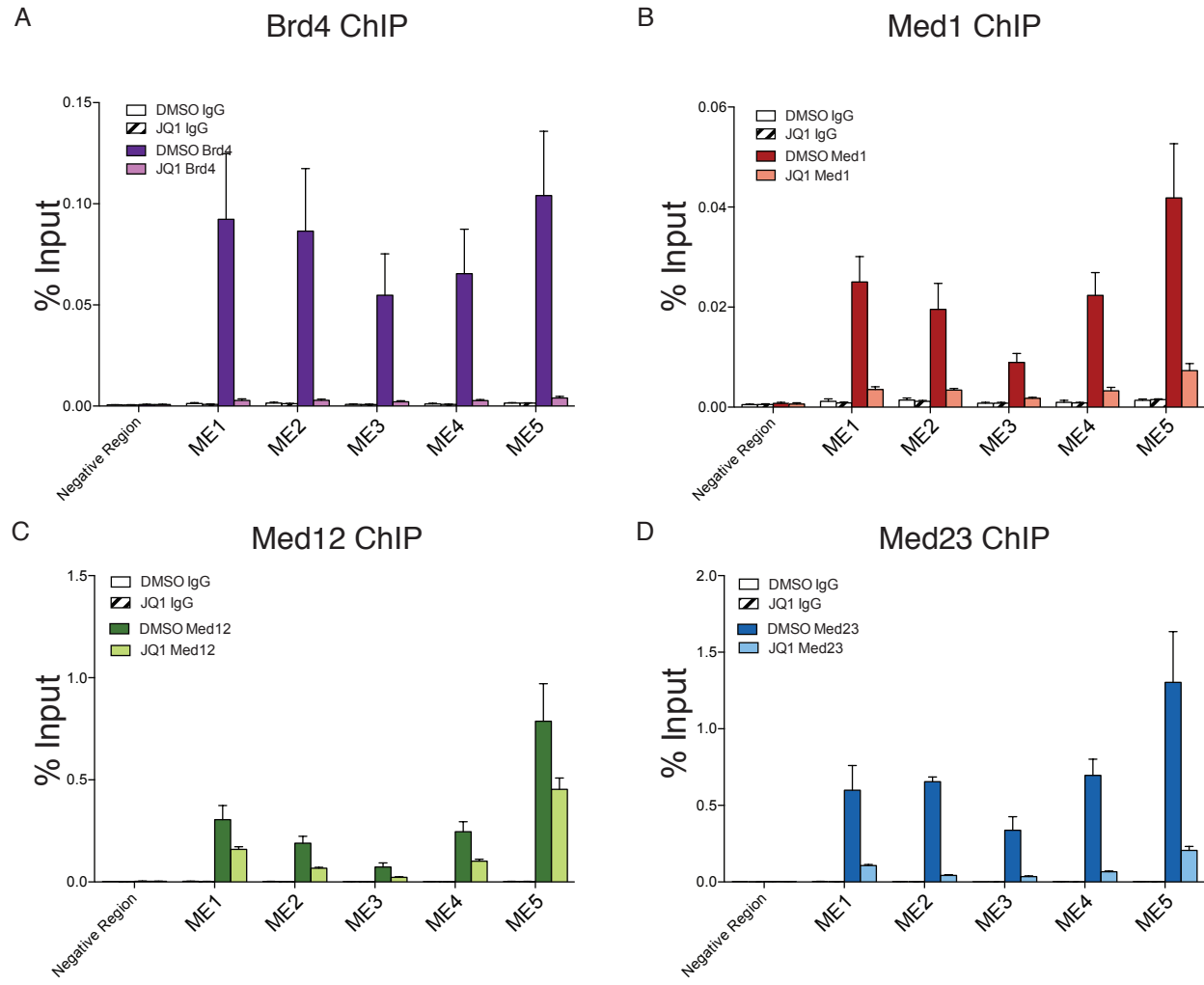
Figure 2-5 JQ1 results in rapid eviction of Mediator from the *Myc* enhancers
A-D) ChIP-qPCR analysis at the Myc enhancer locus of Brd4 or of the indicated
Mediator subunit after 30 min treatment with DMSO or 500nM JQ1.

that Mediator is rapidly released from chromatin as cells are exposed to the molecule (Figure 2-5).

Because BET inhibition has been proposed to selectively perturb Med1 occupancy at super-enhancers, we applied the Rank Ordering of Super-Enhancers (ROSE) algorithm to Med1 ChIP-seq data to define super-enhancers in RN2 cells and used these for the analyses that follow (Figure 2-6A) (Loven et al., 2013; Whyte et al., 2013). We inspected various super-enhancer regions for the impact of JQ1 on Med1 occupancy. *Cdk6* has been previously implicated as a Brd4 target gene in AML and is regulated by an intronic super-enhancer (Dawson et al., 2011; Roe et al., 2015). Similar to the *Myc* locus, we observed parallel reductions of Brd4 and Med1 at the *Cdk6* super-enhancer following BET inhibition (Figure 2-6B). However, not all super-enhancers were susceptible to JQ1-dependent Med1 eviction. The *Lrrfip1* gene harbors a promoter-proximal super-enhancer that displayed reduced Brd4 occupancy but only a minimal reduction of Med1 following exposure to JQ1 (Figure 2-6C). Interestingly, a large domain of Med1 occupancy found at the HoxA locus qualifies as a super-enhancer when applying the ROSE algorithm (Figure 2-6A), yet Med1 is entirely unaltered by JQ1 at this region (Figure 2-6D). We also noted that Med1 displacement often occurred at regions that fell below the threshold of being called as super-enhancers, such as intronic locations at the *Mgat5* locus (Figure 2-6A and 2-6E). For most genomic sites, we observe a largely non-linear relationship between Med1 and Brd4 loss following JQ1 exposure (R^2=0.13) (Figure 2-7). However, we also note that severe Med1 eviction was generally confined to elements exhibiting severe decreases in Brd4 occupancy following JQ1 treatment. Collectively, these findings show that JQ1 causes varying levels of Med1 loss at specific *cis* elements in the leukemia genome.
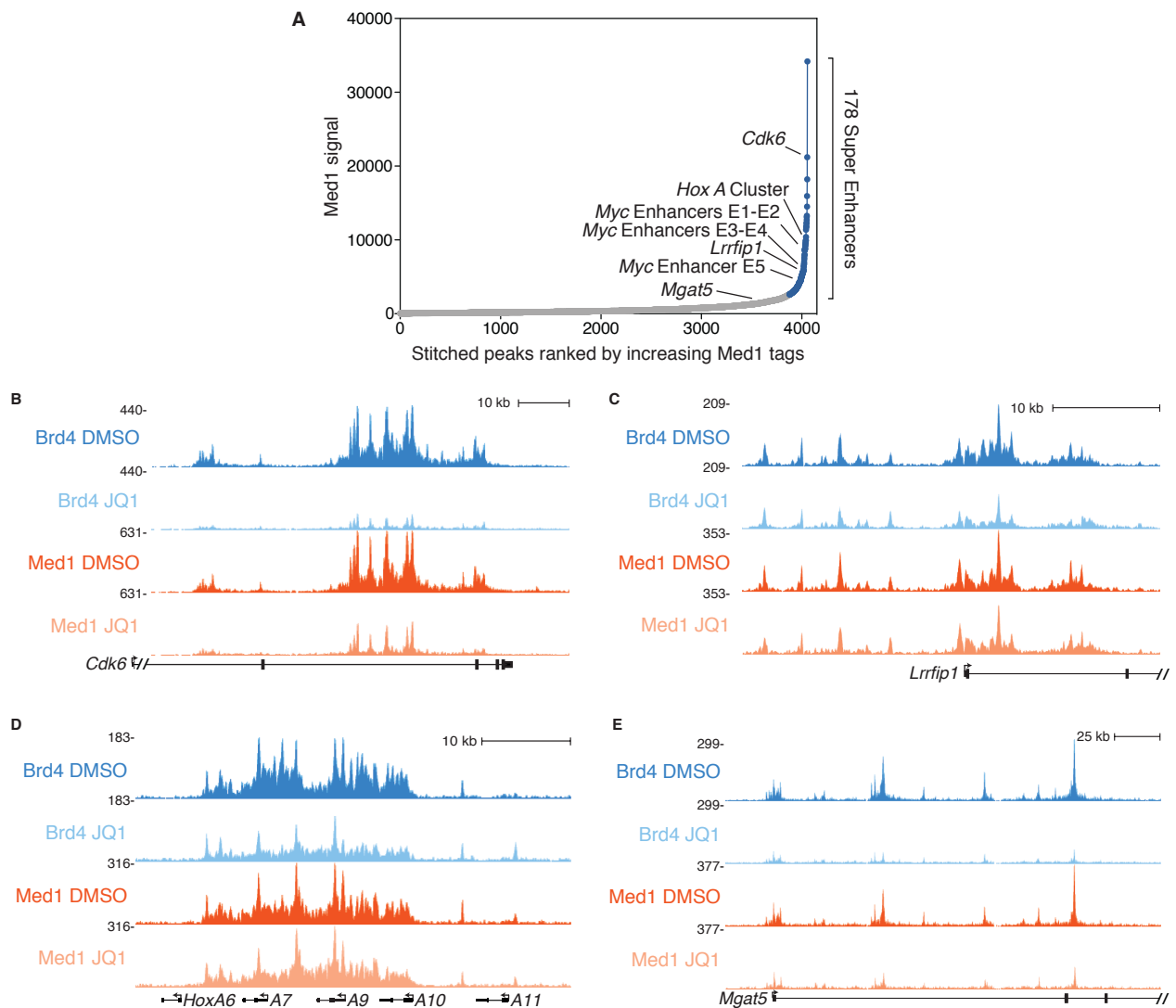
Figure 2-6 The Mediator complex is released from the AML genome in a variable manner following JQ1 exposure

A) 178 Super-enhancers defined by Med1 occupancy at stitched Med1 loci using the ROSE algorithm

B-E) ChIP-Seq occupancy profiles of Brd4 and Med1 at *Cdk6, Lrrfip1*, the *HoxA* cluster, and *Mgat5* following 2 hr treatment with DMSO or 500 nM JQ1.
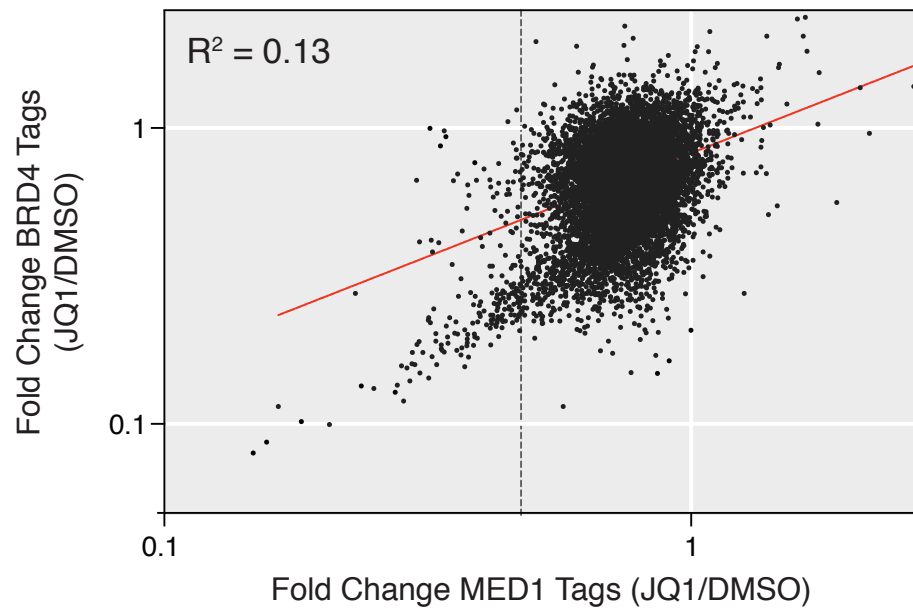
Figure 2-7 Mediator and Brd4 eviction by JQ1 exhibits a largely non-linear relationship
Comparison of fold change in tag counts of BRD4 vs. MED1 ChIP-seq at 10,604 MED1 peaks in the genome after 2 hr 500 nM JQ1 treatment.

2.2.2 – JQ1–induced Mediator eviction correlates with JQ1–induced transcriptional suppression

We next sought an understanding of the transcriptional consequences of JQ1-induced Med1 eviction in RN2 cells. For this purpose, we rank-ordered 10,604 reproducible Med1 peaks, as called by the Model-based Analysis of ChIP-seq (MACS) algorithm, based on the average fold-change of Med1 tag counts following exposure to JQ1 in two independent biological replicates (Zhang et al., 2008). This analysis revealed that the constituent Med1 peaks at the *Myc* E1-E5 super-enhancers were outliers in the genome with regard to the severity of Med1 loss following JQ1 treatment (Figure 2-8A). This result was striking, since *Myc* is also among the most down-regulated mRNAs in AML cells following JQ1 treatment (Dawson et al., 2011; Zuber et al., 2011c) (Figure 2-8B). Furthermore, the severity of Med1 loss at the gene loci highlighted above was correlative with the relative effect of JQ1 on gene expression (Figure 2-8). This raised the possibility that loss of Med1 from the genome was a critical feature of JQ1-induced transcriptional suppression.

To systematically test this hypothesis, we defined 200 regions in the RN2 genome that exhibited the largest JQ1-dependent decrease in Med1 occupancy (Figure 2-8A, blue box). Surprisingly, we found that only 64% of these peaks overlapped with the locations of super-enhancers (Figure 2-9A). We then applied the Genomic Regions Enrichment of Annotations Tool (GREAT) to link each JQ1-sensitive Med1 peak to the nearest expressed gene, an established means of identifying the relevant target gene of *cis*-elements (McLean et al., 2010). We also performed an analogous GREAT analysis to link each Med1-defined super-enhancer to its relevant target
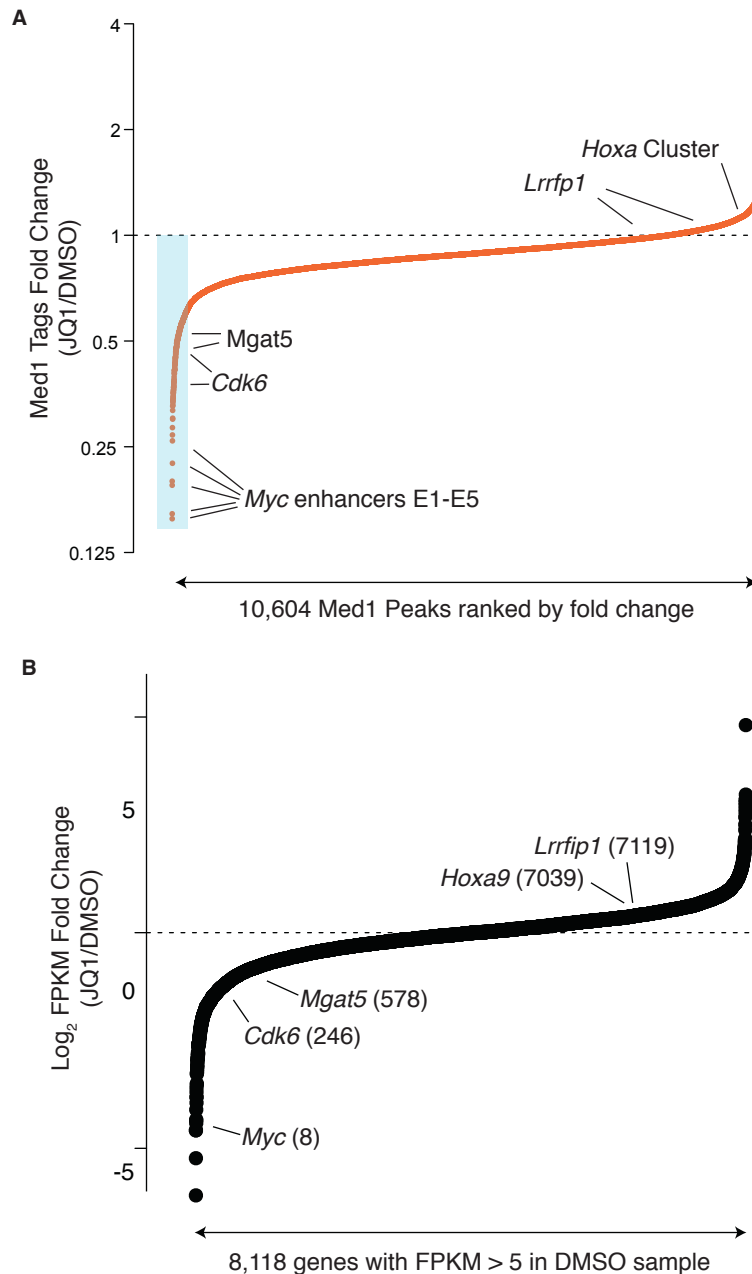
Figure 2-8 JQ1-induced Mediator eviction correlates with JQ1-induced transcriptional suppression.
A) Fold change in occupancy of Med1 at 10,604 individual Med1 peaks in AMLfollowing 2 hr treatment with 500nM JQ1. The peaks are ranked in order of increasing fold change. The blue box highlights the 200 most JQ1-sensitive Med1 elements. Fold changes presented are the average of two independent biological replicates.
B) Fold change in FPKM for 8,118 expressed genes in AML (defined by FPKM > 5 in DMSO sample) following 6 hr of 500nM JQ1 treatment. The genes are ranked in order of increasing fold change. The Numbers in parentheses are the fold-change expression rank of the indicated genes.
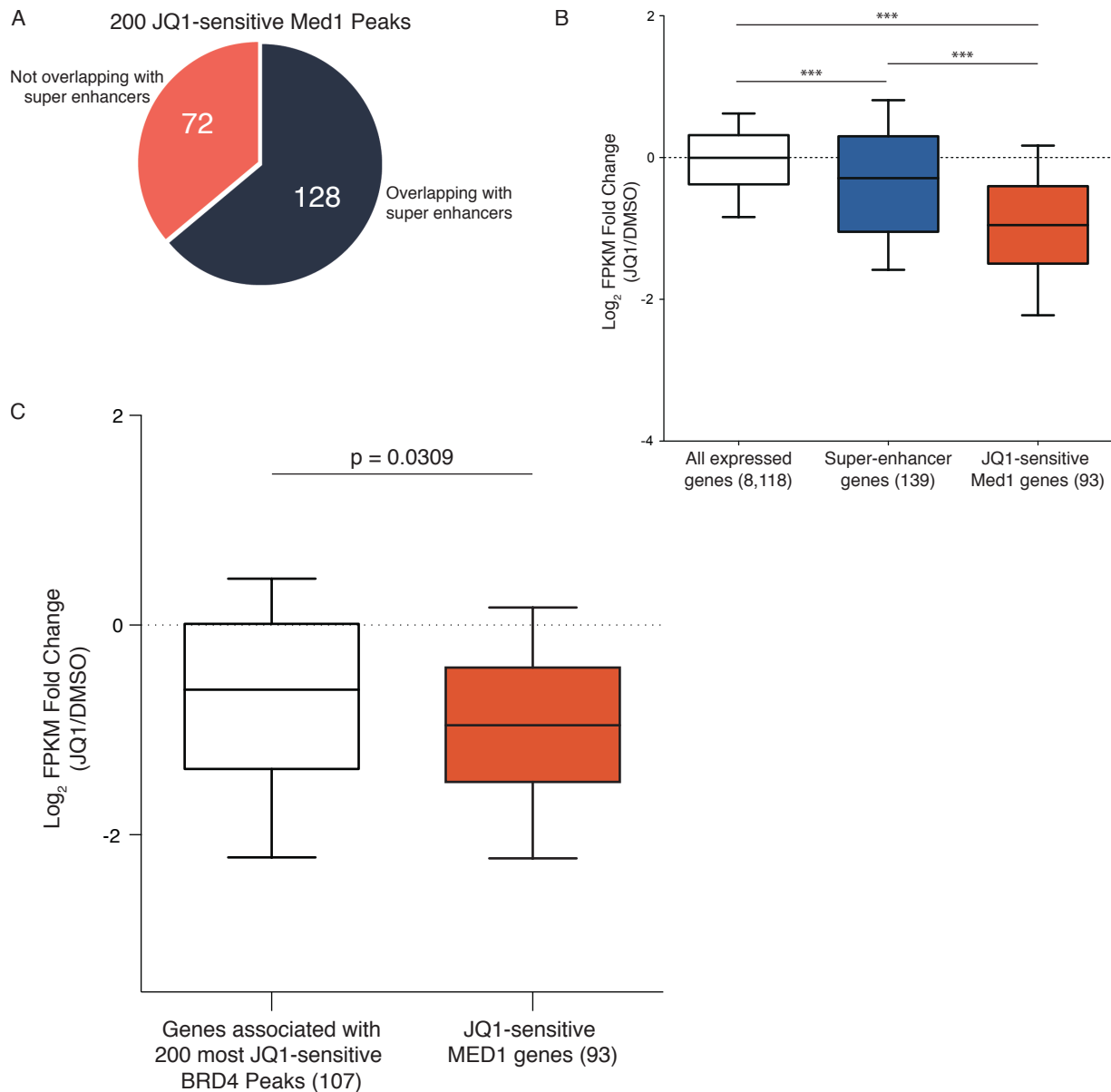
Figure 2-9 JQ1-induced Mediator eviction predicts with transcript sensitivity to JQ1.
A) Stratification of the 200 most JQ1-sensitive Med1 peaks based on whether or not they overlap with a super-enhancer. Minimum overlap 1 bp.

B) Average fold change in FPKM after JQ1 treatment for all expressed genes (left), for genes associated with super-enhancers (center), and for genes associated with JQ1-sensitive Med1 peaks (right). The numbers in parentheses represent the number of genes matched to the class of peaks indicated. *** represents a p value < 0.0001, the result of a Mann-Whitney test.

C) Average fold change in FPKM after 2 hr 500 nM JQ1 treatment for genes associated with the 200 most JQ1-sensitive Brd4 peaks (left) and for genes associated with the 200 most JQ1-sensitive MED1 peaks (right). The numbers in parentheses represent the number of genes matched to the class of peaks indicated. The p value is the result of a Mann-Whitney test.

A

178 Super-enhancers

JQ1-Insensitive Med1

JQ1-Sensitive Med1

103

75

B

Log$_2$ FPKM Fold Change (JQ1/DMSO)

***

JQ1 Sensitive Med1 (52)

JQ1 Insensitive Med1 (87)

Super-enhancer genes
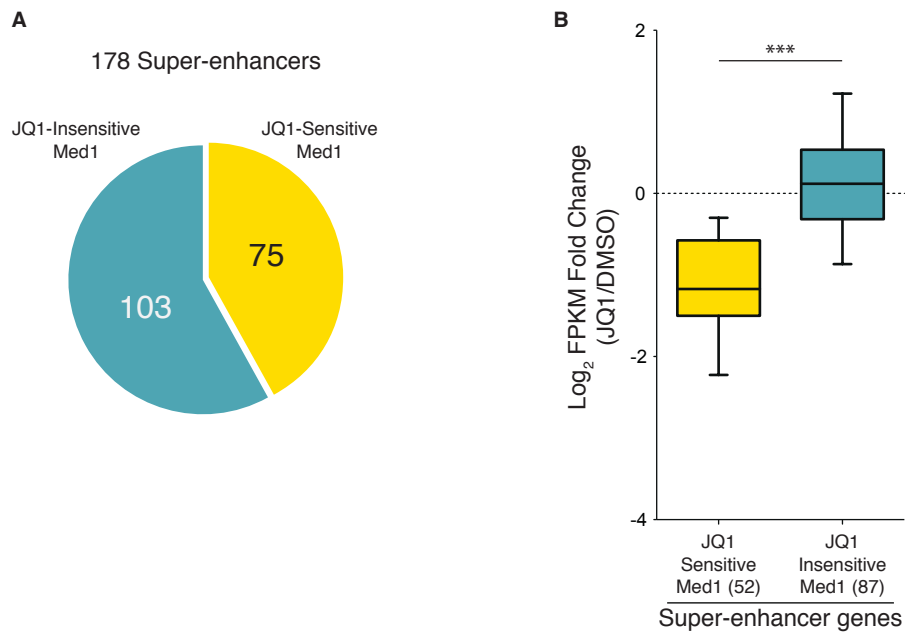
Figure 2-10 JQ1-induced Mediator eviction can stratify super-enhancers and predict transcript sensitivity to JQ1.
A) Stratification of 178 Med1 super-enhancers based on whether or not they overlapwith at least one of the 200 JQ1-sensitive Med1 peaks (minimum overlap 1 bp).
B) Average fold change in FPKM for genes associatd with JQ1-sensitive Med1 super enhancers and for genes associated with JQ1-insensitive Med1 super-enhancers. The numbers in parentheses represent the number of genes in the subclass of super-enhancer indicated. *** represetnts a p value < 0.0001, the result of a Mann-Whitney test.

gene (Table 2-2, at the end of this chapter). These two gene sets were then independently evaluated within RNA-seq data derived from RN2 cells treated with 500 nM JQ1 for 6 hours (Roe et al., 2015). Consistent with prior observations, we found that super-enhancers correlated to some extent with sensitivity of gene expression to JQ1 (Figure 2-9B) (Loven et al., 2013). However, we found that genes located near JQ1-sensitive Med1 peaks were suppressed to a significantly greater degree than genes located in proximity to super-enhancers and genes located in proximity to JQ1-sensitive Brd4 peaks (Figure 2-9B and 2-9C). This result prompted us to consider that the ROSE algorithm definition of super-enhancers might include two distinct classes of *cis* elements that differ with regard to their sensitivity to JQ1-mediated perturbation. We found that 75 of the 178 super-enhancers in RN2 cells overlapped with JQ1-sensitive Med1 peaks (Figure 2-10A), and that only this subset of super-enhancers was associated with JQ1-mediated transcriptional repression (Figure 2-10B). An important implication of this finding is that a large fraction of ROSE-defined super-enhancers (103 out of 178) resist JQ1-mediated Med1 displacement and appear to be unrelated to transcriptional suppression by BET inhibition. JQ1 eviction of Med1 may therefore represent a more reliable correlate of transcriptional repression by JQ1 than pre-existing levels of Med1.

2.2.3 – JQ1-sensitive MED1 peaks are loaded with BRD4-binding TFs and are associated with gene relevant for leukemia

We next sought to understand the unique properties of JQ1-sensitive Med1 peaks in AML cells. We have previously shown that a set of hematopoietic TFs (C/EBPa, C/EBPb, Erg, Fli1, Myb, and Pu.1) directly bind Brd4 and facilitate its recruitment to the genome of AML cells (Roe et

al., 2015). We found that the 200 JQ1-sensitive Med1 peaks were associated with a higher motif density and a higher occupancy of C/EBPa, C/EBPb, and Myb, whereas Erg, Fli1, and Pu.1 levels, and their cognate ETS motifs, were enriched to a lesser extent (Figure 2-11A and 2-11B). We also evaluated whether the genes linked with JQ1-sensitive Med1 peaks were enriched for any particular biological or molecular pathways. For this purpose, we used GREAT to compare the ontology of genes located near 200 JQ1-sensitive Med1 peaks with genes located near 200 random Med1 peaks. This revealed that Mediator release from the genome occurred disproportionately at genes involved in leukemia pathogenesis (Figure 2-12). Within this analysis, Myb target genes comprised the most enriched transcription factor network among the JQ1-sensitive Med1 peaks, in agreement with the higher relative level of Myb occupancy at this class of *cis* elements (Figure 2-11B and 2-12). These results suggest that Mediator is preferentially evicted by JQ1 near Myb target genes that modulate the pathogenesis of leukemia.

2.2.4 – Knockdown of select Mediator subunits triggers differentiation of leukemic blasts

The genomic correlations described above support a model in which Brd4 and Mediator cooperate to regulate a common set of target genes in AML. One prediction of this model is that targeting of specific subunits of Mediator may lead to similar phenotypic and transcriptional ffects as targeting of Brd4. Inhibition of Brd4 with either JQ1 or shRNAs triggers differentiation of AML cells into macrophage-like cells that express higher levels of Mac1 (CD11b) and lower levels of cKit on their cell surface (Zuber et al., 2011c). To evaluate the phenotypic consequences of Mediator perturbation, we constructed a custom library of 190 shRNAs targeting all of the known Mediator subunits (~6 shRNAs/gene) and carried out a negative selection screen to
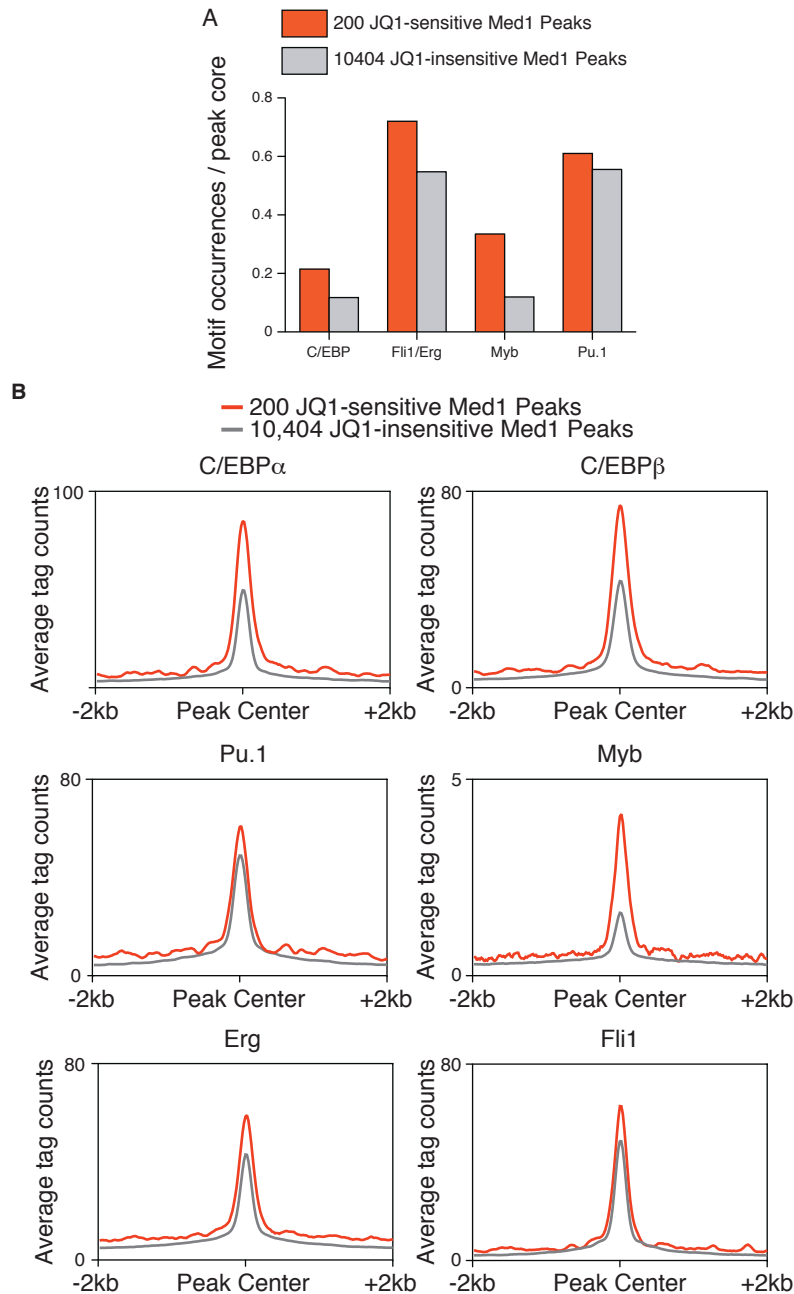
Figure 2-11 TFs preferentially occupy JQ1-sensitive Med1 peaks
A) Motif counts at 200 JQ1-sensitive Med1 peak cores vs. the remaining 10,404 Med1 peak cores (peak cores defined as 400bp centered on peak summits). Motif counts were performed using the FIMO algorithm.
B) ChIP-seq meta-profiles for hematopoietic TFs at 200 JQ1-sensitive Med1 peaks vs. remaining 10,404 Med1 peaks.
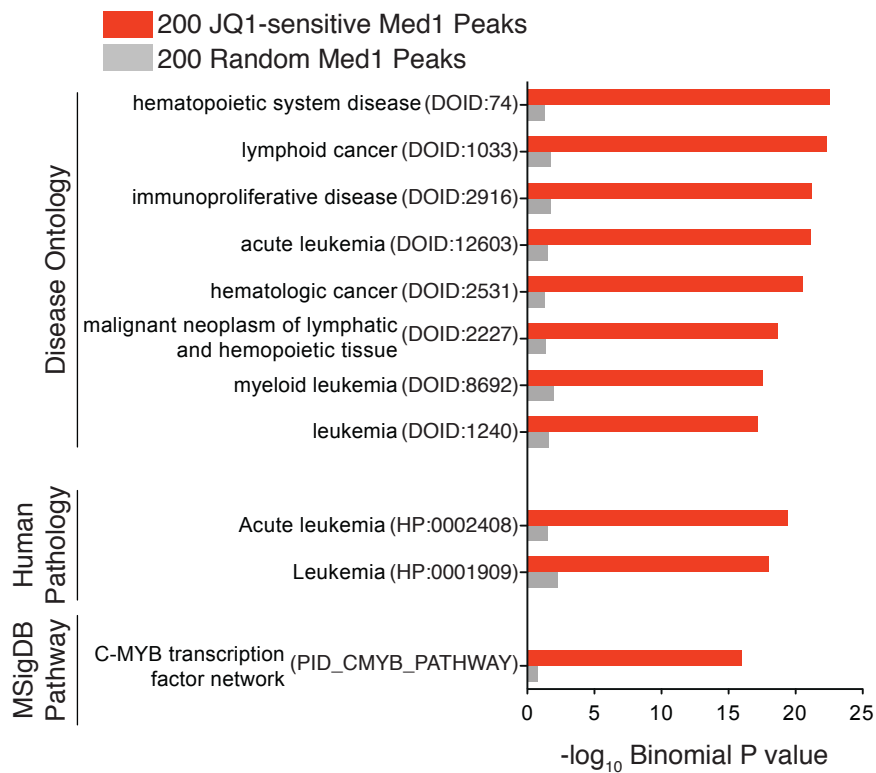
Figure 2-12 JQ1-sensitive Med1 peaks are enriched for genes important for leukemia
GREAT ontology analysis Binomial P values for 200 JQ1-sensitive Med1 peaks vers 200
random Med1 peaks. Top-ranking ontology terms for the JQ1-sensitive peaks are displayed
alongside values for the same ontology terms in the random peaks. Terms in parentheses
represent the ontology identifiers in the GREAT database.

define the Mediator subunits that are essential for the proliferation of RN2 cells. The relative growth arrest observed over 10 days in culture was quantified using GFP reporters in a competition-based assay and the effect of shRNAs were averaged for each gene (Figure 2-13). We set a 3-fold cutoff of depletion in this assay and found that RN2 growth was sensitive to targeting of specific subunits in the complex. This includes components of the head (Med8, Med28, Med30), middle (Med9, Med26), tail (Med16, Med23, Med24, Med25), and kinase (Med12, Med13) modules (Figures 2-13 and 2-14A). On-target knockdown potency for shRNAs was validated using RT-qPCR (Figure 2-14B). We found that the Med12, Med13, Med23, and Med24 requirement for proliferation was unique to AML cells, as shRNAs targeting these subunits in iMEFs did not impair proliferation despite verified knockdown of these subunits (Figures 2-15A and 2-15B). In contrast, shRNAs targeting Med8, Med28, and Med30 impaired the growth of iMEFs (Figure 2-15A). This heterogenous cellular response to genetic perturbation of individual Mediator subunits did not appear to be related to their baseline levels of mRNA expression. Collectively, our findings suggest that, relative to iMEFs, AML cell proliferation is hypersensitive to targeting of Mediator subunits Med12, Med13, Med23, and Med24. Interestingly, Med12 and Med23 have each been previously implicated in the physical interaction with Brd4 (Dawson et al., 2011; Jang et al., 2005; Wang et al., 2013).

We then asked whether knockdown of Mediator subunits in RN2 cells results in a similar myeloid differentiation phenotype as observed following Brd4 inhibition. When expressed conditionally via a doxycycline(dox)-regulated promoter, we found that Med12, Med13, Med23, and Med24 shRNAs, but not Med8 or Med30 shRNAs altered the cell surface expression of cKit and Mac1 in a manner that resembled Brd4 knockdown (Figures 2-16A and 2-16B).

A
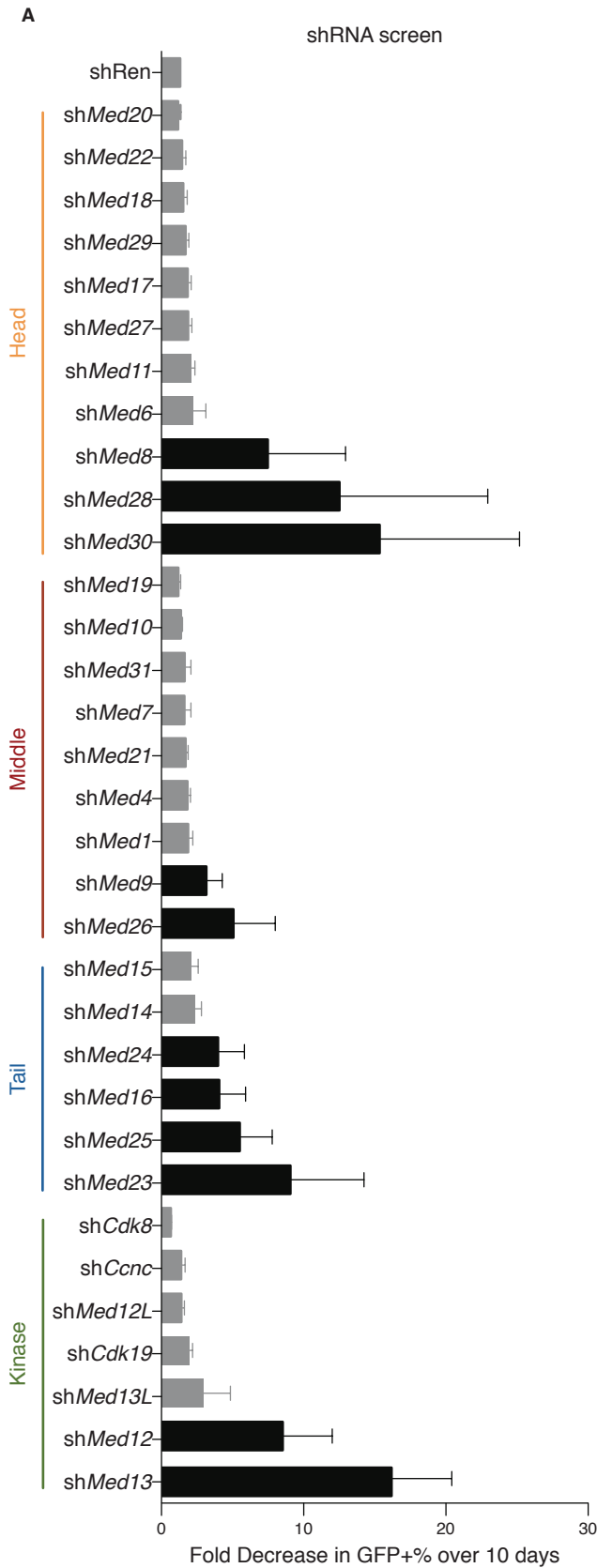
shRNA screen

Figure 2-13 Genetic knockdown of Mediator subunits limits proliferation of AML cells
Summary of negative selection shRNA screen targeting the indicated Mediator subunits. Bars represent the average of all hairpins for each gene. Black bars highlight subunits having at least 3-fold loss of GFP-positive cells with at least two hairpins. shRNAs are expressed using the LMN vector. Data are represented as mean of each hairpin for the corresponding gene ± SEM.
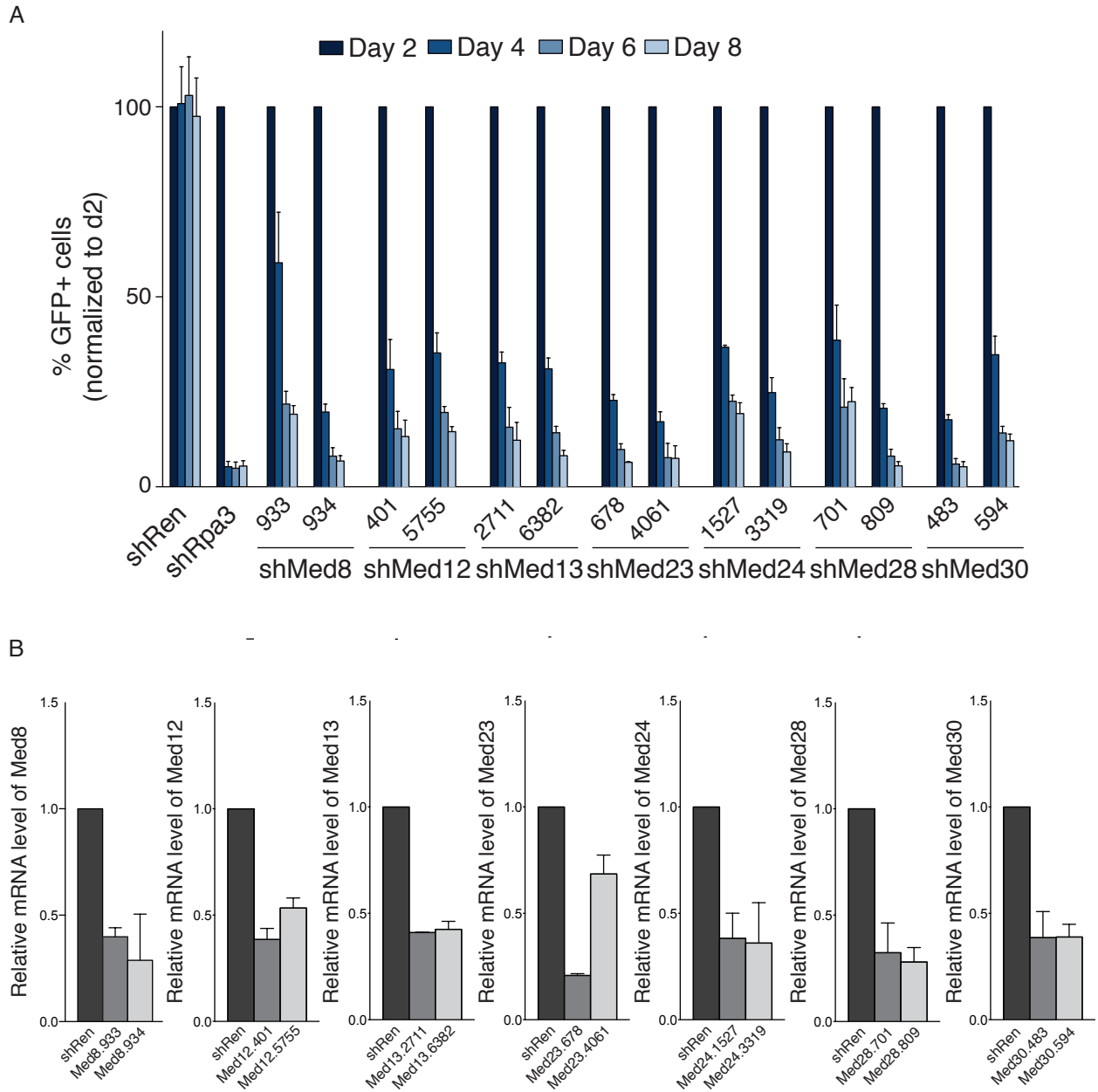
Figure 2-14 Mediator subunit knockdown leads to growth arrest of AML cells
A) Negative-selection experiments using the indicated shRNAs chosen from the screen
in (Figure 2-13). GFP+/shRNA+ percentages were normalized to values taken on day 2
and tracked for 8 days. Data are presented as mean ± SEM and n=3.
B) qRT-PCR analysis to test knockdown efficiency of Mediator subunit shRNAs in RN2
cells. Relative mRNA levels of the indicated Mediator subunits following 48 hr treatment
of RN2 cells with doxycycline to induce expression of the indicated shRNA from the
TRMPV-Neo vector. Values were normalized to Gapdh expression within each sample
and to shRen values across samples. Data are presented as mean ± SEM; n=3.
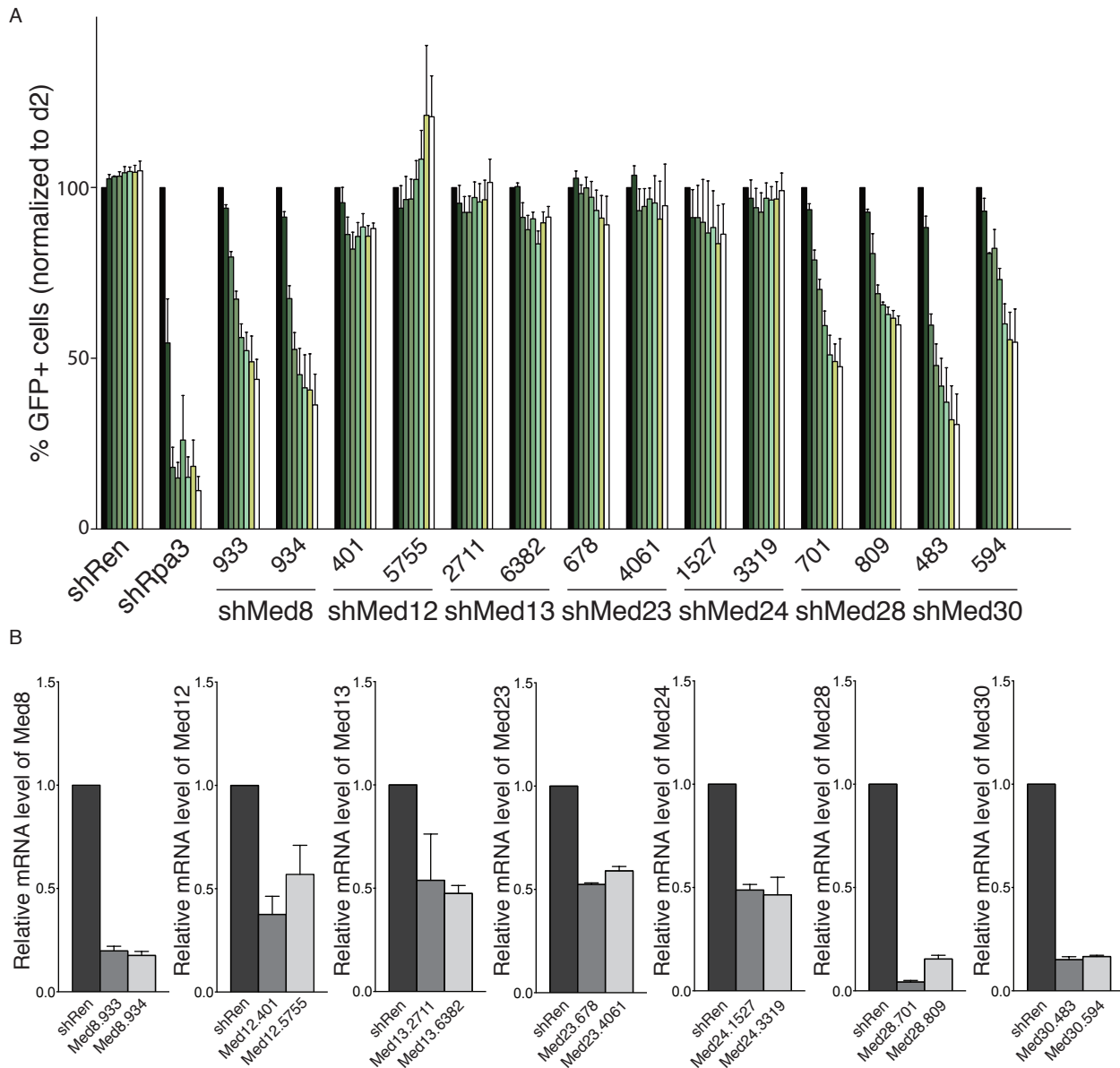
Figure 2-15 Knockdown of some Mediator subunits does not negatively select in a murine fibroblast cell line

A) Negative-selection experiments using the indicated shRNAs chosen from the screen in (Figure 2-13). GFP+/shRNA+ percentages were normalized to values taken on day 2 and tracked for 16 days. Data are presented as mean ± SEM and n=3.

B) qRT-PCR analysis to test knockdown efficiency of Mediator subunit shRNAs in iMEFs. Relative mRNA levels of the indicated Mediator subunits following 48 hr treatment of IMEF cells with doxycycline to induce expression of the indicated shRNA from the TRMPV-Neo vector. Values were normalized to Gapdh expression within each sample and to shRen values across samples. Data are presented as mean ± SEM; n=2.

shRNAs targeting Med15, Med19, and Med28 also induced differentiation, while knockdown of Med25, and Med26 did not. To confirm that differentiation was induced following Mediator subunit knockdown, we imaged May-Grünwald/Giemsa-stained RN2 cells using light microscopy. Consistent with the flow cytometry analysis, knockdown of Med12, Med13, Med23, and Med24, but not of Med8 or Med30, led to morphologic changes, such as cytoplasmic expansion, vacuolation, and multilobular nuclei, consistent with myeloid differentiation as observed after Brd4 inhibition (Figure 2-17). These findings suggest that targeting select Mediator subunits triggers differentiation of AML blasts.

2.2.5 – Mediator subunits are required to sustain expression of Brd4 target genes in AML

We next evaluated the global transcriptional consequences of knocking down Mediator subunits in RN2 cells by performing RNA-seq analysis after 48 hours of dox-induced shRNA expression. In an analogous manner to JQ1 treatment, knockdown of Med12 or of Med23 resulted in reduced mRNA levels of *Myc*, *Mgat5*, and *Cdk6*, but not *Lrrfip1* or *Hoxa9* (Figures 2-18A and 2-18B). To provide an unbiased evaluation of gene signatures altered by Med12 or Med23 knockdown, we performed gene set enrichment analysis (GSEA) to interrogate a database of 10,379 gene sets (Subramanian et al., 2005). Remarkably, several of the most down-regulated gene signatures in this analysis following Med12 or Med23 knockdown corresponded to the known target genes of Myb, Myc, and Brd4 (Figure 2-18C-F). Among the positively enriched gene sets were those related to myeloid cell maturation, consistent with the phenotypic changes observed following Med12 and Med23 knockdown (Figure 2-18C-F). Knockdown of Med8, Med28, and Med30 also led to suppression of Brd4 target genes such as *Myc*, however the global
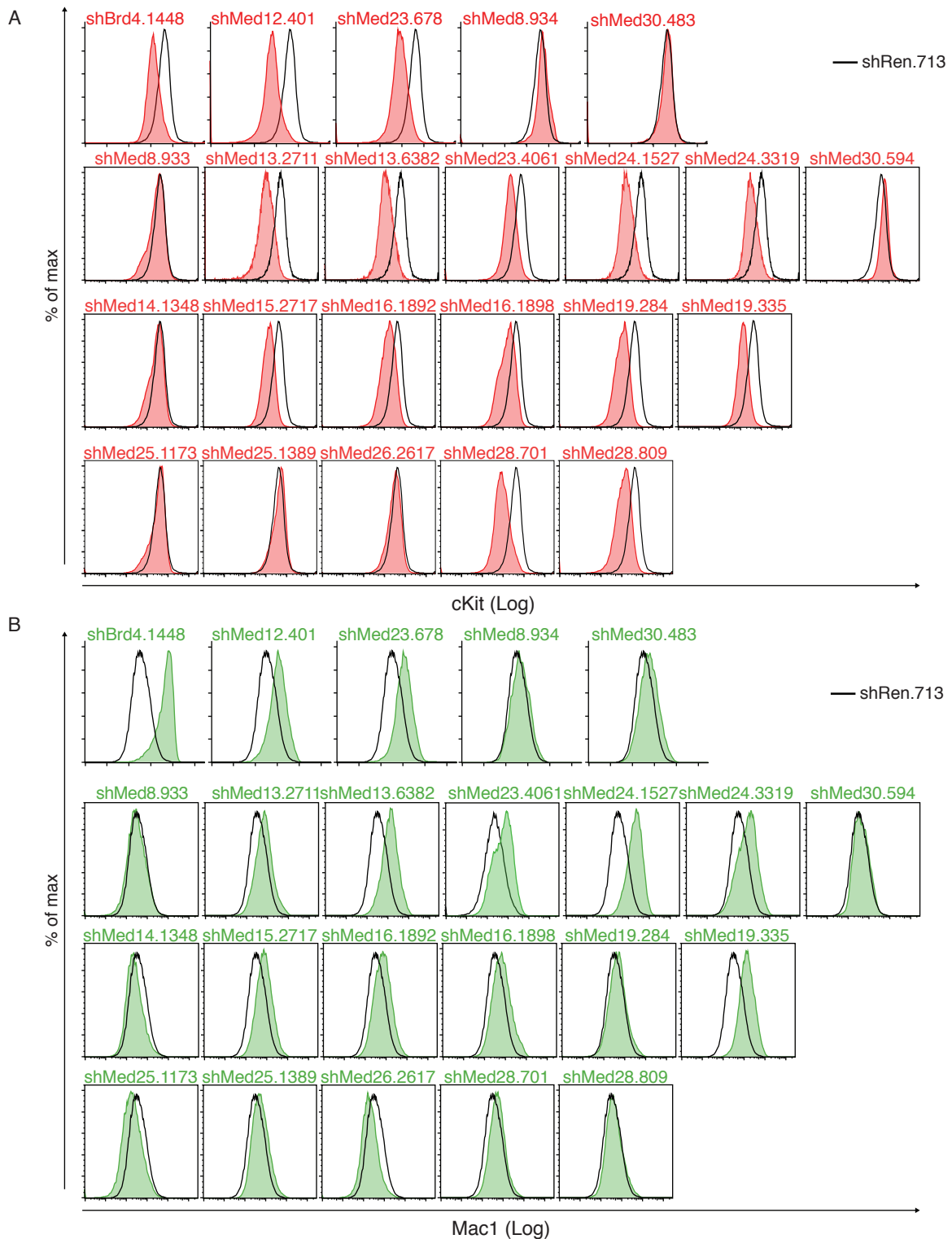
Figure 2-16 Mediator targeting can lead to Myeloid differentiation in AML cells
(A-B) Flow cytometric analysis of cell-surface cKit and Mac1 following 96 h of doxycy-cline-induced expression of indicated shRNAs versus shRen (black trace). shRNAs were expressed using TRMPV-Neo. Gating was performed on GFP+/shRNA+ populations.
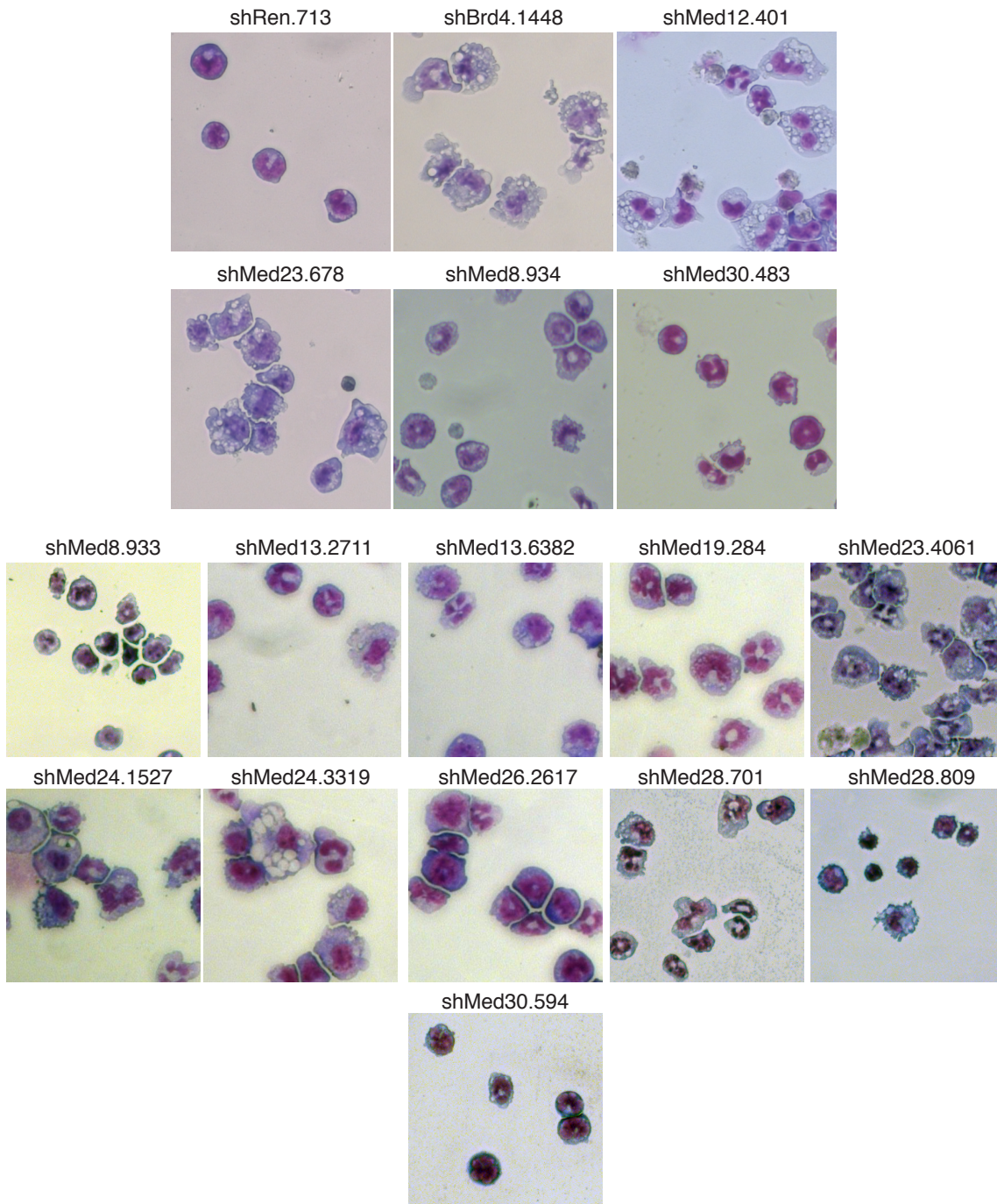
Figure 2-17 Mediator targeting can lead to Myeloid differentiation in AML cells
Light microscopy analysis of May-Grünwald-Giemsa-stained RN2 cells after 96 h of doxycycline-induced expression of the indicated shRNAs. The images were taken with 40X objective.
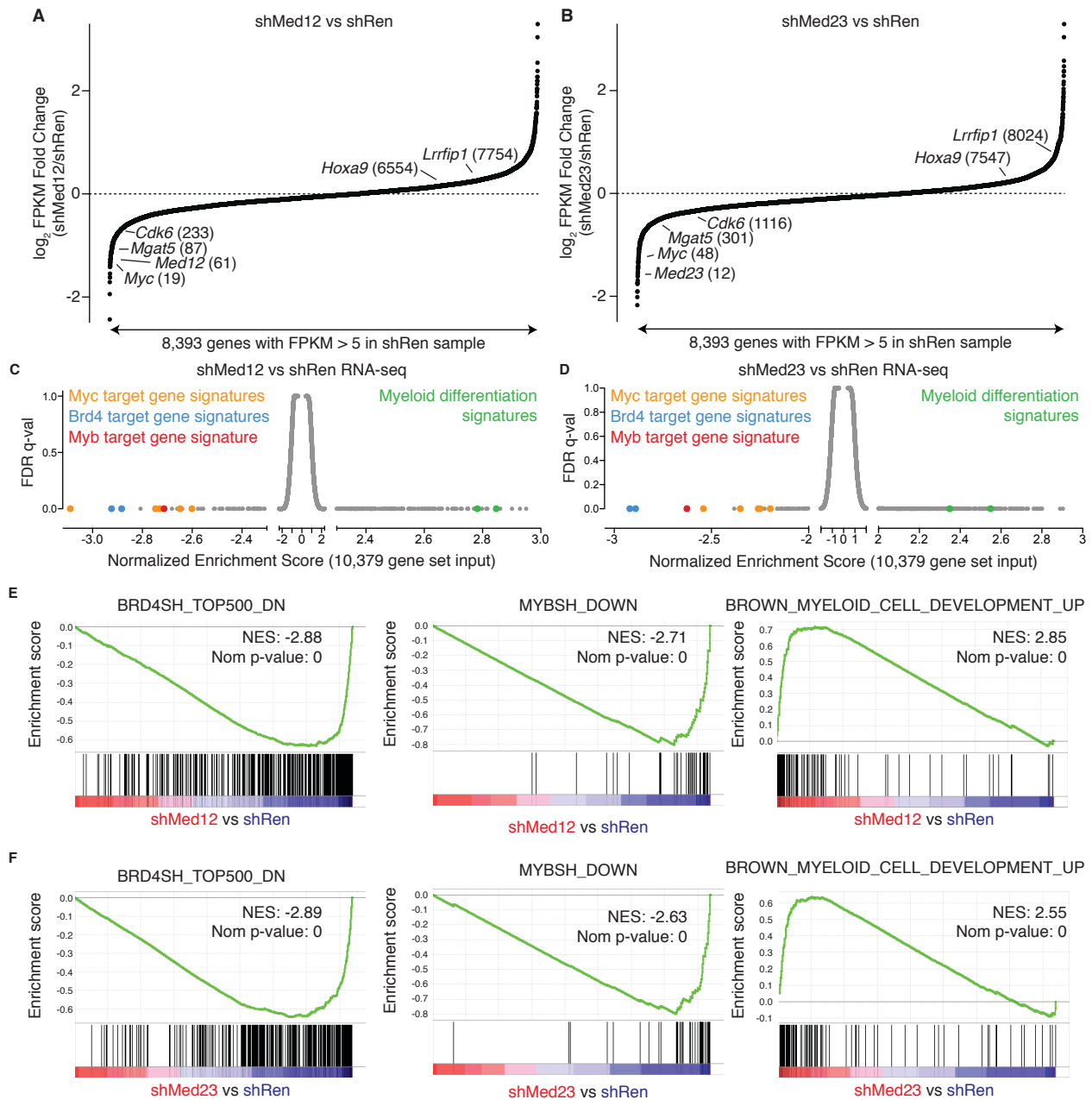
Figure 2-18 Med12 and Med23 are requried to sustain expression of Brd4, Myc, and Myb target genes in AML

A-B) Fold change in FPKM for 8,393 expressed genes in AML (defned by FPKM>5 in shRen sample) following 48h of doxycyline indufcion of two independent shRNAs targeting Med12 or Med23. Fold change values for each gene are the average value of the independent hairpins. The genes are ranked in order of increasing fold change. Nnumbers in parentheses represent the fold change expression rank of the indicated genes.

C-D) Gene Set Enrichment Analysis (GSEA) of Med12 and Med23 RNA-seq using 10,379 gene sets. Signatures are plotted by their Normalized Enrichment Scores and FDR q-values.

E-J) Example GSEA plots from the indicated RNA-seq. Normalized Enrichment Scores (NES) and Nominal p-values (Nom p-value) are provided.

pattern of gene expression following Med8 knockdown was different from what was observed following Med12 or Med23 knockdown (Figure 2-19A-C). GSEA revealed that while Brd4 and Myc signatures were affected by Med8, Med28, and Med30 knockdown, these subunits also perturbed a number of gene signatures, such as metabolic pathways, that are not suppressed by JQ1 treatment or by Med12 or Med23 shRNAs (Figure 2-19D-F and Table 2-1). Though Med8 was most clearly distinct from the pattern of transcriptional change observed after Brd4, Med12, or Med23 inhibition (Figures 2-18A-B, 2-19A-C, 2-20), unsupervised hierarchical clustering analysis of the shMediator RNA-seq datasets placed Med8, Med28, and Med30 in a cluster apart from Med12 and Med23 (Figure 2-21). While it appears that not all Mediator subunits perform identical roles in AML, our findings lend further support for a role of the Mediator complex in supporting Brd4-dependent gene activation.

A recent study in breast cancer has shown that Mediator can facilitate Brd4 chromatin localization in the setting of acquired resistance to BET inhibitors (Shu et al., 2016). We therefore considered whether Mediator plays a reciprocal role in stabilizing Brd4 occupancy in the AML genome. Since Med12 and Med23 knockdown mimicked the phenotypic and transcriptional effects of BRd4 inhibition, we performed Brd4 and Med12 or Med23 ChIP-seq following knockdown of these subunits. This revealed that Med12 and Med23 knockdown resulted in a modest reduction in Med12, Med23, and Brd4 chromatin occupancy at the same *cis* elements at which Med1 is perturbed following BET inhibition (Figure 2-22 and 2-23). This result suggests that an interaction between Brd4 and Mediator can mutually stabilize each other's occupancy at select genomic loci.
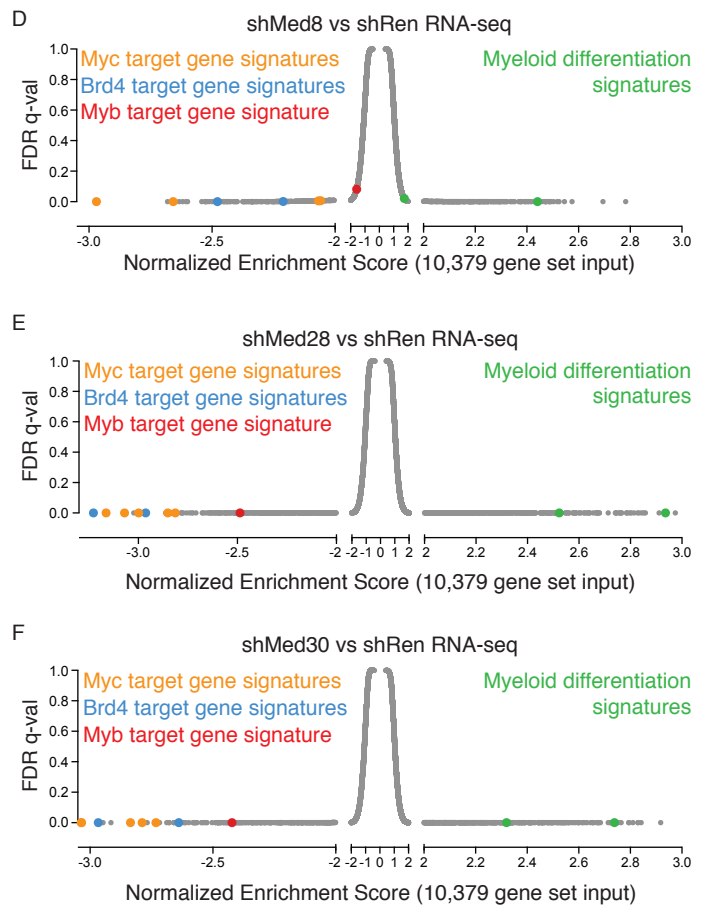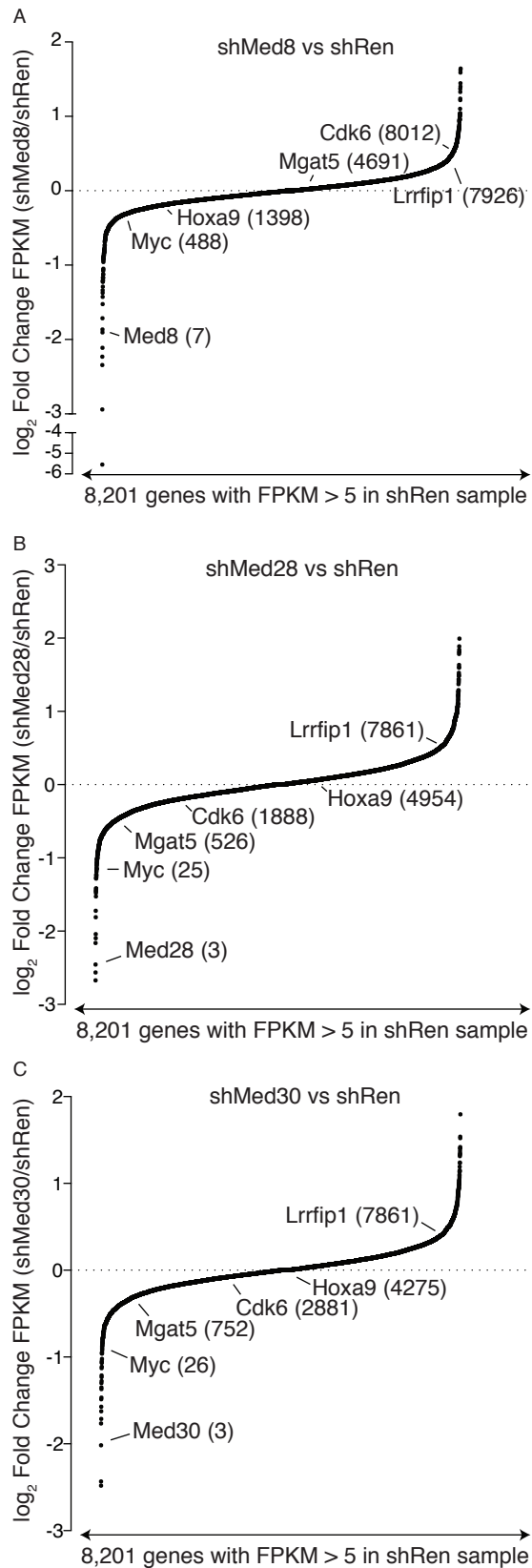
Figure 2-19 Med8, Med28, and Med30 maintain overlapping but distinct genetic pathways as Med12, Med23, and Brd4

A-C) Fold change in FPKM for 8,201 expressed genes in AML (defned by FPKM>5 in shRen sample) following 48h of doxycyline induction of two independent shRNAs targeting Med8, Med28, or Med30. Fold change values for each gene are the average value of the independent hairpins. The genes are ranked in order of increasing fold change. Numbers in parentheses represent the fold change expression rank of the indicated genes.

D-F) Gene Set Enrichment Analysis (GSEA) of Med8, Med28, and Med30 RNA-seq using 10,379 gene sets. Signatures are plotted by their Normalized Enrichment Scores and FDR q-values.

Gene Set	Normalized Enrichment Score					
	shMed12	shMed23	JQ1 6h	shMed8	shMed28	shMed30
BRD4/MYC/Differentiation signatures						
HALLMARK_MYC_TARGETS_V2	-3.09	-2.54	-2.47	-2.66	-3.07	-3.03
BRD4SH_TOP500_DN	-2.88	-2.89	-2.68	-2.21	-2.96	-2.64
MYBSH_DOWN	-2.71	-2.63	-2.35	-1.58	-2.49	-2.42
IVANOVA_HEMATOPOIESIS_EARLY_PROGENITOR	-2.56	-2.23	-2.00	-1.45	-2.28	-2.23
Metabolic processes						
REACTOME_GLUCOSE_METABOLISM	0.78	0.61	0.84	-1.38	-0.87	-0.68
REACTOME_GLYCOLYSIS	0.58	0.92	0.62	-1.45	-1.37	-1.21
REACTOME_TRIGLYCERIDE_BIOSYNTHESIS	1.52	0.75	1.11	-1.77	-1.34	-0.98
REACTOME_CHOLESTEROL_BIOSYNTHESIS	2.03	1.65	1.94	-2.36	-2.03	-1.31
Other Processes						
PLASARI_TGFB1_TARGETS_10HR_UP	1.40	1.58	1.59	-1.57	1.11	-1.16
GROSS_HYPOXIA_VIA_ELK3_DN	1.29	1.66	1.71	-1.81	-1.18	-1.32
SEMENZA_HIF1_TARGETS	1.17	1.63	1.61	-1.42	-0.98	-0.76

Table 2-1 Med8, Med28, and Med30 regulate Brd4 and Myc signatures in addition to other processes in RN2 cells
Normalized enrichment scores of the indicated gene sets, as reported by Gene Set Enrichment Analysis, for RNA-Seq studies following shMed8, shMed12, shMed23, shMed28, shMed30, or 6 h 500 nM JQ1 treatment.
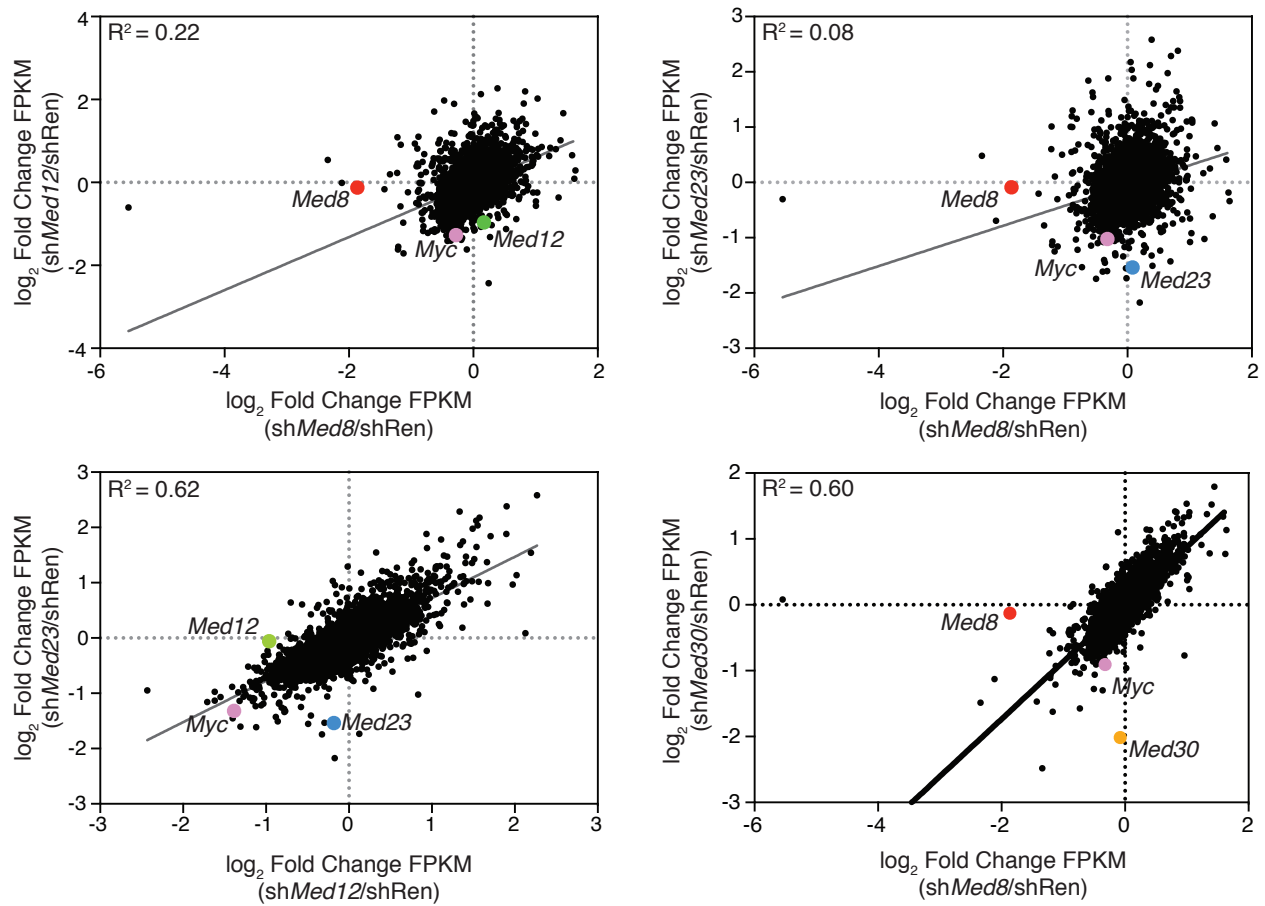
Figure 2-20 shMed8 produces a gene expression change pattern that is largely dissimilar from shMed12 and shMed23
Scatter plots comparing fold change in FPKM values from RNA-Seq data sets of shRen vs. shMed8, shMed12, shMed23, or shMed30. 8,122 genes expressed (FPKM>5) in all shRen samples were used in this analysis
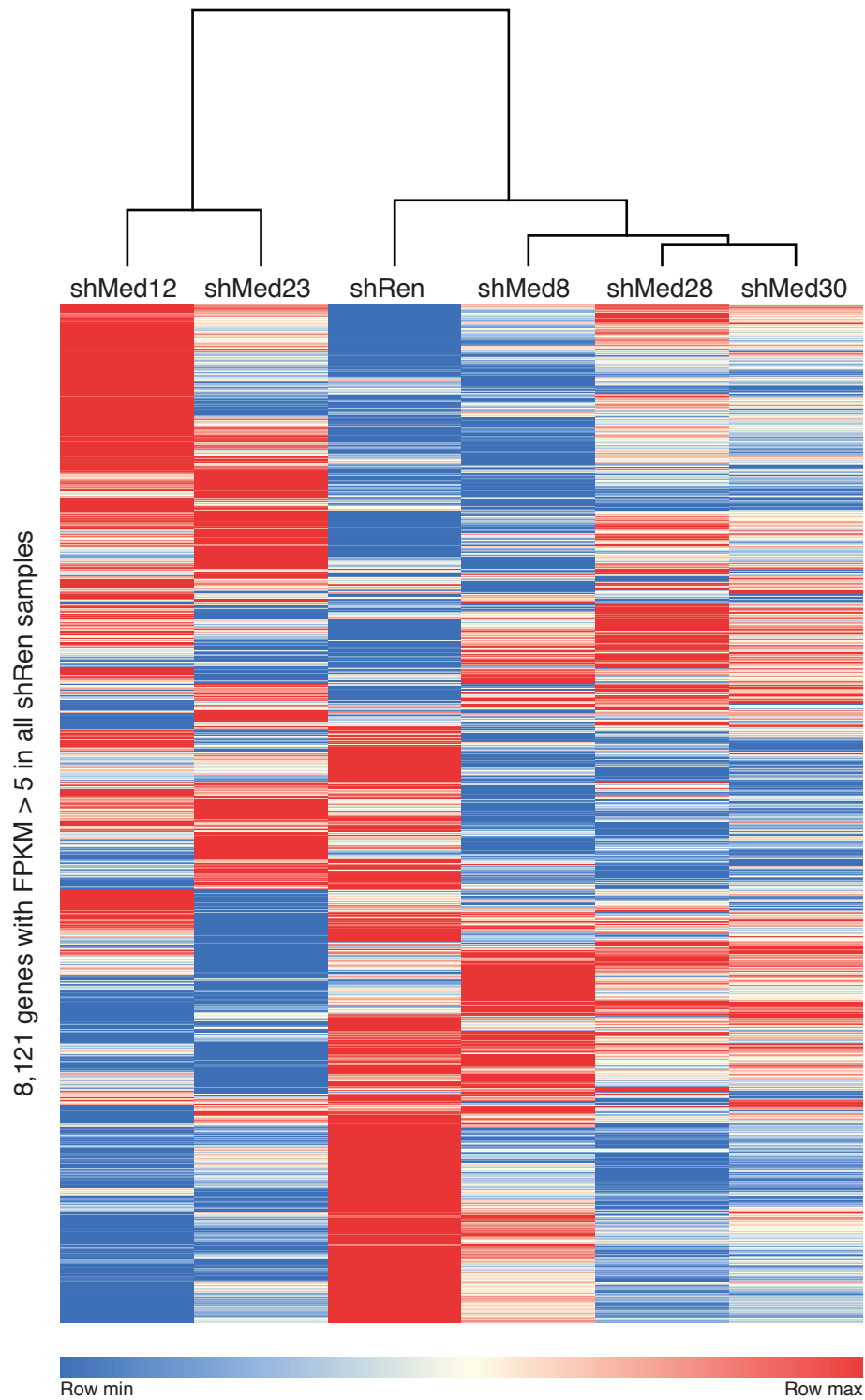
Figure 2-21 shMed8, shMed28, and shMed30 gene expression changes cluster away from shMed12 and shMed23

Average FPKM values in each shMediator RNA-seq data set for 8,121 expressed genes (FPKM > 5 in all four shRen samples) were subjected to unsupervised hierarchical clustering by the GENE-E software.

We next explored the mechanism by which Brd4 and Mediator regulate Pol II activity at their co-regulated target genes. Mediator and Brd4 have each been shown to interact with the kinase P-TEFb, comprised of Cdk9 and Cyclin T, to promote productive Pol II transcription elongation (Donner et al., 2010; Jang et al., 2005; Takahashi et al., 2011; Yang et al., 2005). Using ChIP-qPCR, we found that BET inhibition and Med12 knockdown each led to displacement of Cdk9 and Pol II from the *Myc* super-enhancer and gene body (Figures 2-24 and 2-25). Notably, the loss of Pol II near the TSS was much less severe (3.7-fold for JQ1, 1.3 fold for shMed12) relative to the gene body (15.8-fold for JQ1, 5.4-fold for shMed12). This result is consistent with Brd4 and Mediator supporting release of paused Pol Ii at their co-regulated target genes.

2.3 – Brief Discussion

BRD4 is an essential protein in many myeloid and lymphoid cancers. BRD4 is required for the output of hematopoietic TFs and maintains the expression of important proto-oncogenes (Chapuy et al., 2013; Dawson et al., 2011; Delmore et al., 2011; Roe et al., 2015; Zuber et al., 2011c). BET inhibitors, which result in the displacement of BRD4 from chromatin, are an emerging class of therapy for hematopoietic malignancies. Through an unclear mechanism, JQ1 treatment leads to a loss of transcription of a subset of genes in the genome despite global loss of BRD4 from chromatin (Loven et al., 2013; Zuber et al., 2011c). The findings presented in this study support a model in which Brd4 regulates its downstream target genes by stabilizing the Mediator complex occupancy at specific enhancer and promoter regions of the genome of AML
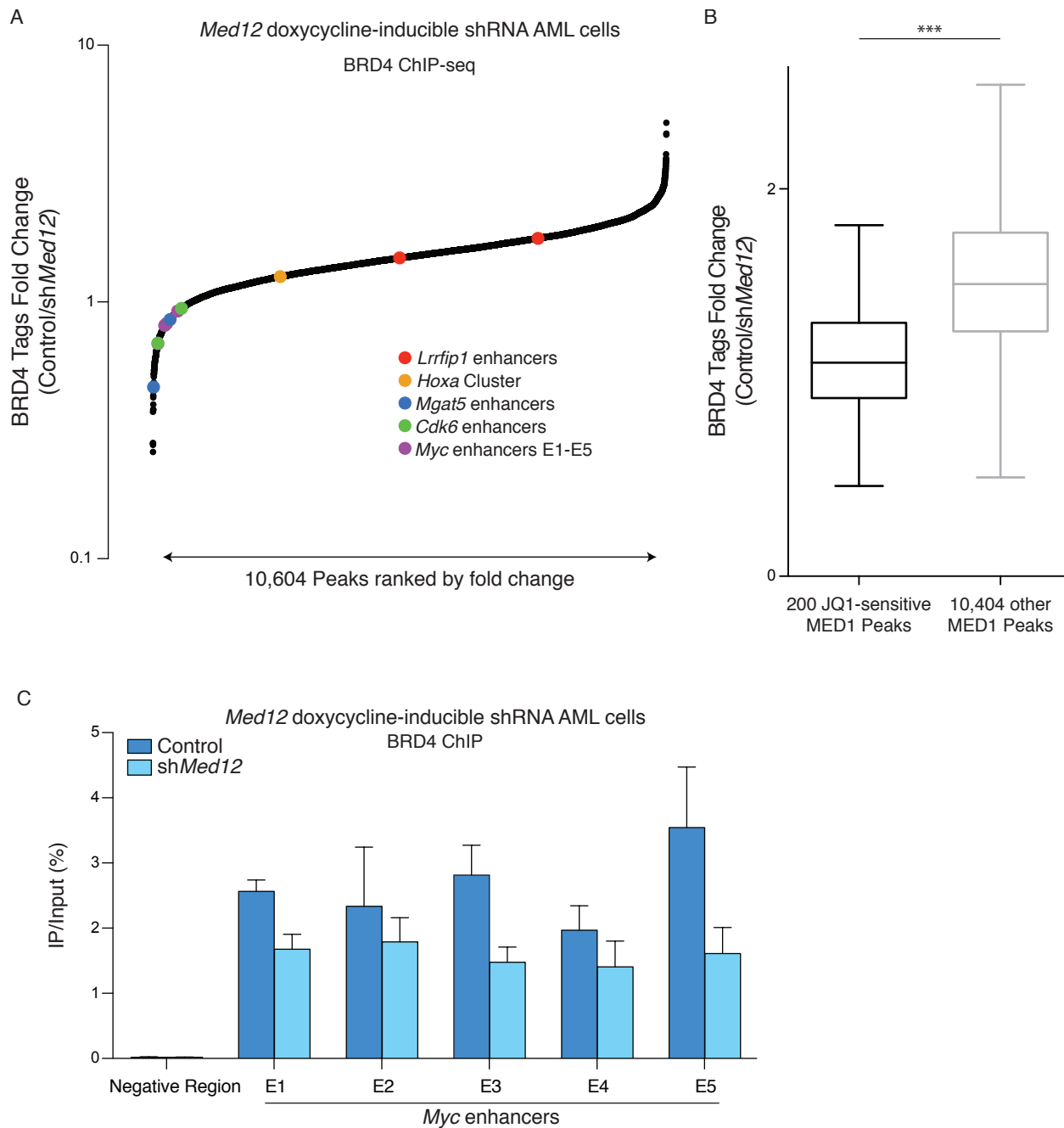
Figure 2-22 shMed12 preferentially reduces Brd4 occupancy at JQ1-sensitive Med1 sites
A) Fold change in occupancy of BRD4 at 10,604 MED1-defined peaks in AML following 48 hr treatment with doxycycline to induce expression of a MED12 shRNA. The peaks are ranked in order of increasing fold change. Colored dots highlight the indicated loci in the genome.
B) Box plot showing fold change of BRD4 occupancy 48 hr treatment with doxycycline to induce a Med12 shRNA at 200 JQ1-sensitive MED1 peaks or at 10,404 remaining peaks in the genome. *** represents a p value < 0.0001, the result of a Mann-Whitney test.
C) ChIP-qPCR analysis of BRD4 at the Myc locus following 48 hr treatment with doxycycline to induce a Med12 shRNA.
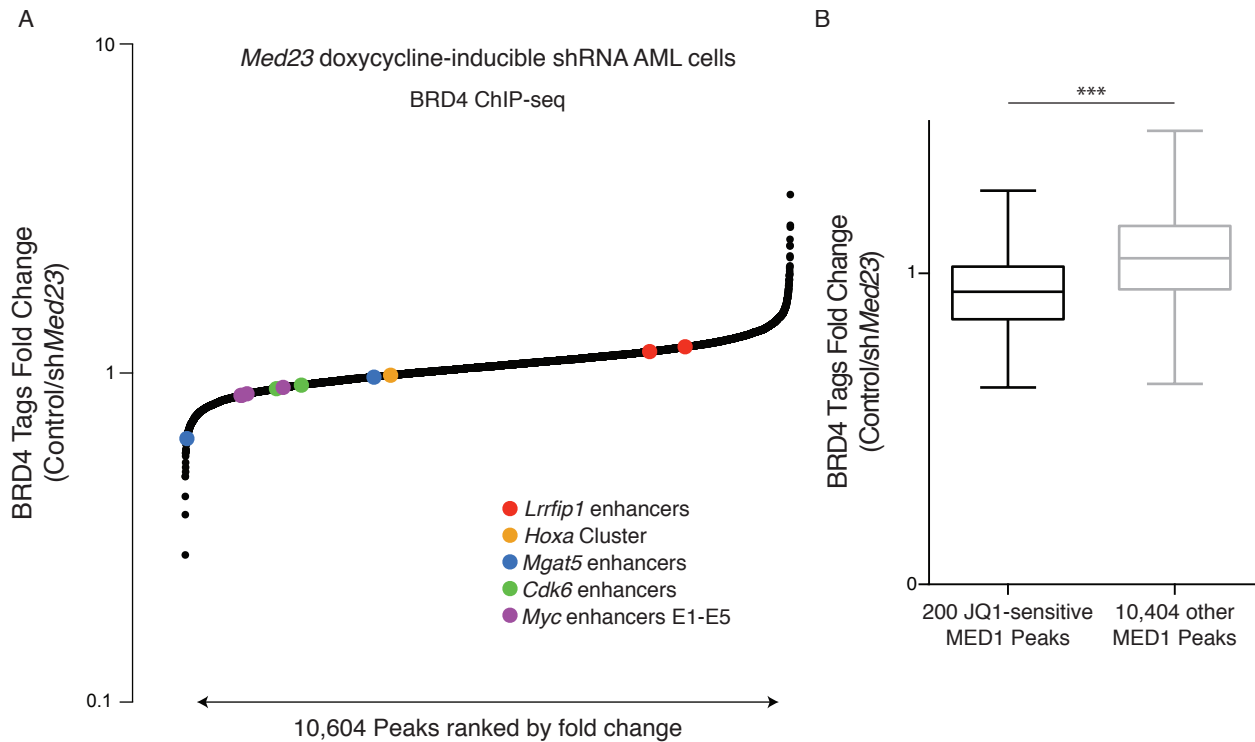
Figure 2-23 shMed23 preferentially reduces Brd4 occupancy at JQ1-sensitive Med1 sites
A) Fold change in occupancy of BRD4 at 10,604 MED1 peaks in AML following 48 hr treatment with doxycycline to induce expression of a MED23 shRNA. The peaks are ranked in order of increasing fold change. Colored dots highlight the indicated loci in the genome.
B) Box plot showing fold change of BRD4 occupancy after 48 hr treatment with doxycycline to induce a Med23 shRNA at 200 JQ1-sensitive MED1 peaks or at 10,404 remaining peaks in the genome. *** represents a p value < 0.0001, the result of a Mann-Whitney test.
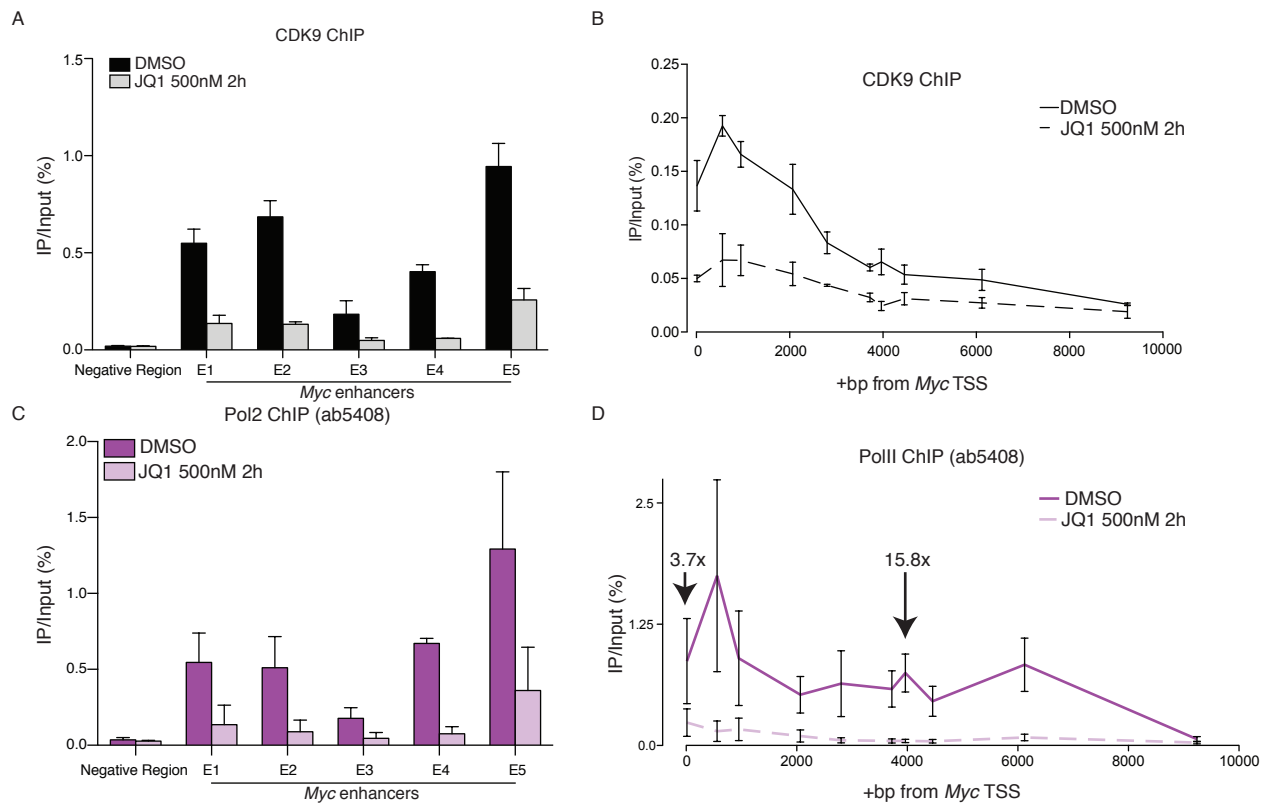
Figure 2-24 JQ1 evicts Cdk9 at the Myc locus and results in a Pol II pause release defect
A) ChIP-qPCR analysis of CDK9 at the Myc enhancer locus following 2 hr treatment with DMSO or with 500 nM JQ1.
B) ChIP-qPCR analysis of CDK9 across the Myc gene body following 2 hr treatment with DMSO or 500 nM JQ1.
C) ChIP-qPCR analysis of PolII at the Myc enhancer locus following 2 hr treatment with DMSO or with 500 nM JQ1.
D) ChIP-qPCR analysis of PolII at the Myc gene body following 2 hr treatment with DMSO or with 500 nM JQ1. Numbers above +14bp and +3965bp data indicate fold change between DMSO and JQ1 ChIPs at these regions.
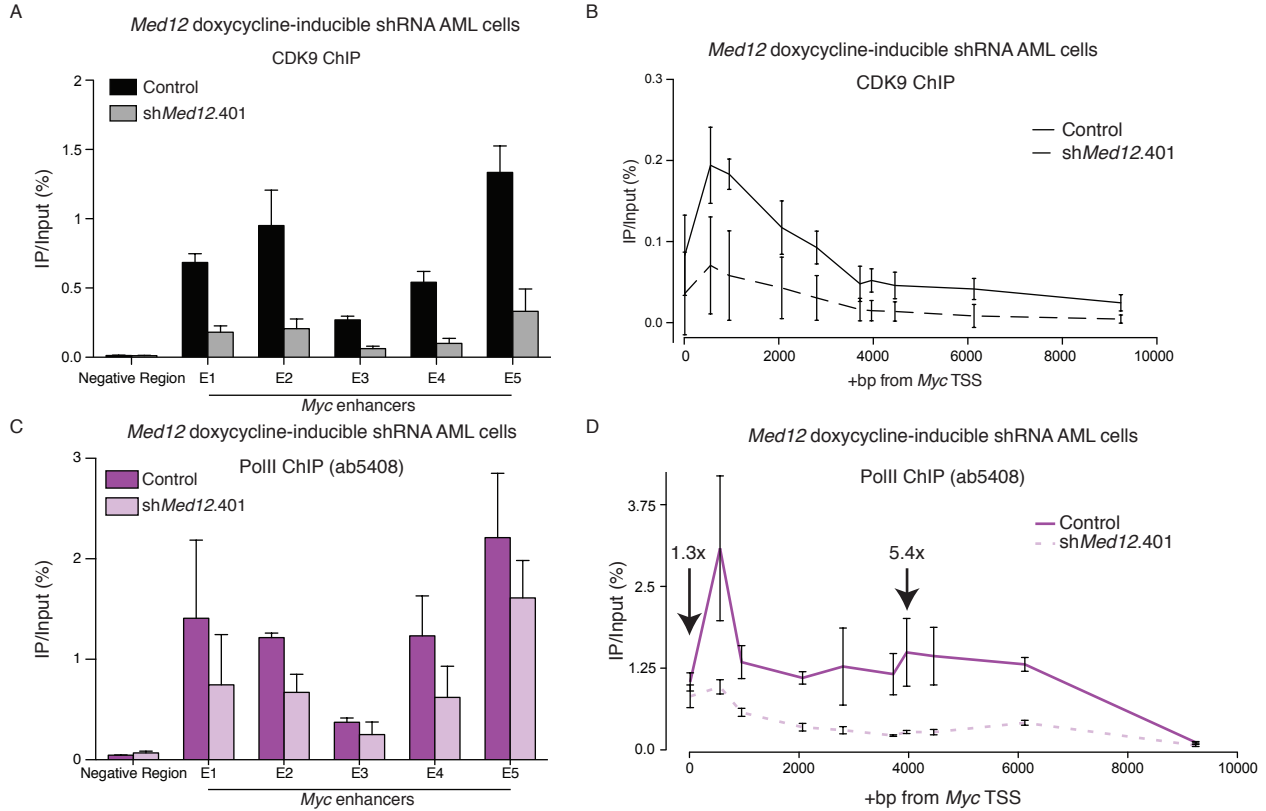
Figure 2-25 JQ1 evicts Cdk9 at the Myc locus and results in a Pol II pause release defect
A) ChIP-qPCR analysis of CDK9 at the Myc enhancer locus following 0- or 48-hour induction of shMed12 with dox.
B) ChIP-qPCR analysis of CDK9 across the Myc gene body following 0- or 48-hour induction of shMed12 with dox.
C) ChIP-qPCR analysis of PolII at the Myc enhancer locus following 0- or 48-hour induction of shMed12 with dox.
D) ChIP-qPCR analysis of PolII across the Myc gene body following 0- or 48-hour induction of shMed12 with dox. Numbers above +14bp and +3965bp data indicate fold change between control and shMed12 ChIPs at these regions.

cells. We have previously shown that Brd4 recruits the short isoform of Nsd3, which acts as a bridge to recruit the Chd8 chromatin remodeler (Shen et al., 2015). In addition, Brd4 is known to recruit the P-TEFb complex to promote transcription elongation of its target genes (Jang et al., 2005; Yang et al., 2005). Notably, Mediator has also been shown to recruit P-TEFb to promote transcription elongation (Donner et al., 2010; Takahashi et al., 2011). Taken together, these observations reinforce a model in which Brd4 acts as a scaffold that recruits several machineries to *cis* elements bound by hyper-acetylated TFs and nucleosomes, and acts cooperatively and reciprocally with Mediator to promote transcription of genes and to sustain the aberrant self-renewal properties of AML cells.

A recent study showed that AML cells are sensitive to chemical inhibition of Cdk8/Cdk19 with Cortistatin A (Pelish et al., 2015). In this study, it was shown that these kinases act in a redundant fashion to restrain super-enhancer activity, thereby antagonizing the activation function of Brd4 (Pelish et al., 2015). Importantly, our shRNA screening results suggest that this repressive function is likely to be confined to the Cdk8/Cdk19 subunits of Mediator, whereas other subunits of Mediator, including the kinase-associated subunit Med12, are involved in supporting Brd4- dependent transcriptional activation. This contrast in roles of Med12/13 and Cdk8/19 is in agreement with prior studies that identified distinct phenotypic and transcriptional consequences after knockdown of kinase module subunits (Gobert et al., 2010; Kuuluvainen et al., 2014).

Mechanistically, our findings suggest that Brd4 and Mediator cooperate to promote recruitment of Cdk9, which is the kinase subunit of P-TEFb, to promote transcriptional elongation of *Myc* and other genes that support leukemia pathogenesis. These findings highlight how various

perturbations of Mediator can destabilize the leukemia cell state through distinct mechanisms.

Our study further provides insights into how JQ1 exerts disproportionate effects cancer-relevant genes while sparing housekeeping gene expression, a property that underlies the therapeutic efficacy of this agent in AML and other malignancies (Shi and Vakoc, 2014). It has previously been proposed that the location of super-enhancers harboring exceptional levels of Brd4 and Mediator provide the molecular basis for the hypersensitivity of specific genes to JQ1-mediated transcriptional suppression (Loven et al., 2013). However, we have shown that less than half of all super-enhancers exhibit JQ1-mediated displacement of the Mediator complex, despite Brd4 being reduced at all super-enhancers by JQ1 (Loven et al., 2013). In other words, the hypersensitivity of Mediator to JQ1-mediated displacement can be uncoupled from the preexisting levels of Mediator occupancy, which is, in turn, reflected in the heterogeneous sensitivity of super-enhancer-linked genes to JQ1-mediated suppression. Importantly, our findings suggest that the degree of Mediator eviction can serve as a more accurate biomarker than the location of super-enhancers in defining the critical *cis* elements that are functionally suppressed by BET inhibition. Measurements of Med1 eviction following JQ1 exposure could be applied more broadly to reveal the critical genes that underlie the therapeutic effects BET inhibition in a variety of cancer and non-cancer contexts.

While Brd4 occupancy genome wide correlates with the occupancy of several hematopoietic TFs (Roe et al., 2015), the sensitivity of Mediator occupancy to JQ1-mediated eviction correlates with *cis* elements harboring higher levels of the TFs C/EBPα, C/EBPβ, and Myb. In addition, our ontology analysis shows that genes associated with JQ1-sensitive Med1 also are enriched for a Myb target gene network. In agreement with a relationship between Myb and Mediator

function, a somatic mutation has been described in T-ALL that produces a Myb binding motif near the *TAL1* gene, which leads to the formation of a Med1-occupied super-enhancer (Mansour et al., 2014). In prior studies, we have also noted that the phenotypic consequences of BET inhibition closely matches the effects of Myb knockdown, which could be accounted for by the biased release of Mediator from *cis* elements with relatively higher levels of Myb recognition motifs (Zuber et al., 2011b; Zuber et al., 2011c). Interestingly, AML cells are known to be more sensitive to Myb knockdown than normal myeloblasts (Zuber et al., 2011b). Since Myb can physically associate with Brd4 (Roe et al., 2015), our results suggest that Myb function might place unique demands on Brd4-Mediator complexes to activate its target genes, which in turn contributes to the hypersensitivity of AML cells to BET inhibition.

In keeping with a model whereby Brd4 recruits Mediator to select *cis*-elements, individual knockdown of each Mediator subunit revealed a number of subunits that recapitulate the phenotype in AML that occurs following Brd4 inhibition. While the Mediator complex has a general role in cellular transcription, and complete loss of the complex might be expected to be incompatible with cell survival, it is well-established that knockdown or knock out of individual subunits can result in viable cells with precise transcriptional deficits (Bai et al., 2011; Carrera et al., 2008; Ito et al., 2000; Stevens et al., 2002; Wang et al., 2009). Several subunits in the head module of Mediator, such as Med8, Med28, and Med30, exhibited more general roles in maintaining cellular proliferation, as evidenced by their requirement in MEF cells. Gene expression profiling supports a broader role for these subunits in transcriptional regulation because, in addition to Brd4 signatures, knockdown of Med8, Med28, and Med30 perturbed a number of other pathways that are largely unaffected by JQ1 treatment. Interestingly, Med17

was previously identified as a key structural linchpin in the Mediator complex (Holstege et al., 1998; Lariviere et al., 2012; Soutourina et al., 2011). Furthermore, Med14 has been demonstrated to serve as a scaffold in reconstituted Mediator complexes and was absolutely required for complex integrity and activation function (Cevher et al., 2014; Plaschka et al., 2015). However, Med17 and Med14 did not score in our shRNA screen. While this may be a result of poor knockdown by all 6 shRNAs targeting each of these subunits, an alternative explanation is that the previously identified roles of Med17 and Med14 are contextual. Med17's essentiality may be restricted to yeast and may also be replaced by some of the metazoan-specific head subunits, such as Med30. Med14's role may be relevant in biochemically reconstituted, artificial complexes on chromatin templates. In live cells, especially AML cells, this subunit appears to have a more limited function.

Some subunits in the tail and kinase modules appeared to be selectively required in AML cells. In particular, we found that Med12 and Med23 induce proliferation arrest and differentiation of AML blasts by regulating the same genes as Brd4 in AML. Notably, Med12 appears in a number of Brd4 IP-MS experiments, and Med23 knockout has been shown to abrogate the association of Brd4 with Mediator complexes (Dawson et al., 2011; Jang et al., 2005; Wang et al., 2013).

Most Mediator occupied regions in the genome are relatively unaffected by JQ1. Since JQ1 does not appear to perturb occupancy of TFs in RN2 cells, this fits with a classical model of direct TF recruitment of Mediator (Malik and Roeder, 2010; Roe et al., 2015). However, our data reveal that Brd4 recruits Mediator to a subset of elements in the AML genome and that Mediator

coactivates transcription of associated Brd4-target genes. This alternative, Brd4-dependent mode of Mediator recruitment to the genome provides a potential means by which JQ1 can achieve a selective impact on gene expression and a therapeutic window for treatment of hematologic cancers.

Table 2-2 – List of mm9 genes associated with peak categories of interest

Genes associated with 200 most JQ1-sensitive Med1 peaks	Genes associated with super-enhancers that overlap with JQ1-sensitive Med1 peaks	Genes associated with super-enhancers that do not overlap with sensitive Med1 peaks	Genes associated with 200 most JQ1-sensitive Brd4 peaks
Ccr2	Ccr2	Bex6	Myc
Myc	Myc	Cd33	F630043A04Rik
Cldn15	Clec12a	Gm14005	Ptpn1
Il12a	Tifab	Spata13	Ift57
Clec12a	Cd93	Tbc1d2b	Erg
Cd28	Erg	Glipr1	Limd1
Hao1	Elk3	Mtus1	Tifab
Tifab	A630001G21Rik	Rin3	Plcg2
Cd93	Parp8	Egln3	Myb
Erg	Igf1r	Zfp608	Med10
Gfi1	Hpgd	Pstpip1	Parp8
Ccnd1	Dgkg	Gsr	Gata2
Kit	Lmo2	Ptpre	Igf1r
BC005764	Cdk6	Adrbk1	Fcho2
Elk3	Susd1	Baz2b	Mrpl33
Serpinb1a	Atp8b4	Fam107b	Cd93
Ift57	Tmed3	Sae1	Sclt1
A630001G21Rik	Zcchc4	Ino80d	Cdk6
Parp8	Gda	Hp1bp3	Cd69
Igf1r	Myb	Tle3	Eif3d
Hpgd	Zeb2	Ldlrap1	Irf2bp2
Dgkg	Ifngr1	Slc16a6	Clec12a
Lmo2	Sgms2	Adssl1	Etv6
Cdk6	Etv6	Sp2	Lta4h
Susd1	Ctsg	Itm2b	Ccr2
B4galnt1	Plac8	Pecr	Tmed3
Atp8b4	Ramp1	Vrk1	Gse1
Tmed3	Mapkapk3	Cep164	Zcchc4
Zcchc4	Rev1	Zfp326	Arid1b
Itga1	Cd69	Ptma	Bcl2
Gda	Haao	B3gnt2	Hpgd
Myb	Dirc2	N4bp1	Mgat5
Zeb2	Bcl2	Fam133b	Rpn1
Ifngr1	Dars	1600014c10rik	Max
Sgms2	Rreb1	Runx2	Zfp217
Plscr3	Prtn3	Rps8	Mis12
Etv6	Ptpre	Plec	Zdhhc17
Plac8	Gata2	Gpi1	Mpdu1
Mthfd1l	B3gnt8	Dhx8	Elk3
Ramp1	Lta4h	Tnrc18	Chsy1
Mapkapk3	Irf2bp2	Itgb2	Dars
Agps	Klhl5	Hmga1	Irf1
Rev1	Mrpl33	Ncf4	Slc31a1
Bckdha	Ly6e	Cnot10	Dgkg
Mgat5	Poc1a	Rhog	Rad18

Oaf	Cd47	Cox4i1	Foxp1
Cd69	Chsy1	Atg12	Cyba
Hk3	Slpi	Rbm38	Tbc1d7
Mcpt8	Dstn	Kif2c	Sipa1l1
Sipa1l1	Tubd1	Fam20c	Cd28
Haao	Os9	Nedd1	Atp8b4
Dirc2	Nfe2l2	Myh9	Ramp1
Bcl2		Hist1h2ab	Anp32e
Elane		Hist1h2an	Eef2k
Foxp1		Mms19	Sec14l1
Dars		Clpx	Cd47
Rreb1		Cyth4	Il12a
Rpn1		Hist1h2ak	Oaf
Kif13a		Ppm1e	Lrp8
Slc35b1		Cotl1	Nup210
Ptpre		Vps33a	Dnajc14
Gata2		Gnai2	Spry2
Lta4h		Vps26a	Itga1
Irf2bp2		Psen2	Lmo2
Klhl5		Ptpn1	Pmaip1
Max		Zbtb7a	Serpinb1a
Mrpl33		Hoxa9	Slc35b1
Ly6c2		Actb	Poc1a
Ly6e		Lrrfip1	Echs1
Poc1a		Pxn	Pcdh7
Cd47		Sec14l1	Pdcd4
Chsy1		Wdr26	Slc3a2
Creb1		Celf1	Bckdha
Slpi		Nfkbia	Hao1
Alas1		Chd2	Ptpre
Plcl2		Hist1h4i	Ptpn2
Ppif		Dusp6	Atg12
Dstn		Plekho2	Rpl39
Arid1b		Midn	Tubd1
Fam133b		Il17ra	Atp6v0a1
Rpl28		Bzrap1	Dirc2
F630043A04Rik		Brd2	Cldn15
Psmd11		Zfp36	Arl8b
Tubd1		Junb	Jarid2
Tfip11		Malat1	Nipbl
Ube2f		Neat1	Ywhag
Fbxo21		Hist1h1c	Ncor2
Zdhhc17			Lrmp
Med10			Arhgap26
Ptpn1			Rbm17
Atf5			Nop14
Malt1			Mpeg1
Papss1			Tex2
			3010026O09Rik
			Creb1
			BC029214
			Haao
			Slpi

			Klhl5
			Mtus1
			Casz1
			Polr1b
			Ifngr1
			Ctss
			Zeb2
			B4galnt1
			Agps

Chapter III – Tethering Mediator to rescue RN2 cells from JQ1

3.1 – Brief Introduction

The results of Chapter II suggest that Mediator complexes might be recruited to some *cis* elements on chromatin by Brd4. Moreover, JQ1-induced release of Mediator from these select elements appears to be a key event in transcriptional suppression following treatment with this inhibitor. However, the possibility still remains that this is simply a reliable collateral effect of JQ1 treatment, and that loss of Mediator from chromatin after BET inhibition is unrelated to the transcriptional output of these molecules. While our functional studies of Mediator in AML, which demonstrated that some Mediator subunits regulate an overlapping gene expression program with Brd4 through an overlapping set of *cis* elements, indicates that this likelihood is minimal, we nevertheless wanted to address this possibility.

To formally test whether Mediator eviction is indeed a contributor to JQ1-mediated transcriptional perturbation, we aimed to force Mediator onto chromatin independently of Brd4. We hypothesized that artificially tethering Mediator to some of these *cis* elements would

uncouple Mediator from its dependence on Brd4 for recruitment to chromatin and would thus "rescue" the associated genes from transcriptional suppression by JQ1. In this model, enforcing Mediator occupancy at sites from which the complex is normally released by JQ1 treatment would undermine the suppressive effects of JQ1 on transcription of associated genes.

Artificial recruitment of Mediator has been accomplished in yeast systems before. Fusing the yeast LexA protein's DNA-binding domain (DBD) to yeast Med20 or Med15 subunits was capable of activating transcription off of a reporter gene (Keaveney and Struhl, 1998). This was the first indication that recruiting a single subunit of Mediator could form transcriptionally active complexes. A later study of the rules governing Swi/Snf and SAGA complex recruitment to chromatin also utilized Mediator tethering (Lemieux and Gaudreau, 2004). By fusing the Gal4 DBD to yeast Gal11 (Med15), the authors were able to show that Swi/Snf and SAGA recruitment to DNA could bypass the TF if Mediator was present (Lemieux and Gaudreau, 2004). Gal4-Med2 fusions were also shown to drive metabolic target gene transcription in yeast (Sakurai and Fukasawa, 2003). Finally, a more recent study, also in yeast, examined transcription at the ADH2 locus under glucose-mediated suppression conditions (Young et al., 2008). In the presence of glucose, the TF Adr1 is prevented from binding to DNA, but in the absence of glucose Adr1 binds in a Swi/Snf-dependent manner (Young et al., 2008). The DBD of Adr1 alone could not bind to the ADH2 locus even in permissive conditions, suggesting that coactivators were required to stabilize Adr1 binding to DNA (Young et al., 2008). Indeed, Adr1-Med15 and –Med3 permitted stable binding of the Adr1-DBD at this locus and coactivated transcription of Adh2. Moreover, the authors found that Adr1-Med15 could integrate into Mediator complexes and rescue a Med15 deletion, suggesting functionality of this

Mediator-TF fusion (Young et al., 2008). Thus, there exists precedent for successful Mediator tethering in live cells.

The recent advent of targeted genome editing using CRISPR/Cas9 systems has led to a cottage industry surrounding the Cas9 protein itself because the ability to direct a protein to precise sequences in a genome can be used in innumerable ways. An important advance was the development of a version of Cas9 with no nuclease activity. This version has two point mutations (D10A and H840A) in its RuvC nuclease and HNH nuclease domains, respectively, that eliminate the ability of Cas9 to cleave DNA (Sander and Joung, 2014). However, the RNA-guided sequence specificity of this catalytically dead Cas9 (dCas9) remains intact, and it can be fused directly to different effector domains in order to confer new activities to the CRISPR/Cas9 system (Sander and Joung, 2014). As an example, dCas9 fusions with TF activations domains has been used to selectively enhance transcription of target genes in the genome, and dCas9-fused to the demethylase domain of LSD1 can be targeted to *cis* elements to selectively repress transcription at their associated genes (Sander and Joung, 2014).

Our goal in these studies was to direct Mediator complexes to select loci in the genome to determine whether uncoupling Mediator recruitment from Brd4 localization could rescue AML cells from the effects of BET inhibition. To this end, fusing Mediator subunits to dCas9 could represent an ideal way to target specific genes for Mediator recruitment in AML genomes. Furthermore, generation of these fusion constructs could open new avenues by which Mediator function in live cells can be studied, thus providing deep insights into the *in vivo* function of this coactivator complex as it relates to eukaryotic transcription.

3.2 - Results

3.2.1 – Generation of dCas9–Mediator fusions

To create dCas9-Mediator fusions, we constructed a vector that contains a 3x-Flag-tagged dCas9 followed by a 10 amino acid linker (Figure 3-1). The MSCV-Puro retroviral vector was chosen as a backbone to allow for puromycin selection of cells containing the dCas9-Mediator fusion construct. There are multiple nuclear localization signals on this vector to ensure proper compartmentalization of dCas9-Mediator fusions, and the 3x-Flag tag allows us to test whether the fusion protein, as would be expected of a dCas9-based chimera, can be localized to specific genomic sites by a guide RNA.

The spatial orientation of Mediator complexes could be crucial to correct complex assembly. If a head subunit is attached to dCas9, for example, and the head is responsible for making contacts with Pol II, then Pol II would necessarily need to be close to the dCas9 molecule. On the other hand, if a tail subunit is tethered to dCas9, then the head (and Pol II) may be less constrained in their locations. In order to cover as many orientations as possible, we began by cloning four subunits into dCas9-fusion constructs, one each from the head (Med10) and middle (Med21) modules of Mediator, and two from the tail module (Med15 and Med25). By anti-Flag immunoblotting, we first noted that dCas9-Med15 did not express in AML cells (Figure 3-2A). This lack of expression may have been due to infrequent expression in a pooled population of AML cells. To address this, we derived single-cell clones from the pool of dCas9-Med15-
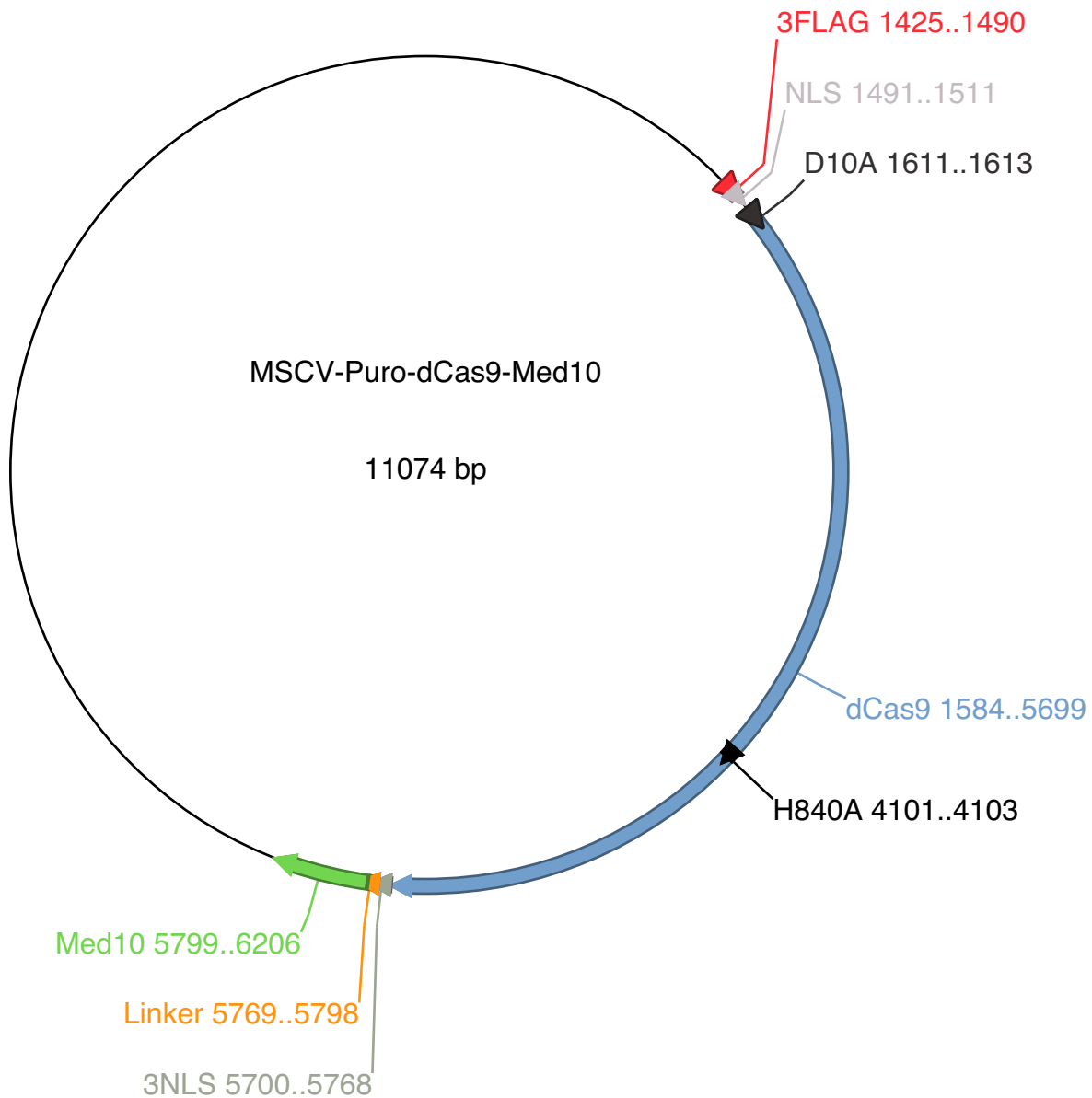
Figure 3-1 Vector designed to tether Mediator subunits to chromatin
This retroviral expression plasmid, based off of the MSCV vector, includes a 3x Flag tag, nuclear localization signals, two point mutants that render the Cas9 catalytically inactive, a (gly-gly-gly-gly-ser)x2 linker, and the Mediator subunit. Depicted here is a dCas9-fusion to Med10.
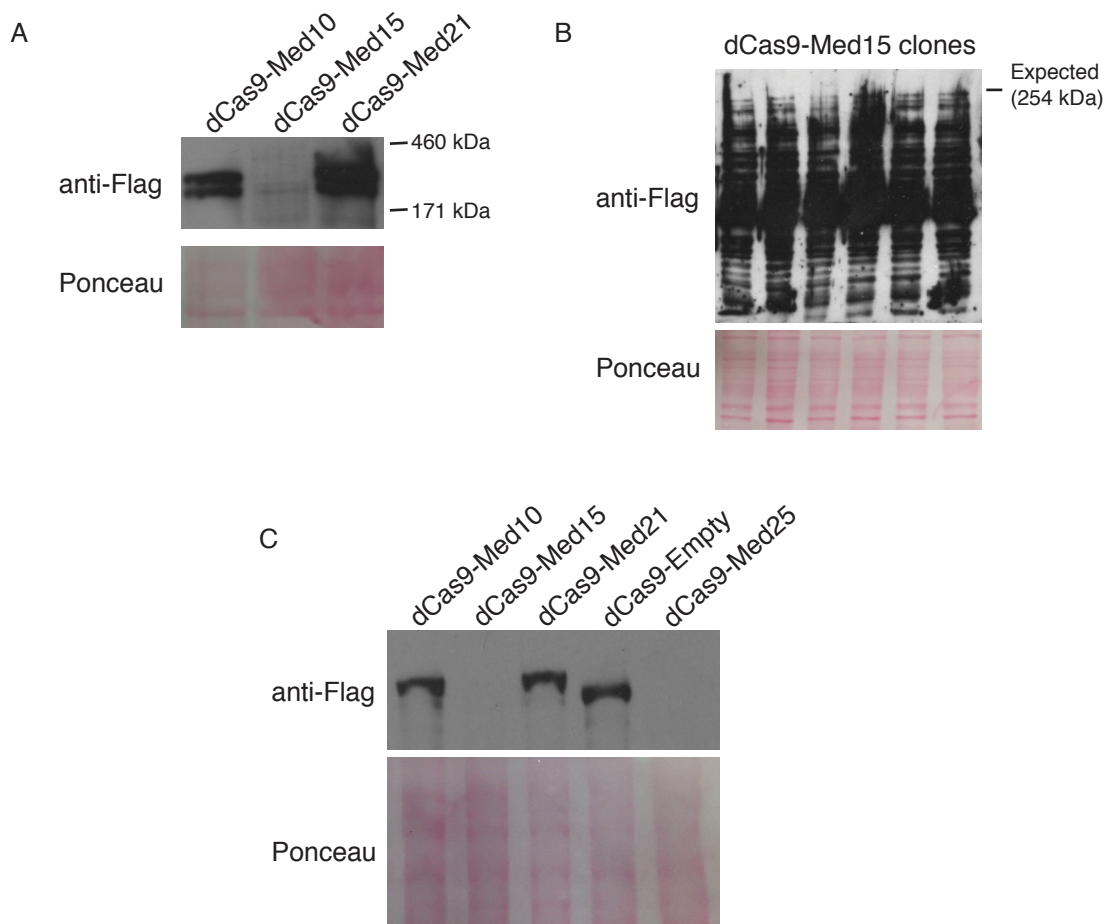
Figure 3-2 dCas9-Mediator fusion expression is limited by size constraints
A) Western blot analysis using whole cell extracts of RN2 cells expressing the indicated constructs. Blot used anti-Flag antibodies directed at dCas9 fused to Med10, Med15 or Med21. The expected size of dCas9 is 168 kDa. Expected Mediator subunit sizes are as follows: Med10 (15.7 kDa), Med15 (86.6 kDa), Med21 (15.6 kDa)
B) Western blot analysis of single-cell RN2 clones of dCas9-Med15 to determine if any express dCas9-Med15 fusions.
C) Western blot analysis of RN2 cells expressing the indicated dCas9-Mediator subunit fusions. The expected size of Med25 is 78.2 kDa

infected, puromycin-selected AML cells. Of 5 clones tested, none expressed any detectable dCas9-Med15, even with long exposure of the film (Figure 3-2B). We thus postulated that this inability to express Med15 as a dCas9-fusion might be due to its large size, an explanation that would also fit with our observed inability to express a subunit of similar size, Med25 (Figure 3-2C).

Because the smaller subunits Med10 and Med21 were successfully expressed in AML cells, we next cloned the Mediator subunits whose predicted molecular weights were below 80kDa, reasoning that these had the best chance of being successfully expressed via a retroviral vector in AML cells. We successfully cloned 11 small Mediator subunits as dCas9 fusions and transduced them into AML cells. Of these subunits, Med4, Med6, Med7, Med9, Med10, Med11, Med27, Med28, Med29, and Med30 are classified as head or middle subunits. In order to be able to include a subunit from the tail, which tend to be too large for this purpose, we cloned the Von Willebrand Factor Type A domain (VWA) of Med25. This 230 amino acid sequence from the amino-terminal end of Med25 has been shown to interact with other Mediator complex subunits and has been used to purify whole, intact Mediator complexes from cell extracts (Sela et al., 2013). Thus, we reasoned that this would be a good candidate fragment from a tail subunit that might still recruit Mediator complexes in our system. With the exception of dCas9-Med17, which was not tested, these subunits all expressed well as determined by Flag western blotting (Figure 3-3), supporting our hypothesis that their large size may have precluded expression of Med15 and Med25 dCas9-fusion constructs.
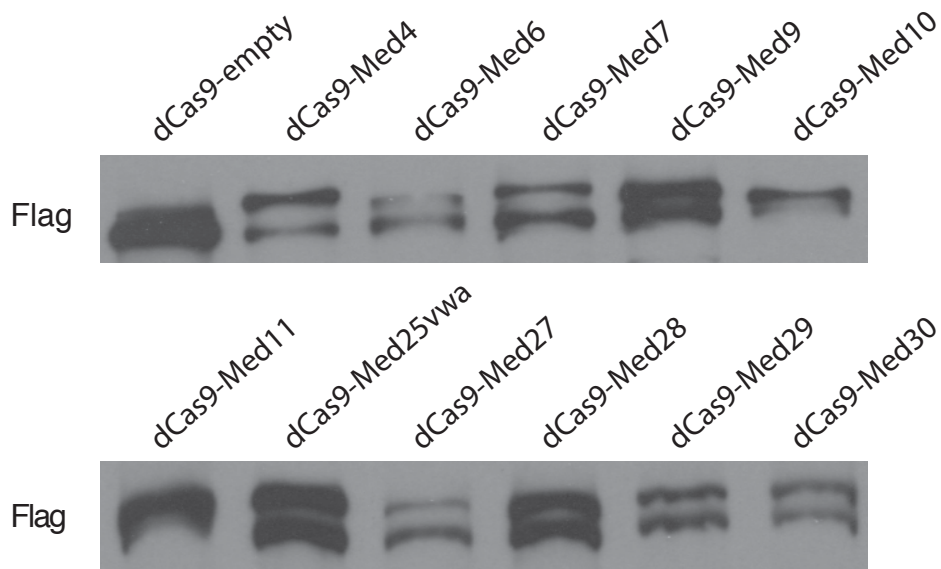
Figure 3-3 Expression of dCas9-Mediator fusion constructs in RN2 cells
Western blot analysis of RN2 cells infected with the indicated dCas9 constructs. Expected sizes are as follows: dCas9 alone (168 kDa), Med4 (29.8 kDa), Med6 (28.4 kDa), Med7 (27.2 kDa), Med9 (15.7 kDa), Med10 (15.7 kDa), Med11 (13.1 kDa), Med25vwa (24.8 kDa), Med27 (35.3 kDA), Med28 (19.5 kDa), Med29 (21.0 kDA), Med30 (20.4 kDa).

3.2.2 – Tethering dCas9–Mediator fusions to the genome

The goal of this line of experimentation was to direct formation of Mediator complexes at precise loci in the AML genome. To test the feasibility of this aim, we introduced guides targeting a region of the genome that we had previously identified as harboring no Mediator occupancy in AML cells (e.g., Figure 2-3, "negative region"). We chose this as the test site because of the simplicity of identifying whether *de novo* Mediator complex formation occurs at this region; at a more biologically relevant site, such as a *Myc* enhancer or promoter, the presence of wild-type Mediator complexes would confound our interpretation of whether complexes were formed around dCas9 fusions.

After introduction of the "negative region" guide, we assessed the proper localization of dCas9 fusions by Flag-ChIP. We noted that all dCas9 fusions, including dCas9 alone, exhibited strong ChIP signal at the target locus but not at other regions tested, including the *Myc* Enhancer element 1 (ME1) (Figure 3-4). This indicated that dCas9's recognition of guide RNAs and its ability to bind complementary DNA was not perturbed by its fusion to Mediator subunit proteins.

We next asked if dCas9-Mediator fusions could recruit or assemble Mediator complexes. We performed ChIP-qPCR analysis of Med1 occupancy at the dCas9 landing pad ("negative") region, and at ME1 as a positive control. As mentioned above and as shown in Figure 2-3 and Figure 2-5, Med1 does not normally show any signal at this region in RN2 cells, so any signal detected here would likely be due to the presence of the dCas9-Mediator fusion proteins. In none of the constructs tested was any Med1 detected at the negative region, despite strong
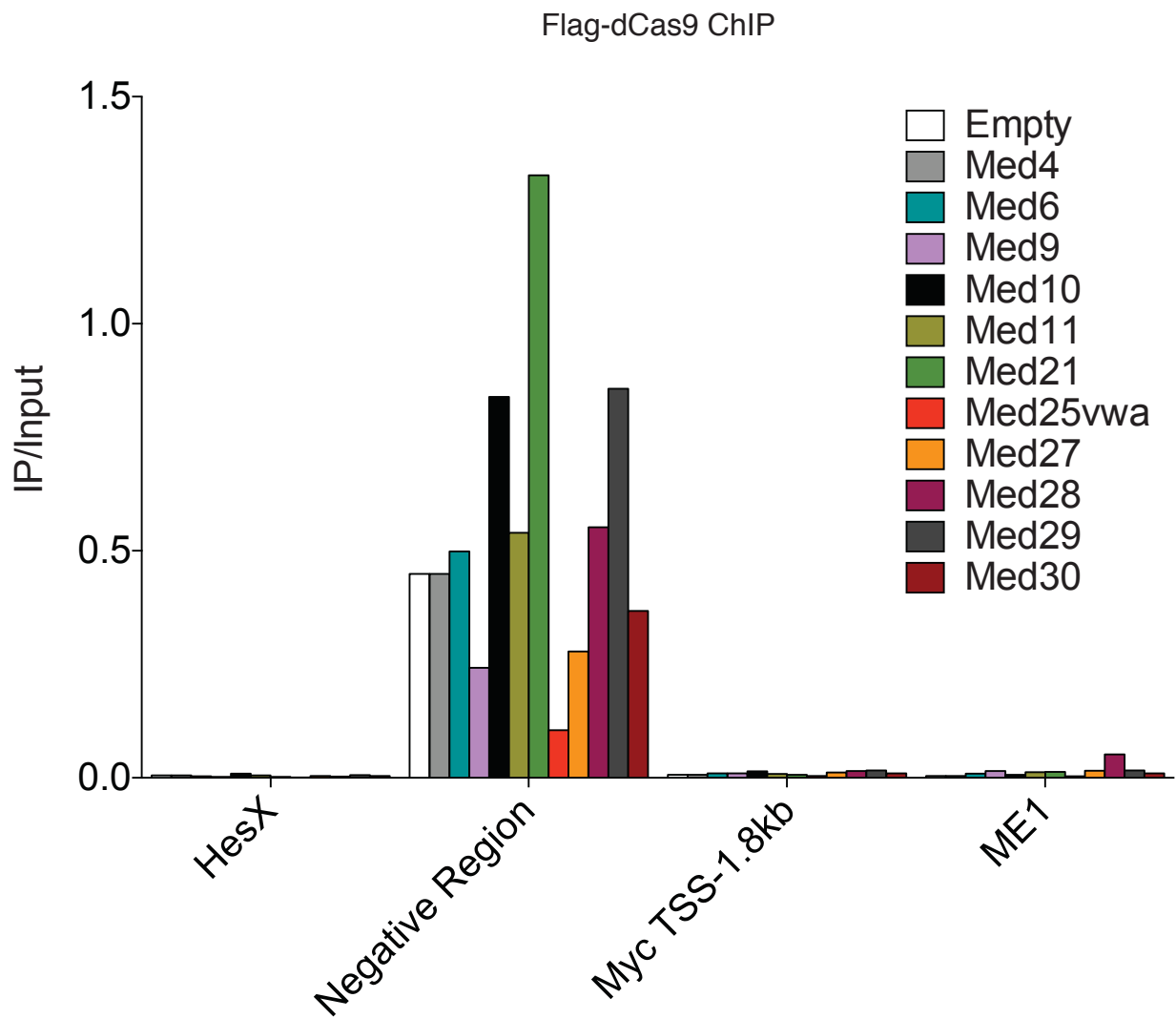
Figure 3-4 Flag ChIP-qPCR results of tethering of dCas9-Mediator fusions
RN2 cells expressing a guide RNA directed to the "Negative Region" were infected with
the indicated dCas9-Mediator fusion constructs and selected with puromycin. After at
least 5 days on puromycin, cells were crosslinked and ChIP-qPCR analysis was
performed with a Flag antibody to determine whether functional dCas9 direction to a
specific chromatin locus was achieved with each construct.

localization of Med1 at the *Myc* enhancer (Figure 3-5). This indicates that dCas9-Mediator fusions are incapable of redirecting Mediator complex formation in AML cells. It was interesting to note that none of the dCas9 fusions could be detected at the ME1 element either, despite strong Med1 signal there. This result suggests that dCas9-Mediator fusions could not serve as a beacon for other Mediator subunits, and that normal Mediator complexes, which form in abundance at ME1, did not incorporate dCas9-Mediator fusion proteins.

3.3 – Brief Discussion

While we successfully expressed dCas9-Mediator fusion proteins in AML and directed them to a chromatin locus, these fusions were unable to redirect assembly of Mediator complexes in the cell. A number of explanations for this are possible. For example, the chromatin landscape has an unclear role in Mediator complex recruitment and assembly. The classical model of TF recruitment of Mediator is unable to uncouple the effects of TFs on histone acetyltransferase recruitment and histone acetylation from the mere presence of a TF serving to recruit Mediator. Furthermore, artificial recruitments of Mediator, which notably have thus far all been performed in the yeast system, used genes, real or constructed, as landing pads for *de novo* Mediator complexes. It is conceivable that the chromatin structure at such elements is more facilitative for Mediator recruitment. Future work on this strategy should attempt targeting to different loci, including promoter and enhancer elements that are capable of hosting Mediator complexes. This may necessitate the use of JQ1 to remove pre-existing Mediator complexes from the chosen locus.
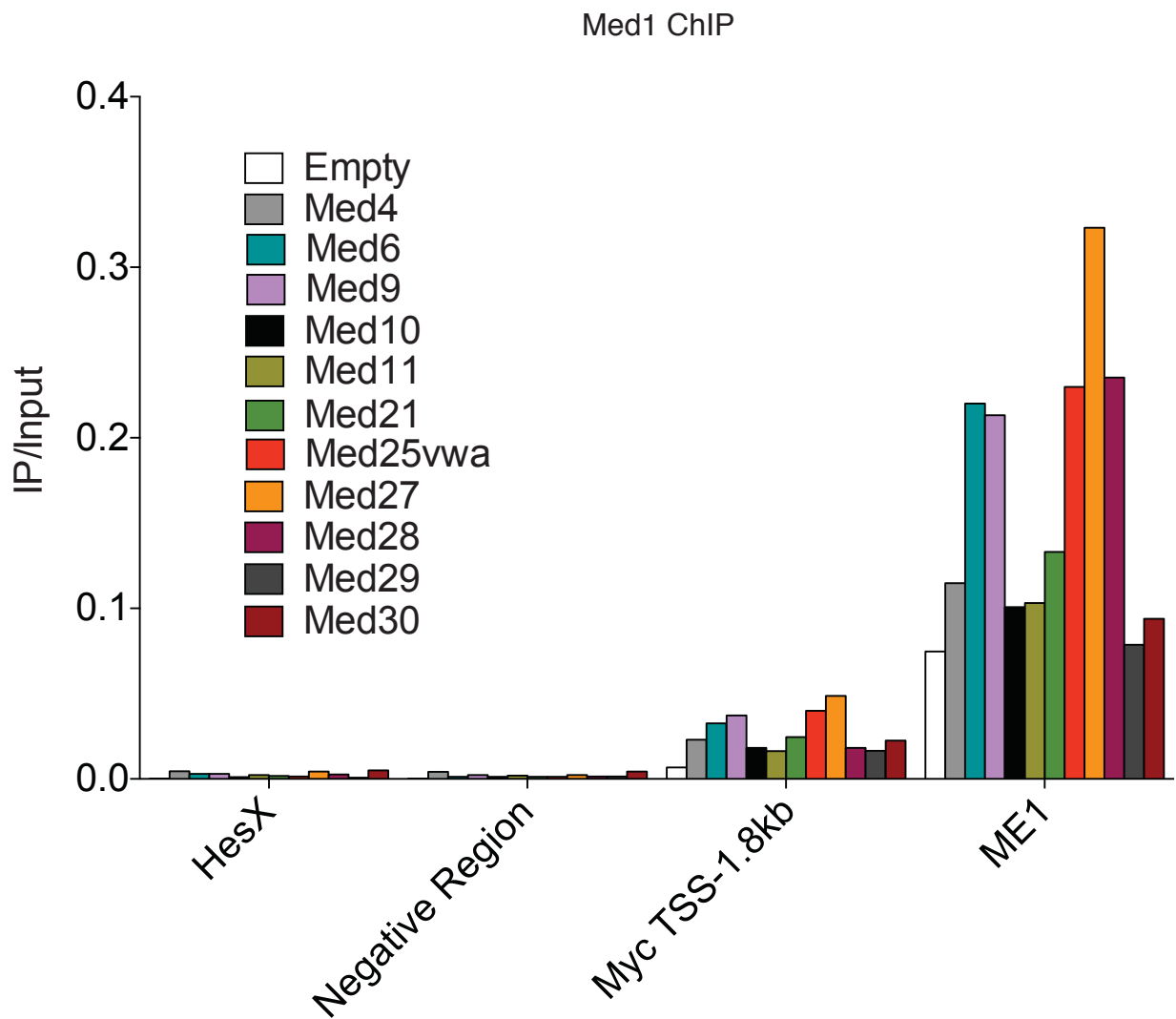
Figure 3-5 Med1 ChIP-qPCR results of tethering of dCas9-Mediator fusions
RN2 cells expressing a guide RNA directed to the "Negative Region" were infected with the indicated dCas9-Mediator fusion constructs and selected with puromycin. After at least 5 days on puromycin, cells were crosslinked and ChIP-qPCR analysis was performed with a Med1 antibody to determine whether Mediator complexes formed at the Negative Region.

Another possibility is that dCas9 simply represents too large a "tag" for Mediator complex formation, perhaps by sterically interfering with the assembly process. Furthermore, it is now well appreciated that different Mediator-cofactor interactions can dramatically reshape the complex conformation. Thus, dCas9-fusions may be incompatible with a stable Mediator assembly. A (G-G-G-G-S)x2 linker was used here to connect dCas9 to Mediator subunits, but it may be that a different linker sequence could have yielded better results.

The potent nuclear localization signals on the dCas9-fusion constructs may also have hindered Mediator complex formation. It is at this point unclear whether Mediator complexes form in the cytoplasm and are imported into the nucleus together or whether they assemble on chromatin. This could be addressed by removing the nuclear localization signals to see if this results in complex formation. In this scenario, free-floating dCas9-Mediator fusions would form Mediator complexes in the cytoplasm, and the addition of the guide RNA would direct these pre-formed complexes to the prescribed chromatin locus in the genome. Another test without guide RNAs present could be a Flag-immunoprecipitation followed by Mediator subunit western blotting to determine whether the dCas9-fusion proteins can ever be incorporated into Mediator complexes independent of chromatin localization.

An alternative strategy to dCas9 tethering is based on the yeast experiments and would utilize a TF DBD-fusion strategy to recruit and assemble Mediator complexes. This strategy would have several advantages, perhaps none more significant than the utilization of a smaller anchor than the large dCas9 protein, permitting the use of larger (and typically TF-binding) tail subunits. Furthermore, TF DBDs will naturally occupy more than one chromatin locus, allowing for a

greater likelihood of true phenotypic rescue of AML from JQ1 treatment rather than a mere gene-specific rescue. Our studies in Chapter II would appear to nominate the DBD of Myb as preferentially enriched at JQ1-sensitive Med1 loci. Thus the Myb DBD is a strong candidate that could be used as an anchor by which Mediator complexes could be tethered to these regions.

Finally, Mediator was first discovered as a limiting reagent in cellular transcription. Thus, simply adding a single subunit to a locus on chromatin may prove futile because all other Mediator subunits may be fully allocated to other sites in the genome. One option would be to knock down the existing, wild-type Mediator subunit that is being used as bait (i.e. shMed10 for dCas9-Med10 fusion cells) in an attempt to force Mediator to incorporate fused Med10 into its complexes. Another option would be to dissociate Mediator from chromatin. It is presently unknown whether BET inhibition, which can evict some Mediator complexes from the genome, do so by breaking apart complexes or by lifting intact Mediator off of chromatin. If the former is the case, then this would allow newly released Mediator subunits to form around a sgRNA-anchored dCas9-Mediator fusion.

Chapter IV - Targeting Mediator Kinases in AML

4.1 – Brief Introduction

The results described in Chapter II provide strong rationale to develop a means to target Mediator for therapeutic purposes in AML. While BET inhibitors are showing promise in early Phase I trials, clinical response has been noted in only 5 out of 28 evaluated patients (Dombret et al., 2014). A number of practical factors could contribute to this level of clinical performance, including the testing of BET inhibitors only in advanced disease and after failure of all other chemotherapies. The ability to orthogonally target the Brd4 pathway by direct inhibition of Mediator subunits is nonetheless compelling.

Design of small molecule inhibitors of protein function has for a variety of practical reasons largely focused on easily tractable enzymatic domains, however the only enzymatic activity contained in the Mediator complex resides the kinase domains of either Cdk8 or Cdk19 (Allen and Taatjes, 2015). Conveniently, this kinase function has been demonstrated to be relevant to transformation and cancer progression (Dale et al., 2015; Firestein et al., 2008). Accordingly a

number of chemical probes have been developed to inhibit Mediator kinase activity (Cee et al., 2009; Dale et al., 2015; Porter et al., 2012; Poss et al., 2013).

Cortistatin A, a chemical isolated from sea squirts, has been demonstrated to be a potent inhibitor of Cdk8 and Cdk19, as well as an inhibitor of the ROCK kinases (Cee et al., 2009). Recently, this molecule was shown to inhibit the growth of AML cells by de-repressing the transcriptional activity of super-enhancer associated genes, fitting with the early, "repressive" concept surrounding the kinase module (Pelish et al., 2015). Interestingly, however, Cortistatin A did not inhibit the growth of HCT116, a colon cancer cell line shown to overexpress Cdk8, to be sensitive to Cdk8 knockdown by shRNAs, and to specifically require a functional kinase domain of Cdk8, raising questions about its mechanism of action (Firestein et al., 2008; Pelish et al., 2015).

Another inhibitor, CCT251545 was discovered in a cell-based screen for WNT pathway inhibitors (Mallinger et al., 2015). Through a competition-based mass spectrometry approach, the targets of this inhibitor were identified as Cdk8 and Cdk19 (Dale et al., 2015). Structures of the inhibitor crystallized with Cdk8 and Cyclin C revealed a type I binding mode (i.e., binding selectively to the active, DMG-in conformation of the kinase), which may explain why this inhibitor, unlike Cortistatin A, showed growth inhibition phenotypes in Cdk8- and β-catenin-dependent cancer cell lines and xenograft models (Dale et al., 2015). It remains to be seen whether this molecule can reproduce the super-enhancer derepression and anti-leukemia effects of Cortistatin A.

Finally, Senexin A was identified in a cell-based screen of molecules that suppressed p21-dependent transcription (Porter et al., 2012). A KinomeScan revealed that the Senexin molecule selectively inhibited Cdk8 and Cdk19 activity (Porter et al., 2012). Optimization of this compound led to the development of Senexin B, a probe that displays improved potency in cellular assays and has been used in combination with chemotherapy to prevent metastasis in a spleen-to-liver colon cancer metastasis model (Porter et al., 2015).

In our shRNA screen performed in MLL-AF9/Nras[G12D] murine leukemia cells, the kinase subunits Cdk8 and Cdk19 did not reach the three-fold threshold we used to call hits. However, Cortistatin A was recently found to have therapeutic impact in AML by inhibiting Cdk8 and Cdk19, thereby further activating transcription at super-enhancer associated genes. We hypothesized that there may be a redundant function of Cdk8 and Cdk19 in AML cells so that individual knockdown of one or the other kinase would not elicit a phenotype. Thus, we sought to determine whether targeting the Mediator kinases could be a viable therapeutic strategy in AML.

4.2 - Results

4.2.1 – Cdk8 and Cdk19 are functionally redundant in AML cells

We first confirmed the results of our Mediator screen (Chapter II) that shRNA-based targeting of Cdk8 and Cdk19 failed to elicit severe proliferation arrest of RN2 cells. Using the same

shRNAs from the screen, we confirmed that individually, these kinases are not dependencies in RN2 cells (Figure 4-1A). This lack of a phenotype occurred despite potent knockdown with some of these shRNAs, suggesting that individual on-target knockdown of Mediator kinases cannot inhibit AML cell growth (Figure 4-1B).

One potential caveat with RNAi for kinases is that the knockdown is seldom complete, and residual kinase activity could be sufficient to mask any potential growth-inhibitory phenotype (Weiss et al., 2007). Indeed, RT-qPCR results showed that, while potent knockdown of both Cdk8 and Cdk19 was being achieved, residual transcript was still being expressed. Thus, to obtain complete functional knockout of these subunits, we utilized a domain-focused approach (Shi et al., 2015) to CRISPR/Cas9 target the kinase domains of Cdk8 alone, of Cdk19 alone, or of both Mediator kinases simultaneously. Individually, guides targeting the kinase domains of Cdk8 or Cdk19 did not affect proliferation of AML cells, consistent with the phenotypes obtained by knocking down these proteins (Figure 4-2, top). In contrast, guides targeting Cdk7, the TFIIH kinase important for Pol II serine 5 phosphorylation and promoter clearance, were negatively selected in AML cells (Adelman and Lis, 2012) (Figure 4-2, bottom).

We then tested the hypothesis that individual targeting of Cdk8 and Cdk19 cannot produce a growth inhibitory phenotype in RN2 cells because the kinases are functionally redundant. To test this, We cloned Cdk8 shRNAs into a vector in which the GFP gene has been replaced with the mCherry gene (LMN-Cherry), allowing for two-color, dual knockdown of Cdk8 and Cdk19. We found that simultaneous shRNA knockdown of both Cdk8 and Cdk19 did indeed lead to a mild negative selection in RN2 cells over 12 days in culture (Figure 4-3A). Similarly,
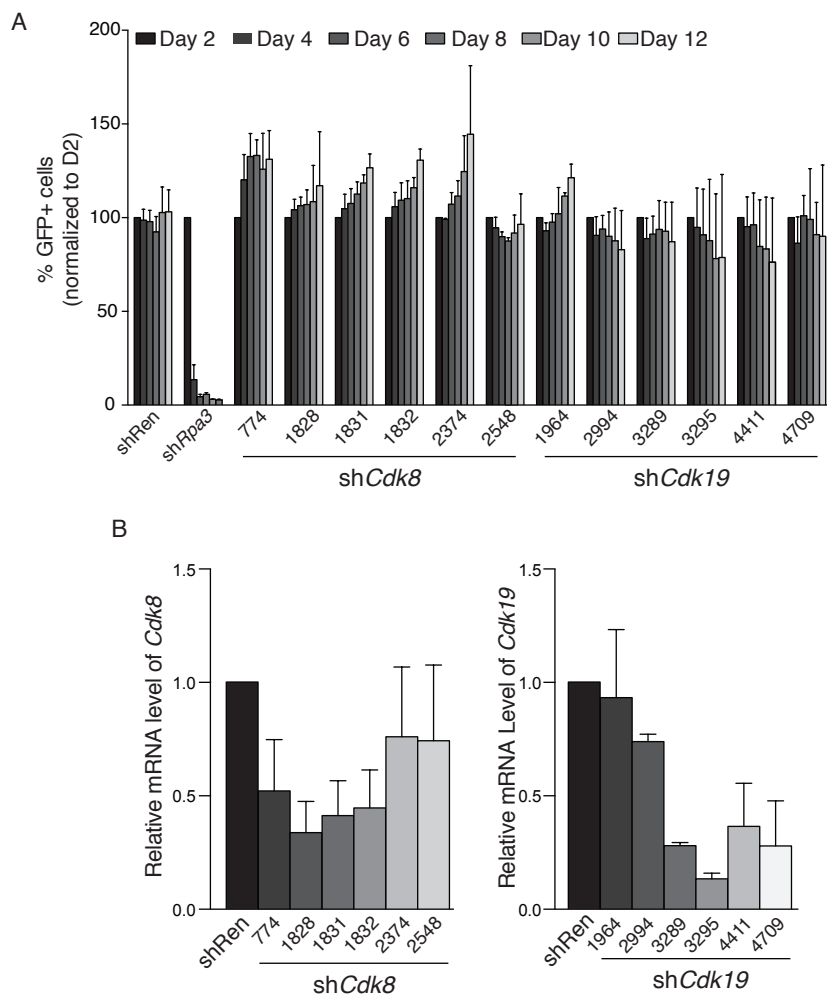
Figure 4-1 shRNAs targeting Cdk8 and Cdk19 do not produce a phenotype in RN2 cells

A) Negative selection experiment performed using RN2 cells that stably express Cas9 and guide RNAs directed against the kinase domains of Cdk8 and Cdk19 (LRG vector). GFP+/gRNA+ cells were measured on the indicated days on a Guava instrument and GFP+% cells were normalized to day 2 post-infection.

B) Relative mRNA levels of the indicated Mediator kinase following knockdown of Cdk8 or Cdk19 with the indicated shRNA (LMN vector) in RN2 cells. Data are presented as mean ± SEM; n=2-3.
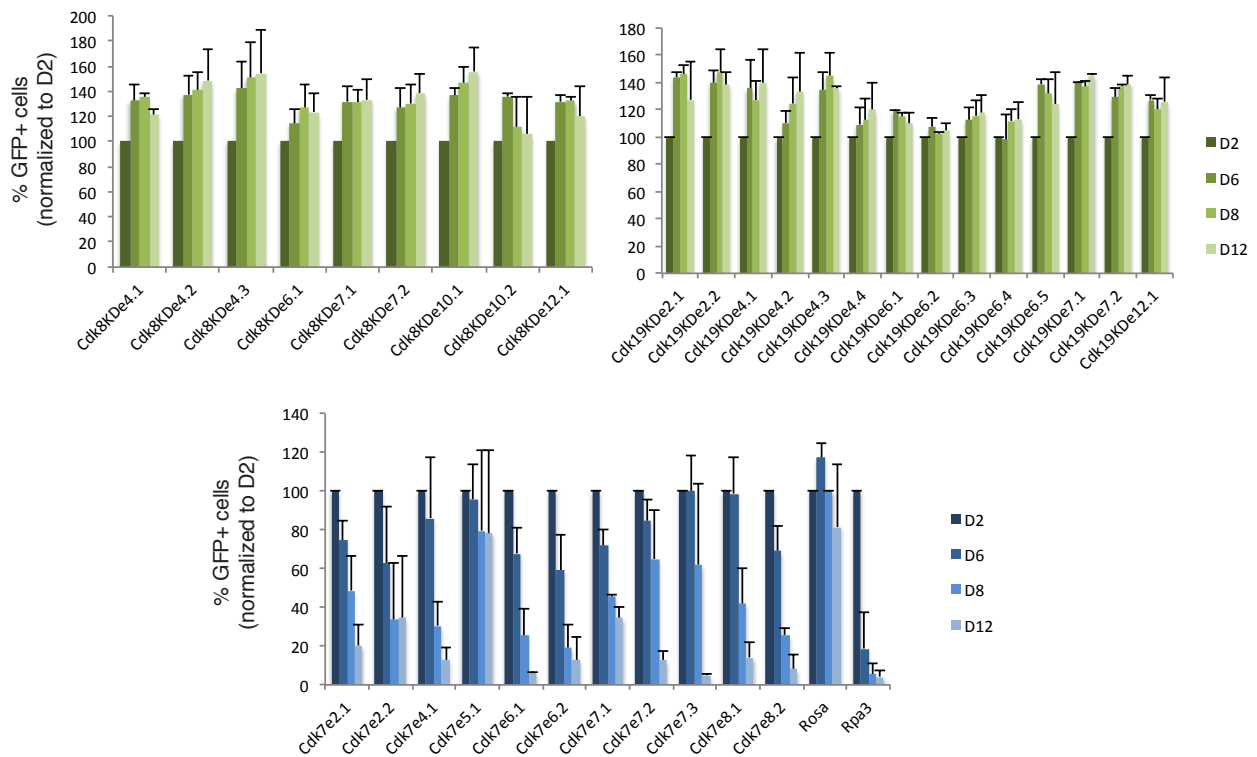
Figure 4-2 CRISPR targeting of Cdk8 or Cdk19 kinase domains does not lead to negative selection in RN2 cells

Negative selection experiment performed using RN2 cells that stably express Cas9 and guide RNAs directed against the kinase domains of Cdk8 and Cdk19 (LRG vector). GFP+/gRNA+ cells were measured on the indicated days on a Guava instrument and GFP+% cells were normalized to day 2 post-infection. On the blue graph, guides targeting the Cdk7 kinase domain or Rpa3 served as positive controls, while a guide targeting the Rosa locus served as a negative control. Data are represented as mean + SEM and n=2.
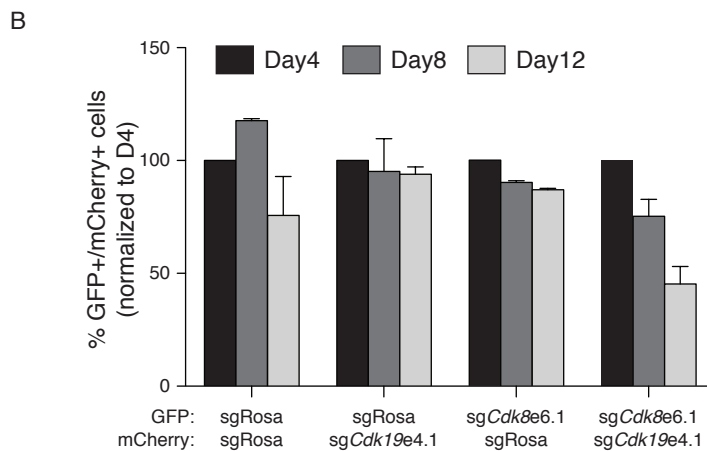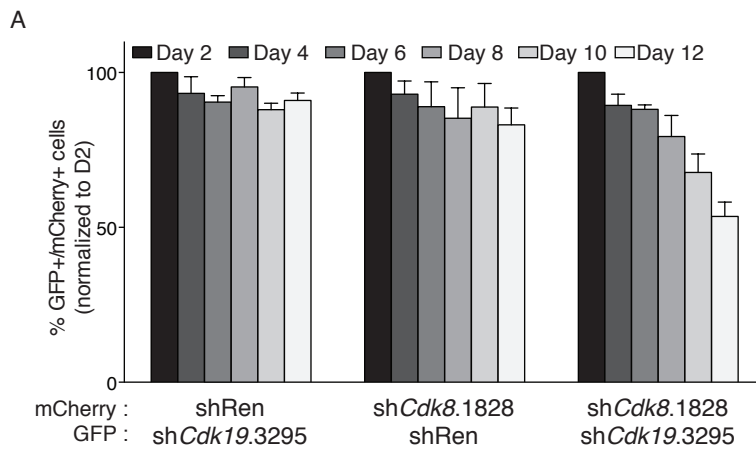
Figure 4-3 Dual targeting of Cdk8 and Cdk19 with shRNA or sgRNA produces a proliferation arrest in RN2 cells

A) Negative-selection competition assay of double shRNA targeting of Cdk8 and Cdk19. Plotted is the percentage of GFP+/mCherry+ cells over time following transduction of RN2 cells with the indicated pair of shRNAs. mCherry-containing constructs (LMN-Cherry) were introduced first, followed by the GFP-containing constructs (LMN vector). Data are presented as mean ± SEM; n=3.

B) Negative-selection competition assay of double CRISPR targeting of Cdk8 and Cdk19 plotting the percentage of GFP+/mCherry+ cells over time following transduction of Cas9-expressing RN2 cells with the indicated sgRNAs (LRG and LR-Cherry vectors). GFP-containing constructs were introduced first, followed by the mCherry-containing constructs, with n=2 for GFP/sgRosa and n=3 for GFP/sgCdk8.

simultaneous CRISPR targeting of Cdk8 and Cdk19 kinase domains resulted in a modestly reduced proliferative capacity relative to control guides (Figure 4-3B).

4.2.2 – Senexin B causes apoptosis of AML cells in cell culture

The results of our dual shRNA- and CRISPR-targeting of the Mediator kinases suggest a redundant function of these two kinase subunits, consistent with a recent study showing that dual Cdk8/Cdk19 inhibition with Cortistatin A suppressed AML cell growth (Pelish et al., 2015). Motivated by these genetic results, we were interested in pursuing a small-molecule-based approach to Mediator kinase inhibition. For this purpose, we were able to obtain Senexin A and Senexin B from Senex, the company that manufactures these molecules (Figure 4-4). We first aimed to test whether or not Senexins could reduce the proliferation of a panel of AML cell lines. After 72 hours of exposure to Senexin A or Senexin B, we observed a strong, dose-dependent reduction in cell accumulation in our murine AML cell line (Figure 4-5). Encouragingly, the more potent Senexin B molecule had a stronger effect than its precursor Senexin A (Figure 4-5). These effects did not appear constricted to any genetically defined subtype of leukemia, as the proliferation of a number of human leukemia cell lines with diverse genetic backgrounds was also affected by Senexin treatment (Figure 4-5). We next took a more detailed measurement of proliferation deficits caused by Senexin B over 5 days (for murine AML cells) or 7 days (for human leukemia cell lines), and again observed a dose-dependent reduction in cell accumulation for each cell line tested (Figure 4-6). While MLL-driven leukemias did appear to be slightly more sensitive to Senexin B, proliferation of all leukemia cell lines tested,
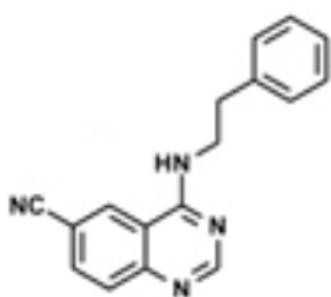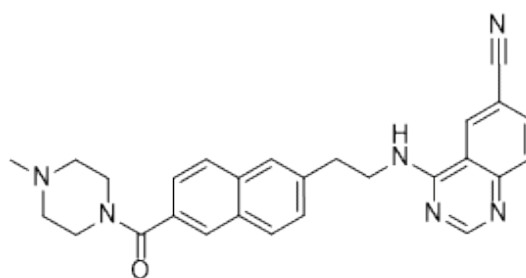
Senexin A   Senexin B

Figure 4-4 Senexin Molecules
Chemical structures of Senexin A and Senexin B, the reported Cdk8/Cdk19 inhibitors
used in this study.
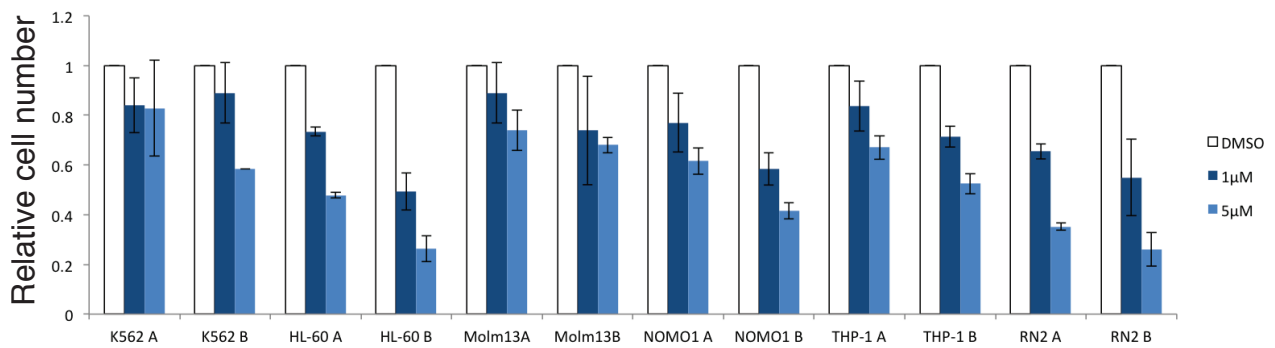
Figure 4-5 Senexins inhibit growth of AML cell lines
10,000 cells were seeded in a dish and treated with either DMSO vehicle control or the inidcated Senexin molecule (A or B) at the indicated concentration. Cells were counted at 72h after seeding and normalized to the DMSO condition. Error bars represent S.E.M. and n=2.
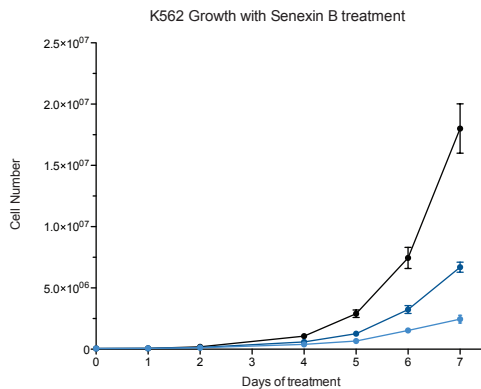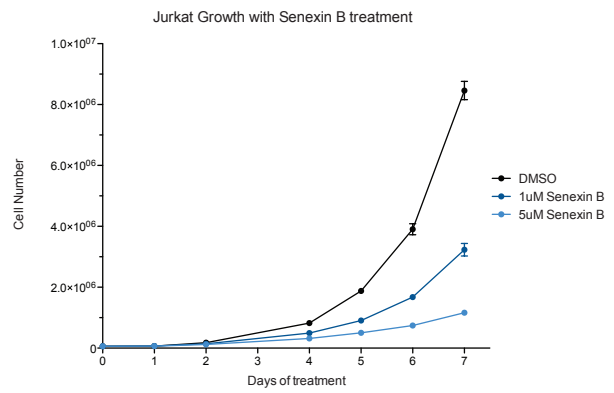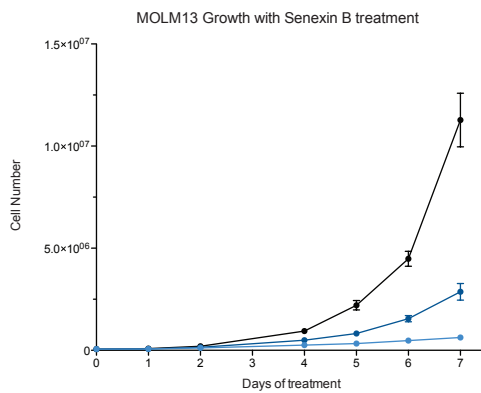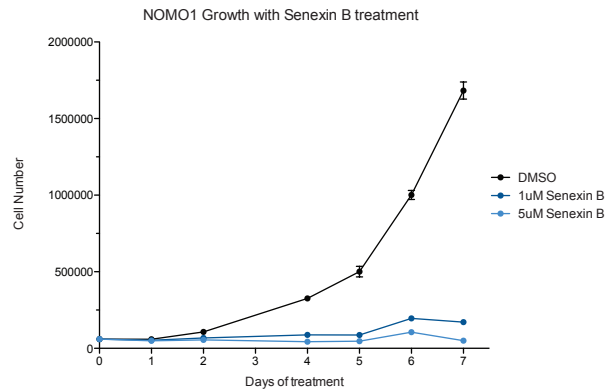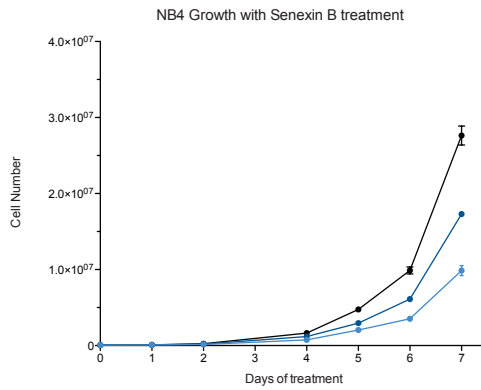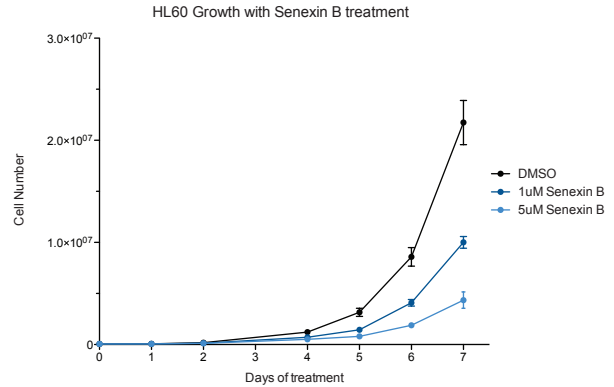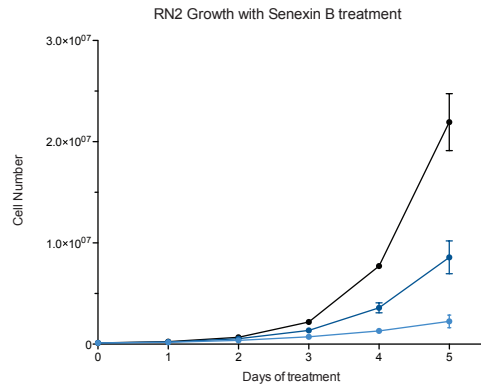
Figure 4-6 Senexin B slows the accumulation of Leukemia cells
Cells were seeded in a dish and treated with the indicated compounds. At each time point displayed, cells were counted on a Guava EasyCyte. Counts were corrected for the degree of passaging. Error bars reprsent SEM and n=3.

including the T-ALL Jurkat and CML blast crisis K562 cell lines, was ultimately inhibited by Senexin B (Figure 4-6).

Knockdown of Mediator complex subunits, including the kinase module subunits Med12 and Med13, led to proliferative inhibition of AML cells by inducing differentiation of leukemic blasts. Thus, we hypothesized that the kinase inhibitor Senexin B would also result in differentiation as measured by cell surface loss of ckit and gain of Mac1 expression. However, flow cytometric analysis of these markers in murine AML cells showed that 1μM Senexin B, despite greater than 50% reduction in cell accumulation, had no effect on differentiation. 5μM Senexin B showed only a very modest change in these markers, despite loss of up to 90% of cell accumulation (Figure 4-7). We then examined whether the loss of cell proliferation instead reflected a greater induction of apoptosis and cell death. Using Annexin V/DAPI staining, we observed that Senexin B induced apoptosis in a concentration-dependent manner in mouse AML cells (Figure 4-7). This result prompted us to measure cell death in the human leukemia cell lines by propidium iodide (PI) staining after 7 days of treatment. Senexin B potently and dose-dependently induced cell death relative to DMSO control in all cell lines tested, as measured by the percent of PI-positive cells in culture (Figure 4-8).

After establishing that Senexin B causes cell death in leukemia cells, we next asked whether these effects would lead to an extension of survival in an animal model of AML. We initiated leukemia in mice by injecting 50,000 murine MLL-AF9/Nras[G12D] AML cells into the tail vein of 10 sublethally irradiated C57Bl/6 mice. Beginning 24 hours after leukemia initiation, 5 of these mice were treated daily with intraperitoneal injection of 40mg/kg Senexin B, while the other 5
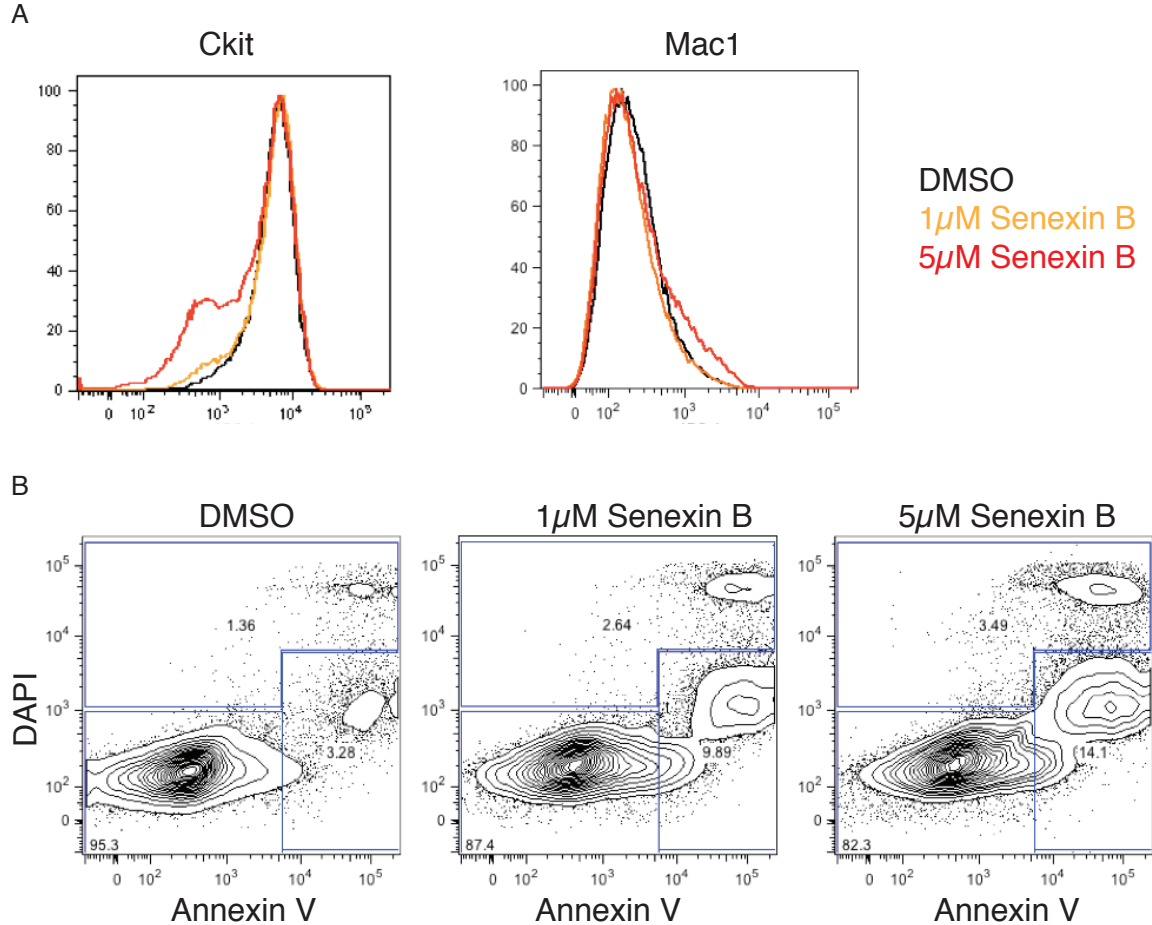
Figure 4-7 Senexin B induces apoptosis in RN2 cells
A) Flow cytometry analysis of cell surface cKit and Mac1 after treatment with Senexin B or DMSO control. RN2 cells were cultured for four days in the indicated concentration of Senexin B or in DMSO (black line). Cells were stained with APC-Ckit or APC-Mac1 antibodies and analyzed on a flow cytometer.
B) Flow cytometry analysis of DAPI staining and Annexin V binding to RN2 cell surface after Senexin B treatment. No gating on live cells was performed for this analysis. RN2 cells were cultured in Senexin B or DMSO and stained with DAPI and APC-Annexin V. Numbers in boxes indicate percentages of the population falling within each gate. The box in the lower right corresponds to apoptotic cells, while the box on the top half of the scatter plot represents dead cells.
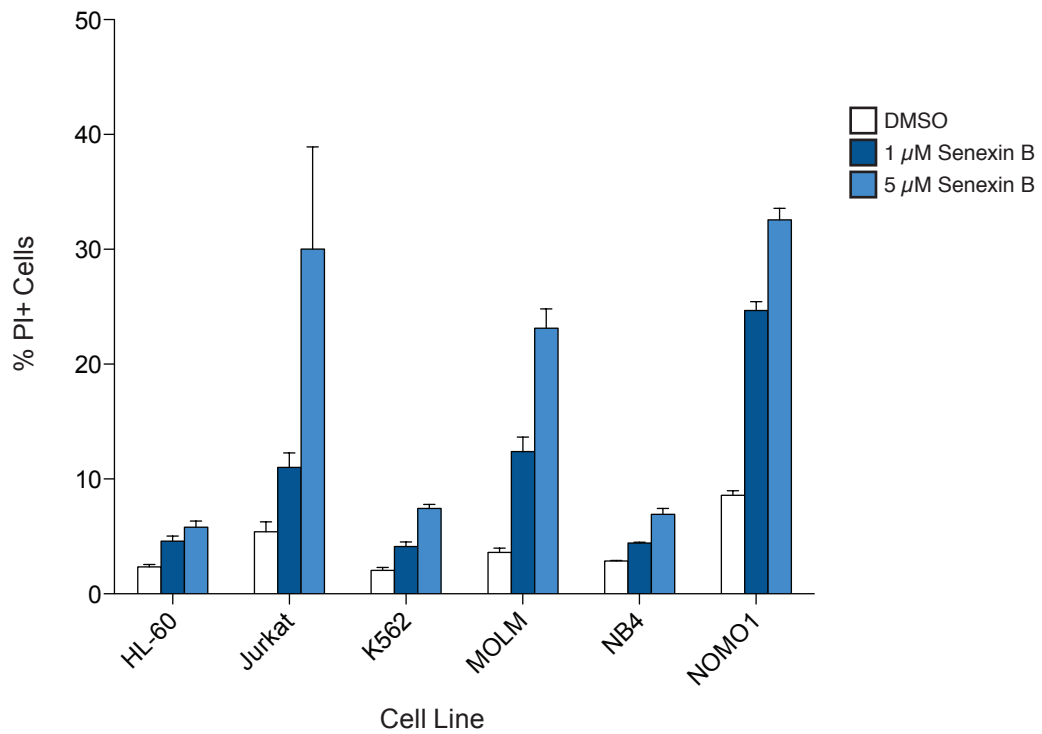
Figure 4-8 Senexin B induces cell death in Human AML cell lines
Cells were cultured in Senexin B for 7 days and stained with propidium iodide (PI).
Percent PI+ cells were normalized to DMSO treated cells. Error bars represent SEM
and n=3.

mice received daily citrate buffer as a vehicle control. Mice were monitored by bioluminescence and for signs of distress. Ultimately, Senexin B treatment did not reduce disease burden or extend survival of leukemic mice (Figure 4-9A and B).

4.3 – Brief Discussion

A recent study using Cortistatin A found that Cdk8 and Cdk19 inhibition hyperactivated transcription of super-enhancer associated genes, antagonistic to the Brd4-like function we identified in other Mediator subunits (Pelish et al., 2015). Whether this result can be validated is unclear, but the lack of differentiation induced by Senexin B (Cortistatin A was also not reported to induce myeloid differentiation), which is in contrast to the phenotype that follows knockdown of Med12 and Med13 (Chapter II) supports a uniquely repressive function of the kinase activity in the Mediator complex (Pelish et al., 2015). It would be interesting to know if, in the *in vivo* setting, doses of Cortistatin A demonstrated to have efficacy in extending survival of leukemic mice remain limited to their Cdk8/Cdk19 targets or whether they begin to inhibit the ROCK kinases, which have already been demonstrated to be therapeutic vulnerabilities in AML (Mali et al., 2011). To this end, leukemia cells bearing one of the Cdk8/Cdk19 tryptophan mutants that are resistant to Cortistatin A could be used to establish the relevant target of this drug (Pelish et al., 2015).

Several alternative factors could explain the lack of Senexin B *in vivo* efficacy. For example, poor bioavailability or a short serum half-life would preclude the drug from having any impact on disease progression. To monitor this, a good biomarker of response is required. Cdk8 and Cdk19
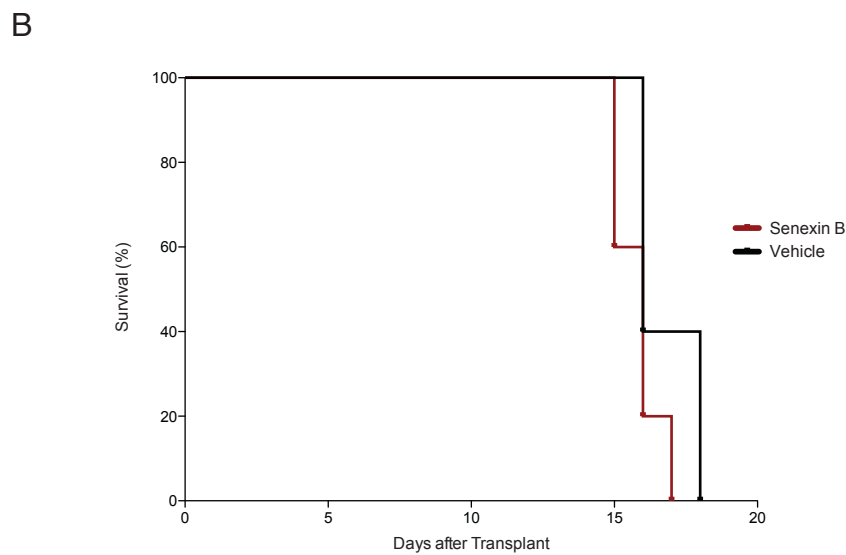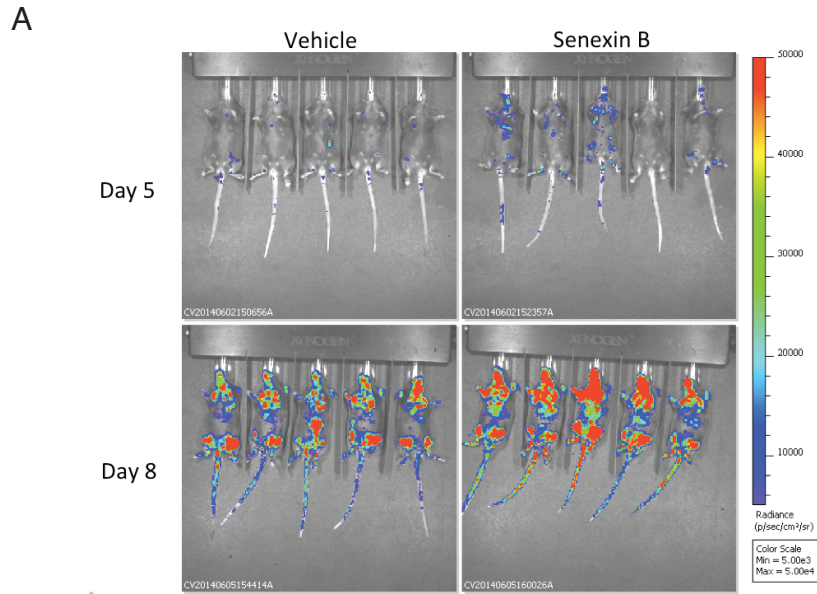
Figure 4-9 Senexin B does not affect the survival of mice with MLL-AF9-driven AML

A) Bioluminescent imaging of MLL-AF9/Nras^{G12D} leukaemia recipient mice at the indicated day after initiation of treatment with Senexin B (40 mg/kg) or citrate buffer vehicle ontrol.

B) Kaplan–Meier survival curves of control and Senexin B-treated mice. In (A) and (B), Senexin B treatment was initiated on day 1 after transplant of 50,000 leukaemia cells.

have been shown to phosphorylate a number of nuclear factors, including TFs, but which substrates are relevant in AML is unclear (Dale et al., 2015; Pelish et al., 2015). One study suggested that pSTAT1^{S727} levels tracked with Cdk8 activity in a number of cell types (Dale et al., 2015), which would support this as a useful correlate of Senexin B on target effects. Whatever the ultimate explanation for the poor outcome of the *in vivo* experiment, the lack of sufficiently available alternatives to Senexin B precluded us from testing Cdk8/19 inhibitors with better pharmacodynamics properties.

Chapter V - Targeting other Mediator subunits

5.1 – Brief Introduction

One of the great promises and challenges of validating Mediator as a viable therapeutic target is the complex's vast surface area for protein interaction. This represents an opportunity to identify a surface that is selectively required in leukemia, but it also represents a daunting task to find these particular surfaces from the many that are present in the highly amorphous Mediator complex. While each subunit in the Mediator complex may have myriad functions, including simply maintaining the structural integrity of the Mediator complex, smaller regions and domains of these subunits may have more specified functions. Mediator subunits interact with basal transcription machinery, activators, and other mediator proteins. In order to have the greatest potential for selective function in leukemia cells, the minimal portion of the Mediator subunit that interacts with a leukemia-driving TF should be identified.

Mediator interaction with TFs can alter the complex's structure and drive its function in cells (Poss et al., 2013). Despite a general lack of available structures to aid identification of likely binding domains, several TF-Mediator interactions have been mapped to discrete regions on the

Mediator complex. For example, LxxLL motifs on Med1 have been shown to facilitate interaction with nuclear hormone receptors, such as the thyroid receptor and estrogen receptor α (Malik and Roeder, 2010). A Med1 LxxLL-mutant mouse was recently generated, and while viable and fertile mice were produced, severe defects in estrogen response gene transcription were observed and were accompanied by impaired pubertal mammary gland development (Jiang et al., 2010).

Two additional TF-binding regions of Mediator that have been characterized by NMR structure are the VP16-binding ACID domain on Med25, and the KIX domain of Med15, which binds the activation domain of the master lipid homeostasis regulating TF SREBP-1a (Malik and Roeder, 2010; Vojnic et al., 2011; Yang et al., 2006). The latter example is particularly exciting because the structural knowledge of Med15's interaction with SREBP-1a has been exploited to develop small molecule inhibitors of this interaction that can restore lipid homeostasis in mouse models (Zhao et al., 2014). Finally, the PQL domain of Med12 interacts with a number of transcription factors, coactivators, and corepressors, including the important oncogene β-catenin (Ding et al., 2008; Kim et al., 2006).

Based on these examples, we hypothesized that the function of Mediator subunits in maintaining AML could be distilled down to specific domains of these subunits that mediate interaction with oncogenic TFs. By binding to and coactivating transcription for these TFs, Mediator could assist in the direction of leukemogenic transcription programs. However, mass-spec-based identification of Mediator associated proteins can yield little actionable information, in part

because the heterogeneity and specificity of Mediator interaction partners across the genome necessarily involves a large number of low-affinity interactions (Herbig et al., 2010). Moreover, Mediator subunits almost always interact with one another and with other components of the PIC, and these more abundant, multi-subunit interacting protein complexes could obscure individual, low-frequency TF interactors. Thus, traditional biochemistry approaches, such as immunoprecipitation coupled with mass spectrometry may not prove fruitful in the search for AML-driving Mediator ligands, and development of a new assay for this purpose is required.

5.2 - Results

5.2.1 – GFP-fused Mediator fragments limit proliferation of RN2 cells

To overcome biochemical difficulties involved with Mediator complexes, we developed an assay that enabled rapid screening of multiple fragments of Mediator for their contribution to AML proliferation. These fragments could then be immunoprecipitated in isolation to identify their putative binding partners in AML cells. We used a GFP-tag directly attached to the fragments by a glycine and alanine linker, in order to be able to track the viability of fragment-expressing cells by the GFP-depletion screening assay used in our shRNA screens. The advantage of a GFP-fused fragment over a bicistronic vector (using IRES-GFP, for example) is that we can attempt to monitor fragment expression; if the GFP-tagged construct fluoresces, it suggests that the GFP-fragment is expressed in cells. The GFP-tag also provides a large, potentially stabilizing fluorescent tag that may permit expression of otherwise unstable peptide fragments of

Mediator proteins. Finally, the unique GFP moiety in the cell could be used to directly immunoprecipitate the fragment of interest and assess binding partners.

We began by arbitrarily dividing Med12 and Med23 into fragments and cloning them into a constitutive vector expressing the GFP-Mediator fusion constructs off of a retroviral promoter. Expression, as determined by GFP intensity, was very low (Figure 5-1A). Despite this, some fragments were expressed and resulted in some level of GFP depletion (Figure 5-1B).

The PQL domain of Med12 has previously been shown to be expressible as an autonomous domain in cells (Kim et al., 2006). However, as a GFP-fusion construct, this domain did not express in AML cells, possibly because the overall vector size was too large for efficient retroviral packaging. We thus instead expressed the PQL domain in AML cells from a bicistronic MIGR1 vector in which GFP is downstream of an IRES element. This construct underwent negative selection in RN2 cells, raising the possibility that the PQL domain has an important role in AML cells (Figure 5-1C).

5.2.2 – Doxycycline–induced expression of the PQL domain results in rapid death of RN2 cells
Encouraged by this result, we aimed to increase the expression of the PQL domain by using a stronger promoter. Because the expressed fragments would have to compete with endogenous Mediator subunits for binding to oncogenic ligands, we hypothesized that sufficiently high fragment expression would be required to observe dominant negative effects. In order to induce higher expression of Mediator fragments, we expressed the PQL domain from the TtIGP vector,
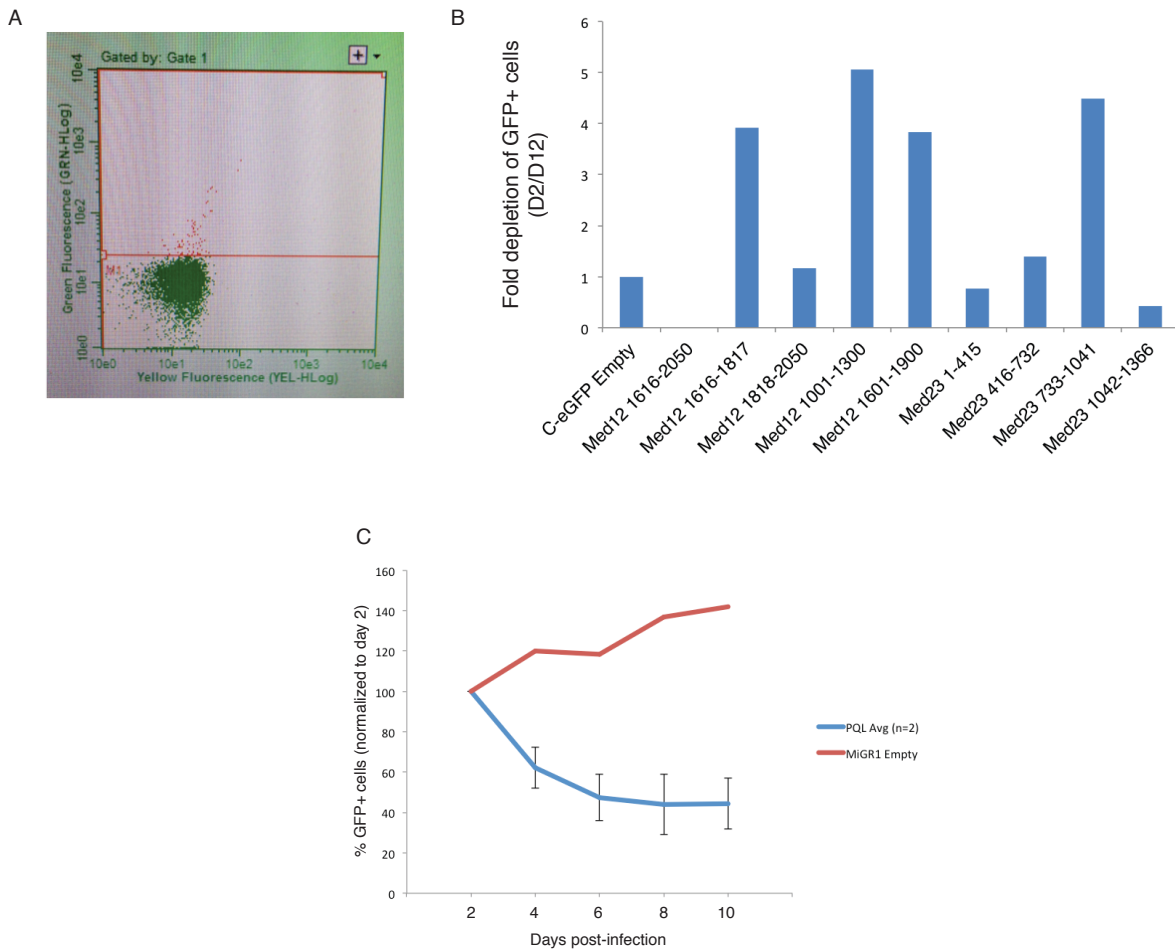
Figure 5-1 Retroviral expression of Mediator fragments results in mild phenotypes in AML cells

A) Expression of fragments, as measured by the GFP fluorescence intensity by Guava EasyCyte machines. Fragments were expressed as fusions to eGFP. Empty vector is an unfused eGFP.

B) Negative selection assay in RN2 cells after 12 days of expression of GFP-fused Mediator fragments from a retroviral vector. Taller bars indicate greater negative selection of the expressed fragment. Depletion value was normalized to empty vector.

C) Expression of the PQL domain from the MIGR1 vector in RN2 cells (blue line) results in negative selection. GFP percentages are normalized to Day 2 and tracked for 10 days. Error bars represent SEM and n=2.

in which it is under the control of a doxycycline-inducible Tetracycline response element. This led to rapid loss of GFP-and PQL domain-expressing cells within 48 hours of doxycycline induction of expression (Figure 5-2A). We hypothesized that Med12 interruption with overexpression of a dominant negative PQL domain would lead to similar phenotypic consequences as Med12 knockdown. In particular, we expected PQL expression to be neutral in MEF cells and to induce cellular differentiation in AML cells. Expression of the PQL domain led to comparable accumulation of GFP- and PQL domain-expressing MEF cells over 6 days, consistent with a non-essential role for Med12 in MEF proliferation (Figure 5-2B). Because of the nature of this dominant negative expression assay, a trivial explanation for this lack of a MEF phenotype would be that the fragment is not expressed in the nucleus where it could interfere with Med12 transcriptional function. To address this, we performed western blot analysis to confirm that the Flag-tagged PQL domain was expressed in the nuclei of both MEF and RN2 cells upon doxycycline treatment (Figure 5-2C).

We next assessed the impact of PQL domain expression on RN2 cell differentiation status. Both 48-hour treatment with 1 μg/mL doxycycline to induce PQL domain expression led to only a mild loss of cell-surface cKit expression and no gain of Mac1 expression despite an observed loss of GFP-expressing cells from the culture (Figure 5-3A). Because this mild induction of differentiation may have been due to expression of an amount of PQL domain that was not tolerated by the cells, we also used lower doses of doxycycline to induce expression. Using 0.1 μg/mL of doxycycline, we could express lower amounts of the PQL domain (Figure 5-2C). We then noted that 0.1μg/mL of doxycycline, one tenth of our standard dose, did modestly decrease
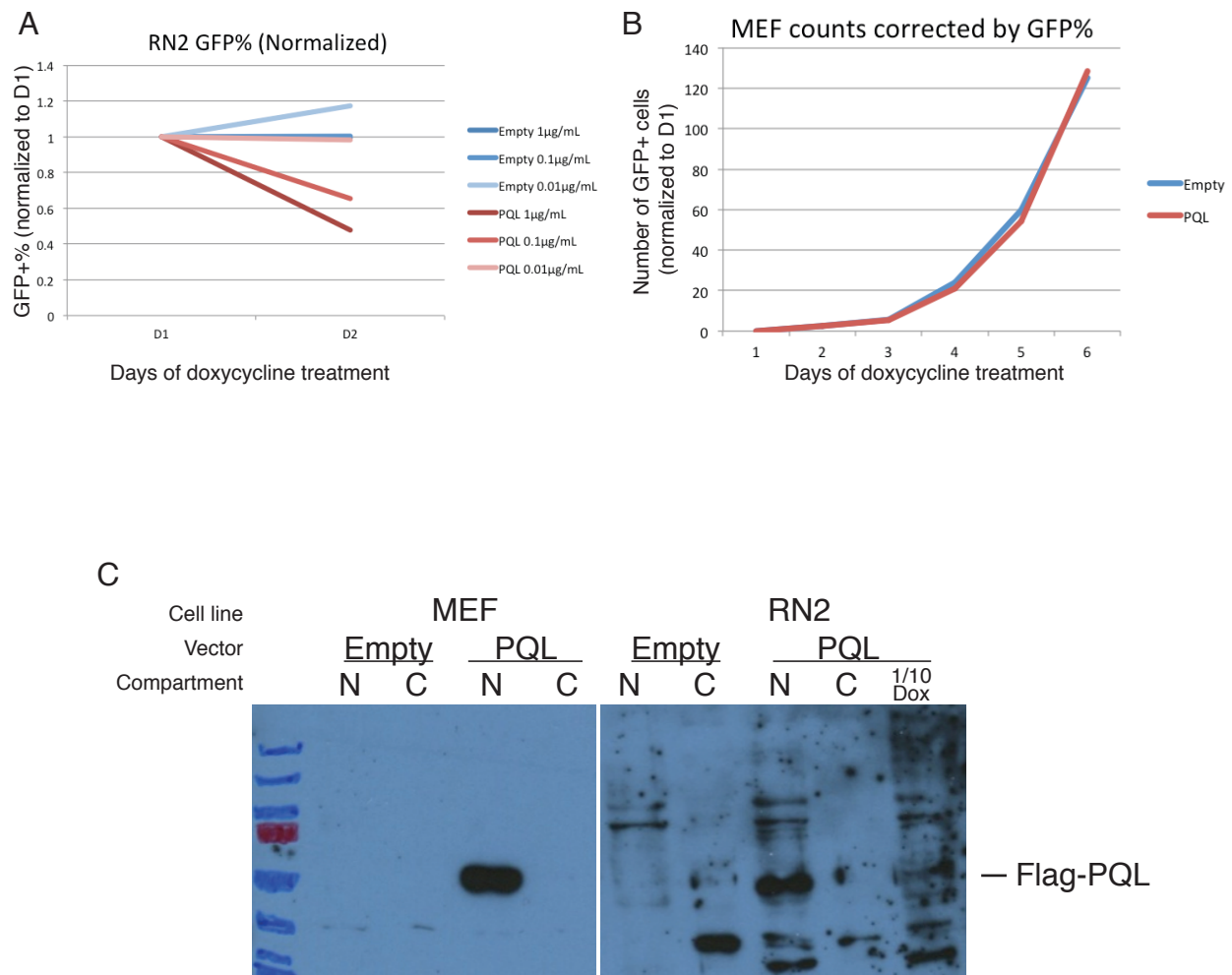
Figure 5-2 TtGIP expression of the Med12 PQL domain is toxic to AML cells but not to MEFs

A) Short-term negative selection experiment in RN2 cells with 48 hr of doxycycline induced expression of the PQL domain. GFP+/PQL+% was measured at 24- and 48-hr time points and normalized to the 24 hr time point.

B) Cell accumulation experiment in which GFP+/PQL+ MEF cells were counted over 6 days of doxycycline treatment and compared to GFP+ MEF cell accumulation rate in cells transduced with TtIGP-empty vector.

C) Flag-Western blot showing PQL expression after 24 hr of doxycyline treatment in MEF cells or RN2 cells. Cells were fractionated and equal amounts of nuclear and cellular extracts were run on a gel and blotted with anti-Flag antibody. Nuclear extract of RN2 cells treated with 1/10th of the normal concentration of doxycycline, or 0.1ng/uL, was also run.
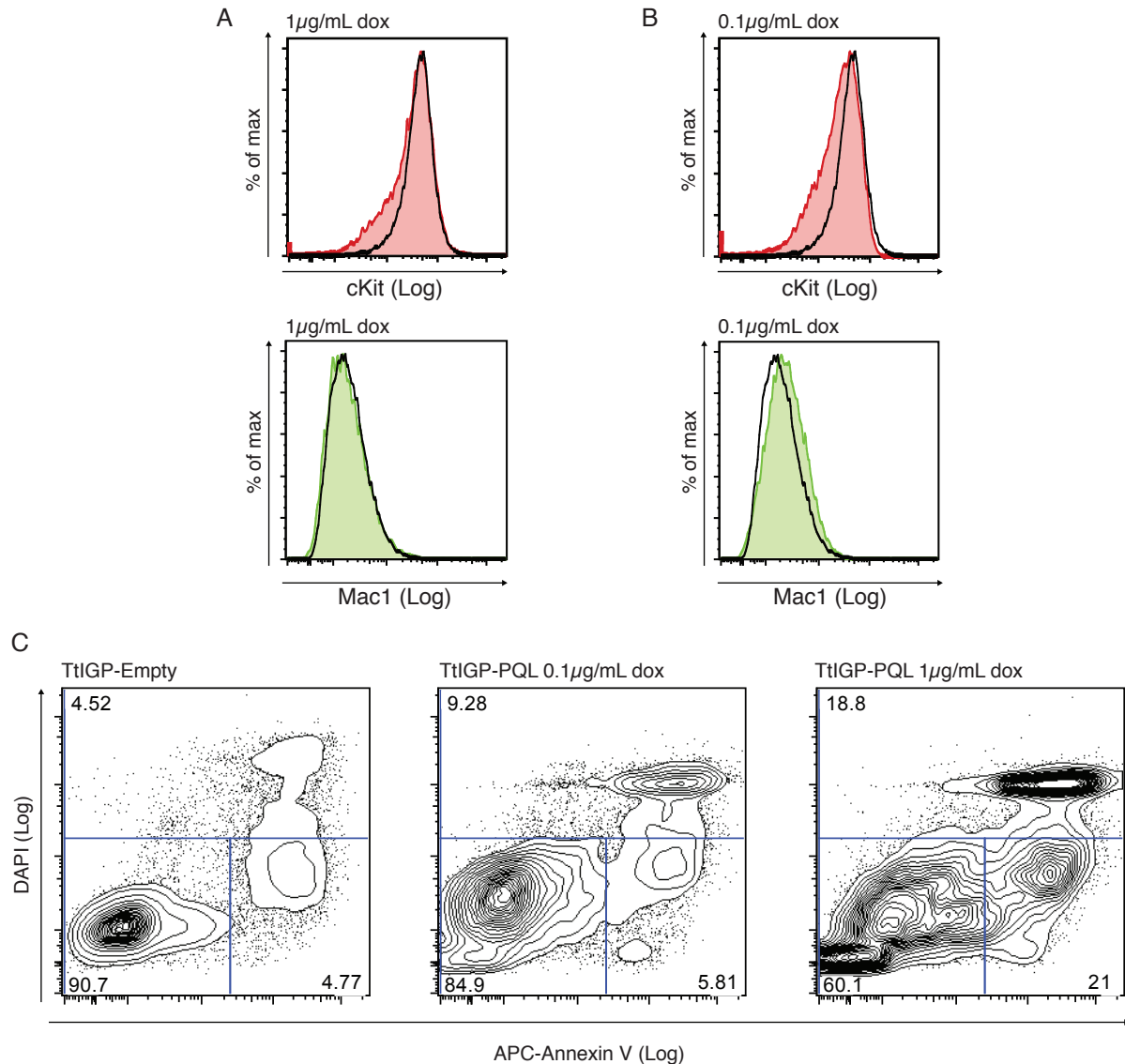
Figure 5-3 Med12 PQL domain expression causes apoptosis in RN2 cells
A-B) Flow cytometric analysis of cell-surface cKit and Mac1 following 48 h of doxycy-cline-induced expression of TtIGP-PQL versus TtIGP-Empty (black trace) at two doses of doxycycline/PQL expression. Gating was performed on GFP+ populations.
C) Flow cytometric analysis of Annexin V binding and DAPI staining following 48 h of doxycycline-induced expression of TtIGP-PQL or TtIGP-Empty. No gating on live cells or GFP+ cells was performed. Because no gating is done in this experiment, a clonal RN2 cell line containing the inducible PQL construct was used for this analysis to avoid con-tamination with non-expressing cells. Numbers in boxes indicate percentages of the population falling within each gate. The box in the lower right corresponds to apoptotic cells, while the box on the top half of the scatter plot represents dead cells.

cKit and modestly increase Mac1 cell surface expression on RN2 cells after 48 hours of doxycycline induction of expression (Figure 5-3B).

Because of the rapid loss of GFP-positive, PQL domain expressing cells from culture but only mild induction of differentiation, we considered whether expression of this domain could induce apoptosis in AML cells. To determine this, we used Annexin V and DAPI staining of cells after 24 hours of doxycycline treatment and PQL induction. We also noted that, despite constant exposure to puromcyin, only approximately 50% of cells expressed the PQL domain as measured by GFP fluorescence. Because gating on live or GFP/PQL-expressing cells cannot be performed for detection of apoptotic and dead cells in this assay, and because PQL-negative cells would dilute the impact of PQL expression in the pooled population, we derived a clone of RN2 cells harboring and inducibly expressing the TtIGP-PQL construct. In this clone, apoptosis was potently induced in a doxycycline dose-dependent manner, as measured by binding of Annexin V and staining with DAPI (Figure 5-3C). In summary, very high levels of expression of the PQL domain induced rapid apoptosis, while slightly lower expression of the PQL domain induced both apoptosis and cellular differentiation.

Motivated by these encouraging results, we attempted to expand this doxycycline-inducible fragment expression assay to include more fragments and more Mediator subunits. We focused on the four subunits we found to be neutral in MEF cells by shRNA knockdown, Med12, Med13, Med23, and Med24. Because within these proteins only the PQL domain of Med12 has been shown to be a standalone, stably expressed domain (Kim et al., 2006), we returned to the method of using GFP-fused constructs in order to monitor expression of fragments by GFP

fluorescence. Mindful of size constraints on expression, we cloned fragments that were 300-400 amino acids in size into the doxycycline-inducible GFP-fusion vector called TtGNP (Figure 5-4). Additionally, we cloned fragments covering halves of the PQL domain in order to obtain a more precise definition of the functionally important region of this domain of Med12 (Figure 5-4).

After 24 hours of doxycycline induction, many of these fragments did not express (as determined by the GFP fluorescence), including the N-terminal 700 amino acids of Med12 and most of Med23 and Med13 (Figure 5-4 and 5-5). However, all of Med24 expressed as GFP-fusion fragments. We next determined which of the fragments, when doxycycline-induced, negatively selected in AML cells. After 5 days on doxycycline, we identified only three fragments in addition to the full-length PQL domain that had a growth inhibitory effect on AML. This included amino acids 1001-1300 of Med12, a region known to be mutated in prostate cancer, the C-terminal 190 amino acids of Med24, and the first half of the PQL domain (amino acids 1616-1817, PQLS) (Figure 5-4 and 5-6). We further dissected Med12 PQLS into three 100 amino acid fragments and found that $Med12_{1616-1717}$ (PQLT) also negatively selected, while $Med12_{1666-1766}$ and $Med12_{1717-1817}$ did not (Figure 5-4 and 5-6).

As mentioned above, Med12 shRNAs have a potent phenotype in AML cells but are neutral in MEF cells. We thus reasoned that expression of the Med12 PQL domain fragments should recapitulate this pattern of sensitivity. We also induced expression of the PQLS and PQLT fragments in MEF cells and also observed little impact on MEF proliferation, similar to what
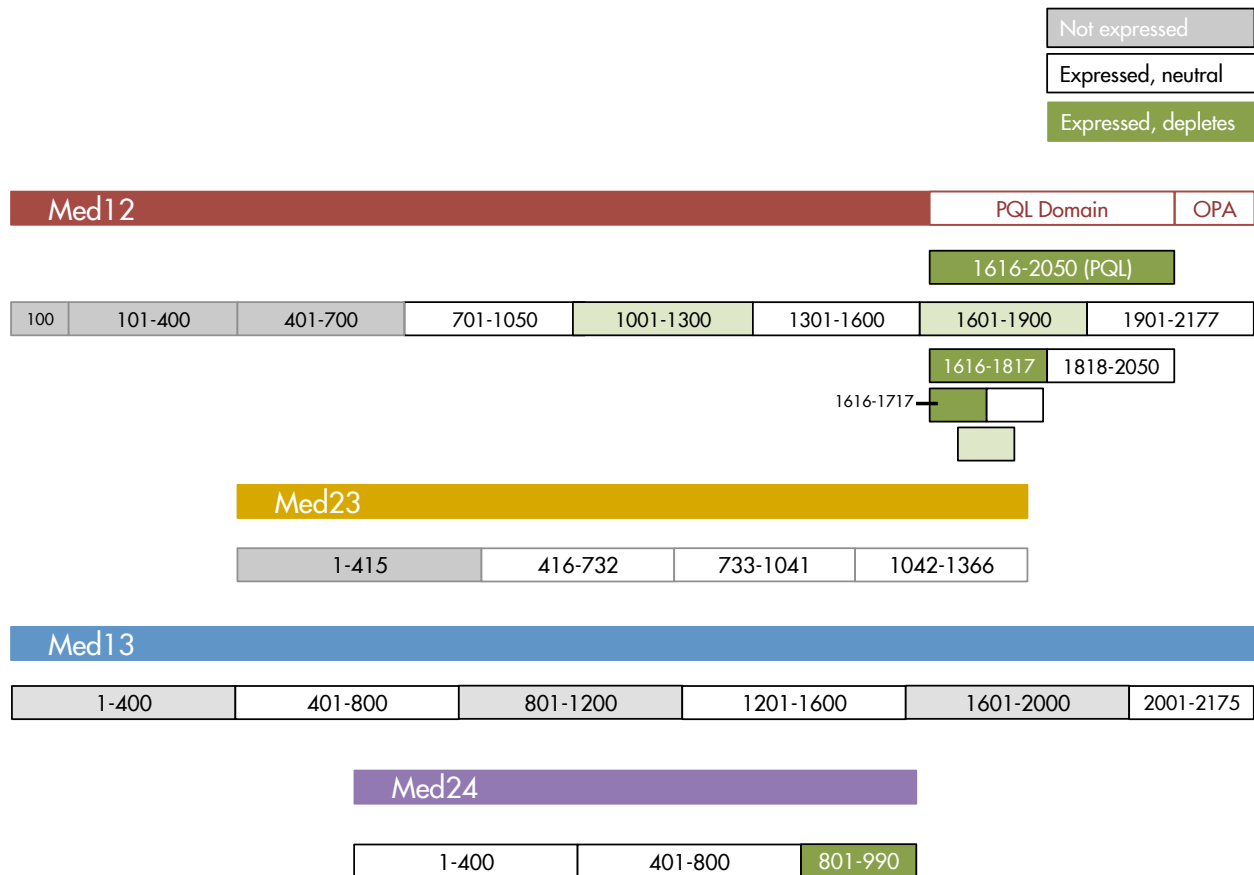
Figure 5-4 Summary of TtNGP Mediator fragment negative-selection studies.
Indicated fragments were cloned into the TtNGP vector and retrovirally introduced into
RN2 cells. Fragments shaded in gray did not express in RN2 cells as measured on a
Guava Easycyte by the GFP fluorescence. Fragments shaded in white expressed but
did not negatively select in RN2 cells, and fragments shaded in green expressed and
negatively seleced either mildly (light green) or potently (bold green).
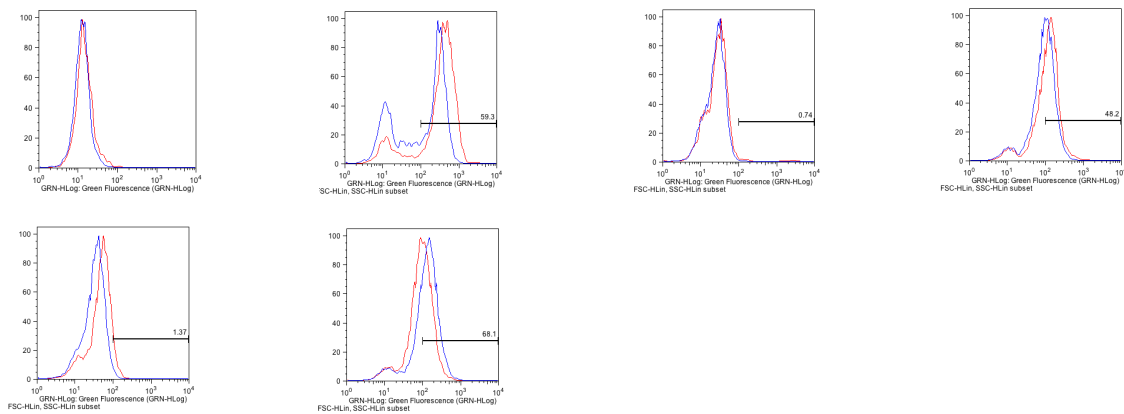
Figure 5-5 Lack of expression of most Med13 fragments from the TtGFP vector
The indicated fragments were retrovirally introduced into RN2cells and induced with doxycycline. GFP intensity was measured on a flow cytometer. Red traces represent baseline measurement of GFP fluorescence intensity (24 hr post-doxycycline). Blue traces represent GFP fluorescence intensity after 5 days of doxycycline treatment (RN2 cells).
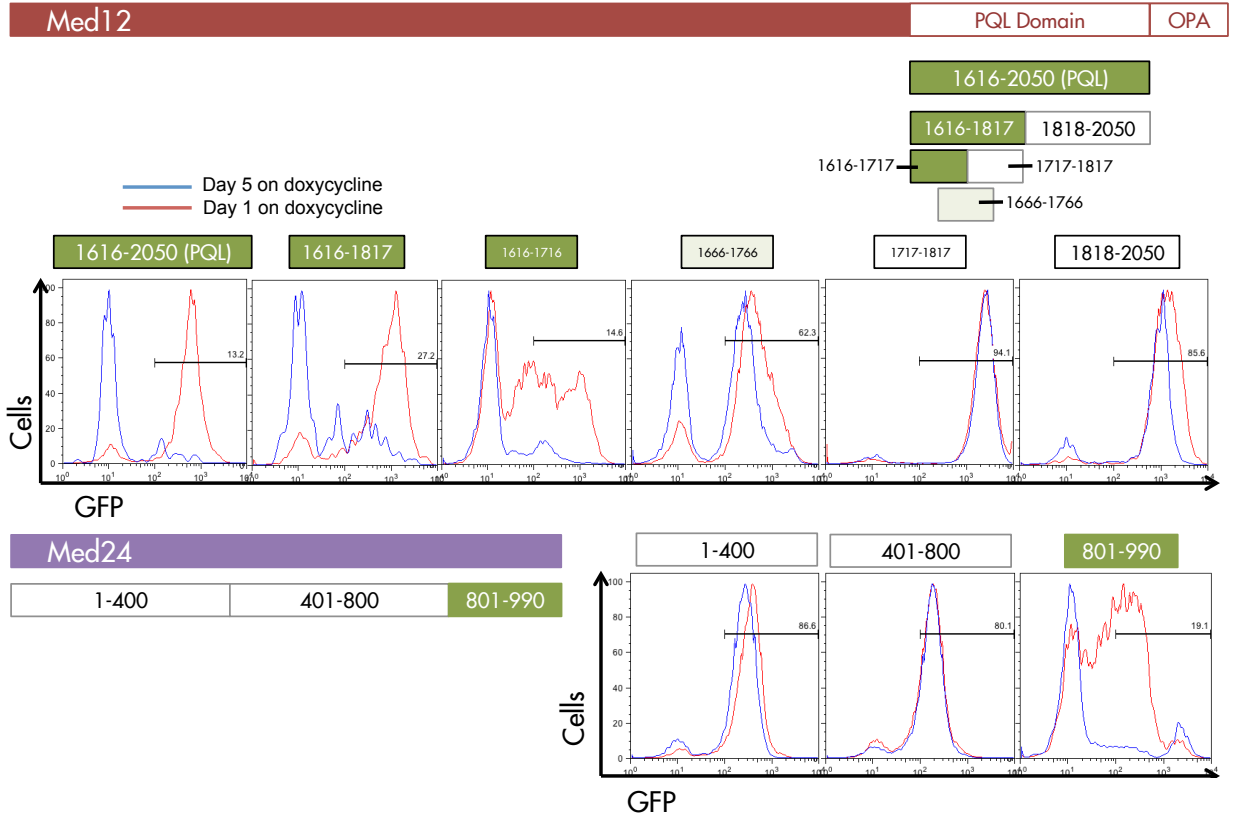
Figure 5-6 Expression of select fragments of Med12 and Med24 are negatively selected in RN2 cells
The indicated fragments were retrovirally introduced into RN2 cells and induced with doxycycline. GFP intensity was measured on a flow cytometer. Red traces represent baseline measurement of GFP fluorescence intensity (24 hr post-doxycycline). Blue traces represent GFP fluorescence intensity after 5 days of doxycycline treatment (RN2 cells).

was observed following TtIGP-PQL expression in MEFs (Figure 5-2B), suggesting that these fragments conform to the AML-selectivity observed after knockdown of Med12 (Figure 5-7).

Our ultimate aim was to identify Mediator interaction partners that function to maintain the leukemia cell state. To this end, we attempted to isolate proteins that interact with the Med12 PQL domain in AML cells. We prepared GST-PQLS proteins and used them as bait to precipitate potential partners from AML cell nuclear lysates. In an initial pilot attempt, silver staining showed several bands that appeared to be unique to the GST-PQLS pulldown (Figure 5-8).

5.3 – Brief Discussion

The pursuit of a means through which Mediator function could be inhibited is hindered by a lack of suitable domains against which small-molecules can be designed. Thus, protein-protein interactions, of which the Mediator complex participates in many, may be the key to inhibiting the leukemia-supporting function of the subunits we identified in our shRNA screen. However, we must first identify specific protein-interaction surfaces on these subunits in order to proceed towards development of inhibitors of these interactions.

Because Mediator is a highly amorphous complex with dynamic, context-dependent structure and many subunits, biochemical approaches to elucidate interaction partners have been difficult. Some studies have identified TFs that bind Mediator, but given the centrality of Mediator in activator-dependent transcription from yeast to man, this number is surprisingly small (Poss et
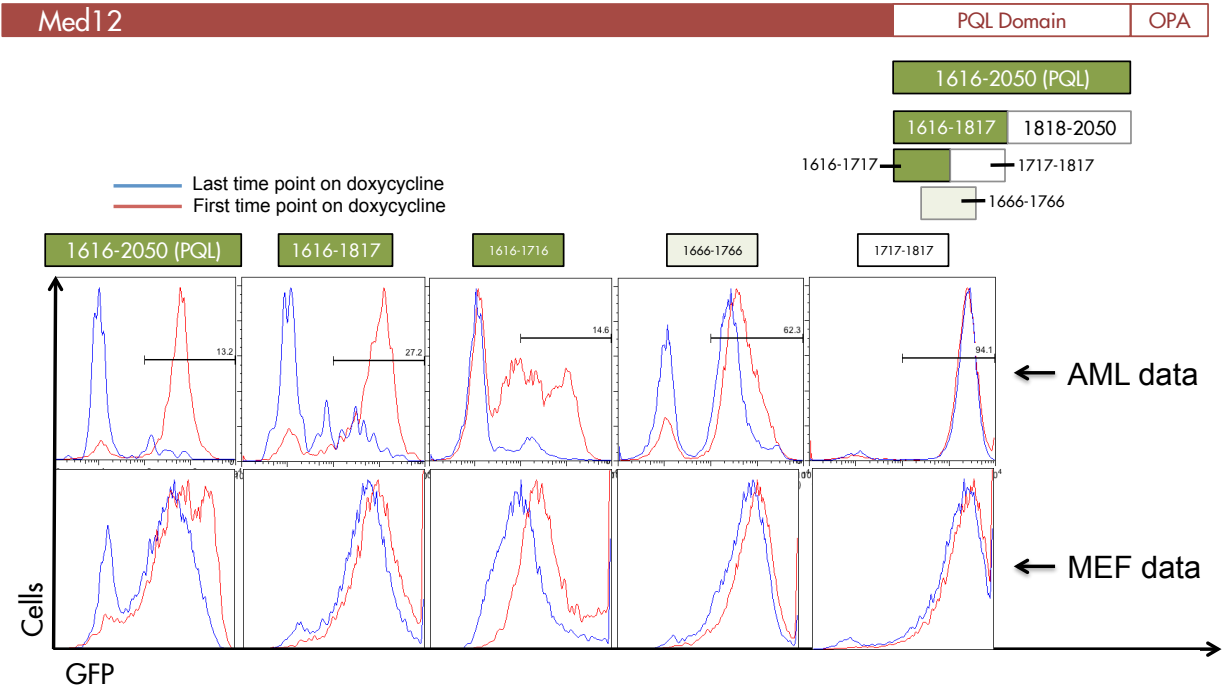
Figure 5-7 Expression of some Med12 PQL fragments negatively select in RN2 cells but not in iMEFs
The indicated fragments were retrovirally introduced into RN2 or iMEF cells and induced with doxycycline. GFP fluorescence was measured on a flow cytometer. Red traces represent baseline measurement of GFP fluorescence intensity (24 hr post-doxycycline). Blue traces represent GFP fluorescence intensity after 5 days of doxycycline treatment (RN2 cells) or 8 days of doxycycline treatment (iMEF).

GST-PQLS	+	+	-	-
GST-alone	-	-	+	+
Nuclear Extract	-	+	-	+
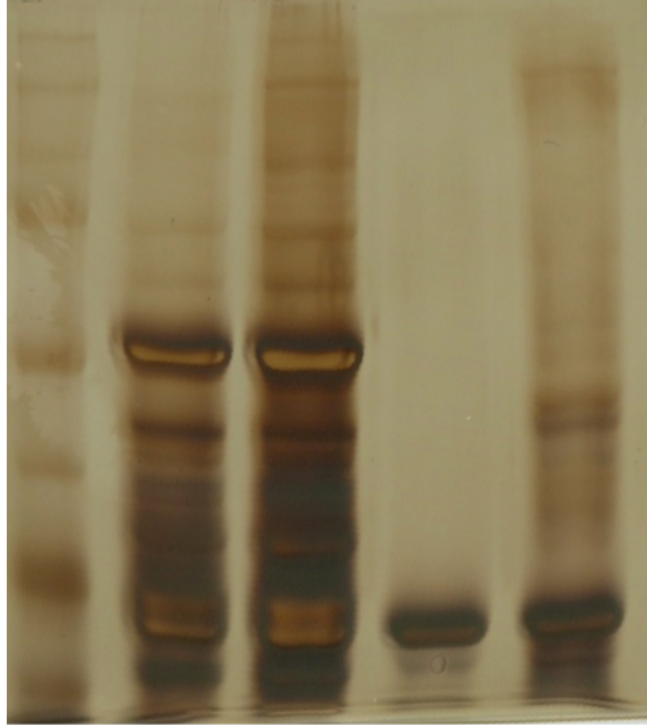
Figure 5-8 GST-PQLS pulldown with RN2 nuclear extract
10µg of bacterially expressed and purified GST-PQLS or 1µg of GST protein alone was incubated with agarose beads followed by 1µg of RN2 nuclear extract. Beads were washed with wash buffer containing 150 mM NaCl and 0.5% NP-40. Pulldown was visualized using silver staining.

al., 2013). As well, they often are identified by studying a TF of interest and finding, via mass spectrometry approaches, Mediator subunits as interaction partners of TF (Malik and Roeder, 2010). Here, we have developed an assay to rapidly screen individual proteins for their functionally important domains. By utilizing a dominant negative expression approach, we can pinpoint key regions of Mediator subunits and utilize these fragments to pinpoint the specific interaction that is being perturbed in cells.

In this chapter, we have used this approach to identify several regions of Med12 that are crucial to its function in AML cells. Med12aa1001-1300 has been described as a region that, when mutated, disrupts the binding of Med12 to Med13 and the core Mediator complex (Kampjarvi et al., 2015b). Thus, this fragment likely displaces Med12 from Mediator complexes rather than blocking TFs from Mediator interactions. While the ultimate outcome for AML cells would be similar, intra-complex-interaction-blocking fragments that disrupt a Med12-Med13 interaction in all cell types might result in less selective growth-inhibitory effects than fragments that block, for example, lineage-specific TFs from binding to Mediator subunits.

Thus, we focused on another region of Med12 that our approach highlighted as essential in AML: the PQL domain. We managed to narrow down the functional unit of the PQL domain in AML cells to its first 100 amino acids. This PQLT region is interestingly the only section of the PQL domain that is not intrinsically disordered, as predicted by GlobPlot (Figure 5-9). This PQLT region, according to JPred contains some predicted helices and sheets that may contribute to TF interaction and that could be used as potential designs for peptide inhibitors (Figure 5-9).
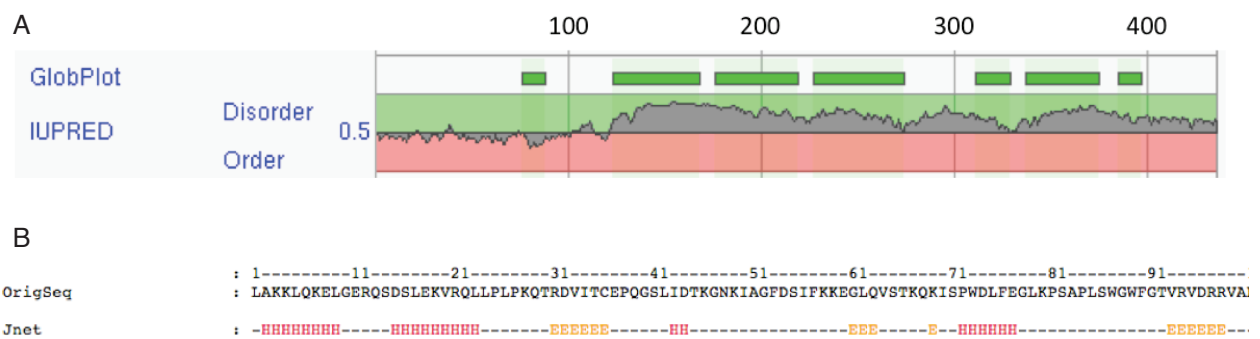
Figure 5-9 Predictions of order and secondary structure within the Med12 PQL domain

A) GlobPlot analysis of disorder within the Med12 PQL domain. The black trace represents a continuous representation of a score of predicted disorder within this amino acid sequence, with higher values indicating greater likelihood of disorder.

B) JPred analysis of PQLT. Red 'H's indicated predicted helices, while yellow 'E's indicate predicted sheet secondary structures.

We were not able to identify any important fragments in Med23 or Med13, which may reflect improper selection of fragment boundaries. Due to a lack of available structural information, we arbitrarily divided up the proteins. However, this may only result in partial domains or even unstructured peptides attached to a GFP molecule. Thus, attempted fragmentation of Med13 and Med23 may benefit from a different set of criteria when choosing fragment boundaries. Respecting boundaries of helical domains or other predicted structural cues might provide better results. Alternatively, the large GFP moiety may interfere with the normal function of these fragments. To solve this problem, we could return to a bicistronic vector system and utilize a smaller tag, such as Flag, to detect expression of Mediator subunit fragments. While measurement of GFP fluorescence would then be uncoupled from expression level of the fragment of interest, this could nevertheless provide valuable information about the roles of pieces of these subunits in AML cells. An alternative approach to this fragmentation study, and one that has become increasingly feasible since the outset of this line of experimentation, is CRISPR scanning with Cas9 and guide RNAs that carpet the protein of interest. This would generate a series of insertions and deletions across the protein that could then be screened in a negative selection manner to determine which regions of these Mediator subunits cannot be altered in AML cells. A preliminary pilot study of Med12 in this manner, using low guide RNA coverage of early exons and the PQL domain only, did indeed pick up the PQL domain as a requirement in RN2 cells. Further density of guide RNA coverage could highlight the exact parts of this domain that facilitate necessary protein-protein interactions in this cell type.

Finally, important interaction surfaces on Mediator subunits may not consist of consecutive sequences of amino acids. Instead, they may involve complex structural conformations that

require fragments of proteins from different regions of the subunit. In this case, our approach would not be successful. As an alternative strategy, we could exploit known or novel interaction partners of Mediator subunits to determine whether they 1) are functionally required in AML cells and 2) whether this requirement results from an interaction with Mediator complexes. For example, TF activation domains are often discrete elements within the protein that could be overexpressed to determine if dominant negative effects—such as squelching—occur. A good candidate to attempt this approach with is Brd4, whose bromodomains, ET domain, and C-terminal domain could all be over-expressed in AML cells to determine if they disrupt crucial interactions. Pulldowns of any critical domains could then be used to identify the specific interaction partner in AML cells that results in negative selection.

Further work on the PQL, PQLS and PQLT domains should be aimed at identifying relevant interaction partners in AML. Mass spectrometry of any unique bands in the pulldowns, or of GST-PQLS-coated beads incubated in AML cell nuclear extracts, could be used identify interaction partners of PQLS. An important control for this would be a parallel pulldown in MEF cells, which display little sensitivity to PQLS expression. In this way, unique protein requirements in AML that operate to maintain leukemogenesis through interaction with this segment of the Mediator complex can be identified. A deep understanding of the binding mechanics between the PQLS, PQLT or whole PQL domain and the identified protein partner could suggest methods to disrupt this interaction for therapeutic purposes in AML.

Finally, it will be important to determine that PQL, PQLS, and PQLT overexpression overlapping gene expression changes as does knockdown of Med12. A number of factors could

contribute to an imperfect overlap, including limited knockdown of Med12 by shRNAs but aggressive overexpression of the PQL domains and the fact that the PQL domain is likely required for only a fraction of the overall function of Med12. Nevertheless, PQL domain overexpression results in myeloid differentiation of AML cells when the level of overexpression is not too high, and this observed phenotypic overlap should be confirmed with RNA-seq experiments.

Chapter VI - Future Directions & Perspectives

The work presented here represents a detailed examination of the role of the Mediator complex in AML. Mediator is a conserved 30-subunit complex that arose in yeast and is required for activator-induced transcription—as well as some basal transcription—in all higher organisms (Poss et al., 2013). Mediator is thought to serve as a molecular bridge that connects sequence-specific TFs with general transcription machinery, including Pol II (Malik and Roeder, 2010). TFs are thought to bind to DNA and then recruit Mediator through interactions with their preferred Mediator complex subunits (Malik and Roeder, 2010). Mediator has been proposed to have key roles at every subsequent step of transcription, including enhancer-promoter looping, assembly of the pre-initiation complex, including recruitment of Pol II, and regulation of Pol II pausing (Allen and Taatjes, 2015).

Given that AML frequently harbors transcription that is perturbed at various levels, including via mutant transcription factors, aberrant DNA methylation patterns, and deregulated chromatin architecture, we reasoned that this disease would depend on the function of this crucial mediator of RNA Polymerase II-dependent transcription (Dohner et al., 2015; Figueroa et al., 2010b). Moreover, alterations in transcription programs that contribute to the divergence of normal and

leukemic blood development could be exploited by a differential dependence on certain Mediator subunits. Thus, we had strong rationale to obtain a better understanding the role of Mediator in AML. In particular, we were interested in determining whether the modular nature of Mediator—that is, the fact that individual subunits can be knocked out with only very precise transcriptional deficits—might provide a means to harness the aberrant transcriptional processes in AML for therapeutic purposes. In addition, because Mediator's first mammalian isolation included Brd4, we asked whether, in AML, Mediator cooperates with Brd4 to maintain leukemogenic gene expression programs (Jiang et al., 1998).

6.1 – BET inhibition and super-enhancers in AML

We previously showed that AML is hypersensitive to Brd4 inhibition, and that the BET inhibitor JQ1 selectively suppresses some transcripts in AML cells while leaving many unaffected (Zuber et al., 2011c). Ever since a therapeutic window for BET inhibition in hematologic malignancies was demonstrated, the mechanism by which these molecules achieve transcriptional selectivity has been an area of immense interest (Loven et al., 2013). The prevailing model proposes that sites of extraordinary Brd4, histone acetylation, and Mediator occupancy, termed super-enhancers, are preferentially perturbed by JQ1 treatment and can thus explain its selectivity (Loven et al., 2013). This is in part because it was noted that, on average, Brd4 occupancy is more sensitive to JQ1 treatment at super-enhancer elements than at other elements in the genome (Loven et al., 2013). Super-enhancers are often located near cell state-defining genes, and are disproportionately affected by disease-associated polymporphisms (Hnisz et al., 2013).

These properties are attractive features of elements that can explain the cell type-specific and selective transcriptional output of BET inhibition.

There are a number of possible explanations for the observation that super-enhancers are sensitive to JQ1 treatment, none of which have yet been verified. Firstly, the biophysical properties of these elements and their associated genes may be inherently different. For example, a more rapid turnover of super-enhancer-associated proteins may lead to an apparently quicker effect of BET inhibitors, which block Brd4 from re-binding to acetylated proteins it has disengaged. This may be supported by studies of chromatin localization of JQ1 that found a greater localization of the drug to super-enhancer elements, suggesting that Brd4 proteins at these elements is more accessible to the drug, perhaps through a great on/off rate (Anders et al., 2014).

The half-life of super-enhancer-associated gene transcripts may also be inherently shorter. Transcript measurements such as RNA-seq and RT-qPCR assess the steady-state pool of RNA in a cell at a given time point after perturbation. Even if all transcription were affected equally by JQ1, shorter half-life transcripts would appear to be more severely affected by these types of assays. Measurements of nascent transcription, such as GRO-seq or similar methods, could help address whether super-enhancer-associated genes are indeed preferentially affected by BET inhibition. Measurement of typical- and super-enhancer-associated transcript half-lives, such as with actinomycin treatment, could also shed light on this aspect of super-enhancers. It should be noted, however, that an inherent instability of, for example, the *Myc* mRNA, would not explain why *Myc* transcription is selectively sensitive to JQ1 treatment in AML but not MEF cells, for

example. Nevertheless, a recent study found that translation of some transcripts, including a familiar list of Myc, Myb, Cdk6, and a number of ETS TFs, is preferentially affected in T-ALL by a natural drug product—silvestrol, which is believed to inhibit eIF4a—because of the presence of G-quadruplexes in the 5'-UTRs of their mRNAs that render them dependent on this particular RNA helicase for their efficient translation (Wolfe et al., 2014). Thus, precedent exists for context-dependent alterations in biophysical properties of nucleotides.

Teleological explanations for these hypothetical properties of super-enhancers and their associated genes' transcripts could center on the finding that super-enhancers are often cell type-specific and disease relevant (Hnisz et al., 2013). These types of genes, in contrast to housekeeping genes, may be under much tighter regulation and may thus be more sensitive to external stimuli.

An alternative hypothesis regarding the hypersensitivity of Brd4 to JQ1 at super-enhancers arises from the observation that many different TFs can be found at these elements (Hnisz et al., 2013; Roe et al., 2015). This accumulation of a diverse complement of TFs occupying one element could result in a large number of low-affinity interactions for Brd4. With many opposing TFs vying for Brd4's attention, their interactions may be more transient in nature and this could be reflected in a greater impact of JQ1 on these elements. Additionally, the fact that so many different proteins occupy the same regions, as determined by ChIP studies, may indeed be a reflection of a dynamic type of locus with a high rate of exchange of factors, since not all proteins can occupy the same DNA sequences at a single time.

A more trivial explanation for the super-enhancer bias could be the "further to fall" idea. Super-enhancers are simply defined as the most heavily occupied regions of the genome. Thus, any perceived increase in sensitivity may simply be due to a greater ease of detecting changes in occupancy at this larger scale.

While we do find super-enhancer associated genes to be transcriptionally suppressed slightly more than the average gene in response to JQ1 treatment in AML cells, we also observed that many super-enhancer associated genes, including *Hoxa9*, are wholly unaffected by BET inhibition (Eaton et al., 2015; Zuber et al., 2011c). Thus the super-enhancer concept, though compelling, leaves much to be explained about how BET inhibition works.

6.1.1 – JQ1 evicts Mediator from a subset of cis elements in AML

In our studies in Chapter II, we found that JQ1 rapidly evicts Mediator complexes at only at a small number of genomic elements in AML cells. When overlapped with Med1-defined super-enhancers, over a third of these JQ1-sensitive Mediator elements are not super-enhancers, and less than half of super-enhancers experience a severe loss of Mediator in response to JQ1 treatment. Importantly, JQ1-sensitive Mediator elements are associated with genes that are suppressed to a significantly greater degree than simply super-enhancer-associated genes. Moreover, those super-enhancers at which Mediator is lost following JQ1 treatment appear to be the only super-enhancers associated with JQ1-suppressed transcripts. Put another way, loss of Mediator occupancy in the genome appears to be a defining feature of JQ1-mediated transcriptional suppression in AML.

Mediator has frequently been described as a molecular bridge that is recruited to chromatin by direct interaction with TFs and that then aids in assembly of the pre-initiation complex (Allen and Taatjes, 2015; Malik and Roeder, 2010; Poss et al., 2013). Its discovery was prompted by the observation that exogenous expression of a TF could siphon Mediator complexes away from other TFs, suggesting that TFs are an attractive force for Mediator (Gill and Ptashne, 1988). Thus, our results are surprising because it appears that at a subset of elements in the AML genome, BET-inhibitor-induced loss of Brd4 is sufficient to displace Mediator. At this subset of elements, we have previously shown that TF occupancy is unperturbed by JQ1 treatment, suggesting the observed loss of Mediator occupancy is not an indirect consequence of a JQ1 effect on TF occupancy. This implies that Brd4 can support or replace the function of TFs to recruit Mediator. Importantly, the vast majority of Mediator occupancy seems to be stable in the face of BET inhibition, suggesting that the existing paradigm of TF recruitment of Mediator is not irrelevant in the AML context. Nevertheless, the subset of loci at which JQ1 treatment leads to Mediator displacement, and therefore the subset at which Mediator depends on Brd4 for chromatin occupancy, is related to genes with known importance in leukemia disease pathogenesis.

This finding raised the possibility that Mediator undergoes alternative, Brd4-dependent recruitment to some locations in the genome. To better understand the properties of the elements at which this happens, we analyzed the JQ1-sensitive Med1 regions for the TFs that occupy them. By utilizing TF DNA-sequence motif searching, we found that JQ1-sensitive Med1 sites harbor a greater density of motifs recognized by C/EBP and Myb TFs. This also corresponded with a greater occupancy of these TFs in AML cells by ChIP-sequencing.

Notably, we previously identified a direct interaction between C/EBP, Myb and Brd4 (Roe et al., 2015), raising the possibility that in certain contexts, this direct TF-Brd4 interaction intercepts any potential affinity between the TF and Mediator and leads to Brd4-dependent recruitment of the complex. Because this Brd4-dependent recruitment of Mediator also does not occur at all TF sites in the genome, biochemical validation of this TF preference for Brd4 binding could be used to shed light onto the nature of this interaction. For example, an *in vitro* competition assay may reveal that acetylated Myb or C/EBP TFs have a higher affinity for Brd4 than for Mediator. In this case, the coactivators at these sites, particularly the activity of lysine acetyltransferases, could have a profound impact on the occupancy of Mediator. Given that higher levels of Myb and C/EBPα and β were found at JQ1-sensitive Mediator sites, a simple explanation of the JQ1-eviction result may be that basal levels of TFs still directly recruit Mediator, but excess levels of these TFs instead attract Brd4, which is then somehow required to stabilize Mediator occupancy.

Notably, our genomewide analysis of Brd4 occupancy after Med12 or Med23 knockdown also highlighted the same regions as preferentially sensitive to Mediator perturbation. This suggests that an inherent property of these elements, such as a higher degree of lability, results in their sensitivity to various perturbations. Whatever the reason, it is clear that both Brd4 and Mediator closely regulate this shared set of *cis* elements and their associated genes.

6.2.2 – The function of select Mediator subunits is required in AML

Our analysis of Mediator occupancy and the transcriptional response to JQ1 suggested that Mediator might be required for the maintenance of the AML state in a manner analogous to Brd4. Since we determined that Brd4 is required for Mediator occupancy at key elements in the AML genome, that loss of Mediator from these elements led to loss of transcription at the associated genes, and that knockdown of Med12 and Med23 preferentially evicted Brd4 from these elements, we reasoned that directly perturbing Mediator would result in similar phenotypic consequences as JQ1 inhibition of Brd4 in AML.

To this end, we designed an shRNA library targeting each of the 33 subunits of Mediator. This study identified a number of Mediator subunits that are required for the proliferation of AML cells. Crucially, shRNAs targeting four of these subunits—Med12, Med13, Med23, and Med24—did not affect the proliferation of untransformed iMEFs despite equivalent knockdown in AML and MEF cells. This result supported a selective requirement of these subunits in AML maintenance. Our MEF counter-screen also suggested a general role for some Mediator subunits, such as Med8, Med28, and Med30, in supporting cell proliferation.

An important consequence of BET inhibition in AML cells is the release of a differentiation blockade and subsequent myeloid maturation of AML blasts (Zuber et al., 2011c). Supporting an overlapping function of Brd4 and Mediator, we found that knockdown of Mediator subunits, similarly induced myeloid differentiation of RN2 cells. In contrast, some subunits, such as Med8 and Med26, did not result in similar differentiation of AML cells. Interestingly, Med26 has been described to preferentially occur in Mediator complexes that lack a kinase module, raising the

possibility that kinase module-containing Mediator complexes functionally overlap with Brd4 while kinase-independent Mediator does not (Malik and Roeder, 2010). Finally, we also found via RNA-seq analysis that the phenotypic overlap of Brd4 and Med12 or Med23 knockdown occurs as a result of perturbation of the same genes. This suggests that these coactivator proteins are responsible for maintaining the same leukemogenic transcription programs in AML.

The three head subunits we identified as general requirements for cell proliferation subunits have not before been described to have general roles in transcription. Med8 has previously been found to bind the Rpb4 subunit of Pol II and the TATA Binding Protein of TFIID (Lariviere et al., 2006; Sharma et al., 2006). Interestingly, Med28 and Med30 are metazoan-specific subunits. Thus, while our screen did not highlight some Mediator subunits that had been previously described as essential, such as Med17 (Holstege et al., 1998), it raises the possibility that the function of such subunits has been replaced from yeast to mammals. Med28 was initially discovered as Magicin, a cytoskeletal-associated protein that interacts with Merlin and Grb2, although it is now a well-appreciated member of the Mediator complex (Wiederhold et al., 2004). Interestingly, Med28 knockdown was found to result in a loss of Med8 expression in NIH3T3 cells (Beyer et al., 2007). It was also found to associate preferentially with kinase-module-containing Mediator complexes (Paoletti et al., 2006). Our RNA-seq analysis indicated that knockdown of Med28 resulted in gene expression changes that overlapped with Brd4 and Med12/Med23 in RN2 cells, and unlike the other head subunits we identified as essential in RN2 cells, Med28 knockdown induced myeloid differentiation of this cell type. It would therefore be interesting to determine whether this is a result of an increased association with Brd4-interacting Mediator complexes. Interestingly, Med28 knockdown also led to smooth-

muscle differentiation in NIH3T3 cells and Med28 deletion leads to embryonic lethality that results in part from a reduced pluripotency (Beyer et al., 2007; Li et al., 2015). This raises the possibility that Med28 plays a more general role in maintaining undifferentiated states, a model supported by studies that identified an enhanced capacity for reprogramming in MEF cells overexpressing Med28 (Li et al., 2015). Further, it is important to understand whether our observed effects of Med28 knockdown in iMEFs are due to loss of nuclear or cytoskeletal Med28. To determine this, Med28 knockdown could be rescued with a Med28 transgene that is modified to contain a nuclear localization or a nuclear export signal. If the nuclear export signal-Med28 rescues knockdown of Med28 in MEF cells, it would suggest that cytoskeletal Med28, and not Mediator complex-associated Med28, is essential for iMEF proliferation.

6.2 – Artificial localization of Mediator to study Mediator function in live cells

We next attempted to validate the role of Mediator as a partner of Brd4 in AML. We hypothesized that forcing Mediator complex localization to a site where it is normally released after JQ1 treatment would subvert the suppressive effects of JQ1 on the transcription of associated genes. We attempted to tether Mediator complexes the genome using dCas9, but were unsuccessful in forming intact complexes on chromatin. While our efforts did not result in the tethering of Mediator complexes to discrete loci in the genome, this remains a worthwhile pursuit. As discussed in Chapter III, there are a number of strategies that could be attempted in order to achieve Mediator tethering *in vivo*. For example, changing the length of the linker that connects dCas9 and the Mediator subunit could result in a greater degree of freedom for the "bait" subunit to assume the necessary conformation to recruit Mediator complexes. A different

chromatin context than the nucleosome-, TF-, and coactivator-free region that we chose as the landing pad may also improve the chances of complex formation. Additionally, an alternate "anchor" to dCas9, such as a TF DBD, may better recapitulate necessary features to tether Mediator on chromatin. This last option is most compelling because it also would provide the opportunity to simultaneously rescue many genes from the transcriptional effects of JQ1. These efforts would help establish the role of Mediator as an effector of Brd4 in AML.

However even beyond this system's ability to define Mediator's role in Brd4 target gene transcription, Mediator tethering has a lot of utility in a number of other systems. Despite its discovery necessitating heroic feats of biochemistry, Mediator is most often studied in the *in vitro* system (Conaway et al., 2005; Malik and Roeder, 2010). Even recently, a Mediator complex was reconstituted from purified proteins to define the minimal composition of Mediator in a test tube, and this was used to suggest that Med14 is an absolutely essential scaffold subunit for any Mediator activity in solutions (Cevher et al., 2014). Yet much of what we know about Mediator underscores the highly context-dependent nature of this complex's function in actual cells, including its subunit composition, structure, and positive or negative effects on transcription (Poss et al., 2013). Thus, studying Mediator biology on chromatin templates in solutions may limit our ability to truly understand its contributions to transcription. The ability to direct formation of Mediator complexes could provide powerful insights into Mediator biology *in vivo*. For example, tethering Mediator with various tagged TF DBDs could shed light onto the long-standing question of whether each Mediator complex necessarily contains the full complement of non-kinase-module subunits. Furthermore, while Mediator has been demonstrated to assist in PIC formation, this is difficult to uncouple from the contribution of

144

the recruiting TF and the TFs other interacting partners, including acetyltransferases and chromatin remodelers. Indeed, some studies find that Mediator requires chromatin remodelers to be recruited to chromatin, while others find the inverse relationship (Bhoite et al., 2001; Lemieux and Gaudreau, 2004). By tethering Mediator to an "off" gene in a cell, we could begin to understand the actual contribution of Mediator alone to PIC formation, or the proper coactivator- and chromatin-context required for this fundamental function of the Mediator complex.

Using tethering, we can also attempt to understand the actual role of Mediator in enhancer-promoter looping. While knockdown of Mediator subunits was shown to abrogate such loops in ES cells, this effect was observed after a number of days, long after transcription of associated genes was lost (Kagey et al., 2010). Thus, it was unclear whether the looping effect was direct or an indirect consequence of transcriptional shutdown. Notably, short-term treatment of JQ1 only modestly perturbs looping at the Myc locus despite dramatic loss of Mediator from Myc enhancer and promoter elements (Shi et al., 2013). This raises the possibility that Mediator is involved in formation but not maintenance of loops, if it is involved in looping at all. By tethering Mediator to enhancer and promoter elements in cells, we can observe the contribution of Mediator to relevant enhancer-promoter loops in an inducible manner.

Furthermore, in combination with knockdown of select subunits, we may be able to use Mediator tethering to define precise contributions of these individual subunits to the various described Mediator functions. For example, we know that certain TFs recruit Mediator through interactions with preferred subunits. However once Mediator is recruited, it is unclear whether

the partner subunit plays any further role beyond its requirement for the recruitment event itself. By tethering Mediator in, for example, Med23 knockdown conditions, we may be able to understand whether Elk1 uses Med23 for steps subsequent to Mediator recruitment. We may also begin to understand, in a similar manner, how the various observed shapes of Mediator affect its functional output. By tethering Mediator in different conformations at a gene (perhaps via different anchors), we may observe different transcriptional outputs that shed light on the impact of structure on function in this amorphous complex.

Mediator tethering could also be used to dissect enhancer and promoter properties. Tethering Mediator in between two genes could result in the establishment of an active enhancer-like element that, given Mediator's purported role in enhancer-promoter contacts, could attempt to loop to one of the two neighboring genes. This choice of which gene is chosen for the loop with a *de novo* Mediator enhancer could be studied to understand this process.

Finally, tethered Mediator complexes could add to our understanding of the properties of eRNAs. These noncoding, enhancer-derived transcripts have been reported to be essential for the recruitment of Mediator complexes to some enhancer elements, and knockdown of select eRNAs resulted in loss of Mediator at its associated enhancer and loss of looping between that enhancer and its chosen promoter (Lai et al., 2013). However, consistent with its crucial role in Pol II-dependent transcription, Mediator was also shown in the same study to be essential for the production of eRNAs (Lai et al., 2013). By tethering Mediator to an enhancer element, we can determine whether Mediator is indeed required for the production of eRNAs. Furthermore, by knocking down the eRNA transcript, we can determine whether the eRNAs are functional for

anything beyond Mediator recruitment and attempt to understand the roles of eRNAs and Mediator in loop formation and maintenance. Deleting a TSS or TATA box at an enhancer, and thus deleting the eRNA, but tethering Mediator to this enhancer could also parse out the recruitment of Mediator from the production of the eRNA and from the rest of eRNA and Mediator functions at enhancers.

6.3 - Identifying crucial domains of Mediator in AML

Given the described roles of Mediator in transcription regulation and our results that suggest a hypersensitivity of AML cells to Mediator perturbation, we attempted to understand what gives rise to the differential sensitivity to some subunits between untransformed cells and AML cells and whether this could be exploited for therapeutic purposes. In Chapter V, we identified a small region of Med12 whose overexpression appears to be selectively toxic to AML cells relative to iMEFs. This region, termed PQLT, comprises the first 100 amino acids of the PQL domain, the region of Med12 that has been demonstrated to interface with transcription coactivators, corepressors, and TFs (Ding et al., 2008; Kim et al., 2006; Zhou et al., 2012). Notably, the overexpression of the Med12 fragment has a much faster phenotype than knockdown of Med12, possibly because there is no lag before protein turnover can occur after knockdown. This raises the intriguing possibility of leveraging this fragment of Med12 as a novel peptide therapeutic. One possible way to convert this genetic tool into a therapy is to use an 11-R methodology, adapted from the HIV TAT protein, to create a cell-permeable peptide (Matsui et al., 2003). Similar techniques have been used to create a peptide inhibitor of SALL4 TF function in AML

and hepatocellular carcinomas (Gao et al., 2013; Yong et al., 2013). The peptide fragment screening method developed here could also be widely applied to other intrinsically disordered proteins.

Using a first-pass set of fragments, we were able to define key regions of both Med12 and Med24. While similar analysis of Med13 and Med23 did not reveal dominant negative fragments, proper delineation of fragment boundaries could improve this success rate. Moreover, further application of this methodology could help to define heuristics that would aid in fragment boundary choice. Furthermore, this approach could be complemented with site-specific genetic disruption by CRISPR/Cas9 to insure that the effects observed with fragment overexpression are not simply due to unintended toxic consequences, such as unfolded protein responses. Similarly, initial CRISPR scanning of targets of interest could identify hotspot regions that do not tolerate small insertions and deletions. Fragment design, which has the advantage over CRISPR of generating potentially therapeutic peptides, could then focus on the area encompassing these identified regions rather than spanning whole genes at low coverage.

A key basic question that arises from this work is how the interaction between Mediator and Brd4 occurs in AML. We have identified numerous Mediator subunits that appear to regulate similar pathways as Brd4 in AML, thus nominating potential candidate subunits as Brd4 interaction partners. Given the amorphous and dynamic nature of Mediator's structure and composition, it is possible that in AML a number of different subunits can interact with Brd4 either separately or in concert. Previous studies have identified interactions of Brd4 with Med12 (Dawson et al., 2011; Jang et al., 2005) and demonstrated a key role for Med23 in mediating this

interaction (Wang et al., 2013). Our transcriptomic data support critical Brd4-supporting functions of these subunits in AML, as shRNA perturbation of Med12 and Med23 regulated an identical set of genes as Brd4 in RN2 cells and both of these subunits were rapidly removed from chromatin following JQ1 treatment. A recent study supports an interaction between Brd4 and Med1, a subunit that did not score in our shRNA screen (Shu et al., 2016). This appears to be bromodomain-dependent, as JQ1 perturbs the interaction (Shu et al., 2016), although hyperphosphorylation of Brd4 changes the nature of the Med1 interaction to make it bromodomain-independent (Shu et al., 2016).

Understanding the interaction between Brd4 and Mediator would allow us to understand the unexpected mode of Mediator recruitment to chromatin that we found in our study. Numerous IP-MS studies of Mediator and Brd4 have been conducted with variable results that may be due to a weak or dynamic interaction between Mediator and Brd4. Thus, a functional genetic approach may be useful to understand the nature of the Brd4-Mediator interaction. While the approach we developed to identify the PQL domain as an important fragment of Med12 could be useful here, in order to more rapidly identify key Brd4-interacting Mediator surfaces across the entire complex, a more high-throughput approach would be useful. To this end, CRISPR scanning of the Mediator complex could be employed. In this endeavor, guide RNAs that cover the coding sequence of all Mediator subunits could be introduced into RN2 cells that stably express Cas9. Guide RNAs that lead to erroneous editing of crucial regions of Mediator, thereby creating insertions, deletions, and mutations in these regions, would be negatively selected from the pool of guide RNAs.

Scanning Mediator subunits with a high density of guide RNAs should accomplish a number of things. As confirmation of proper assay function, subunits that scored in our shRNA screen should be confirmed by this alternative screening approach. More importantly, many aspects of Mediator biology may be highlighted by this approach. For example, essential Mediator interactions will be defined by this CRISPR scan, including the interaction with Brd4. In addition, hotspot regions on Mediator subunits may also represent regions that interact with TFs, with GTFs, or with other Mediator subunits. All of these possibilities warrant follow-up. Because of the vast number of potentially critical interactions that Mediator may participate in, this approach could be coupled with scanning of specific genes of interest, such as Brd4, the Myb TF, or any transcriptional machinery, to identify regions on these proteins that, when mutagenized, disrupt interactions with purified Mediator complexes. As stated in Chapter V, an important pursuit prompted by our studies is to understand the Mediator-interacting TFs that hijack the complex to drive leukemia. A CRISPR-created mutation in a Mediator subunit that disrupts interaction with a key leukemogenic TF, such as Myb, would provide valuable information not only regarding the identity of the Mediator subunit interaction partner, but also of the specific region on the Mediator subunit involved in that interaction.

Further interesting information that could arise from CRISPR scanning of Mediator involves the subunits that interact with general transcription machinery, including GTFs. Earlier studies identified subunits such as Med17 and Med11 as participating in key interactions with Rbp3 and TFIIH, respectively (Esnault et al., 2008; Soutourina et al., 2011). However, neither Med17 nor Med11 scored in our screen, suggesting that either these subunits do not participate in these interactions in mammalian AML cells or that these interactions might not be critical for

transcriptional output in AML. Alternatively, as discussed earlier, shRNA knockdown of these subunits may have been insufficient to identify these subunits as essential for AML proliferation. CRISPR mutagenesis of these subunits may generate alleles that negatively select in AML cells to address this possibility, and may further highlight crucial regions of these subunits that mediate interaction with transcription machinery components. Alternatively, since the Mediator head subunits Med8, Med28, and Med30 scored in our screen, these subunits may participate in previously undescribed interactions with general transcription machinery, including RNA Pol II and GTFs. Scanning these subunits with CRISPR can highlight regions important for the interaction of these subunits with any transcriptional partners.

This approach also has the potential to map the architecture of the AML Mediator complex. Some of the negatively selected guides will mutagenize regions of Mediator subunits that are involved in intra-complex interactions. For example, a region of Med12 that is responsible for connecting it to Med13 and the rest of the core Mediator complex would likely be essential for the function of Med12 in AML. Because Mediator assumes highly dynamic and context-dependent conformations, these intra-Mediator interactions could prove distinct between cell types or even between loci in the AML genome. For example, Med13 at the *Myc* enhancers may be connected to core Mediator via one region of the protein, while at the GAPDH promoter, because Mediator may assume a different conformation, Med13 may be connected to core Mediator via a different region. In an untransformed cell type, recruitment of Mediator to the *Myc* locus may similarly result in a different conformation of Mediator. Thus, disruption of CRISPR-highlighted regions of Mediator subunits might result in functional consequences only under select, AML conditions. This would ultimately leverage the highly dynamic nature of the

Mediator complex into a compelling means by which oncogenic transcription can be specifically disrupted while normal transcription is spared.

6.4 - Perspectives and Implications

Taken together, the results presented here highlight the essentiality of the Mediator complex in AML. In this disease, we have identified Mediator's place in the Brd4 pathway, where it serves as a coactivator in the leukemogenic transcription network maintained by this BET protein. This is in contrast to the only other defined role of Mediator. The Mediator kinases Cdk8 and Cdk19 have been shown to restrain expression of super-enhancer associated genes, essentially working in opposition to Brd4. Interestingly, other subunits of the kinase module, despite being absolutely required for functional Cdk8/Cdk19 kinase activity, do not harbor this repressive function. Instead, Med12, of the kinase module, as well as the tail module subunit Med23, positively regulate the Brd4 gene network and their inhibition leads to identical phenotypic consequences, as does Brd4 inhibition. The identification of Mediator subunits that are required in AML cells but not in MEF cells, a pattern that recapitulates the Brd4 phenotype, raises the possibility that Mediator can be an important therapeutic target in AML.

Importantly, targeting Mediator would, based on our results, target the same pathway as the BET inhibitors that are currently being evaluated in clinic. Thus far, approximately 25% of patients have demonstrated responses to BET inhibition (Dombret et al., 2014). While this is an extremely encouraging result at such an early stage in the clinical development of BET inhibitors, it does raise the possibility that patients will not experience universal therapeutic

benefit from this class of molecules. We demonstrated Mediator displacement to be a faithful predictor of transcriptional response to JQ1 in AML cells. Thus, one possibility is that Mediator displacement, or lack thereof, could be a useful biomarker of clinical response to BET inhibition. Alternative modes of Mediator recruitment, such as classical, direct binding of TFs to Mediator, could also result in resistance to this class of therapeutic by uncoupling Mediator chromatin localization from BET proteins. A recent report suggests that resistance to BET inhibitors in triple-negative breast cancer can result from hyperphosphorylation of Brd4 that leads to its increased association with Med1 (Shu et al., 2016). In these resistant cells, Brd4 is no longer evicted from chromatin following JQ1 treatment, and it was suggested that the stronger interaction with Med1 stabilizes Brd4 on chromatin (Shu et al., 2016). While our data would support a different route of Mediator-Brd4 co-localization on chromatin, this result is nonetheless intriguing as it highlights the importance of this coactivator crosstalk. It will be interesting to determine whether this mechanism can be recapitulated in leukemias or whether Mediator's dependence on Brd4 for its localization to certain chromatin loci in leukemia precludes this Mediator-dependent route of BET inhibitor resistance. Intriguingly, a report of BET inhibitor-resistant AML cells identified a recurrent point mutation in Med15 (Fong et al., 2015). While the impact of this mutation on resistance and on Mediator-Brd4 interaction is unknown, it is conceivable that it results in a gain-of-function interaction between Mediator and a new TF or in a gain of affinity for an existing Mediator interaction with a TF or with Brd4. Another study found that gain of β-catenin function resulted in resistance to BET inhibition in AML cells (Rathert et al., 2015). Since Med12 is known to directly interact with β-catenin through its PQL domain, it would be interesting to determine whether this direct TF-Mediator

interaction confers on-chromatin stability to Mediator and thus contributes to BET inhibitor resistance in these cells (Kim et al., 2006).

While resistance to BET inhibition has not yet emerged clinically, another possible means of generating BET inhibitor resistance could be gatekeeper mutations in the bromodomains of Brd4 that preserve acetyl-lysine binding capacity but have reduced or eliminated affinity for pocket-binding chemical probes. In this hypothetical case, our data nominate Mediator as a useful alternative target to therapeutically disrupt the same transcriptional pathway. While it has been reported that targeting Mediator kinases in AML leads to opposing, activating effects on Brd4 transcriptional target genes, we have identified subunits in Mediator that are instead required for support of the Brd4-driven AML transcription network. Developing ways to target these subunits could thus prove useful in patients that develop resistance to BET inhibitors in the clinic.

Chapter VII - Methods

Cell culture

RN2 cells were derived as previously described (hematopoietic stem and progenitor cells were isolated from C57BL/6 fetal livers (embryonic days 13.5-15) and retrovirally transduced with MLL-AF9-rtTA3 and $NRAS^{G12D}$-firefly luciferase transgenes (Zuber et al., 2011a)). RN2 cells were cultured in RPMI-1640 with 10% FBS and Penicillin/streptomycin at 7.5% CO_2. iMEF cells, Plat-E cells, and 293T cells were cultured in DMEM with 10% FBS and penicillin/streptomycin at 5% CO_2. Transfections were carried out using Calcium phosphate or PEI transfection methods.

shRNA screen

LMN-shRNA vectors were individually packaged in retroviruses using the Plat E cell line and calcium phosphate transfection methods. Media was changed 6 hours after transfection and virus was collected 24 hours and 32 hours post-transfection. A murine MLL-AF9/$Nras^{G12D}$ cell line was infected with these viruses in a one-by-one manner with the addition of polybrene. GFP percentage, corresponding to the percent of cells that were infected with an shRNA, was tracked using a Guava Easycyte (Millipore). The loss of GFP over time corresponds to the loss of the shRNA from the population (in favor of uninfected cells), and thus is a suitable measure of the

toxicity of an shRNA. Results were normalized to day 2 post-infection, the first time point recorded for this study. The sequences of all Mediator shRNAs used in this study can be found at the end of this chapter.

RT-qPCR

Total RNA was extracted from cells using TRIzol (Invitrogen) according to the manufacturer's instructions. Isolated RNA was treated with DNase I to eliminate contaminating genomic DNA. qScript reverse transcriptase mix was used to synthesize cDNA according to the manufacturer's protocol. The resulting 20μL of cDNA was diluted 1:10 in water. Results were quantified by qPCR performed using SYBR green on an ABI 7900HT Fast Real-Time PCR machine, and normalized to *Gapdh* within each sample and to shRen across all samples.

Antibodies for ChIP

Brd4: Bethyl A301-985 (2μg/IP)

Med1: Bethyl A300-793A (2μg/IP)

Med12: Bethyl A300-774 (5μg/IP)

Med23: Bethyl A300-423A (5μg/IP)

Cdk9: SC-484(1.6μg/IP)

Pol2: Ab5408 (2μg/IP)

Flag-M2: Sigma F1804 (5μg/IP)

ChIP-qPCR

5-20 million RN2 cells were crosslinked in 1% formaldehyde for 20 minutes and quenched for 10 minutes in 0.125M Glycine. Nuclear lysates were sonicated in 5-20-million cell batches using a BioRuptor water bath sonicator for 10 minutes (30 seconds on, 30 seconds off). Sonicated chromatin was pre-cleared using rabbit IgG and agarose beads followed by addition of the antibody and beads (Brd4 and Med1) or was directly incubated with the relevant antibody for two hours followed by addition of magnetic beads (Med12, Med23, Cdk9, Pol2S2, Flag, and Brd4 in shMed12 and shMed23 conditions) and overnight rotation at 4°C. After extensive washing, crosslinks were reversed overnight at 65°C. DNA was treated with RNAse and proteinase K, purified using the QIAGEN PCR purification kit, and analyzed using an ABI 7900HT Fast Real-Time PCR machine and SYBR green. Input samples were diluted for a standard curve and ChIP results were normalized to these standards.

ChIP-Seq

120 million RN2 cells were crosslinked in 1% formaldhyde for 20 minutes and quenched for 10 minutes in 0.125M Glycine. Nuclear lysates were sonicated in 20-million cell batches using a BioRuptor water bath sonicator. Sonicated chromatin was pre-cleared using rabbit IgG and agarose beads (for Brd4 and Med1 ChIP-seq in DMSO or JQ1 conditions) or was directly incubated with the relevant antibody for two hours followed by addition of magnetic beads (for Brd4 ChIP-seq in shMed12 and shMed23 conditions, for Med12, and for Med23. IP with the relevant antibodies was done overnight at 4°C with rotation. After extensive washing as previously described (Steger et al., 2008), crosslinks were reversed overnight at 65°C. DNA was treated with RNAse and proteinase K and purified using the QIAGEN PCR purification kit. 1µL of ChIP samples were diluted 1:20 to test ChIP success by qPCR. For detailed procedure of

library construction, see the end of this section. Briefly, libraries were then constructed using the TruSeq ChIP Sample Prep kit from lllumina. Libraries underwent a final amplification step of 15 PCR cycles and were analyzed using a Bioanalyzer with a High Sensitivity chip (Agilent). Libraries were single-end sequenced on a HiSeq2000 with reads of 50bp.

ChIP-seq analysis

1. Analysis of previously published data:

    a. 5,135 high confidence Brd4 peaks were previously defined (Roe et al., 2015) based on overlapping multiple Brd4 ChIP-sequencing data sets and selection of MACS-called peaks with a false discovery rate below 1 and a fold enrichment over input of greater than 10.

    b. For density plots, these 5,135 high confidence Brd4 peaks were used.

        i. To construct these density plots, sequencing reads from each ChIP-seq dataset used were binned into 500 20bp bins around the MACS-defined summit of the 5,135 high confidence Brd4 peaks. These peaks were ranked in descending order of Brd4 sequencing reads. The resulting matrices were converted into a heat map using Java TreeView 1.1.6r4.

    c. The following RN2 ChIP-seq datasets from (Roe et al., 2015) were used:

        i. C/EBPα, C/EBPβ, Myb, Erg, Fli1, Pu.1, Brd4 (untreated).

2. Analysis of new ChIP-seq datasets

a. For all new ChIP-seq datasets, 50bp sequence reads were mapped to the mm9 reference murine genome using the BOWTIE algorithm. To call peaks, the MACS algorithm, version 1.4.2, was used.

b. To define a set of high confidence Med1 peaks in the AML genome, the MACS output for each of the three Med1 ChIP-seq replicates generated for these studies (untreated, and two DMSO-treated replicates) was intersected as follows:

   i. MACS-called peaks were filtered to retain only those peaks with an FDR value of less than or equal to one and a fold-enrichment over input of at least 10.

   ii. The intervals of each data set were intersected sequentially (intersection was defined as a minimum overlap of 1bp) to retain only those peaks that appeared in all three Med1 ChIP-seq data sets.

   iii. The result of this was a set of 10,604 high confidence Med1 peaks. Overlapping these peak boundaries with the areas within 2kb from a RefSeq-defined transcription start site in the mm9 genome resulted in 6328 Med1 peaks being assigned to putative promoter elements. The remaining 4276, TSS-distal Med1 peaks were considered putative enhancer elements.

3. Identification of Med1 super-enhancers

   a. As described before (Loven et al., 2013), the ROSE algorithm was used to stitch together any of the 10,604 Med1 peaks that occurred within 12.5kb of each other. The recommended TSS-exclusion zone of ±2.5kb was used.

From the resulting 4,056 stitched regions, 178 super enhancers were called by ROSE.

4. Defining JQ1-sensitivity at Med1 peaks

   a. For all subsequent analyses, including calculations of fold change in Med1 occupancy after JQ1 treatment, BOWTIE-mapped *.bam files were filtered to remove redundant reads. This helps to reduce PCR bias that is gained during the ChIP-seq library generation steps.

   b. To calculate the fold change of Mediator and Brd4 following JQ1 treatment, ChIP-seq reads that mapped to high confidence Med1 intervals (a minimum overlap of 1bp was required for a read to be considered as mapping to a MACS peak) were counted in both replicates of DMSO and JQ1 datasets as well as for Brd4 DMSO- and JQ1-treated datasets used here. Normalization to the total number of unique mapped reads between paired DMSO and JQ1 datasets was applied. A fold change of Med1 at each peak was then calculated by dividing the number of each reads in the JQ1 sample by the number of reads at each peak in the corresponding DMSO sample. The fold change at each peak across both replicates of the Med1 DMSO and JQ1 ChIP-seq experiment was averaged, and this average fold change of Med1 was used to plot the fold changes and to identify the 200 most JQ1-sensitive Med1 regions in RN2 cells.

   c. To calculate the fold change at super-enhancers, the same methodology was used, but the stitched intervals supplied by ROSE were used instead of the 10,604 high confidence Med1 peaks.

d. Subsequently, the ROSE-stitched intervals were intersected with the 200 most sensitive Med1 unstitched peaks (minimum overlap of 1bp was required). This resulted in 75 super-enhancers being defined as "sensitive" and 103 super-enhancers defined as "insensitive" to JQ1.

5. Associating Med1 peaks with genes

    a. The GREAT algorithm (McLean et al., 2010) defines "gene neighborhoods" in several ways. The default method of gene neighborhood definition is -1kb from a gene body to +5kb from the end of a gene body, plus an extension of up to 1Mb until the next gene neighborhood. Peaks falling within these gene neighborhoods are then attributed to these genes. The default GREAT definition of gene neighborhoods was used for the results presented here. Using the alternative gene neighborhood definition (e.g., using the two nearest genes to a peak) produced similar results. We supplied GREAT with the 10,604 Med1 regions as well as with the 178 stitched super-enhancer regions for further gene assignments.

    b. To improve accuracy of gene assignment, the genes assigned to the 200-sensitive Med1 peaks and to the 178 super enhancers were manually corrected in the following ways when possible:

        i. If a peak occurred in the intron of an expressed gene (FPKM > 5) and GREAT did not assign it to that gene, this expressed gene was used instead.

        ii. If GREAT assigned a peak to a gene that is not expressed in RN2 cells (FPKM < 5), the following corrections were attempted:

161

1. If GREAT also assigned a second possible gene to a peak, and if this second gene is expressed in RN2 cells, this gene was used.

2. If GREAT did not assign a second gene, or if the second gene was also not expressed, the expressed genes in the immediate vicinity (i.e. the closest gene in either direction) was used.

3. The *Myc* enhancers we have previously characterized as looping to the *Myc* gene in RN2 cells (Shi et al., 2013), were assigned to *Myc* instead of the nearby (unexpressed) *Gsdmc*.

4. If none of the above criteria could be met, the peak was left unassigned to a gene.

c. Genes assigned to 200 JQ1-sensitive Med1 peaks and to super-enhancers can be found in Table S3.

6. Calculating the fold change in gene expression of Med1 peak-associated genes.

a. Calculating the fold change in gene expression as was done using the RN2 DMSO vs RN2 6h JQ1 RNA-seq from Roe et al, 2015. "All expressed genes" refers to all genes with FPKM > 5 in this data set. "JQ1 Insensitive Med1 Peaks" refers to all genes assigned to the 10,404 Med1 peaks not included in the set of 200 most JQ1-sensitive Med1 peaks. If a gene was associated with multiple peaks (e.g., Myc enhancers corresponding to Myc), only one instance of that gene was counted.

RNA isolation for RNA-seq

Cells were lysed in 1mL TRIzol reagent and incubated for 3 minutes at room temperature. 200µL chloroform was added and samples were shaken and incubated for 10 minutes at room temperature. After 15 minutes of centrifugation, supernatants were added to 500µL isopropanol. RNA was precipitated and immediately used for library construction.

RNA-seq library construction

For detailed procedure of library construction, see the end of this section. Briefly, the Illumina TruSeq sample prep kit v2 was used to make libraries for RNA-sequencing. From the RNA isolated as described above, 2µg of RNA was poly-A selected and enzymatically fragmented. cDNA was synthesized from this fragmented RNA using Super Script II master mix (Life Technologies). cDNA was then end-repaired and A-tailed, and finally adapters were ligated onto the cDNA.

Libraries were single-end sequenced on a HiSeq2000 machine with 50bp reads.

RNA-seq Data Analysis

Reads were trimmed for quality purposes and mapped to the mm9 reference genome using the Tophat algorithm. Differentially expressed genes were identified using the Cuffdiff algorithm. Structural RNAs were masked for this purpose. Transcripts with an FPKM value of greater than 5 were used for subsequent analyses. Average fold change of a transcript between two independent hairpins targeting Med12, two independent hairpins targeting Med23, or two replicates of a hairpin targeting Renilla luciferase were averaged. shMed12 and shMed23 values were then compared to shRen values to calculate the fold change in gene expression for these experiments.

Gene Set Enrichment Analysis

Gene set enrichment analysis was performed using the preranked GSEA option for RNA-seq. To the library of 10,348, a number of additional gene sets were added, including those defined in RN2 cells based on Brd4 shRNA experiments, Myb shRNA experiments, and based on JQ1 treatment.

Flow Cytometry differentiation analysis

RN2 cells transduced with doxycycline-inducible TRMPV-Neo shRNAs were treated with 0.1 μg/mL doxycycline for 4 days to induce shRNA expression. Cells were inclubated in APC-cKit or APC–Mac1 antibodies (BioLegend) at a 1:200 dilution in FACS buffer for 1 hour at 4°C. Cells were washed three times in FACS buffer and analyzed on an LSRII. Analysis was done using FlowJo.

May-Grünwald-Giemsa staining

RN2 cells transduced with doxycycline-inducible TRMPV-Neo shRNAs were treated with 0.1 μg/mL doxycycline for 4 days to induce shRNA expression. 500,000 cells/mL were resuspended in FACS buffer and spun onto glass slides using a Cytospin 2 Centrifuge at 500rpm for 5 min. Staining was done using May-Grünwald and Giemsa solutions (Sigma) according to manufacturer's protocols. Images were acquired on a Zeiss Observer Microscope at 40x.

CRISPR targeting of kinase domains

Guides were designed targeting the kinase domains of Cdk8 and Cdk19 and cloned into the LRG vector or LRCherry vector. They were introduced into RN2s expressing Cas9 and negative selection was carried out as previously described (Shi et al., 2015). GFP+/mCherry+ cells were measured on an LSRII.

dCas9 fusion constructs

dCas9 was obtained as a gift from the Blobel lab. From their MSCV-dCas9-mCherry plasmid, the 3x-Flag-NLS-dCas9 was PCR-amplified and isolated. The stop codon was removed and replaced with a linker sequence of Gly-Gly-Gly-Gly-Ser-Gly-Gly-Gly-Gly-Ser. This was cloned into the MSCV-Puromycin vector using the XhoI AND ClaI sites. Mediator subunits were PCR amplified from RN2 cell cDNA (using the longest isoform when applicable) and cloned into a ClaI-digested MSCV-dCas9-Puro vector using the InFusionHD kit (ClonTech).

Annexin V staining

RN2 cells were treated with doxycycline for 48-96 hours to induce expression of Med12 fragments or with Senexin B at the indicated concentration. Cells were resuspended in Annexin V binding buffer (which contains 0.14M NaCl and Calcium, necessary for Annexin V binding) and incubated for 15 minutes at room temperature with DAPI and APC-Annexin V. Stained cells were analyzed on an LSR-II flow cytometer.

Senexin use

For cell culture experiments, Senexin compounds were received in solution in DMSO and were diluted to working concentrations.

For *in vivo* experiments, solid free-base Senexin B was first dissolved in 0.2M HCl (1mL per 50mg Senexin). The mixture was heated at 55°C until fully dissolved, and then dried in a speed vac for 2 hours at 45°C. Dry compound was transferred to a 50 mL tube and dissolved in isotonic buffer (10mM Citrate pH 6.0, 150 mM NaCl). Concentration was checked on a nano-drop (OD ~1.10), filtered in a 0.2 μm syringe, and stored at -20°C. Solutions were heated at 55°C prior to injection. As a vehicle control, isotonic buffer (citrate buffer) was used.

Animal studies

The Cold Spring Harbor Animal Care and Use Committee approved all mouse experiments included in this work. To enrich for engraftment-competent leukemia cells, $1x10^6$ RN2 cells were injected into the tail vein of sub-lethally irradiated mice. As the mice succumbed to disease (based on moribund appearance), they were sacrificed and their spleens were harvested by gently mashing between two glass slides, filtered through 100 μm cell strainers, and frozen. For drug trial leukemia transplantation, $5x10^4$ of these cells were injected in the tail vein of sub-lethally irradiated recipient mice (5.5 Gy, 24 h before transplantation). Whole-body bioluminescent imaging was performed every other day using an IVIS100 system (Caliper LifeSciences). Leukemic mice were sacrificed at terminal disease stage, as determined by whole body signal in bioluminescent imaging and moribund appearance.

Western Blotting

For whole-cell extracts, cells were lysed directly with 2x Laemmli Sample Buffer (BioRad) supplemented with β-mercaptoethanol. Extracts from ~50,000 cells were loaded into each lane of an SDS-PAGE gel, followed by transfer to nitrocellulose membrane for immunoblotting with the appropriate antibodies. For nuclear extracts, RN2 or iMEF cell pellets were washed in PBS, resuspended in Buffer A2 (10 mM Hepes-KOH pH 7.9, 1.5 mM $MgCl_2$, 10 mM KCL) and incubated on ice for 30 min to allow cell lysis to occur. Nuclei were separated by centrifugation, resuspended in Buffer C2 (20 mM Hepes-KOH pH 7.9, 25 % glycerol, 420 mM NaCl, 1.5 mM $MgCl_2$, 0.2 mM EDTA) and incubated on ice for 30 min, prior to spinning in a table-top centrifuge at 13,200 rpm, 4 °C for 10 min.

Generation and use of TtNGP vector

The TtIGP vector was modified as follows: IRES-GFP was digested out using XhoI and ClaI, followed by insertion of an NLS-GFP construct to create the TtGFP-empty vector. Mediator subunits were then PCR cloned from HeLa cDNA and inserted into a ClaI-digested TtGFP-empty vector using the InFusionHD cloning kit.

GST-PQLS expression and purification

When *e. coli* culture OD600 was 0.6-0.8, it was induced with 0.2 mM IPTG (Roche) and returned to a 30°C incubator for 3 hours. Bacteria was then spun down at 7200 RCF at 4°C for 5 minutes and resuspended in BC500 buffer (20 mM Tris-HCl, PH 8.0, 500 mM KCl, 0.5 mM EDTA, 1% NP-40, 20% glycerol, 1 mM DTT, 0.5 mM PMSF, 2 μl/ml Protease Inhibitor Cocktail (Sigma-Aldrich)) plus 2 mg/mL of lysozyme (Sigma-Aldrich). After incubation at room temperature for 5 minutes, 1% Triton-X 100 was added and cells were further lysed with

sonication (5 seconds on/off at 40% amplitude) for 2 minutes. Cells were spun down at 14,000 RCF for 10 minutes and supernatant was incubated with GST-sepharose 4B beads (GE) overnight at 4°C. After four washes with BC500 and one wash with PBS (supplemented with 20% glycerol, 1% NP-40 and 0.5 mM PMSF), proteins were eluted with Reduced Glutathione Solution (10 mM glutathione dissolved in 50 mM Tris, pH 8; Sigma-Aldrich) and stored at - 80°C.

RNA-seq Library Construction

Make RNA Bead Plate
1) Dilute 2ug total RNA to 25µL with RNA water in a PCR plate with an RBP barcode
2) Vortex RNA Purification (Oligo-dT beads), add 25µL to each well, mix by pipetting
3) Seal with adhesive film
     a. 65°C – 5 min, 4°C forever
4) Incubate at RT on bench for 5 min
5) Remove adhesive film, place the plate on the magnetic stand for 5 min
6) Discard all supernatant, remove plate from stand
7) Add 100µL Bead Washing Buffer, pipette up and down, magnetic stand for 5 min, remove supernatant
8) Add 25µL centrifuged, thawed Elution Buffer to each well, mix by pipetting
9) Cover with a film, centrifuge, then elute the RNA
     a. 80°C for 2 min, 25°C forever
10) Remove the seal. Add 25µL centrifuged, thawed Bead Binding Buffer to each well. Incubate at RT for 5 min, then place on magnetic stand for 5 min.
11) Remove all supernatant, take the plate off the stand
12) Add 10µL Fragment, Prime, Finish Mix to each well, pipette up and down to mix
13) Seal the plate, centrifuge, then
     a. 94°C for 8 min, 4°C forever

Synthesize first strand cDNA
1) Remove seal, place plate on magnetic stand
2) Transfer 8.5µL to a new row
3) Mix 0.5µL SuperScriptII with 3.5µL First Strand Synthesis Act D Mix for each sample
4) Add 4µL of FSSADM/SSII mix to each well, pipette to mix, seal, spin, then
     a. 25°C for 10m, 42°C for 50m, 70°C for 15m, 4°C forever
5) Remove plate, spin, remove seal

Synthesize second strand cDNA
1) Add 12.5µL of thawed, centrifuged Second Strand Marking Master Mix to each well, pipette to mix
2) Seal the plate, spin, incubate at 16°C for 1 hour, remove the seal, let plate stand at RT until at RT
3) Vortex AMPure XP beads, add 45µL of beads to each well, pipette up and down to mix
4) Incubate at RT for 15 min, then put on the magnetic stand
5) Remove and discard 135µL supernatant
6) Add 200µL 80% EtOH, remove, repeat (two washes)
7) Air dry (remove any EtOH carefully with the vacuum!)
8) Add 27.5µL Resuspension Buffer to each well, pipette up and down to mix, incubate for 2 min, then place on the magnetic stand
9) Transfer 25µL of supernatant (dsCDNA) to a new row.

End Repair
1) Add 5µL Resuspension Buffer to each sample with 25µL dsCDNA
2) Add 20µL End Repair Mix to each well, pipette up and down to mix, seal
3) Incubate 30°C for 30 min, spin

4) Add 80µL vortexed AMPure XP beads, pipette up and down to mix
5) Incubate at RT for 15 min, place on magnetic stand until clear
6) Remove 127.5µL supernatant, remove 127.5µL supernatant again
7) Add 200µL of 80% EtOH without disturbing beads, incubate 30s, remove, repeat
8) Air dry for 15 min (remove residual with a vacuum CAREFULLY!)
9) Add 9.8µL Resuspension buffer to each well, pipette up and down to mix, incubate for 2 min, then place on magnetic stand.
10) Transfer 8.75µL of supernatant (end-repaired dsCDNA) to a new row

Adenylate 3' Ends
1) Add 6.25µL of thawed A-Tailing Mix to each well, pipette to mix
2) Seal plate, centrifuge, then
   a. 37°C for 30min, 70°C for 5min, 4°C forever
3) Remove the plate, spin

Ligate Adapters
1) Add 1.25µL Resuspension Buffer to each well
2) Add 1.25µL Ligation Mix to each well
3) Add 1.25µL of appropriate RNA Adapter to each well. Pipette up and down to mix.
4) Seal/centrifuge the plate, then
   a. Incubate at 30°C for 12 minutes (Cold Start)
5) Remove the plate, spin, then add 2.5µL of Stop Ligation Buffer to each well, pipette to mix.
6) Vortex AMPure XP beads, add 21µL of beads to each well, mix well
7) Incubate the plate at RT for 15 minutes
8) Place on the magnetic stand, then remove 79.5 µL of supernatant
9) Wash twice with 180µL of 80% EtOH, remove all ethanol in the latter wash
10) Add 11.5µL of Resuspension buffer to each well, resuspend well
11) Transfer 10µL to a new well. Freeze at -20°C.

Day 2
Enrich DNA fragments
1) Add 2.5µL of PCR Primer cocktail to each well
2) Add 12.5µL of PCR Master Mix to each well
3) Seal the plate, centrifuge, then
   a. 98°C for 30s
   b. 15 cycles: 98°C for 10s, 60°C for 30s, 72°C for 30s
   c. 72°C for 5min, 4°C forever
4) Remove the plate, centrifuge
5) Add 25µL vortexed AMPure XP beads to each well, mix well
6) Incubate at RT for 15 min
7) Place on the magnetic stand, remove as much supernatant as possible
8) Wash with 180µL 80% EtOH twice, removing ethanol with vacuum at the end
9) Add 21.5µL Resuspension buffer to each well, mixing well, then incubate for 2 min
10) Place on the magnetic stand, save 20µL as the library!

ChIP-seq Library preparation

End repair on ChIP DNA
- Thaw "End Repair Mix" and "Resuspension buffer" at RT

1) Add 10µL of Resuspension buffer to 50µL of ChIP DNA *in a PCR plate.*
2) Add 40µL of End Repair Mix to the 60µL of Resuspended ChIP DNA. Cover with a strip of adhesive film (for qPCR plates) Vortex gently to mix, spin at 2k RPM for 1 minute.
   a. Incubate at 30°C for 32 minutes (cold start)
3) Clean up with MinElute kit:
   a. 500µL PB, 750µL PE, 16.5µL EB

3' Adenylation
- Thaw "A-tailing Mix" at RT
1) Add 2.5µL of Resuspension buffer to each well.
2) Add 12.5µL of A-Tailing mix to each well, gently pipette up and down 10 times to mix, spin plate.
3) Run the following program in a thermocycler with a 100°C heated lid:
   a. 37°C for 30 min
   b. 70°C for 5 min
4) Immediately proceed to *ligate adapters* after the program drops to 4°C
5) In this incubation time, pour the gel!
   a. 150mL, 2% agarose gel (3g Agarose), 10µL EtBr. Enough wells for spacer lanes on either side of samples

Ligate Adapters
- Prepare:
   a. Thaw at RT: Stop ligation buffer
2) Add 2.5µL of resuspension buffer to each well
3) Add 2.5µL of Ligation Mix to each tube (put this mix back at -20°C immediately)
4) Add 2.5µL of the appropriate RNA adapter index to each well, pipette up and down (thaw them right before use, freeze again immediately).
5) Centrifuge the PCR plate
6) Place the tubes in the 30°C cycler for 12 minutes (cold start).
7) Remove the plate, add 5µL of Stop Ligation Buffer, mix by pipetting.
8) Vortex the beads, add 42.5µL of beads to each well, pipette up and down to mix.
   a. Incubate at RT for 15 min
9) Place the plate on the magnetic stand for a couple minutes
10) Remove as much supernatant as possible from each well
11) Wash with 180µL of fresh 80% EtOH, incubate for 30 seconds, and remove all supernatant. Do all of this without disturbing the beads. Repeat (two washes).
   a. After the second wash, wait briefly to dry a bit and then get rid of ALL the ethanol (use a vacuum carefully to help).
12) Resuspend the dried pellet with 52.5µL resuspension buffer, gently mix by pipetting.
13) Incubate at RT for 2 min.

14) Place the plate back on the stand for 2 min.
15) Transfer 50μL of supernatant to new wells.

Purify ligation products
1) Add 10μL of 6x Gel Loading Dye to each well of the PCR plate
    a. 5μL 100bp ladder
2) Load all of the samples into their own wells, with a one-well gap btwn ladder and sample. Run.
3) Photograph the gel before slicing
4) Slice the gel at exactly 250bp-300bp using a razor blade.
5) Use the MinElute Gel Extraction kit to purify each sample
    a. Only incubate in QC at ***ROOM TEMPERATURE*** (not 50°C), vortexing every 2 minutes instead.
    b. Elute in 25μL of EB
6) Transfer 20μL of each eluted sample into a well of a PCR plate

Enrich DNA fragments
1) Add 5μL of PCR primer cocktail to each well
2) Add 25μL of PCR master mix to each well. Pipette up and down to mix.
3) Perform the following with a 100°C pre-heated lid to amplify the plate:
    a. 98°C for 30 s
    b. 15x: 98°C for 10s, 60°C for 30 s, 72°C for 30s
    c. 72°C for 5min
4) Remove the plate. Add 50μL of vortexed beads to each well (which already has 50μL of PCR sample). Pipette up and down to mix.
5) Incubate at RT for 15m
6) Place on magnetic stand for 5 min
7) Discard 95μL of supernatant
8) Add 200μL of 80% EtOH, wait 30 sec, remove all supernatant. Repeat (2 washes).
9) Air Dry on the stand for 15 min, remove from the magnetic stand.
10) Resuspend the dried pellet in 17.5μL resuspension buffer
11) Incubate at RT for 2 min
12) Place on the magnetic stand for 5 min.
13) Transfer 15μL of the supernatant to a new plate.
14) Bioanalyze the DNA!

Table 7-1 – Mediator-targeting shRNA sequences used in Chapter II

Ccnc.337	TGCTGTTGACAGTGAGCGCTAGGTGAACATCTTAAATTAATAGTGAAGCCACAGA TGTATTAATTTAAGATGTTCACCTAATGCCTACTGCCTCGGA
Ccnc.374	TGCTGTTGACAGTGAGCGATACTGCTACAGTCTATTTCAATAGTGAAGCCACAGA TGTATTGAAATAGACTGTAGCAGTAGTGCCTACTGCCTCGGA
Ccnc.573	TGCTGTTGACAGTGAGCGCTACAGGATGAATCATATACTATAGTGAAGCCACAGA TGTATAGTATATGATTCATCCTGTAATGCCTACTGCCTCGGA
Ccnc.575	TGCTGTTGACAGTGAGCGCCAGGATGAATCATATACTAGATAGTGAAGCCACAGA TGTATCTAGTATATGATTCATCCTGTTGCCTACTGCCTCGGA
Ccnc.576	TGCTGTTGACAGTGAGCGAAGGATGAATCATATACTAGAATAGTGAAGCCACAGA TGTATTCTAGTATATGATTCATCCTGTGCCTACTGCCTCGGA
Ccnc.878	TGCTGTTGACAGTGAGCGCCAGGGTTATTTTAAAACTGTATAGTGAAGCCACAGA TGTATACAGTTTTAAAATAACCCTGATGCCTACTGCCTCGGA
Cdk19.1964	TGCTGTTGACAGTGAGCGCCACGCTGTAGCAATCATTATATAGTGAAGCCACAGA TGTATATAATGATTGCTACAGCGTGATGCCTACTGCCTCGGA
Cdk19.2994	TGCTGTTGACAGTGAGCGACAGAATCAAGAGGAAATGTAATAGTGAAGCCACAGA TGTATTACATTTCCTCTTGATTCTGGTGCCTACTGCCTCGGA
Cdk19.3289	TGCTGTTGACAGTGAGCGCCAGCATAAGGATGCTTATAAATAGTGAAGCCACAGA TGTATTTATAAGCATCCTTATGCTGATGCCTACTGCCTCGGA
Cdk19.3295	TGCTGTTGACAGTGAGCGCAAGGATGCTTATAAACAGTAATAGTGAAGCCACAGA TGTATTACTGTTTATAAGCATCCTTATGCCTACTGCCTCGGA
Cdk19.4411	TGCTGTTGACAGTGAGCGATAGATACTATTTTGTTCTCTATAGTGAAGCCACAGA TGTATAGAGAACAAAATAGTATCTACTGCCTACTGCCTCGGA
Cdk19.4709	TGCTGTTGACAGTGAGCGAAGAGATCAAGAGACAAGTCTATAGTGAAGCCACAGA TGTATAGACTTGTCTCTTGATCTCTGTGCCTACTGCCTCGGA
Cdk8.1828	TGCTGTTGACAGTGAGCGCAACACAGATTATGTTAACAAATAGTGAAGCCACAGA TGTATTTGTTAACATAATCTGTGTTTTGCCTACTGCCTCGGA
Cdk8.1831	TGCTGTTGACAGTGAGCGAACAGATTATGTTAACAAAATATAGTGAAGCCACAGA TGTATATTTTGTTAACATAATCTGTGTGCCTACTGCCTCGGA
Cdk8.1832	TGCTGTTGACAGTGAGCGCCAGATTATGTTAACAAATAATAGTGAAGCCACAGA TGTATTATTTTGTTAACATAATCTGTTGCCTACTGCCTCGGA
Cdk8.2374	TGCTGTTGACAGTGAGCGCAAGGTTGTTCGCACATTTTTATAGTGAAGCCACAGA TGTATAAAAATGTGCGAACAACCTTTTGCCTACTGCCTCGGA
Cdk8.2548	TGCTGTTGACAGTGAGCGCAACAAGGTGTTATGTAATAAATAGTGAAGCCACAGA TGTATTTATTACATAACACCTTGTTTTGCCTACTGCCTCGGA
Cdk8.774	TGCTGTTGACAGTGAGCGATGGACAGAATATTCAATGTAATAGTGAAGCCACAGA TGTATTACATTGAATATTCTGTCCAGTGCCTACTGCCTCGGA
Med1.1096	TGCTGTTGACAGTGAGCGACACTGCTATTTTCTCAATAAATAGTGAAGCCACAGA TGTATTTATTGAGAAAATAGCAGTGCTGCCTACTGCCTCGGA
Med1.1449	TGCTGTTGACAGTGAGCGATACAGACGACTTCATTGCCAATAGTGAAGCCACAGA TGTATTGGCAATGAAGTCGTCTGTACTGCCTACTGCCTCGGA
Med1.1466	TGCTGTTGACAGTGAGCGACCAAAGTTGTTCAAAGATGTATAGTGAAGCCACAGA TGTATACATCTTTGAACAACTTTGGCTGCCTACTGCCTCGGA
Med1.445	TGCTGTTGACAGTGAGCGCAAGGGTCTTGTTAATCTGTATTAGTGAAGCCACAGA TGTAATACAGATTAACAAGACCCTTATGCCTACTGCCTCGGA
Med10.195	TGCTGTTGACAGTGAGCGCCAGGACATAGATAAATGCAGATAGTGAAGCCACAGA TGTATCTGCATTTATCTATGTCCTGTTGCCTACTGCCTCGGA
Med10.341	TGCTGTTGACAGTGAGCGACAAGATCGACACAATGAAGAATAGTGAAGCCACAGA TGTATTCTTCATTGTGTCGATCTTGCTGCCTACTGCCTCGGA
Med10.342	TGCTGTTGACAGTGAGCGAAAGATCGACACAATGAAGAAATAGTGAAGCCACAGA TGTATTTCTTCATTGTGTCGATCTTGTGCCTACTGCCTCGGA
Med10.346	TGCTGTTGACAGTGAGCGCTCGACACAATGAAGAAATTTATAGTGAAGCCACAGA TGTATAAATTTCTTCATTGTGTCGATTGCCTACTGCCTCGGA
Med10.381	TGCTGTTGACAGTGAGCGCCAGGAACTTTCTAAAGTGTTTTAGTGAAGCCACAGA

	TGTAAAACACTTTAGAAAGTTCCTGATGCCTACTGCCTCGGA
Med10.795	TGCTGTTGACAGTGAGCGCCAGATGTTGTGTATAAGAACATAGTGAAGCCACAGA TGTATGTTCTTATACACAACATCTGATGCCTACTGCCTCGGA
Med11.311	TGCTGTTGACAGTGAGCGAAAGGACTGTCAAATGGCTCTATAGTGAAGCCACAGA TGTATAGAGCCATTTGACAGTCCTTCTGCCTACTGCCTCGGA
Med11.501	TGCTGTTGACAGTGAGCGAAAGGCAGAAAGGAGAACTGAATAGTGAAGCCACAGA TGTATTCAGTTCTCCTTTCTGCCTTGTGCCTACTGCCTCGGA
Med11.509	TGCTGTTGACAGTGAGCGCAAGGAGAACTGAAGAATCCAATAGTGAAGCCACAGA TGTATTGGATTCTTCAGTTCTCCTTTTGCCTACTGCCTCGGA
Med11.583	TGCTGTTGACAGTGAGCGCTCCACTATGCAAGATCAGACATAGTGAAGCCACAGA TGTATGTCTGATCTTGCATAGTGGAATGCCTACTGCCTCGGA
Med11.844	TGCTGTTGACAGTGAGCGCAAACAGGAACTAAGTGTTTTATAGTGAAGCCACAGA TGTATAAAACACTTAGTTCCTGTTTTTGCCTACTGCCTCGGA
Med11.847	TGCTGTTGACAGTGAGCGCCAGGAACTAAGTGTTTTAATATAGTGAAGCCACAGA TGTATATTAAAACACTTAGTTCCTGTTGCCTACTGCCTCGGA
Med12.3321	TGCTGTTGACAGTGAGCGCCCGCTATAGCTTTGTGTGCAATAGTGAAGCCACAGA TGTATTGCACACAAAGCTATAGCGGTTGCCTACTGCCTCGGA
Med12.401	TGCTGTTGACAGTGAGCGCTCGCAGAGAAGTTAAGGTGTATAGTGAAGCCACAGA TGTATACACCTTAACTTCTCTGCGATTGCCTACTGCCTCGGA
Med12.5755	TGCTGTTGACAGTGAGCGACCCGTGCGATTACCAATGCAATAGTGAAGCCACAGA TGTATTGCATTGGTAATCGCACGGGGTGCCTACTGCCTCGGA
Med12.7441	TGCTGTTGACAGTGAGCGCCAGAAGTTCCGACTAGTTCTATAGTGAAGCCACAGA TGTATAGAACTAGTCGGAACTTCTGTTGCCTACTGCCTCGGA
Med12.8092	TGCTGTTGACAGTGAGCGATAGGTCAAGTGGATAGGTGTATAGTGAAGCCACAGA TGTATACACCTATCCACTTGACCTAGTGCCTACTGCCTCGGA
Med12.8105	TGCTGTTGACAGTGAGCGCTAGGTGTATTACATATAGAAATAGTGAAGCCACAGA TGTATTTCTATATGTAATACACCTATTGCCTACTGCCTCGGA
Med12l.2149	TGCTGTTGACAGTGAGCGCGAGCAGAAGACTGTCAGTCAATAGTGAAGCCACAGA TGTATTGACTGACAGTCTTCTGCTCATGCCTACTGCCTCGGA
Med12l.2476	TGCTGTTGACAGTGAGCGACCCGGAAAATGTGTTCACGAATAGTGAAGCCACAGA TGTATTCGTGAACACATTTTCCGGGGTGCCTACTGCCTCGGA
Med12l.2477	TGCTGTTGACAGTGAGCGACCGGAAAATGTGTTCACGAAATAGTGAAGCCACAGA TGTATTTCGTGAACACATTTTCCGGGTGCCTACTGCCTCGGA
Med12l.3148	TGCTGTTGACAGTGAGCGCCCGGTACAGCTTTGTGTGCAATAGTGAAGCCACAGA TGTATTGCACACAAAGCTGTACCGGTTGCCTACTGCCTCGGA
Med12l.9419	TGCTGTTGACAGTGAGCGCACGGTGAAATATGAAAATAAATAGTGAAGCCACAGA TGTATTTATTTTCATATTTCACCGTATGCCTACTGCCTCGGA
Med13.2219	TGCTGTTGACAGTGAGCGCCACGAAGAAGATGCTATGTCATAGTGAAGCCACAGA TGTATGACATAGCATCTTCTTCGTGTTGCCTACTGCCTCGGA
Med13.2711	TGCTGTTGACAGTGAGCGACCCGAAAATTGTCAAGTTCTATAGTGAAGCCACAGA TGTATAGAACTTGACAATTTTCGGGCTGCCTACTGCCTCGGA
Med13.6382	TGCTGTTGACAGTGAGCGCCAGGTTTGTTTTGGAACAGTATAGTGAAGCCACAGA TGTATACTGTTCCAAAACAAACCTGATGCCTACTGCCTCGGA
Med13.9029	TGCTGTTGACAGTGAGCGACAGGATGATAGATCTAACTTATAGTGAAGCCACAGA TGTATAAGTTAGATCTATCATCCTGCTGCCTACTGCCTCGGA
Med13.9615	TGCTGTTGACAGTGAGCGAAAGCACTATGTTAATACTGTATAGTGAAGCCACAGA TGTATACAGTATTAACATAGTGCTTGTGCCTACTGCCTCGGA
Med13.9618	TGCTGTTGACAGTGAGCGACACTATGTTAATACTGTAATATAGTGAAGCCACAGA TGTATATTACAGTATTAACATAGTGCTGCCTACTGCCTCGGA
Med13l.4998	TGCTGTTGACAGTGAGCGCCAGGATGGACAAGACAGTGTTTAGTGAAGCCACAGA TGTAAACACTGTCTTGTCCATCCTGTTGCCTACTGCCTCGGA
Med13l.7236	TGCTGTTGACAGTGAGCGCCAGCTGCATTCTGTTTATTTATAGTGAAGCCACAGA TGTATAAATAAACAGAATGCAGCTGTTGCCTACTGCCTCGGA
Med13l.7682	TGCTGTTGACAGTGAGCGCTAGGAATATTGTTTCAAAGAATAGTGAAGCCACAGA TGTATTCTTTGAAACAATATTCCTATTGCCTACTGCCTCGGA

Med13l.7683	TGCTGTTGACAGTGAGCGCAGGAATATTGTTTCAAAGAAATAGTGAAGCCACAGA TGTATTTCTTTGAAACAATATTCCTATGCCTACTGCCTCGGA
Med13l.7953	TGCTGTTGACAGTGAGCGATGGGAGAGTCATGCAAACTAATAGTGAAGCCACAGA TGTATTAGTTTGCATGACTCTCCCACTGCCTACTGCCTCGGA
Med14.1200	TGCTGTTGACAGTGAGCGCTCGCTTCAACTAGAAGTATTATAGTGAAGCCACAGA TGTATAATACTTCTAGTTGAAGCGATTGCCTACTGCCTCGGA
Med14.1348	TGCTGTTGACAGTGAGCGCCAGCATCTGTTCACAAAGTTATAGTGAAGCCACAGA TGTATAACTTTGTGAACAGATGCTGTTGCCTACTGCCTCGGA
Med14.1491	TGCTGTTGACAGTGAGCGCAAGCTCCTGATTGACAGTGTATAGTGAAGCCACAGA TGTATACACTGTCAATCAGGAGCTTTTGCCTACTGCCTCGGA
Med14.2425	TGCTGTTGACAGTGAGCGCTCCGATTACAAGGTAGAAATATAGTGAAGCCACAGA TGTATATTTCTACCTTGTAATCGGAATGCCTACTGCCTCGGA
Med14.3568	TGCTGTTGACAGTGAGCGAACCCTAGTTCTCCATATACTATAGTGAAGCCACAGA TGTATAGTATATGGAGAACTAGGGTCTGCCTACTGCCTCGGA
Med14.3981	TGCTGTTGACAGTGAGCGACAGCTGATCAATTCCAATGAATAGTGAAGCCACAGA TGTATTCATTGGAATTGATCAGCTGCTGCCTACTGCCTCGGA
Med15.2717	TGCTGTTGACAGTGAGCGCAAGCATCTCTGTTTTGCAATATAGTGAAGCCACAGA TGTATATTGCAAAACAGAGATGCTTTTGCCTACTGCCTCGGA
Med15.3030	TGCTGTTGACAGTGAGCGCAGGGCTGTCAGTGCTATGATATAGTGAAGCCACAGA TGTATATCATAGCACTGACAGCCCTTTGCCTACTGCCTCGGA
Med15.3053	TGCTGTTGACAGTGAGCGCCAGGCAGATAGGCAGATACTATAGTGAAGCCACAGA TGTATAGTATCTGCCTATCTGCCTGTTGCCTACTGCCTCGGA
Med15.308	TGCTGTTGACAGTGAGCGCTCCGAGATATTCATAACAAGATAGTGAAGCCACAGA TGTATCTTGTTATGAATATCTCGGAATGCCTACTGCCTCGGA
Med15.310	TGCTGTTGACAGTGAGCGACGAGATATTCATAACAAGAAATAGTGAAGCCACAGA TGTATTTCTTGTTATGAATATCTCGGTGCCTACTGCCTCGGA
Med15.718	TGCTGTTGACAGTGAGCGACAGCAACAGTTCCAAGCAGTATAGTGAAGCCACAGA TGTATACTGCTTGGAACTGTTGCTGCTGCCTACTGCCTCGGA
Med16.1098	TGCTGTTGACAGTGAGCGATCGCCTGTGGTTGGTGACAAATAGTGAAGCCACAGA TGTATTTGTCACCAACCACAGGCGAGTGCCTACTGCCTCGGA
Med16.1871	TGCTGTTGACAGTGAGCGACGCCAAGATCACCGATGTTGATAGTGAAGCCACAGA TGTATCAACATCGGTGATCTTGGCGCTGCCTACTGCCTCGGA
Med16.1880	TGCTGTTGACAGTGAGCGCCACCGATGTTGACATCGACAATAGTGAAGCCACAGA TGTATTGTCGATGTCAACATCGGTGATGCCTACTGCCTCGGA
Med16.1881	TGCTGTTGACAGTGAGCGAACCGATGTTGACATCGACAAATAGTGAAGCCACAGA TGTATTTGTCGATGTCAACATCGGTGTGCCTACTGCCTCGGA
Med16.1892	TGCTGTTGACAGTGAGCGCCATCGACAAAGTCATGATCAATAGTGAAGCCACAGA TGTATTGATCATGACTTTGTCGATGTTGCCTACTGCCTCGGA
Med16.1898	TGCTGTTGACAGTGAGCGCCAAAGTCATGATCAACCTGAATAGTGAAGCCACAGA TGTATTCAGGTTGATCATGACTTTGTTGCCTACTGCCTCGGA
Med17.1882	TGCTGTTGACAGTGAGCGCCCGAAGAGTGATGTTTTACAATAGTGAAGCCACAGA TGTATTGTAAAACATCACTCTTCGGATGCCTACTGCCTCGGA
Med17.2803	TGCTGTTGACAGTGAGCGAAAGCTCAAGAGTTCAAGTTCATAGTGAAGCCACAGA TGTATGAACTTGAACTCTTGAGCTTCTGCCTACTGCCTCGGA
Med17.2816	TGCTGTTGACAGTGAGCGCCAAGTTCAGCTTGATCTGCAATAGTGAAGCCACAGA TGTATTGCAGATCAAGCTGAACTTGATGCCTACTGCCTCGGA
Med17.3098	TGCTGTTGACAGTGAGCGACAGATTCAAGCTCCAGACTTATAGTGAAGCCACAGA TGTATAAGTCTGGAGCTTGAATCTGGTGCCTACTGCCTCGGA
Med17.387	TGCTGTTGACAGTGAGCGCTACAGAGATGTGTGTTCTCTATAGTGAAGCCACAGA TGTATAGAGAACACACATCTCTGTAATGCCTACTGCCTCGGA
Med17.768	TGCTGTTGACAGTGAGCGCTAAGAAGATACCAGAAGATTATAGTGAAGCCACAGA TGTATAATCTTCTGGTATCTTCTTATTGCCTACTGCCTCGGA
Med18.1644	TGCTGTTGACAGTGAGCGACCAGCATTGTGTGGTAATAAATAGTGAAGCCACAGA TGTATTTATTACCACACAATGCTGGCTGCCTACTGCCTCGGA
Med18.336	TGCTGTTGACAGTGAGCGATCCGAGGTTTGTGTGACAACATAGTGAAGCCACAGA

	TGTATGTTGTCACACAAACCTCGGAGTGCCTACTGCCTCGGA
Med18.640	TGCTGTTGACAGTGAGCGCCATGAAGGTTGTGGTGTACAATAGTGAAGCCACAGA TGTATTGTACACCACAACCTTCATGATGCCTACTGCCTCGGA
Med18.644	TGCTGTTGACAGTGAGCGAAAGGTTGTGGTGTACAAGATTTAGTGAAGCCACAGA TGTAAATCTTGTACACCACAACCTTCTGCCTACTGCCTCGGA
Med18.835	TGCTGTTGACAGTGAGCGCAAGGCTGATGTGATGAAGAAATAGTGAAGCCACAGA TGTATTTCTTCATCACATCAGCCTTTTGCCTACTGCCTCGGA
Med19.1805	TGCTGTTGACAGTGAGCGCTAGCAAGAGATTCAACAGAGATAGTGAAGCCACAGA TGTATCTCTGTTGAATCTCTTGCTATTGCCTACTGCCTCGGA
Med19.1824	TGCTGTTGACAGTGAGCGCGAGGATGTATTTGTTATGAAATAGTGAAGCCACAGA TGTATTTCATAACAAATACATCCTCTTGCCTACTGCCTCGGA
Med19.284	TGCTGTTGACAGTGAGCGACACCAATTTAATCACACACTATAGTGAAGCCACAGA TGTATAGTGTGTGATTAAATTGGTGCTGCCTACTGCCTCGGA
Med19.335	TGCTGTTGACAGTGAGCGATGGGAAGAAAGTGAAGGAGAATAGTGAAGCCACAGA TGTATTCTCCTTCACTTTCTTCCCACTGCCTACTGCCTCGGA
Med19.631	TGCTGTTGACAGTGAGCGCCAGATCACAAGAAGAAGAAAATAGTGAAGCCACAGA TGTATTTTCTTCTTCTTGTGATCTGATGCCTACTGCCTCGGA
Med19.680	TGCTGTTGACAGTGAGCGCAAGGAAGAAGAAAGAAAGAATAGTGAAGCCACAGA TGTATTCTTTTCTTTCTTCTTCCTTTTGCCTACTGCCTCGGA
Med20.1456	TGCTGTTGACAGTGAGCGAACACATGTTCCTGACACTCAATAGTGAAGCCACAGA TGTATTGAGTGTCAGGAACATGTGTCTGCCTACTGCCTCGGA
Med20.1559	TGCTGTTGACAGTGAGCGCCACCTACTACAGAGACATTTATAGTGAAGCCACAGA TGTATAAATGTCTCTGTAGTAGGTGATGCCTACTGCCTCGGA
Med20.1560	TGCTGTTGACAGTGAGCGAACCTACTACAGAGACATTTAATAGTGAAGCCACAGA TGTATTAAATGTCTCTGTAGTAGGTGTGCCTACTGCCTCGGA
Med20.1566	TGCTGTTGACAGTGAGCGATACAGAGACATTTAACACAAATAGTGAAGCCACAGA TGTATTTGTGTTAAATGTCTCTGTAGTGCCTACTGCCTCGGA
Med20.1614	TGCTGTTGACAGTGAGCGCCAAAGTGTAGGCTGTCAGTTATAGTGAAGCCACAGA TGTATAACTGACAGCCTACACTTTGTTGCCTACTGCCTCGGA
Med20.1988	TGCTGTTGACAGTGAGCGCCAGCTCCTCTCAGCTTCTAAATAGTGAAGCCACAGA TGTATTTAGAAGCTGAGAGGAGCTGATGCCTACTGCCTCGGA
Med21.151	TGCTGTTGACAGTGAGCGCACAGCAATTAATAAAGATCAATAGTGAAGCCACAGA TGTATTGATCTTTATTAATTGCTGTTTGCCTACTGCCTCGGA
Med21.418	TGCTGTTGACAGTGAGCGCCAGCTGAAGACCAGAAGTGTTTAGTGAAGCCACAGA TGTAAACACTTCTGGTCTTCAGCTGTTGCCTACTGCCTCGGA
Med21.707	TGCTGTTGACAGTGAGCGCCAGGATAGATACTGTACTAATTAGTGAAGCCACAGA TGTAATTAGTACAGTATCTATCCTGATGCCTACTGCCTCGGA
Med21.708	TGCTGTTGACAGTGAGCGAAGGATAGATACTGTACTAATATAGTGAAGCCACAGA TGTATATTAGTACAGTATCTATCCTGTGCCTACTGCCTCGGA
Med21.728	TGCTGTTGACAGTGAGCGCAAGGTTCATGATATAATTAAATAGTGAAGCCACAGA TGTATTTAATTATATCATGAACCTTATGCCTACTGCCTCGGA
Med22.1194	TGCTGTTGACAGTGAGCGCTAGGTTCAGGTTCTATAGAGATAGTGAAGCCACAGA TGTATCTCTATAGAACCTGAACCTAATGCCTACTGCCTCGGA
Med22.1341	TGCTGTTGACAGTGAGCGCTGAGATGAGACTGTTGAATAATAGTGAAGCCACAGA TGTATTATTCAACAGTCTCATCTCAATGCCTACTGCCTCGGA
Med22.145	TGCTGTTGACAGTGAGCGAACGGAGCTGTTGTATCGGAAATAGTGAAGCCACAGA TGTATTTCCGATACAACAGCTCCGTCTGCCTACTGCCTCGGA
Med22.477	TGCTGTTGACAGTGAGCGCCAAGCAGTTTCTGATCCTCAATAGTGAAGCCACAGA TGTATTGAGGATCAGAAACTGCTTGATGCCTACTGCCTCGGA
Med22.872	TGCTGTTGACAGTGAGCGATAGGGCCTAGTTTATCAGAAATAGTGAAGCCACAGA TGTATTTCTGATAAACTAGGCCCTAGTGCCTACTGCCTCGGA
Med23.2252	TGCTGTTGACAGTGAGCGAAGGGAACTTGGTGTAAAGATATAGTGAAGCCACAGA TGTATATCTTTACACCAAGTTCCCTGTGCCTACTGCCTCGGA
Med23.2642	TGCTGTTGACAGTGAGCGACAGGAGGTCAGCAACTCAATATAGTGAAGCCACAGA TGTATATTGAGTTGCTGACCTCCTGCTGCCTACTGCCTCGGA

Med23.4061	TGCTGTTGACAGTGAGCGCAAGAGCAAGTAGAGAAGATTATAGTGAAGCCACAGA TGTATAATCTTCTCTACTTGCTCTTTTGCCTACTGCCTCGGA
Med23.4313	TGCTGTTGACAGTGAGCGACACCATGTTCAGATTGGTTTATAGTGAAGCCACAGA TGTATAAACCAATCTGAACATGGTGGTGCCTACTGCCTCGGA
Med23.678	TGCTGTTGACAGTGAGCGCCACAGAGATCAGAAAACTATATAGTGAAGCCACAGA TGTATATAGTTTTCTGATCTCTGTGATGCCTACTGCCTCGGA
Med24.1080	TGCTGTTGACAGTGAGCGAACAGGTCTTGGTGAAGTTGAATAGTGAAGCCACAGA TGTATTCAACTTCACCAAGACCTGTGTGCCTACTGCCTCGGA
Med24.1377	TGCTGTTGACAGTGAGCGACACGGTCACAAACATTCTCAATAGTGAAGCCACAGA TGTATTGAGAATGTTTGTGACCGTGGTGCCTACTGCCTCGGA
Med24.1527	TGCTGTTGACAGTGAGCGACCGGAAATTCATCAATCTGAATAGTGAAGCCACAGA TGTATTCAGATTGATGAATTTCCGGGTGCCTACTGCCTCGGA
Med24.2640	TGCTGTTGACAGTGAGCGCCAGAGAGGACATTGAGGACTATAGTGAAGCCACAGA TGTATAGTCCTCAATGTCCTCTCTGTTGCCTACTGCCTCGGA
Med24.3318	TGCTGTTGACAGTGAGCGACACAGTGTGTATATAAGTTTTTAGTGAAGCCACAGA TGTAAAAACTTATATACACACTGTGGTGCCTACTGCCTCGGA
Med24.3319	TGCTGTTGACAGTGAGCGAACAGTGTGTATATAAGTTTTATAGTGAAGCCACAGA TGTATAAAACTTATATACACACTGTGTGCCTACTGCCTCGGA
Med25.1173	TGCTGTTGACAGTGAGCGATGGGCAGCAGTCAGTATCCAATAGTGAAGCCACAGA TGTATTGGATACTGACTGCTGCCCACTGCCTACTGCCTCGGA
Med25.1398	TGCTGTTGACAGTGAGCGCCCGGAACTCAAGAATGGTTCATAGTGAAGCCACAGA TGTATGAACCATTCTTGAGTTCCGGATGCCTACTGCCTCGGA
Med25.1416	TGCTGTTGACAGTGAGCGCTCAGTTCCACTTCACCAACAATAGTGAAGCCACAGA TGTATTGTTGGTGAAGTGGAACTGAATGCCTACTGCCTCGGA
Med25.1617	TGCTGTTGACAGTGAGCGACCAGGTCATCACCAACCACAATAGTGAAGCCACAGA TGTATTGTGGTTGGTGATGACCTGGCTGCCTACTGCCTCGGA
Med25.2249	TGCTGTTGACAGTGAGCGAACCCAATAAAGTTCCTTTTAATAGTGAAGCCACAGA TGTATTAAAAGGAACTTTATTGGGTGTGCCTACTGCCTCGGA
Med25.237	TGCTGTTGACAGTGAGCGAAGAGTCCTATGTACAATGTCATAGTGAAGCCACAGA TGTATGACATTGTACATAGGACTCTGTGCCTACTGCCTCGGA
Med26.1206	TGCTGTTGACAGTGAGCGCTCGGAGCTCTTACATACCCAATAGTGAAGCCACAGA TGTATTGGGTATGTAAGAGCTCCGATTGCCTACTGCCTCGGA
Med26.2223	TGCTGTTGACAGTGAGCGCCCAGTTTACTAACGATTGCAATAGTGAAGCCACAGA TGTATTGCAATCGTTAGTAAACTGGTTGCCTACTGCCTCGGA
Med26.2268	TGCTGTTGACAGTGAGCGACAGATAGATGGCTGAAATCTATAGTGAAGCCACAGA TGTATAGATTTCAGCCATCTATCTGCTGCCTACTGCCTCGGA
Med26.2398	TGCTGTTGACAGTGAGCGAAAGAGGTTACCTTAACAGCAATAGTGAAGCCACAGA TGTATTGCTGTTAAGGTAACCTCTTCTGCCTACTGCCTCGGA
Med26.2617	TGCTGTTGACAGTGAGCGCCAGTTCAGTCCCAGTTCTTAATAGTGAAGCCACAGA TGTATTAAGAACTGGGACTGAACTGATGCCTACTGCCTCGGA
Med27.203	TGCTGTTGACAGTGAGCGACGGGACCTCAATGAACTGGAATAGTGAAGCCACAGA TGTATTCCAGTTCATTGAGGTCCCGGTGCCTACTGCCTCGGA
Med27.322	TGCTGTTGACAGTGAGCGCCAGCCAGCTTCTGCAAGCATATAGTGAAGCCACAGA TGTATATGCTTGCAGAAGCTGGCTGTTGCCTACTGCCTCGGA
Med27.326	TGCTGTTGACAGTGAGCGACAGCTTCTGCAAGCATACAAATAGTGAAGCCACAGA TGTATTTGTATGCTTGCAGAAGCTGGTGCCTACTGCCTCGGA
Med27.530	TGCTGTTGACAGTGAGCGCCCAGAGATGTCCATTCACTTATAGTGAAGCCACAGA TGTATAAGTGAATGGACATCTCTGGATGCCTACTGCCTCGGA
Med27.712	TGCTGTTGACAGTGAGCGACAGCTACCAAGTGTTCCAGAATAGTGAAGCCACAGA TGTATTCTGGAACACTTGGTAGCTGGTGCCTACTGCCTCGGA
Med28.1955	TGCTGTTGACAGTGAGCGCTCCCTTAATTAGAATATATAATAGTGAAGCCACAGA TGTATTATATATTCTAATTAAGGGAATGCCTACTGCCTCGGA
Med28.2029	TGCTGTTGACAGTGAGCGAAGGAAGGAAGCTCAAAGTGTATAGTGAAGCCACAGA TGTATACACTTTGAGCTTCCTTCCTCTGCCTACTGCCTCGGA
Med28.3454	TGCTGTTGACAGTGAGCGCAACGATGATCAGGTGAGACAATAGTGAAGCCACAGA

	TGTATTGTCTCACCTGATCATCGTTTTGCCTACTGCCTCGGA
Med28.4152	TGCTGTTGACAGTGAGCGCAAGGTGGATATAGAAATGTCATAGTGAAGCCACAGA TGTATGACATTTCTATATCCACCTTATGCCTACTGCCTCGGA
Med28.701	TGCTGTTGACAGTGAGCGCTGGAAGGACTCTGTTGGATAATAGTGAAGCCACAGA TGTATTATCCAACAGAGTCCTTCCAATGCCTACTGCCTCGGA
Med28.809	TGCTGTTGACAGTGAGCGCCAGCTCCTCTAGTACTCTAAATAGTGAAGCCACAGA TGTATTTAGAGTACTAGAGGAGCTGATGCCTACTGCCTCGGA
Med29.1271	TGCTGTTGACAGTGAGCGCTAGCTCCAAAGCAGAAGTGAATAGTGAAGCCACAGA TGTATTCACTTCTGCTTTGGAGCTAATGCCTACTGCCTCGGA
Med29.1521	TGCTGTTGACAGTGAGCGAACCAGGTTCCTGTGTCTACAATAGTGAAGCCACAGA TGTATTGTAGACACAGGAACCTGGTGTGCCTACTGCCTCGGA
Med29.1523	TGCTGTTGACAGTGAGCGACAGGTTCCTGTGTCTACAAAATAGTGAAGCCACAGA TGTATTTTGTAGACACAGGAACCTGGTGCCTACTGCCTCGGA
Med29.1583	TGCTGTTGACAGTGAGCGACCAGATCATCACACTAGGAAATAGTGAAGCCACAGA TGTATTTCCTAGTGTGATGATCTGGGTGCCTACTGCCTCGGA
Med29.500	TGCTGTTGACAGTGAGCGCCAGTACCTGGCTGTCATCAAATAGTGAAGCCACAGA TGTATTTGATGACAGCCAGGTACTGTTGCCTACTGCCTCGGA
Med29.675	TGCTGTTGACAGTGAGCGCCAGGTGGTTCCTGTTGCTGATTAGTGAAGCCACAGA TGTAATCAGCAACAGGAACCACCTGTTGCCTACTGCCTCGGA
Med30.483	TGCTGTTGACAGTGAGCGAACGAGAAATTGTAGAAGTAAATAGTGAAGCCACAGA TGTATTTACTTCTACAATTTCTCGTCTGCCTACTGCCTCGGA
Med30.535	TGCTGTTGACAGTGAGCGAAAGCAGATTATGGATCAATTATAGTGAAGCCACAGA TGTATAATTGATCCATAATCTGCTTCTGCCTACTGCCTCGGA
Med30.594	TGCTGTTGACAGTGAGCGCGAGGAACTAAAGCGATATTTATAGTGAAGCCACAGA TGTATAAATATCGCTTTAGTTCCTCATGCCTACTGCCTCGGA
Med30.595	TGCTGTTGACAGTGAGCGAAGGAACTAAAGCGATATTTAATAGTGAAGCCACAGA TGTATTAAATATCGCTTTAGTTCCTCTGCCTACTGCCTCGGA
Med30.720	TGCTGTTGACAGTGAGCGCAAGTTTCTGTTTTCACTTTAATAGTGAAGCCACAGA TGTATTAAAGTGAAAACAGAAACTTTTGCCTACTGCCTCGGA
Med30.804	TGCTGTTGACAGTGAGCGCTAGGGTATAAATTTTGGTTAATAGTGAAGCCACAGA TGTATTAACCAAAATTTATACCCTATTGCCTACTGCCTCGGA
Med31.1026	TGCTGTTGACAGTGAGCGCTAGGACGTGTATATAATGTATTAGTGAAGCCACAGA TGTAATACATTATATACACGTCCTAATGCCTACTGCCTCGGA
Med31.364	TGCTGTTGACAGTGAGCGATAGCAGGACTCTGAGACCTAATAGTGAAGCCACAGA TGTATTAGGTCTCAGAGTCCTGCTACTGCCTACTGCCTCGGA
Med31.722	TGCTGTTGACAGTGAGCGCAAGAGGTTACTTCAAAGACAATAGTGAAGCCACAGA TGTATTGTCTTTGAAGTAACCTCTTTTGCCTACTGCCTCGGA
Med31.723	TGCTGTTGACAGTGAGCGCAGAGGTTACTTCAAAGACAAATAGTGAAGCCACAGA TGTATTTGTCTTTGAAGTAACCTCTTTGCCTACTGCCTCGGA
Med31.742	TGCTGTTGACAGTGAGCGCAAGCTTTTGTTAATTATCTTATAGTGAAGCCACAGA TGTATAAGATAATTAACAAAAGCTTTTGCCTACTGCCTCGGA
Med31.787	TGCTGTTGACAGTGAGCGACAGAATATGCCAAATATCTAATAGTGAAGCCACAGA TGTATTAGATATTTGGCATATTCTGGTGCCTACTGCCTCGGA
Med4.1018	TGCTGTTGACAGTGAGCGATGGCATGAGACTGAAGAGGAATAGTGAAGCCACAGA TGTATTCCTCTTCAGTCTCATGCCAGTGCCTACTGCCTCGGA
Med4.269	TGCTGTTGACAGTGAGCGCCAGGGAAAAGTTCACCACGAATAGTGAAGCCACAGA TGTATTCGTGGTGAACTTTTCCCTGATGCCTACTGCCTCGGA
Med4.270	TGCTGTTGACAGTGAGCGAAGGGAAAAGTTCACCACGAAATAGTGAAGCCACAGA TGTATTTCGTGGTGAACTTTTCCCTGTGCCTACTGCCTCGGA
Med4.293	TGCTGTTGACAGTGAGCGACAGGCTTTAGAGAAAGAAGTATAGTGAAGCCACAGA TGTATACTTCTTTCTCTAAAGCCTGCTGCCTACTGCCTCGGA
Med4.408	TGCTGTTGACAGTGAGCGATCAAGTCAATAGAGAAAGCAATAGTGAAGCCACAGA TGTATTGCTTTCTCTATTGACTTGAGTGCCTACTGCCTCGGA
Med4.470	TGCTGTTGACAGTGAGCGACACAGGATTAGTGCAAGCAATTAGTGAAGCCACAGA TGTAATTGCTTGCACTAATCCTGTGCTGCCTACTGCCTCGGA

Med6.181	TGCTGTTGACAGTGAGCGCTCAGATGGTTGGAATCGAATATAGTGAAGCCACAGA TGTATATTCGATTCCAACCATCTGATTGCCTACTGCCTCGGA
Med6.460	TGCTGTTGACAGTGAGCGCACAAGAGAAAGTCAAACCTAATAGTGAAGCCACAGA TGTATTAGGTTTGACTTTCTCTTGTTTGCCTACTGCCTCGGA
Med6.461	TGCTGTTGACAGTGAGCGCCAAGAGAAAGTCAAACCTAAATAGTGAAGCCACAGA TGTATTTAGGTTTGACTTTCTCTTGTTGCCTACTGCCTCGGA
Med6.564	TGCTGTTGACAGTGAGCGACACCCAGATTTGTTCAGCAAATAGTGAAGCCACAGA TGTATTTGCTGAACAAATCTGGGTGGTGCCTACTGCCTCGGA
Med6.565	TGCTGTTGACAGTGAGCGAACCCAGATTTGTTCAGCAAAATAGTGAAGCCACAGA TGTATTTTGCTGAACAAATCTGGGTGTGCCTACTGCCTCGGA
Med6.686	TGCTGTTGACAGTGAGCGCCAGCAGACTGTGAGCACTAAATAGTGAAGCCACAGA TGTATTTAGTGCTCACAGTCTGCTGATGCCTACTGCCTCGGA
Med7.1496	TGCTGTTGACAGTGAGCGATAGCACAGTTCTAATCACAAATAGTGAAGCCACAGA TGTATTTGTGATTAGAACTGTGCTACTGCCTACTGCCTCGGA
Med7.1846	TGCTGTTGACAGTGAGCGCAAGATGGTGCTTGTAATTCTATAGTGAAGCCACAGA TGTATAGAATTACAAGCACCATCTTATGCCTACTGCCTCGGA
Med7.193	TGCTGTTGACAGTGAGCGCCAGCTACATGATGTTTGGCAATAGTGAAGCCACAGA TGTATTGCCAAACATCATGTAGCTGTTGCCTACTGCCTCGGA
Med7.395	TGCTGTTGACAGTGAGCGCAAGCTAGAAGATCTTAAGCTATAGTGAAGCCACAGA TGTATAGCTTAAGATCTTCTAGCTTTTGCCTACTGCCTCGGA
Med7.410	TGCTGTTGACAGTGAGCGCAAGCTACTTTTTGTACATGTATAGTGAAGCCACAGA TGTATACATGTACAAAAAGTAGCTTATGCCTACTGCCTCGGA
Med7.894	TGCTGTTGACAGTGAGCGATAGGTGGTAATTTAACACTAATAGTGAAGCCACAGA TGTATTAGTGTTAAATTACCACCTACTGCCTACTGCCTCGGA
Med8.1339	TGCTGTTGACAGTGAGCGACAGGTGGAAGAGCTCTTAAGATAGTGAAGCCACAGA TGTATCTTAAGAGCTCTTCCACCTGCTGCCTACTGCCTCGGA
Med8.1669	TGCTGTTGACAGTGAGCGCAAGGGTTTCTTTGTTTAATAATAGTGAAGCCACAGA TGTATTATTAAACAAAGAAACCCTTTTGCCTACTGCCTCGGA
Med8.1670	TGCTGTTGACAGTGAGCGCAGGGTTTCTTTGTTTAATAAATAGTGAAGCCACAGA TGTATTTATTAAACAAAGAAACCCTTTGCCTACTGCCTCGGA
Med8.385	TGCTGTTGACAGTGAGCGAAAGCCTGACCCTGAAGTTGAATAGTGAAGCCACAGA TGTATTCAACTTCAGGGTCAGGCTTGTGCCTACTGCCTCGGA
Med8.933	TGCTGTTGACAGTGAGCGATAGGGTTGTTGTGAGGATTAATAGTGAAGCCACAGA TGTATTAATCCTCACAACAACCCTACTGCCTACTGCCTCGGA
Med8.934	TGCTGTTGACAGTGAGCGCAGGGTTGTTGTGAGGATTAAATAGTGAAGCCACAGA TGTATTTAATCCTCACAACAACCCTATGCCTACTGCCTCGGA
Med9.1311	TGCTGTTGACAGTGAGCGCTAGCTGTGTTCTACTTGTAGATAGTGAAGCCACAGA TGTATCTACAAGTAGAACACAGCTATTGCCTACTGCCTCGGA
Med9.1424	TGCTGTTGACAGTGAGCGAAAGGTGAGAAGAACCCAGTTATAGTGAAGCCACAGA TGTATAACTGGGTTCTTCTCACCTTCTGCCTACTGCCTCGGA
Med9.1689	TGCTGTTGACAGTGAGCGCTGGGACTGTTACTGAACTGAATAGTGAAGCCACAGA TGTATTCAGTTCAGTAACAGTCCCAATGCCTACTGCCTCGGA
Med9.2416	TGCTGTTGACAGTGAGCGACAAGGAGATCTTGGTCACAAATAGTGAAGCCACAGA TGTATTTGTGACCAAGATCTCCTTGCTGCCTACTGCCTCGGA
Med9.2937	TGCTGTTGACAGTGAGCGAACCTCACACAATAGAAATGTATAGTGAAGCCACAGA TGTATACATTTCTATTGTGTGAGGTCTGCCTACTGCCTCGGA
Med9.2943	TGCTGTTGACAGTGAGCGCCACAATAGAAATGTAGAGATTTAGTGAAGCCACAGA TGTAAATCTCTACATTTCTATTGTGTTGCCTACTGCCTCGGA
Rpa3.457	TGCTGTTGACAGTGAGCGCAAGGAAGACTCCTGCAGTTTATAGTGAAGCCACAGA TGTATAAACTGCAGGAGTCTTCCTTATGCCTACTGCCTCGGA

References

Adelman, K., and Lis, J.T. (2012). Promoter-proximal pausing of RNA polymerase II: emerging roles in metazoans. Nat Rev Genet *13*, 720-731.

Alarcon, C., Zaromytidou, A.I., Xi, Q., Gao, S., Yu, J., Fujisawa, S., Barlas, A., Miller, A.N., Manova-Todorova, K., Macias, M.J., *et al.* (2009). Nuclear CDKs drive Smad transcriptional activation and turnover in BMP and TGF-beta pathways. Cell *139*, 757-769.

Alekseyenko, A.A., Walsh, E.M., Wang, X., Grayson, A.R., Hsi, P.T., Kharchenko, P.V., Kuroda, M.I., and French, C.A. (2015). The oncogenic BRD4-NUT chromatin regulator drives aberrant transcription within large topological domains. Genes Dev *29*, 1507-1523.

Allen, B.L., and Taatjes, D.J. (2015). The Mediator complex: a central integrator of transcription. Nat Rev Mol Cell Biol *16*, 155-166.

Anders, L., Guenther, M.G., Qi, J., Fan, Z.P., Marineau, J.J., Rahl, P.B., Loven, J., Sigova, A.A., Smith, W.B., Lee, T.I., *et al.* (2014). Genome-wide localization of small molecules. Nat Biotechnol *32*, 92-96.

Asturias, F.J., Jiang, Y.W., Myers, L.C., Gustafsson, C.M., and Kornberg, R.D. (1999). Conserved structures of mediator and RNA polymerase II holoenzyme. Science *283*, 985-987.

Baek, H.J., Kang, Y.K., and Roeder, R.G. (2006). Human Mediator enhances basal transcription by facilitating recruitment of transcription factor IIB during preinitiation complex assembly. J Biol Chem *281*, 15172-15181.

Bai, L., Jia, Y., Viswakarma, N., Huang, J., Vluggens, A., Wolins, N.E., Jafari, N., Rao, M.S., Borensztajn, J., Yang, G., *et al.* (2011). Transcription coactivator mediator subunit MED1 is required for the development of fatty liver in the mouse. Hepatology *53*, 1164-1174.

Bancerek, J., Poss, Z.C., Steinparzer, I., Sedlyarov, V., Pfaffenwimmer, T., Mikulic, I., Dolken, L., Strobl, B., Muller, M., Taatjes, D.J., *et al.* (2013). CDK8 kinase phosphorylates transcription factor STAT1 to selectively regulate the interferon response. Immunity *38*, 250-262.

Barbieri, C.E., Baca, S.C., Lawrence, M.S., Demichelis, F., Blattner, M., Theurillat, J.P., White, T.A., Stojanov, P., Van Allen, E., Stransky, N., *et al.* (2012). Exome sequencing identifies recurrent SPOP, FOXA1 and MED12 mutations in prostate cancer. Nat Genet *44*, 685-689.

Becker, A.J., Mc, C.E., and Till, J.E. (1963). Cytological demonstration of the clonal nature of spleen colonies derived from transplanted mouse marrow cells. Nature *197*, 452-454.

Bennett, J.M., Catovsky, D., Daniel, M.T., Flandrin, G., Galton, D.A., Gralnick, H.R., and Sultan, C. (1976). Proposals for the classification of the acute leukaemias. French-American-British (FAB) co-operative group. Br J Haematol *33*, 451-458.

Bernt, K.M., Zhu, N., Sinha, A.U., Vempati, S., Faber, J., Krivtsov, A.V., Feng, Z., Punt, N., Daigle, A., Bullinger, L., *et al.* (2011). MLL-rearranged leukemia is dependent on aberrant H3K79 methylation by DOT1L. Cancer Cell *20*, 66-78.

Beyer, K.S., Beauchamp, R.L., Lee, M.F., Gusella, J.F., Naar, A.M., and Ramesh, V. (2007). Mediator subunit MED28 (Magicin) is a repressor of smooth muscle cell differentiation. J Biol Chem *282*, 32152-32157.

Bhoite, L.T., Yu, Y., and Stillman, D.J. (2001). The Swi5 activator recruits the Mediator complex to the HO promoter without RNA polymerase II. Genes Dev *15*, 2457-2469.

Bisgrove, D.A., Mahmoudi, T., Henklein, P., and Verdin, E. (2007). Conserved P-TEFb-interacting domain of BRD4 inhibits HIV transcription. Proc Natl Acad Sci U S A *104*, 13690-13695.

Black, J.C., Choi, J.E., Lombardo, S.R., and Carey, M. (2006). A mechanism for coordinating chromatin modification and preinitiation complex assembly. Mol Cell *23*, 809-818.

Boulais, P.E., and Frenette, P.S. (2015). Making sense of hematopoietic stem cell niches. Blood *125*, 2621-2629.

Bourbon, H.M., Aguilera, A., Ansari, A.Z., Asturias, F.J., Berk, A.J., Bjorklund, S., Blackwell, T.K., Borggrefe, T., Carey, M., Carlson, M., *et al.* (2004). A unified nomenclature for protein subunits of mediator complexes linking transcriptional regulators to RNA polymerase II. Mol Cell *14*, 553-557.

Boyer, T.G., Martin, M.E., Lees, E., Ricciardi, R.P., and Berk, A.J. (1999). Mammalian Srb/Mediator complex is targeted by adenovirus E1A protein. Nature *399*, 276-279.

Burke, M.J. (2016). Minimal Residual Disease in NPM1-Mutated AML. N Engl J Med.

Busque, L., Patel, J.P., Figueroa, M.E., Vasanthakumar, A., Provost, S., Hamilou, Z., Mollica, L., Li, J., Viale, A., Heguy, A., *et al.* (2012). Recurrent somatic TET2 mutations in normal elderly individuals with clonal hematopoiesis. Nat Genet *44*, 1179-1181.

Butler, J.M., Nolan, D.J., Vertes, E.L., Varnum-Finney, B., Kobayashi, H., Hooper, A.T., Seandel, M., Shido, K., White, I.A., Kobayashi, M., *et al.* (2010). Endothelial cells are essential for the self-renewal and repopulation of Notch-dependent hematopoietic stem cells. Cell Stem Cell *6*, 251-264.

Cancer Genome Atlas Research, N. (2013). Genomic and epigenomic landscapes of adult de novo acute myeloid leukemia. N Engl J Med *368*, 2059-2074.

Carrera, I., Janody, F., Leeds, N., Duveau, F., and Treisman, J.E. (2008). Pygopus activates Wingless target gene transcription through the mediator complex subunits Med12 and Med13. Proc Natl Acad Sci U S A *105*, 6644-6649.

Cee, V.J., Chen, D.Y., Lee, M.R., and Nicolaou, K.C. (2009). Cortistatin A is a high-affinity ligand of protein kinases ROCK, CDK8, and CDK11. Angew Chem Int Ed Engl *48*, 8952-8957.

Cevher, M.A., Shi, Y., Li, D., Chait, B.T., Malik, S., and Roeder, R.G. (2014). Reconstitution of active human core Mediator complex reveals a critical role of the MED14 subunit. Nat Struct Mol Biol *21*, 1028-1034.

Chapuy, B., McKeown, M.R., Lin, C.Y., Monti, S., Roemer, M.G., Qi, J., Rahl, P.B., Sun, H.H., Yeda, K.T., Doench, J.G., *et al.* (2013). Discovery and characterization of super-enhancer-associated dependencies in diffuse large B cell lymphoma. Cancer Cell *24*, 777-790.

Chen, C.W., and Armstrong, S.A. (2015). Targeting DOT1L and HOX gene expression in MLL-rearranged leukemia and beyond. Exp Hematol *43*, 673-684.

Chen, C.W., Koche, R.P., Sinha, A.U., Deshpande, A.J., Zhu, N., Eng, R., Doench, J.G., Xu, H., Chu, S.H., Qi, J., *et al.* (2015). DOT1L inhibits SIRT1-mediated epigenetic silencing to maintain leukemic gene expression in MLL-rearranged leukemia. Nat Med *21*, 335-343.

Chen, X.F., Lehmann, L., Lin, J.J., Vashisht, A., Schmidt, R., Ferrari, R., Huang, C., McKee, R., Mosley, A., Plath, K., *et al.* (2012). Mediator and SAGA have distinct roles in Pol II preinitiation complex assembly and function. Cell Rep *2*, 1061-1067.

Cheshier, S.H., Morrison, S.J., Liao, X., and Weissman, I.L. (1999). In vivo proliferation and cell cycle kinetics of long-term self-renewing hematopoietic stem cells. Proc Natl Acad Sci U S A *96*, 3120-3125.

Chipumuro, E., Marco, E., Christensen, C.L., Kwiatkowski, N., Zhang, T., Hatheway, C.M., Abraham, B.J., Sharma, B., Yeung, C., Altabef, A., *et al.* (2014). CDK7 inhibition suppresses super-enhancer-linked oncogenic transcription in MYCN-driven cancer. Cell *159*, 1126-1139.

Conaway, R.C., Sato, S., Tomomori-Sato, C., Yao, T., and Conaway, J.W. (2005). The mammalian Mediator complex and its role in transcriptional regulation. Trends Biochem Sci *30*, 250-255.

Daigle, S.R., Olhava, E.J., Therkelsen, C.A., Majer, C.R., Sneeringer, C.J., Song, J., Johnston, L.D., Scott, M.P., Smith, J.J., Xiao, Y., *et al.* (2011). Selective killing of mixed lineage leukemia cells by a potent small-molecule DOT1L inhibitor. Cancer Cell *20*, 53-65.

Dale, T., Clarke, P.A., Esdar, C., Waalboer, D., Adeniji-Popoola, O., Ortiz-Ruiz, M.J., Mallinger, A., Samant, R.S., Czodrowski, P., Musil, D., *et al.* (2015). A selective chemical probe for exploring the role of CDK8 and CDK19 in human disease. Nat Chem Biol.

Dawson, M.A., Prinjha, R.K., Dittmann, A., Giotopoulos, G., Bantscheff, M., Chan, W.I., Robson, S.C., Chung, C.W., Hopf, C., Savitski, M.M., *et al.* (2011). Inhibition of BET recruitment to chromatin as an effective treatment for MLL-fusion leukaemia. Nature *478*, 529-533.

Delmore, J.E., Issa, G.C., Lemieux, M.E., Rahl, P.B., Shi, J., Jacobs, H.M., Kastritis, E., Gilpatrick, T., Paranal, R.M., Qi, J., *et al.* (2011). BET bromodomain inhibition as a therapeutic strategy to target c-Myc. Cell *146*, 904-917.

Deng, W., Lee, J., Wang, H., Miller, J., Reik, A., Gregory, P.D., Dean, A., and Blobel, G.A. (2012). Controlling long-range genomic interactions at a native locus by targeted tethering of a looping factor. Cell *149*, 1233-1244.

Deshpande, A.J., Bradner, J., and Armstrong, S.A. (2012). Chromatin modifications as therapeutic targets in MLL-rearranged leukemia. Trends Immunol *33*, 563-570.

Deshpande, A.J., Deshpande, A., Sinha, A.U., Chen, L., Chang, J., Cihan, A., Fazio, M., Chen, C.W., Zhu, N., Koche, R., *et al.* (2014). AF10 regulates progressive H3K79 methylation and HOX gene expression in diverse AML subtypes. Cancer Cell *26*, 896-908.

Dey, A., Chitsaz, F., Abbasi, A., Misteli, T., and Ozato, K. (2003). The double bromodomain protein Brd4 binds to acetylated chromatin during interphase and mitosis. Proc Natl Acad Sci U S A *100*, 8758-8763.

Di Micco, R., Fontanals-Cirera, B., Low, V., Ntziachristos, P., Yuen, S.K., Lovell, C.D., Dolgalev, I., Yonekubo, Y., Zhang, G., Rusinova, E., *et al.* (2014). Control of embryonic stem cell identity by BRD4-dependent transcriptional elongation of super-enhancer-associated pluripotency genes. Cell Rep *9*, 234-247.

Ding, L., Ley, T.J., Larson, D.E., Miller, C.A., Koboldt, D.C., Welch, J.S., Ritchey, J.K., Young, M.A., Lamprecht, T., McLellan, M.D., *et al.* (2012a). Clonal evolution in relapsed acute myeloid leukaemia revealed by whole-genome sequencing. Nature *481*, 506-510.

Ding, L., Saunders, T.L., Enikolopov, G., and Morrison, S.J. (2012b). Endothelial and perivascular cells maintain haematopoietic stem cells. Nature *481*, 457-462.

Ding, N., Zhou, H., Esteve, P.O., Chin, H.G., Kim, S., Xu, X., Joseph, S.M., Friez, M.J., Schwartz, C.E., Pradhan, S., *et al.* (2008). Mediator links epigenetic silencing of neuronal gene expression with x-linked mental retardation. Mol Cell *31*, 347-359.

Dohner, H., Weisdorf, D.J., and Bloomfield, C.D. (2015). Acute Myeloid Leukemia. N Engl J Med *373*, 1136-1152.

Dombret, H., and Gardin, C. (2015). An update of current treatments for adult acute myeloid leukemia. Blood.

Dombret, H., Preudhomme, C., Berthon, C., Raffoux, E., Thomas, X., Vey, N., Gomez-Roca, C., Ethell, M., Yee, K., Bourdel, F., *et al.* (2014). A Phase 1 Study of the BET-Bromodomain Inhibitor OTX015 in Patients with Advanced Acute Leukemia. Blood *124*, 117-117.

Donner, A.J., Ebmeier, C.C., Taatjes, D.J., and Espinosa, J.M. (2010). CDK8 is a positive regulator of transcriptional elongation within the serum response network. Nat Struct Mol Biol *17*, 194-201.

Dotson, M.R., Yuan, C.X., Roeder, R.G., Myers, L.C., Gustafsson, C.M., Jiang, Y.W., Li, Y., Kornberg, R.D., and Asturias, F.J. (2000). Structural organization of yeast and mammalian mediator complexes. Proc Natl Acad Sci U S A *97*, 14307-14310.

Eaton, M., Corces-Zimmerman, R., Lopez, J., Fritz, C., Olson, E., Majeti, R., and Loven, J. (2015). Abstract 2212: Super-enhancer landscapes specify molecular subtypes and novel targets in acute myeloid leukemia. Cancer Research *75*, 2212.

Eaves, C.J. (2015). Hematopoietic stem cells: concepts, definitions, and the new reality. Blood *125*, 2605-2613.

Elmlund, H., Baraznenok, V., Lindahl, M., Samuelsen, C.O., Koeck, P.J., Holmberg, S., Hebert, H., and Gustafsson, C.M. (2006). The cyclin-dependent kinase 8 module sterically blocks Mediator interactions with RNA polymerase II. Proc Natl Acad Sci U S A *103*, 15788-15793.

Ernst, P., Fisher, J.K., Avery, W., Wade, S., Foy, D., and Korsmeyer, S.J. (2004). Definitive hematopoiesis requires the mixed-lineage leukemia gene. Dev Cell *6*, 437-443.

Esnault, C., Ghavi-Helm, Y., Brun, S., Soutourina, J., Van Berkum, N., Boschiero, C., Holstege, F., and Werner, M. (2008). Mediator-dependent recruitment of TFIIH modules in preinitiation complex. Mol Cell *31*, 337-346.

Figueroa, M.E., Abdel-Wahab, O., Lu, C., Ward, P.S., Patel, J., Shih, A., Li, Y., Bhagwat, N., Vasanthakumar, A., Fernandez, H.F., *et al.* (2010a). Leukemic IDH1 and IDH2 mutations result in a hypermethylation phenotype, disrupt TET2 function, and impair hematopoietic differentiation. Cancer Cell *18*, 553-567.

Figueroa, M.E., Lugthart, S., Li, Y., Erpelinck-Verschueren, C., Deng, X., Christos, P.J., Schifano, E., Booth, J., van Putten, W., Skrabanek, L., *et al.* (2010b). DNA methylation signatures identify biologically distinct subtypes in acute myeloid leukemia. Cancer Cell *17*, 13-27.

Filippakopoulos, P., Qi, J., Picaud, S., Shen, Y., Smith, W.B., Fedorov, O., Morse, E.M., Keates, T., Hickman, T.T., Felletar, I., *et al.* (2010). Selective inhibition of BET bromodomains. Nature *468*, 1067-1073.

Firestein, R., Bass, A.J., Kim, S.Y., Dunn, I.F., Silver, S.J., Guney, I., Freed, E., Ligon, A.H., Vena, N., Ogino, S., *et al.* (2008). CDK8 is a colorectal cancer oncogene that regulates beta-catenin activity. Nature *455*, 547-551.

Flanagan, P.M., Kelleher, R.J., 3rd, Sayre, M.H., Tschochner, H., and Kornberg, R.D. (1991). A mediator required for activation of RNA polymerase II transcription in vitro. Nature *350*, 436-438.

Fondell, J.D., Ge, H., and Roeder, R.G. (1996). Ligand induction of a transcriptionally active thyroid hormone receptor coactivator complex. Proc Natl Acad Sci U S A *93*, 8329-8333.

Fong, C.Y., Gilan, O., Lam, E.Y., Rubin, A.F., Ftouni, S., Tyler, D., Stanley, K., Sinha, D., Yeh, P., Morison, J., *et al.* (2015). BET inhibitor resistance emerges from leukaemia stem cells. Nature *525*, 538-542.

Fryer, C.J., White, J.B., and Jones, K.A. (2004). Mastermind recruits CycC:CDK8 to phosphorylate the Notch ICD and coordinate activation with turnover. Mol Cell *16*, 509-520.

Galbraith, M.D., Allen, M.A., Bensard, C.L., Wang, X., Schwinn, M.K., Qin, B., Long, H.W., Daniels, D.L., Hahn, W.C., Dowell, R.D., *et al.* (2013). HIF1A employs CDK8-mediator to stimulate RNAPII elongation in response to hypoxia. Cell *153*, 1327-1339.

Gao, C., Dimitrov, T., Yong, K.J., Tatetsu, H., Jeong, H.W., Luo, H.R., Bradner, J.E., Tenen, D.G., and Chai, L. (2013). Targeting transcription factor SALL4 in acute myeloid leukemia by interrupting its interaction with an epigenetic complex. Blood *121*, 1413-1421.

Garcia-Cuellar, M.P., Fuller, E., Mathner, E., Breitinger, C., Hetzner, K., Zeitlmann, L., Borkhardt, A., and Slany, R.K. (2014). Efficacy of cyclin-dependent-kinase 9 inhibitors in a murine model of mixed-lineage leukemia. Leukemia *28*, 1427-1435.

Ge, K., Guermah, M., Yuan, C.X., Ito, M., Wallberg, A.E., Spiegelman, B.M., and Roeder, R.G. (2002). Transcription coactivator TRAP220 is required for PPAR gamma 2-stimulated adipogenesis. Nature *417*, 563-567.

Genovese, G., Kahler, A.K., Handsaker, R.E., Lindberg, J., Rose, S.A., Bakhoum, S.F., Chambert, K., Mick, E., Neale, B.M., Fromer, M., *et al.* (2014). Clonal hematopoiesis and blood-cancer risk inferred from blood DNA sequence. N Engl J Med *371*, 2477-2487.

Gill, G., and Ptashne, M. (1988). Negative effect of the transcriptional activator GAL4. Nature *334*, 721-724.

Gobert, V., Osman, D., Bras, S., Auge, B., Boube, M., Bourbon, H.M., Horn, T., Boutros, M., Haenlin, M., and Waltzer, L. (2010). A genome-wide RNA interference screen identifies a differential role of the mediator CDK8 module subunits for GATA/ RUNX-activated transcription in Drosophila. Mol Cell Biol *30*, 2837-2848.

Godley, L.A. (2014). Inherited predisposition to acute myeloid leukemia. Semin Hematol *51*, 306-321.

Goyama, S., Yamamoto, G., Shimabe, M., Sato, T., Ichikawa, M., Ogawa, S., Chiba, S., and Kurokawa, M. (2008). Evi-1 is a critical regulator for hematopoietic stem cells and transformed leukemic cells. Cell Stem Cell *3*, 207-220.

Graham, J.M., Jr., and Schwartz, C.E. (2013). MED12 related disorders. Am J Med Genet A *161A*, 2734-2740.

Grimwade, D., Ivey, A., and Huntly, B.J. (2015). Molecular landscape of acute myeloid leukemia in younger adults and its clinical relevance. Blood.

Groschel, S., Sanders, M.A., Hoogenboezem, R., de Wit, E., Bouwman, B.A., Erpelinck, C., van der Velden, V.H., Havermans, M., Avellino, R., van Lom, K., *et al.* (2014). A single oncogenic enhancer rearrangement causes concomitant EVI1 and GATA2 deregulation in leukemia. Cell *157*, 369-381.

Grueter, C.E., van Rooij, E., Johnson, B.A., DeLeon, S.M., Sutherland, L.B., Qi, X., Gautron, L., Elmquist, J.K., Bassel-Duby, R., and Olson, E.N. (2012). A cardiac microRNA governs systemic energy homeostasis by regulation of MED13. Cell *149*, 671-683.

Han, S.J., Lee, Y.C., Gim, B.S., Ryu, G.H., Park, S.J., Lane, W.S., and Kim, Y.J. (1999). Activator-specific requirement of yeast mediator proteins for RNA polymerase II transcriptional activation. Mol Cell Biol *19*, 979-988.

Hanoun, M., Zhang, D., Mizoguchi, T., Pinho, S., Pierce, H., Kunisaki, Y., Lacombe, J., Armstrong, S.A., Duhrsen, U., and Frenette, P.S. (2014). Acute myelogenous leukemia-induced sympathetic neuropathy promotes malignancy in an altered hematopoietic stem cell niche. Cell Stem Cell *15*, 365-375.

Harris, N.L., Jaffe, E.S., Diebold, J., Flandrin, G., Muller-Hermelink, H.K., Vardiman, J., Lister, T.A., and Bloomfield, C.D. (1999). The World Health Organization classification of neoplastic diseases of the hematopoietic and lymphoid tissues. Report of the Clinical Advisory Committee meeting, Airlie House, Virginia, November, 1997. Ann Oncol *10*, 1419-1432.

Hasemann, M.S., Lauridsen, F.K., Waage, J., Jakobsen, J.S., Frank, A.K., Schuster, M.B., Rapin, N., Bagger, F.O., Hoppe, P.S., Schroeder, T., *et al.* (2014). C/EBPalpha is required for long-term self-renewal and lineage priming of hematopoietic stem cells and for the maintenance of epigenetic configurations in multipotent progenitors. PLoS Genet *10*, e1004079.

Herbig, E., Warfield, L., Fish, L., Fishburn, J., Knutson, B.A., Moorefield, B., Pacheco, D., and Hahn, S. (2010). Mechanism of Mediator recruitment by tandem Gcn4 activation domains and three Gal11 activator-binding domains. Mol Cell Biol *30*, 2376-2390.

Hnisz, D., Abraham, B.J., Lee, T.I., Lau, A., Saint-Andre, V., Sigova, A.A., Hoke, H.A., and Young, R.A. (2013). Super-enhancers in the control of cell identity and disease. Cell *155*, 934-947.

Holstege, F.C., Jennings, E.G., Wyrick, J.J., Lee, T.I., Hengartner, C.J., Green, M.R., Golub, T.R., Lander, E.S., and Young, R.A. (1998). Dissecting the regulatory circuitry of a eukaryotic genome. Cell *95*, 717-728.

Huang, M.E., Ye, Y.C., Chen, S.R., Chai, J.R., Lu, J.X., Zhoa, L., Gu, L.J., and Wang, Z.Y. (1988). Use of all-trans retinoic acid in the treatment of acute promyelocytic leukemia. Blood *72*, 567-572.

Huang, M.E., Ye, Y.C., Chen, S.R., Zhao, J.C., Gu, L.J., Cai, J.R., Zhao, L., Xie, J.X., Shen, Z.X., and Wang, Z.Y. (1987). All-trans retinoic acid with or without low dose cytosine arabinoside in acute promyelocytic leukemia. Report of 6 cases. Chin Med J (Engl) *100*, 949-953.

Huang, S., Holzel, M., Knijnenburg, T., Schlicker, A., Roepman, P., McDermott, U., Garnett, M., Grernrum, W., Sun, C., Prahallad, A.*, et al.* (2012). MED12 controls the response to multiple cancer drugs through regulation of TGF-beta receptor signaling. Cell *151*, 937-950.

Illendula, A., Pulikkan, J.A., Zong, H., Grembecka, J., Xue, L., Sen, S., Zhou, Y., Boulton, A., Kuntimaddi, A., Gao, Y.*, et al.* (2015). Chemical biology. A small-molecule inhibitor of the aberrant transcription factor CBFbeta-SMMHC delays leukemia in mice. Science *347*, 779-784.

Imasaki, T., Calero, G., Cai, G., Tsai, K.L., Yamada, K., Cardelli, F., Erdjument-Bromage, H., Tempst, P., Berger, I., Kornberg, G.L.*, et al.* (2011). Architecture of the Mediator head module. Nature *475*, 240-243.

Ito, M., Yuan, C.X., Okano, H.J., Darnell, R.B., and Roeder, R.G. (2000). Involvement of the TRAP220 component of the TRAP/SMCC coactivator complex in embryonic development and thyroid hormone action. Mol Cell *5*, 683-693.

Jacobson, L.O., Simmons, E.L., Marks, E.K., and Eldredge, J.H. (1951). Recovery from radiation injury. Science *113*, 510-511.

Jaiswal, S., Fontanillas, P., Flannick, J., Manning, A., Grauman, P.V., Mar, B.G., Lindsley, R.C., Mermel, C.H., Burtt, N., Chavez, A.*, et al.* (2014). Age-related clonal hematopoiesis associated with adverse outcomes. N Engl J Med *371*, 2488-2498.

Jang, M.K., Mochizuki, K., Zhou, M., Jeong, H.S., Brady, J.N., and Ozato, K. (2005). The bromodomain protein Brd4 is a positive regulatory component of P-TEFb and stimulates RNA polymerase II-dependent transcription. Mol Cell *19*, 523-534.

Jiang, P., Hu, Q., Ito, M., Meyer, S., Waltz, S., Khan, S., Roeder, R.G., and Zhang, X. (2010). Key roles for MED1 LxxLL motifs in pubertal mammary gland development and luminal-cell differentiation. Proc Natl Acad Sci U S A *107*, 6765-6770.

Jiang, Y.W., Veschambre, P., Erdjument-Bromage, H., Tempst, P., Conaway, J.W., Conaway, R.C., and Kornberg, R.D. (1998). Mammalian mediator of transcriptional regulation and its possible role as an end-point of signal transduction pathways. Proc Natl Acad Sci U S A *95*, 8538-8543.

Johnson, K.M., and Carey, M. (2003). Assembly of a mediator/TFIID/TFIIA complex bypasses the need for an activator. Curr Biol *13*, 772-777.

Jonkers, I., and Lis, J.T. (2015). Getting up to speed with transcription elongation by RNA polymerase II. Nat Rev Mol Cell Biol *16*, 167-177.

Kagey, M.H., Newman, J.J., Bilodeau, S., Zhan, Y., Orlando, D.A., van Berkum, N.L., Ebmeier, C.C., Goossens, J., Rahl, P.B., Levine, S.S., *et al.* (2010). Mediator and cohesin connect gene expression and chromatin architecture. Nature *467*, 430-435.

Kampen, K.R., Ter Elst, A., Mahmud, H., Scherpen, F.J., Diks, S.H., Peppelenbosch, M.P., de Haas, V., Guryev, V., and de Bont, E.S. (2014). Insights in dynamic kinome reprogramming as a consequence of MEK inhibition in MLL-rearranged AML. Leukemia *28*, 589-599.

Kampjarvi, K., Jarvinen, T.M., Heikkinen, T., Ruppert, A.S., Senter, L., Hoag, K.W., Dufva, O., Kontro, M., Rassenti, L., Hertlein, E., *et al.* (2015a). Somatic MED12 mutations are associated with poor prognosis markers in chronic lymphocytic leukemia. Oncotarget *6*, 1884-1888.

Kampjarvi, K., Kim, N.H., Keskitalo, S., Clark, A.D., von Nandelstadh, P., Turunen, M., Heikkinen, T., Park, M.J., Makinen, N., Kivinummi, K., *et al.* (2015b). Somatic MED12 mutations in prostate cancer and uterine leiomyomas promote tumorigenesis through distinct mechanisms. Prostate.

Kapoor, A., Goldberg, M.S., Cumberland, L.K., Ratnakumar, K., Segura, M.F., Emanuel, P.O., Menendez, S., Vardabasso, C., Leroy, G., Vidal, C.I., *et al.* (2010). The histone variant macroH2A suppresses melanoma progression through regulation of CDK8. Nature *468*, 1105-1109.

Keaveney, M., and Struhl, K. (1998). Activator-mediated recruitment of the RNA polymerase II machinery is the predominant mechanism for transcriptional activation in yeast. Mol Cell *1*, 917-924.

Kelleher, R.J., 3rd, Flanagan, P.M., and Kornberg, R.D. (1990). A novel mediator between activator proteins and the RNA polymerase II transcription apparatus. Cell *61*, 1209-1215.

Kim, S., Xu, X., Hecht, A., and Boyer, T.G. (2006). Mediator is a transducer of Wnt/beta-catenin signaling. J Biol Chem *281*, 14066-14075.

Kim, Y.J., Bjorklund, S., Li, Y., Sayre, M.H., and Kornberg, R.D. (1994). A multiprotein mediator of transcriptional activation and its interaction with the C-terminal repeat domain of RNA polymerase II. Cell *77*, 599-608.

Knuesel, M.T., Meyer, K.D., Bernecky, C., and Taatjes, D.J. (2009a). The human CDK8 subcomplex is a molecular switch that controls Mediator coactivator function. Genes Dev *23*, 439-451.

Knuesel, M.T., Meyer, K.D., Donner, A.J., Espinosa, J.M., and Taatjes, D.J. (2009b). The human CDK8 subcomplex is a histone kinase that requires Med12 for activity and can function independently of mediator. Mol Cell Biol *29*, 650-661.

Kode, A., Manavalan, J.S., Mosialou, I., Bhagat, G., Rathinam, C.V., Luo, N., Khiabanian, H., Lee, A., Murty, V.V., Friedman, R., *et al.* (2014). Leukaemogenesis induced by an activating beta-catenin mutation in osteoblasts. Nature *506*, 240-244.

Kon, A., Shih, L.Y., Minamino, M., Sanada, M., Shiraishi, Y., Nagata, Y., Yoshida, K., Okuno, Y., Bando, M., Nakato, R., *et al.* (2013). Recurrent mutations in multiple components of the cohesin complex in myeloid neoplasms. Nat Genet *45*, 1232-1237.

Kretzschmar, M., Stelzer, G., Roeder, R.G., and Meisterernst, M. (1994). RNA polymerase II cofactor PC2 facilitates activation of transcription by GAL4-AH in vitro. Mol Cell Biol *14*, 3927-3937.

Kuuluvainen, E., Hakala, H., Havula, E., Sahal Estime, M., Ramet, M., Hietakangas, V., and Makela, T.P. (2014). Cyclin-dependent kinase 8 module expression profiling reveals requirement of mediator subunits 12 and 13 for transcription of Serpent-dependent innate immunity genes in Drosophila. J Biol Chem *289*, 16252-16261.

Lai, F., Orom, U.A., Cesaroni, M., Beringer, M., Taatjes, D.J., Blobel, G.A., and Shiekhattar, R. (2013). Activating RNAs associate with Mediator to enhance chromatin architecture and transcription. Nature *494*, 497-501.

Landau, D.A., Carter, S.L., Stojanov, P., McKenna, A., Stevenson, K., Lawrence, M.S., Sougnez, C., Stewart, C., Sivachenko, A., Wang, L., *et al.* (2013). Evolution and impact of subclonal mutations in chronic lymphocytic leukemia. Cell *152*, 714-726.

Lariviere, L., Geiger, S., Hoeppner, S., Rother, S., Strasser, K., and Cramer, P. (2006). Structure and TBP binding of the Mediator head subcomplex Med8-Med18-Med20. Nat Struct Mol Biol *13*, 895-901.

Lariviere, L., Plaschka, C., Seizl, M., Wenzeck, L., Kurth, F., and Cramer, P. (2012). Structure of the Mediator head module. Nature *492*, 448-451.

Lavallee, V.P., Baccelli, I., Krosl, J., Wilhelm, B., Barabe, F., Gendron, P., Boucher, G., Lemieux, S., Marinier, A., Meloche, S., *et al.* (2015). The transcriptomic landscape and directed chemical interrogation of MLL-rearranged acute myeloid leukemias. Nat Genet *47*, 1030-1037.

Lemieux, K., and Gaudreau, L. (2004). Targeting of Swi/Snf to the yeast GAL1 UAS G requires the Mediator, TAF IIs, and RNA polymerase II. EMBO J *23*, 4040-4050.

Ley, T.J., Ding, L., Walter, M.J., McLellan, M.D., Lamprecht, T., Larson, D.E., Kandoth, C., Payton, J.E., Baty, J., Welch, J., *et al.* (2010). DNMT3A mutations in acute myeloid leukemia. N Engl J Med *363*, 2424-2433.

Li, L., Walsh, R.M., Wagh, V., James, M.F., Beauchamp, R.L., Chang, Y.S., Gusella, J.F., Hochedlinger, K., and Ramesh, V. (2015). Mediator Subunit Med28 Is Essential for Mouse Peri-Implantation Development and Pluripotency. PLoS One *10*, e0140192.

Li, N., Fassl, A., Chick, J., Inuzuka, H., Li, X., Mansour, M.R., Liu, L., Wang, H., King, B., Shaik, S., *et al.* (2014). Cyclin C is a haploinsufficient tumour suppressor. Nat Cell Biol *16*, 1080-1091.

Li, Y., Bjorklund, S., Jiang, Y.W., Kim, Y.J., Lane, W.S., Stillman, D.J., and Kornberg, R.D. (1995). Yeast global transcriptional regulators Sin4 and Rgr1 are components of mediator complex/RNA polymerase II holoenzyme. Proc Natl Acad Sci U S A *92*, 10864-10868.

Lichtinger, M., Ingram, R., Hannah, R., Muller, D., Clarke, D., Assi, S.A., Lie, A.L.M., Noailles, L., Vijayabaskar, M.S., Wu, M., *et al.* (2012). RUNX1 reshapes the epigenetic landscape at the onset of haematopoiesis. EMBO J *31*, 4318-4333.

Lim, W.K., Ong, C.K., Tan, J., Thike, A.A., Ng, C.C., Rajasegaran, V., Myint, S.S., Nagarajan, S., Nasir, N.D., McPherson, J.R., *et al.* (2014). Exome sequencing identifies highly recurrent MED12 somatic mutations in breast fibroadenoma. Nat Genet *46*, 877-880.

Ling, K.W., Ottersbach, K., van Hamburg, J.P., Oziemlak, A., Tsai, F.Y., Orkin, S.H., Ploemacher, R., Hendriks, R.W., and Dzierzak, E. (2004). GATA-2 plays two functionally distinct roles during the ontogeny of hematopoietic stem cells. J Exp Med *200*, 871-882.

Lo-Coco, F., Avvisati, G., Vignetti, M., Thiede, C., Orlando, S.M., Iacobelli, S., Ferrara, F., Fazi, P., Cicconi, L., Di Bona, E., *et al.* (2013). Retinoic acid and arsenic trioxide for acute promyelocytic leukemia. N Engl J Med *369*, 111-121.

Loven, J., Hoke, H.A., Lin, C.Y., Lau, A., Orlando, D.A., Vakoc, C.R., Bradner, J.E., Lee, T.I., and Young, R.A. (2013). Selective inhibition of tumor oncogenes by disruption of super-enhancers. Cell *153*, 320-334.

Makinen, N., Mehine, M., Tolvanen, J., Kaasinen, E., Li, Y., Lehtonen, H.J., Gentile, M., Yan, J., Enge, M., Taipale, M., *et al.* (2011). MED12, the mediator complex subunit 12 gene, is mutated at high frequency in uterine leiomyomas. Science *334*, 252-255.

Mali, R.S., Ramdas, B., Ma, P., Shi, J., Munugalavadla, V., Sims, E., Wei, L., Vemula, S., Nabinger, S.C., Goodwin, C.B., *et al.* (2011). Rho kinase regulates the survival and transformation of cells bearing oncogenic forms of KIT, FLT3, and BCR-ABL. Cancer Cell *20*, 357-369.

Malik, S., Gu, W., Wu, W., Qin, J., and Roeder, R.G. (2000). The USA-derived transcriptional coactivator PC2 is a submodule of TRAP/SMCC and acts synergistically with other PCs. Mol Cell *5*, 753-760.

Malik, S., and Roeder, R.G. (2010). The metazoan Mediator co-activator complex as an integrative hub for transcriptional regulation. Nat Rev Genet *11*, 761-772.

Mallinger, A., Crumpler, S., Pichowicz, M., Waalboer, D., Stubbs, M., Adeniji-Popoola, O., Wood, B., Smith, E., Thai, C., Henley, A.T., *et al.* (2015). Discovery of potent, orally bioavailable, small-molecule inhibitors of WNT signaling from a cell-based pathway screen. J Med Chem *58*, 1717-1735.

Mansour, M.R., Abraham, B.J., Anders, L., Berezovskaya, A., Gutierrez, A., Durbin, A.D., Etchin, J., Lawton, L., Sallan, S.E., Silverman, L.B., *et al.* (2014). Oncogene regulation. An oncogenic super-enhancer formed through somatic mutation of a noncoding intergenic element. Science *346*, 1373-1377.

Matsui, H., Tomizawa, K., and Matsushita, M. (2003). [Protein transduction by poly-arginine]. Nihon Yakurigaku Zasshi *121*, 435-439.

McLean, C.Y., Bristor, D., Hiller, M., Clarke, S.L., Schaar, B.T., Lowe, C.B., Wenger, A.M., and Bejerano, G. (2010). GREAT improves functional interpretation of cis-regulatory regions. Nat Biotechnol *28*, 495-501.

Mehine, M., Kaasinen, E., Makinen, N., Katainen, R., Kampjarvi, K., Pitkanen, E., Heinonen, H.R., Butzow, R., Kilpivaara, O., Kuosmanen, A., *et al.* (2013). Characterization of uterine leiomyomas by whole-genome sequencing. N Engl J Med *369*, 43-53.

Meyer, M.E., Gronemeyer, H., Turcotte, B., Bocquel, M.T., Tasset, D., and Chambon, P. (1989). Steroid hormone receptors compete for factors that mediate their enhancer function. Cell *57*, 433-442.

Mittal, P., Shin, Y.H., Yatsenko, S.A., Castro, C.A., Surti, U., and Rajkovic, A. (2015). Med12 gain-of-function mutation causes leiomyomas and genomic instability. J Clin Invest *125*, 3280-3284.

Morris, E.J., Ji, J.Y., Yang, F., Di Stefano, L., Herr, A., Moon, N.S., Kwon, E.J., Haigis, K.M., Naar, A.M., and Dyson, N.J. (2008). E2F1 represses beta-catenin transcription and is antagonized by both pRB and CDK8. Nature *455*, 552-556.

Mullenders, J., Aranda-Orgilles, B., Lhoumaud, P., Keller, M., Pae, J., Wang, K., Kayembe, C., Rocha, P.P., Raviram, R., Gong, Y., *et al.* (2015). Cohesin loss alters adult hematopoietic stem cell homeostasis, leading to myeloproliferative neoplasms. J Exp Med *212*, 1833-1850.

Muncke, N., Jung, C., Rudiger, H., Ulmer, H., Roeth, R., Hubert, A., Goldmuntz, E., Driscoll, D., Goodship, J., Schon, K., *et al.* (2003). Missense mutations and gene interruption in PROSIT240, a novel TRAP240-like gene, in patients with congenital heart defect (transposition of the great arteries). Circulation *108*, 2843-2850.

Myers, L.C., Gustafsson, C.M., Bushnell, D.A., Lui, M., Erdjument-Bromage, H., Tempst, P., and Kornberg, R.D. (1998). The Med proteins of yeast and their function through the RNA polymerase II carboxy-terminal domain. Genes Dev *12*, 45-54.

Myers, L.C., Gustafsson, C.M., Hayashibara, K.C., Brown, P.O., and Kornberg, R.D. (1999). Mediator protein mutations that selectively abolish activated transcription. Proc Natl Acad Sci U S A *96*, 67-72.

Naar, A.M., Beaurang, P.A., Zhou, S., Abraham, S., Solomon, W., and Tjian, R. (1999). Composite co-activator ARC mediates chromatin-directed transcriptional activation. Nature *398*, 828-832.

Nonet, M.L., and Young, R.A. (1989). Intragenic and extragenic suppressors of mutations in the heptapeptide repeat domain of Saccharomyces cerevisiae RNA polymerase II. Genetics *123*, 715-724.

Okuda, T., van Deursen, J., Hiebert, S.W., Grosveld, G., and Downing, J.R. (1996). AML1, the target of multiple chromosomal translocations in human leukemia, is essential for normal fetal liver hematopoiesis. Cell *84*, 321-330.

Othus, M., Kantarjian, H., Petersdorf, S., Ravandi, F., Godwin, J., Cortes, J., Pierce, S., Erba, H., Faderl, S., Appelbaum, F.R., *et al.* (2014). Declining rates of treatment-related mortality in patients with newly diagnosed AML given 'intense' induction regimens: a report from SWOG and MD Anderson. Leukemia *28*, 289-292.

Ott, C.J., Kopp, N., Bird, L., Paranal, R.M., Qi, J., Bowman, T., Rodig, S.J., Kung, A.L., Bradner, J.E., and Weinstock, D.M. (2012). BET bromodomain inhibition targets both c-Myc and IL7R in high-risk acute lymphoblastic leukemia. Blood *120*, 2843-2852.

Paoletti, A.C., Parmely, T.J., Tomomori-Sato, C., Sato, S., Zhu, D., Conaway, R.C., Conaway, J.W., Florens, L., and Washburn, M.P. (2006). Quantitative proteomic analysis of distinct mammalian Mediator complexes using normalized spectral abundance factors. Proc Natl Acad Sci U S A *103*, 18928-18933.

Parmar, K., Mauch, P., Vergilio, J.A., Sackstein, R., and Down, J.D. (2007). Distribution of hematopoietic stem cells in the bone marrow according to regional hypoxia. Proc Natl Acad Sci U S A *104*, 5431-5436.

Pelish, H.E., Liau, B.B., Nitulescu, II, Tangpeerachaikul, A., Poss, Z.C., Da Silva, D.H., Caruso, B.T., Arefolov, A., Fadeyi, O., Christie, A.L.*, et al.* (2015). Mediator kinase inhibition further activates super-enhancer-associated genes in AML. Nature *526*, 273-276.

Plaschka, C., Lariviere, L., Wenzeck, L., Seizl, M., Hemann, M., Tegunov, D., Petrotchenko, E.V., Borchers, C.H., Baumeister, W., Herzog, F.*, et al.* (2015). Architecture of the RNA polymerase II-Mediator core initiation complex. Nature *518*, 376-380.

Porter, D.C., Chen, M., Liang, J., Kaza, V., Chumanevich, A., Altilia, S., Farmaki, E., Pena, M., Schools, G.P., Chatzistamou, I.*, et al.* (2015). Abstract PR08: Targeting tumor microenvironment with selective small-molecule inhibitors of CDK8/19. Cancer Research *75*, PR08.

Porter, D.C., Farmaki, E., Altilia, S., Schools, G.P., West, D.K., Chen, M., Chang, B.D., Puzyrev, A.T., Lim, C.U., Rokow-Kittell, R.*, et al.* (2012). Cyclin-dependent kinase 8 mediates chemotherapy-induced tumor-promoting paracrine activities. Proc Natl Acad Sci U S A *109*, 13799-13804.

Poss, Z.C., Ebmeier, C.C., and Taatjes, D.J. (2013). The Mediator complex and transcription regulation. Crit Rev Biochem Mol Biol *48*, 575-608.

Pulte, D., Gondos, A., and Brenner, H. (2010). Expected long-term survival of patients diagnosed with acute myeloblastic leukemia during 2006-2010. Ann Oncol *21*, 335-341.

Rachez, C., Suldan, Z., Ward, J., Chang, C.P., Burakov, D., Erdjument-Bromage, H., Tempst, P., and Freedman, L.P. (1998). A novel protein complex that interacts with the vitamin D3 receptor in a ligand-dependent manner and enhances VDR transactivation in a cell-free system. Genes Dev *12*, 1787-1800.

Rahman, S., Sowa, M.E., Ottinger, M., Smith, J.A., Shi, Y., Harper, J.W., and Howley, P.M. (2011). The Brd4 extraterminal domain confers transcription activation independent of pTEFb by recruiting multiple proteins, including NSD3. Mol Cell Biol *31*, 2641-2652.

Rathert, P., Roth, M., Neumann, T., Muerdter, F., Roe, J.S., Muhar, M., Deswal, S., Cerny-Reiterer, S., Peter, B., Jude, J., *et al.* (2015). Transcriptional plasticity promotes primary and acquired resistance to BET inhibition. Nature *525*, 543-547.

Reddy, V.A., Iwama, A., Iotzova, G., Schulz, M., Elsasser, A., Vangala, R.K., Tenen, D.G., Hiddemann, W., and Behre, G. (2002). Granulocyte inducer C/EBPalpha inactivates the myeloid master regulator PU.1: possible role in lineage commitment decisions. Blood *100*, 483-490.

Rekhtman, N., Radparvar, F., Evans, T., and Skoultchi, A.I. (1999). Direct interaction of hematopoietic transcription factors PU.1 and GATA-1: functional antagonism in erythroid cells. Genes Dev *13*, 1398-1411.

Rice, K.L., and de The, H. (2014). The acute promyelocytic leukaemia success story: curing leukaemia through targeted therapies. J Intern Med *276*, 61-70.

Roe, J.S., Mercan, F., Rivera, K., Pappin, D.J., and Vakoc, C.R. (2015). BET Bromodomain Inhibition Suppresses the Function of Hematopoietic Transcription Factors in Acute Myeloid Leukemia. Mol Cell *58*, 1028-1039.

Rosenbauer, F., and Tenen, D.G. (2007). Transcription factors in myeloid development: balancing differentiation with transformation. Nat Rev Immunol *7*, 105-117.

Rowe, J.M., and Tallman, M.S. (2010). How I treat acute myeloid leukemia. Blood *116*, 3147-3156.

Russler-Germain, D.A., Spencer, D.H., Young, M.A., Lamprecht, T.L., Miller, C.A., Fulton, R., Meyer, M.R., Erdmann-Gilmore, P., Townsend, R.R., Wilson, R.K., *et al.* (2014). The R882H DNMT3A mutation associated with AML dominantly inhibits wild-type DNMT3A by blocking its ability to form active tetramers. Cancer Cell *25*, 442-454.

Ryu, S., Zhou, S., Ladurner, A.G., and Tjian, R. (1999). The transcriptional cofactor complex CRSP is required for activity of the enhancer-binding protein Sp1. Nature *397*, 446-450.

Sakurai, H., and Fukasawa, T. (2003). Artificial recruitment of certain Mediator components affects requirement of basal transcription factor IIE. Genes Cells *8*, 41-50.

Sander, J.D., and Joung, J.K. (2014). CRISPR-Cas systems for editing, regulating and targeting genomes. Nat Biotechnol *32*, 347-355.

Sanyal, A., Lajoie, B.R., Jain, G., and Dekker, J. (2012). The long-range interaction landscape of gene promoters. Nature *489*, 109-113.

Sato, S., Tomomori-Sato, C., Parmely, T.J., Florens, L., Zybailov, B., Swanson, S.K., Banks, C.A., Jin, J., Cai, Y., Washburn, M.P., *et al.* (2004). A set of consensus mammalian mediator subunits identified by multidimensional protein identification technology. Mol Cell *14*, 685-691.

Sela, D., Conkright, J.J., Chen, L., Gilmore, J., Washburn, M.P., Florens, L., Conaway, R.C., and Conaway, J.W. (2013). Role for human mediator subunit MED25 in recruitment of mediator to promoters by endoplasmic reticulum stress-responsive transcription factor ATF6alpha. J Biol Chem *288*, 26179-26187.

Shaikhibrahim, Z., Offermann, A., Braun, M., Menon, R., Syring, I., Nowak, M., Halbach, R., Vogel, W., Ruiz, C., Zellweger, T., *et al.* (2014). MED12 overexpression is a frequent event in castration-resistant prostate cancer. Endocr Relat Cancer *21*, 663-675.

Shalem, O., Sanjana, N.E., Hartenian, E., Shi, X., Scott, D.A., Mikkelsen, T.S., Heckl, D., Ebert, B.L., Root, D.E., Doench, J.G., *et al.* (2014). Genome-scale CRISPR-Cas9 knockout screening in human cells. Science *343*, 84-87.

Sharma, N., Marguerat, S., Mehta, S., Watt, S., and Bahler, J. (2006). The fission yeast Rpb4 subunit of RNA polymerase II plays a specialized role in cell separation. Mol Genet Genomics *276*, 545-554.

Shen, C., Ipsaro, J.J., Shi, J., Milazzo, J.P., Wang, E., Roe, J.S., Suzuki, Y., Pappin, D.J., Joshua-Tor, L., and Vakoc, C.R. (2015). NSD3-Short Is an Adaptor Protein that Couples BRD4 to the CHD8 Chromatin Remodeler. Mol Cell *60*, 847-859.

Shi, J., and Vakoc, C.R. (2014). The mechanisms behind the therapeutic activity of BET bromodomain inhibition. Mol Cell *54*, 728-736.

Shi, J., Wang, E., Milazzo, J.P., Wang, Z., Kinney, J.B., and Vakoc, C.R. (2015). Discovery of cancer drug targets by CRISPR-Cas9 screening of protein domains. Nat Biotechnol *33*, 661-667.

Shi, J., Whyte, W.A., Zepeda-Mendoza, C.J., Milazzo, J.P., Shen, C., Roe, J.S., Minder, J.L., Mercan, F., Wang, E., Eckersley-Maslin, M.A., *et al.* (2013). Role of SWI/SNF in acute leukemia maintenance and enhancer-mediated Myc regulation. Genes Dev *27*, 2648-2662.

Shih, A.H., Jiang, Y., Meydan, C., Shank, K., Pandey, S., Barreyro, L., Antony-Debre, I., Viale, A., Socci, N., Sun, Y., *et al.* (2015). Mutational cooperativity linked to combinatorial epigenetic gain of function in acute myeloid leukemia. Cancer Cell *27*, 502-515.

Shu, S., Lin, C.Y., He, H.H., Witwicki, R.M., Tabassum, D.P., Roberts, J.M., Janiszewska, M., Jin Huh, S., Liang, Y., Ryan, J., *et al.* (2016). Response and resistance to BET bromodomain inhibitors in triple-negative breast cancer. Nature.

Sigova, A.A., Abraham, B.J., Ji, X., Molinie, B., Hannett, N.M., Guo, Y.E., Jangi, M., Giallourakis, C.C., Sharp, P.A., and Young, R.A. (2015). Transcription factor trapping by RNA in gene regulatory elements. Science.

Slany, R.K. (2009). The molecular biology of mixed lineage leukemia. Haematologica *94*, 984-993.

Soutourina, J., Wydau, S., Ambroise, Y., Boschiero, C., and Werner, M. (2011). Direct interaction of RNA polymerase II and mediator required for transcription in vivo. Science *331*, 1451-1454.

Spencer, J.A., Ferraro, F., Roussakis, E., Klein, A., Wu, J., Runnels, J.M., Zaher, W., Mortensen, L.J., Alt, C., Turcotte, R., *et al.* (2014). Direct measurement of local oxygen concentration in the bone marrow of live animals. Nature *508*, 269-273.

Staber, P.B., Zhang, P., Ye, M., Welner, R.S., Nombela-Arrieta, C., Bach, C., Kerenyi, M., Bartholdy, B.A., Zhang, H., Alberich-Jorda, M., *et al.* (2013). Sustained PU.1 levels balance cell-cycle regulators to prevent exhaustion of adult hematopoietic stem cells. Mol Cell *49*, 934-946.

Steger, D.J., Lefterova, M.I., Ying, L., Stonestrom, A.J., Schupp, M., Zhuo, D., Vakoc, A.L., Kim, J.E., Chen, J., Lazar, M.A., *et al.* (2008). DOT1L/KMT4 recruitment and H3K79 methylation are ubiquitously coupled with gene transcription in mammalian cells. Mol Cell Biol *28*, 2825-2839.

Stein, E.M., Altman, J.K., Collins, R., DeAngelo, D.J., Fathi, A.T., Flinn, I., Frankel, A., Levine, R.L., Medeiros, B.C., Patel, M., *et al.* (2014). AG-221, an Oral, Selective, First-in-Class, Potent Inhibitor of the IDH2 Mutant Metabolic Enzyme, Induces Durable Remissions in a Phase I Study in Patients with IDH2 Mutation Positive Advanced Hematologic Malignancies. Blood *124*, 115-115.

Stevens, J.L., Cantin, G.T., Wang, G., Shevchenko, A., Shevchenko, A., and Berk, A.J. (2002). Transcription control by E1A and MAP kinase pathway via Sur2 mediator subunit. Science *296*, 755-758.

Stumpf, M., Waskow, C., Krotschel, M., van Essen, D., Rodriguez, P., Zhang, X., Guyot, B., Roeder, R.G., and Borggrefe, T. (2006). The mediator complex functions as a coactivator for GATA-1 in erythropoiesis via subunit Med1/TRAP220. Proc Natl Acad Sci U S A *103*, 18504-18509.

Subramanian, A., Tamayo, P., Mootha, V.K., Mukherjee, S., Ebert, B.L., Gillette, M.A., Paulovich, A., Pomeroy, S.L., Golub, T.R., Lander, E.S., *et al.* (2005). Gene set enrichment analysis: a knowledge-based approach for interpreting genome-wide expression profiles. Proc Natl Acad Sci U S A *102*, 15545-15550.

Suda, T., Takubo, K., and Semenza, G.L. (2011). Metabolic regulation of hematopoietic stem cells in the hypoxic niche. Cell Stem Cell *9*, 298-310.

Taatjes, D.J., Naar, A.M., Andel, F., 3rd, Nogales, E., and Tjian, R. (2002). Structure, function, and activator-induced conformations of the CRSP coactivator. Science *295*, 1058-1062.

Takahashi, H., Parmely, T.J., Sato, S., Tomomori-Sato, C., Banks, C.A., Kong, S.E., Szutorisz, H., Swanson, S.K., Martin-Brown, S., Washburn, M.P., *et al.* (2011). Human mediator subunit MED26 functions as a docking site for transcription elongation factors. Cell *146*, 92-104.

Takubo, K., Goda, N., Yamada, W., Iriuchishima, H., Ikeda, E., Kubota, Y., Shima, H., Johnson, R.S., Hirao, A., Suematsu, M., *et al.* (2010). Regulation of the HIF-1alpha level is essential for hematopoietic stem cells. Cell Stem Cell *7*, 391-402.

Tan, J., Ong, C.K., Lim, W.K., Ng, C.C., Thike, A.A., Ng, L.M., Rajasegaran, V., Myint, S.S., Nagarajan, S., Thangaraju, S., *et al.* (2015). Genomic landscapes of breast fibroepithelial tumors. Nat Genet *47*, 1341-1345.

Tenen, D.G. (2003). Disruption of differentiation in human cancer: AML shows the way. Nat Rev Cancer *3*, 89-101.

Triezenberg, S.J., Kingsbury, R.C., and McKnight, S.L. (1988). Functional dissection of VP16, the trans-activator of herpes simplex virus immediate early gene expression. Genes Dev *2*, 718-729.

Tsai, K.L., Tomomori-Sato, C., Sato, S., Conaway, R.C., Conaway, J.W., and Asturias, F.J. (2014). Subunit architecture and functional modular rearrangements of the transcriptional mediator complex. Cell *157*, 1430-1444.

Turunen, M., Spaeth, J.M., Keskitalo, S., Park, M.J., Kivioja, T., Clark, A.D., Makinen, N., Gao, F., Palin, K., Nurkkala, H., *et al.* (2014). Uterine leiomyoma-linked MED12 mutations disrupt mediator-associated CDK activity. Cell Rep *7*, 654-660.

Vardiman, J.W., Harris, N.L., and Brunning, R.D. (2002). The World Health Organization (WHO) classification of the myeloid neoplasms. Blood *100*, 2292-2302.

Vassiliou, G.S., Cooper, J.L., Rad, R., Li, J., Rice, S., Uren, A., Rad, L., Ellis, P., Andrews, R., Banerjee, R., *et al.* (2011). Mutant nucleophosmin and cooperating pathways drive leukemia initiation and progression in mice. Nat Genet *43*, 470-475.

Viny, A.D., Ott, C.J., Spitzer, B., Rivas, M., Meydan, C., Papalexi, E., Yelin, D., Shank, K., Reyes, J., Chiu, A., *et al.* (2015). Dose-dependent role of the cohesin complex in normal and malignant hematopoiesis. J Exp Med *212*, 1819-1832.

Vojnic, E., Mourao, A., Seizl, M., Simon, B., Wenzeck, L., Lariviere, L., Baumli, S., Baumgart, K., Meisterernst, M., Sattler, M., *et al.* (2011). Structure and VP16 binding of the Mediator Med25 activator interaction domain. Nat Struct Mol Biol *18*, 404-409.

Wada, T., Takagi, T., Yamaguchi, Y., Ferdous, A., Imai, T., Hirose, S., Sugimoto, S., Yano, K., Hartzog, G.A., Winston, F., *et al.* (1998). DSIF, a novel transcription elongation factor that regulates RNA polymerase II processivity, is composed of human Spt4 and Spt5 homologs. Genes Dev *12*, 343-356.

Wander, S.A., Levis, M.J., and Fathi, A.T. (2014). The evolving role of FLT3 inhibitors in acute myeloid leukemia: quizartinib and beyond. Ther Adv Hematol *5*, 65-77.

Wang, W., Huang, L., Huang, Y., Yin, J.W., Berk, A.J., Friedman, J.M., and Wang, G. (2009). Mediator MED23 links insulin signaling to the adipogenesis transcription cascade. Dev Cell *16*, 764-771.

Wang, W., Yao, X., Huang, Y., Hu, X., Liu, R., Hou, D., Chen, R., and Wang, G. (2013). Mediator MED23 regulates basal transcription in vivo via an interaction with P-TEFb. Transcription *4*, 39-51.

Weiss, W.A., Taylor, S.S., and Shokat, K.M. (2007). Recognizing and exploiting differences between RNAi and small-molecule inhibitors. Nat Chem Biol *3*, 739-744.

Welch, J.S., Ley, T.J., Link, D.C., Miller, C.A., Larson, D.E., Koboldt, D.C., Wartman, L.D., Lamprecht, T.L., Liu, F., Xia, J., *et al.* (2012). The origin and evolution of mutations in acute myeloid leukemia. Cell *150*, 264-278.

Whyte, W.A., Orlando, D.A., Hnisz, D., Abraham, B.J., Lin, C.Y., Kagey, M.H., Rahl, P.B., Lee, T.I., and Young, R.A. (2013). Master transcription factors and mediator establish super-enhancers at key cell identity genes. Cell *153*, 307-319.

Wiederhold, T., Lee, M.F., James, M., Neujahr, R., Smith, N., Murthy, A., Hartwig, J., Gusella, J.F., and Ramesh, V. (2004). Magicin, a novel cytoskeletal protein associates with the NF2 tumor suppressor merlin and Grb2. Oncogene *23*, 8815-8825.

Wolfe, A.L., Singh, K., Zhong, Y., Drewe, P., Rajasekhar, V.K., Sanghvi, V.R., Mavrakis, K.J., Jiang, M., Roderick, J.E., Van der Meulen, J., *et al.* (2014). RNA G-quadruplexes cause eIF4A-dependent oncogene translation in cancer. Nature *513*, 65-70.

Wong, T.N., Ramsingh, G., Young, A.L., Miller, C.A., Touma, W., Welch, J.S., Lamprecht, T.L., Shen, D., Hundal, J., Fulton, R.S., *et al.* (2015). Role of TP53 mutations in the origin and evolution of therapy-related acute myeloid leukaemia. Nature *518*, 552-555.

Wu, S.Y., and Chiang, C.M. (2007). The double bromodomain-containing chromatin adaptor Brd4 and transcriptional regulation. J Biol Chem *282*, 13141-13145.

Wu, T., Pinto, H.B., Kamikawa, Y.F., and Donohoe, M.E. (2015). The BET family member BRD4 interacts with OCT4 and regulates pluripotency gene expression. Stem Cell Reports *4*, 390-403.

Yamaguchi, Y., Takagi, T., Wada, T., Yano, K., Furuya, A., Sugimoto, S., Hasegawa, J., and Handa, H. (1999). NELF, a multisubunit complex containing RD, cooperates with DSIF to repress RNA polymerase II elongation. Cell *97*, 41-51.

Yamazaki, S., Ema, H., Karlsson, G., Yamaguchi, T., Miyoshi, H., Shioda, S., Taketo, M.M., Karlsson, S., Iwama, A., and Nakauchi, H. (2011). Nonmyelinating Schwann cells maintain hematopoietic stem cell hibernation in the bone marrow niche. Cell *147*, 1146-1158.

Yang, F., Vought, B.W., Satterlee, J.S., Walker, A.K., Jim Sun, Z.Y., Watts, J.L., DeBeaumont, R., Saito, R.M., Hyberts, S.G., Yang, S., *et al.* (2006). An ARC/Mediator subunit required for SREBP control of cholesterol and lipid homeostasis. Nature *442*, 700-704.

Yang, Z., Yik, J.H., Chen, R., He, N., Jang, M.K., Ozato, K., and Zhou, Q. (2005). Recruitment of P-TEFb for stimulation of transcriptional elongation by the bromodomain protein Brd4. Mol Cell *19*, 535-545.

Yates, J.W., Wallace, H.J., Jr., Ellison, R.R., and Holland, J.F. (1973). Cytosine arabinoside (NSC-63878) and daunorubicin (NSC-83142) therapy in acute nonlymphocytic leukemia. Cancer Chemother Rep *57*, 485-488.

Yeamans, C., Wang, D., Paz-Priel, I., Torbett, B.E., Tenen, D.G., and Friedman, A.D. (2007). C/EBPalpha binds and activates the PU.1 distal enhancer to induce monocyte lineage commitment. Blood *110*, 3136-3142.

Yong, K.J., Gao, C., Lim, J.S., Yan, B., Yang, H., Dimitrov, T., Kawasaki, A., Ong, C.W., Wong, K.F., Lee, S., *et al.* (2013). Oncofetal gene SALL4 in aggressive hepatocellular carcinoma. N Engl J Med *368*, 2266-2276.

Yoshida, M., Sekine, S., Ogawa, R., Yoshida, H., Maeshima, A., Kanai, Y., Kinoshita, T., and Ochiai, A. (2015). Frequent MED12 mutations in phyllodes tumours of the breast. Br J Cancer *112*, 1703-1708.

Young, E.T., Tachibana, C., Chang, H.W., Dombek, K.M., Arms, E.M., and Biddick, R. (2008). Artificial recruitment of mediator by the DNA-binding domain of Adr1 overcomes glucose repression of ADH2 expression. Mol Cell Biol *28*, 2509-2516.

Zarrinkar, P.P., Gunawardane, R.N., Cramer, M.D., Gardner, M.F., Brigham, D., Belli, B., Karaman, M.W., Pratz, K.W., Pallares, G., Chao, Q., *et al.* (2009). AC220 is a uniquely potent and selective inhibitor of FLT3 for the treatment of acute myeloid leukemia (AML). Blood *114*, 2984-2992.

Zhang, P., Behre, G., Pan, J., Iwama, A., Wara-Aswapati, N., Radomska, H.S., Auron, P.E., Tenen, D.G., and Sun, Z. (1999). Negative cross-talk between hematopoietic regulators: GATA proteins repress PU.1. Proc Natl Acad Sci U S A *96*, 8705-8710.

Zhang, X.W., Yan, X.J., Zhou, Z.R., Yang, F.F., Wu, Z.Y., Sun, H.B., Liang, W.X., Song, A.X., Lallemand-Breitenbach, V., Jeanne, M., *et al.* (2010). Arsenic trioxide controls the fate of the PML-RARalpha oncoprotein by directly binding PML. Science *328*, 240-243.

Zhang, Y., Liu, T., Meyer, C.A., Eeckhoute, J., Johnson, D.S., Bernstein, B.E., Nusbaum, C., Myers, R.M., Brown, M., Li, W., *et al.* (2008). Model-based analysis of ChIP-Seq (MACS). Genome Biol *9*, R137.

Zhao, X., Xiaoli, Zong, H., Abdulla, A., Yang, E.S., Wang, Q., Ji, J.Y., Pessin, J.E., Das, B.C., and Yang, F. (2014). Inhibition of SREBP transcriptional activity by a boron-containing compound improves lipid homeostasis in diet-induced obesity. Diabetes *63*, 2464-2473.

Zhou, H., Spaeth, J.M., Kim, N.H., Xu, X., Friez, M.J., Schwartz, C.E., and Boyer, T.G. (2012). MED12 mutations link intellectual disability syndromes with dysregulated GLI3-dependent Sonic Hedgehog signaling. Proc Natl Acad Sci U S A *109*, 19763-19768.

Zhu, J., Gianni, M., Kopf, E., Honore, N., Chelbi-Alix, M., Koken, M., Quignon, F., Rochette-Egly, C., and de The, H. (1999). Retinoic acid induces proteasome-dependent degradation of retinoic acid receptor alpha (RARalpha) and oncogenic RARalpha fusion proteins. Proc Natl Acad Sci U S A *96*, 14807-14812.

Zuber, J., McJunkin, K., Fellmann, C., Dow, L.E., Taylor, M.J., Hannon, G.J., and Lowe, S.W. (2011a). Toolkit for evaluating genes required for proliferation and survival using tetracycline-regulated RNAi. Nat Biotechnol *29*, 79-83.

Zuber, J., Rappaport, A.R., Luo, W., Wang, E., Chen, C., Vaseva, A.V., Shi, J., Weissmueller, S., Fellmann, C., Taylor, M.J., *et al.* (2011b). An integrated approach to dissecting oncogene addiction implicates a Myb-coordinated self-renewal program as essential for leukemia maintenance. Genes Dev *25*, 1628-1640.

Zuber, J., Shi, J., Wang, E., Rappaport, A.R., Herrmann, H., Sison, E.A., Magoon, D., Qi, J., Blatt, K., Wunderlich, M., *et al.* (2011c). RNAi screen identifies Brd4 as a therapeutic target in acute myeloid leukaemia. Nature *478*, 524-528.

Appendix I – Targeting Transcription Factors in Cancer

Review

Targeting Transcription Factors in Cancer

Anand S. Bhagwat[1] and Christopher R. Vakoc[1,*]

Transcription factors (TFs) are commonly deregulated in the pathogenesis of human cancer and are a major class of cancer cell dependencies. Consequently, targeting of TFs can be highly effective in treating particular malignancies, as highlighted by the clinical efficacy of agents that target nuclear hormone receptors. In this review we discuss recent advances in our understanding of TFs as drug targets in oncology, with an emphasis on the emerging chemical approaches to modulate TF function. The remarkable diversity and potency of TFs as drivers of cell transformation justifies a continued pursuit of TFs as therapeutic targets for drug discovery.

Introduction

DNA-binding TFs regulate gene expression by influencing RNA polymerase activity in a gene-specific manner. To carry out this function, TFs minimally employ two distinct interaction surfaces: a sequence-specific DNA-binding domain (e.g., zinc finger, homeodomain, basic helix-loop-helix) and an activation/repression domain that interacts with various cofactors. In eukaryotes, TF cofactors include large, multisubunit protein complexes that either directly activate RNA polymerase II or modify local chromatin structure to allow an increased rate of transcription [1]. TFs regulate many of their target genes by occupying distal enhancer DNA elements, which loop over large genomic distances to regulate target gene promoters [2]. The human genome encodes over 2000 different TFs, many of which are expressed in a cell type-specific manner to coordinate gene expression programs underlying a vast array of cellular processes [2].

Deregulation of TFs is a pervasive theme across many, if not all, forms of human cancer [2]. In tumor cells, genes encoding TFs are often amplified, deleted, rearranged via chromosomal translocation, or subjected to point mutations that result in a gain- or loss-of-function [3]. As prominent examples, *TP53* and *MYC*, which encode the TFs p53 (tumor protein 53) and c-Myc, are among the most commonly altered genes across all cancers [4,5]. Cancer genome studies have also revealed that mutation of TF cofactors (e.g., SWI/SNF, p300/CBP, and Mediator) is also a major mechanism of tumorigenesis [6]. Furthermore, many oncogenic signal transduction cascades alter the function of downstream TFs to implement gene expression changes that drive cell transformation [3]. The myriad mechanisms of TF deregulation in cancer highlight the centrality of aberrant gene expression in cellular transformation and justify consideration of TFs as therapeutic targets in these diseases.

We discuss below recent insights into the therapeutic strategies to modulate TFs in cancer, and emphasize agents with established clinical efficacy or with promising effects in preclinical models. This review naturally covers the agents that exploit ligand-binding domains (LBDs) of nuclear hormone receptors (NHRs), which are among the most successful targeted therapies in all of oncology. We also highlight some of the emerging chemical strategies to target oncogenic TFs outside the NHR family, which includes methods to stabilize or degrade TFs or to interfere with the function of cofactors.

Trends

TFs are commonly deregulated in the pathogenesis of human and are a major class of cancer cell dependencies. This makes TFs attractive targets for cancer therapy.

Drugs that target nuclear hormone receptors are among the most impactful targeted therapies in all of oncology. Insights into their mechanism of action and mechanisms of resistance have illuminated fundamental concepts of TF-targeting therapeutics.

Therapeutic targeting of general transcriptional cofactors can lead to remarkable efficacy in animal cancer models with surprisingly little toxicity to normal tissues.

Chemical targeting of TFs for proteolysis is among the few curative strategies in cancer therapeutics today and is an emerging approach to suppress intractable protein targets.

[1]Cold Spring Harbor Laboratory, 1 Bungtown Road, Cold Spring Harbor, NY 11724, USA

*Correspondence. vakoc@cshl.edu (C.R. Vakoc).

Pharmacological Induction or Restoration of TF Function as a Cancer Therapy

One established means of undermining the cancer cell state is by pharmacologically elevating the function of specific TFs, in particular those related to tumor-suppressor pathways. In addition, chemical approaches have been devised that restore physiological transcriptional regulation to bypass the aberrant properties of genetically altered TFs or cofactors.

Reversal of PML–RARA-Mediated Repression with All-*trans* Retinoic Acid (ATRA)

PML (promyelocytic leukemia)–RARA (retinoic acid receptor α) is an oncogenic fusion TF produced as a result of the t(15;17) translocation, which occurs in over 98% of acute promyelocytic leukemias (APLs) [7]. This TF retains an N-terminal zinc-finger region of the PML protein and the DNA-binding domain and LBD of RARA [8]. The fusion protein undergoes aberrant dimerization and assembly with corepressor complexes to deregulate the normal function of RARA, thereby blocking myeloid differentiation (Figure 1) [7]. Empirical evaluation of drug sensitivity led to the discovery that APL cells were highly sensitive to treatment with various retinoid ligands of RARA, including all-*trans* retinoic acid (ATRA) [9]. This finding was remarkable because the therapeutic activity of ATRA was discovered before the identification of PML–RARA as the causative oncogene in this disease [10,11]. Notably, combination therapy using ATRA and A_2O_3 (the latter discussed below) cures more than 90% of APL patients [12].
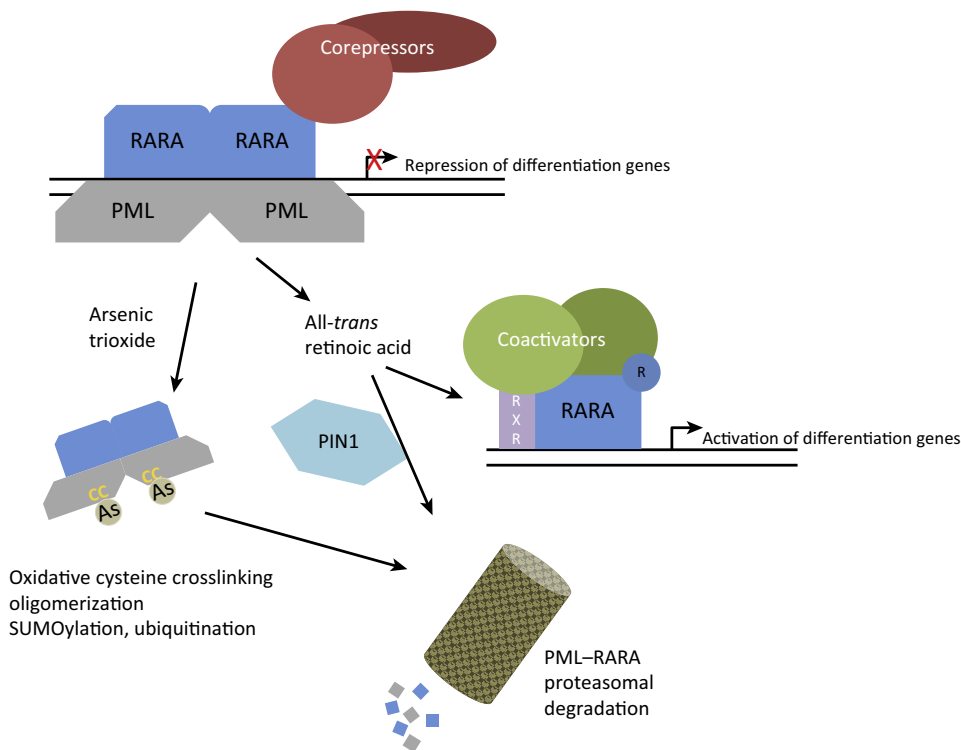
Trends in Cancer

Figure 1. Targeting of PML–RARA in Acute Promyelocytic Leukemia. The PML–RARA fusion protein binds to RARA sites in the genome, recruiting co-repressors and repressing RAR-target genes. All-*trans* retinoic acid (ATRA, labeled as R) binds to PML–RARA and switches it from a repressor of myeloid differentiation genes to an activator. ATRA also induces degradation of PML–RARA through a direct effect on the PIN1 prolyl isomerase. Arsenic trioxide also binds directly to the fusion protein and induces its degradation interacting with the zinc finger of the PML moiety. Arsenic leads to ROS production and subsequent disulfide crosslinking of the cysteines, resulting in oligomerization, SUMOylation, and subsequent ubiquitin-mediated proteolysis. Abbreviations: PIN1, peptidylprolyl *cis/trans* isomerase 1; PML, promyelocytic leukemia; RARA, retinoic acid receptor α; ROS, reactive oxygen species; SUMO, small ubiquitin-related modifier.

Early work demonstrated that the interaction of ATRA with the LBD of PML–RARA leads to a conformational change that disrupts its association with histone deacetylase-containing corepressors in favor of acetyltransferase coactivators [13]. Hence, one outcome of ATRA binding to PML–RARA is its conversion from a repressor to an activator of transcription through the elevation of local histone acetylation at sites occupied by PML–RARA [7,13,14]. Because many of the genes repressed by PML–RARA have roles in promoting myeloid differentiation, the net effect of ATRA is the induction of terminal neutrophil differentiation of leukemic blasts (Figure 1) [14].

Chemical Restoration of CBFβ–RUNX1 Complexes in inv(16) Acute Myeloid Leukemia (AML)

Another subtype of acute leukemia is characterized by an inversion on chromosome 16 that fuses core binding factor β (CBFβ) with the smooth-muscle myosin heavy chain (SMMHC) [15]. CBFβ is a cofactor for the RUNX (Runt-related) family of TFs, and CBFβ–RUNX1 heterodimers perform essential roles in normal hematopoiesis [16]. The CBFβ–SMMHC fusion forms aberrant oligomers that sequester RUNX1 away from the wild-type form of CBFβ, thereby resulting in leukemogenesis [17]. A recent study employed a high-throughput chemical screen for molecules that disrupt complexes of CBFβ–SMMHC and RUNX1 using a FRET (fluorescence resonance energy transfer)-based approach [15]. While the lead molecule identified from the screen exhibited moderate potency and a lack of selectivity for the fusion protein, the authors sought to selectively inhibit the oligomeric CBFβ–SMMHC by generating bivalent derivatives of the compound, named AI-10-49 (Figure 2) [15]. Exposing inv(16) AML cells to AI-10-49 led to the selective disruption of CBFβ–SMMHC interactions with RUNX1 and restored the formation of wild-type CBFβ–RUNX1 heterodimers (Figure 2) [15]. Notably, only AML cell lines and patient samples harboring CBFβ–SMMHC were sensitive to AI-10-49, and this molecule led to impressive survival benefit in a genetically engineered mouse model of this disease [15]. This study
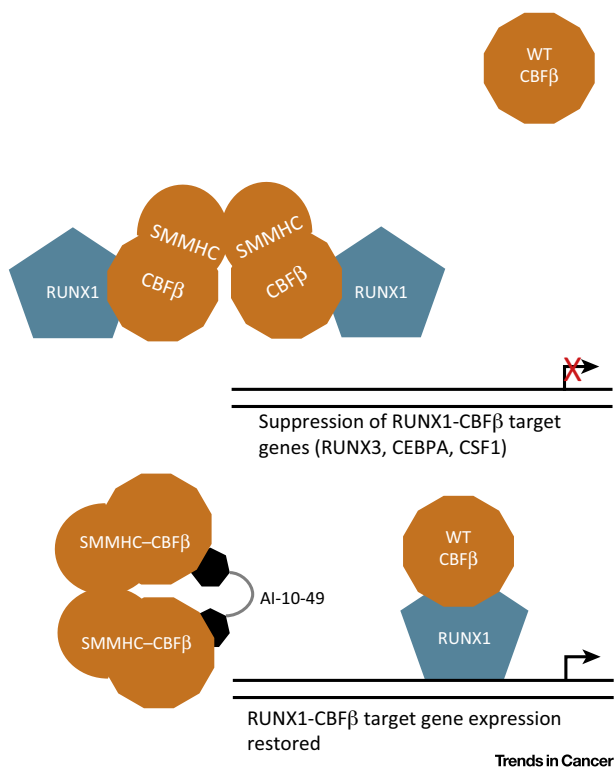
Figure 2. Targeting of CBFβ–SMMHC in inv(16) AML. CBFβ is a cofactor for the TF RUNX1. Together these proteins regulate normal hematopoiesis. The inv(16) lesion that defines a subtype of AML results in the joining of smooth-muscle myosin heavy chain to CBFβ. This fusion product is oligomeric and outcompetes wild-type CBFβ for RUNX1 binding. AI-10-49 is a bivalent inhibitor of CBFβ-SMMHC that prevents its interaction with RUNX1, thus restoring the formation of RUNX1–CBFβ heterodimers. Abbreviations: AML, acute myeloid leukemia; CBFβ, core-binding factor, β subunit, RUNX, Runt-related transcription factor; SMMHC, myosin heavy chain 11, smooth muscle.

highlights the utility of bivalent molecules for selectively targeting an aberrantly oligomerized transcriptional cofactor to restore the formation of physiological TF–cofactor interactions.

Ligand-Induced Activation of the Glucocorticoid Receptor (GR) Leads to Apoptosis in Lymphoid Cancers

Glucocorticoids are steroid hormones that exert pleiotropic, stress-associated effects on multiple human tissues by activating the function of GR [18]. One of the effects of GR activation with synthetic agonists (e.g., dexamethasone and prednisolone) is a severe defect in the proliferation and survival of lymphocytes, which has led to a widespread use of glucocorticoids as immunosuppressants and as a therapy for acute lymphoblastic leukemia (ALL) and other lymphoid neoplasms (Figure 3) [19,20]. Part of the mechanism underlying the induction of lymphocyte apoptosis by glucocorticoids is the role of GR in regulating the expression of genes encoding the BCL2 (B cell lymphoma 2) family of apoptosis regulators [21,22]. Specifically, GR activates expression of the proapoptotic *BIM* (BCL2 interacting mediator of cell death) gene, which is required for glucocorticoid-induced apoptosis of transformed lymphoid cells [21,22]. The clinical use of glucocorticoids in lymphoid cancers illustrates how chemical augmentation of TF function can cause lethality in cancer cells in a manner specific to the cell lineage from which the tumor is derived.

Despite the well-established efficacy of GR modulation in lymphoid cancers, the clinical response to glucocorticoids is heterogeneous and limited by the emergence of resistance. It has been found that GR occupancy at an intronic *BIM* enhancer occurs in dexamethasone-sensitive ALLs, but not in dexamethasone-resistant ALL, highlighting how TF genomic
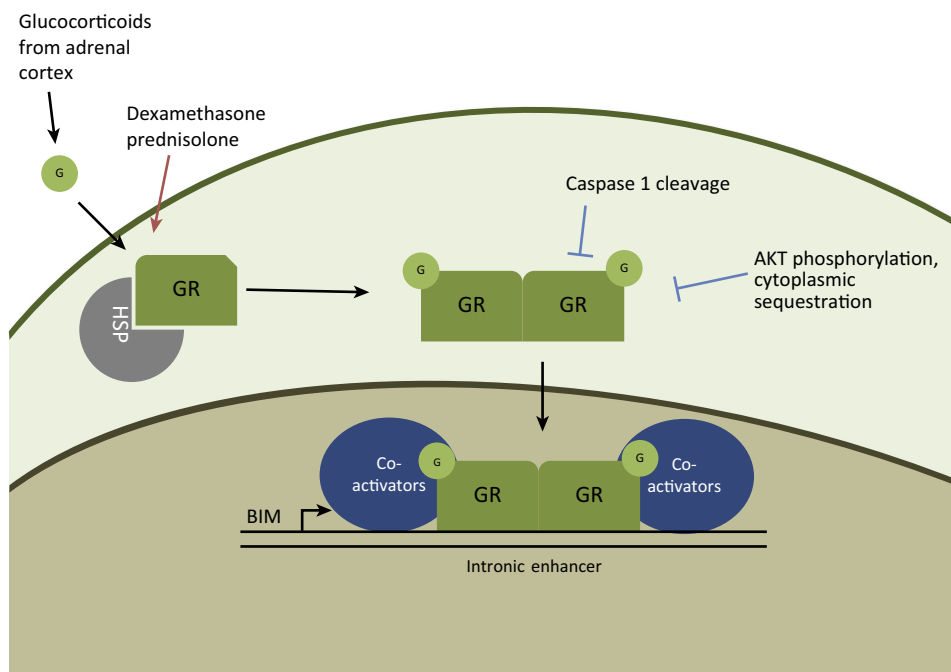
Trends in Cancer

Figure 3. Targeting the Glucocorticoid Receptor (GR) in Lymphoid Cancers. Endogenous glucocorticoids (G) or synthetic glucocorticoids such as dexamethasone and prednisolone enter a leukemia cell and bind to the GR. Upon binding its ligand, GR is released from heat shock protein (HSP) chaperones, dimerizes, and enters the nucleus. Its key target genes for cancer therapy include the proapoptotic gene *BIM* (BCL2 interacting mediator of cell death). GR binds to a regulatory element in an intron of BIM, and recruits coactivators to drive expression of BIM to promote apoptosis of normal and neoplastic lymphoid cells. Abbreviations: AKT, protein kinase B.

occupancy can be utilized as a therapeutic response biomarker [23]. In a separate study it was found that increased expression of caspase 1 confers resistance to glucocorticoids via caspase 1-mediated cleavage of GR to antagonize its transcriptional output [24]. Resistance to gluco-corticoid therapy can also be conferred via the genetic loss of *PTEN* (phosphatase and tensin homology), which leads to AKT (protein kinase B)-mediated hyperphosphorylation of GR to block its nuclear entry [25]. Loss-of-function mutations or transcriptional silencing of GR coactivators (e.g., CBP and SWI/SNF) has also been associated with dexamethasone resis-tance in ALL [26,27]. Collectively, these studies raise the possibility that targeting of caspase 1, AKT, or GR cofactors could improve the efficacy of glucocorticoid therapy in ALL.

Stabilization of p53 by Antagonizing MDM2

Mutations in *TP53* are among the most frequent genetic alterations in human cancer. However, many cancers retain wild-type *TP53* and instead depend on the E3 ligase protein MDM2 (double minute 2) for ubiquitin-mediated destruction of p53 via the proteasome, or on MDMX/MDM4, which directly binds to and inhibits the function of p53 [28]. Because genetic restoration of p53 function can lead to profound tumor regression in animal models, several groups have devel-oped MDM2 inhibitors as a targeted therapy for *TP53* wild-type cancers [29–31]. The first of such inhibitors, nutlins, were identified via a high-throughput chemical screen for molecules that disrupted the binding of MDM2 and p53 [32]. Preclinical studies with nutlins have demonstrated strong effects in suppressing tumor growth in mouse xenografts via induction of p53-mediated apoptosis and several molecules based on the nutlin chemical structure are currently in clinical development [28,31].

Targeting of Lineage-Specific Non-Oncogene TF Dependencies

While genetically altered TFs, such c-Myc and PML–RARA, represent compelling targets, non-oncogene TFs that support growth of discrete tissues can also be suitable for therapeutic intervention in cancer. The unique requirement for the estrogen receptor α (ERα) and the androgen receptor (AR) for the growth of reproductive tissues has afforded the development of highly-effective and well-tolerated cancer therapeutics in breast and prostate cancer, respectively.

ER in Breast Cancer

Approximately 70% of breast cancers rely on estrogen for sustained cell growth, a feature that cancer cells share with the ductal epithelium cell-of-origin [33,34]. These effects are largely mediated through the interaction of estrogen with the LBD of a single NHR, ERα [33,35]. While not an oncogene *per se*, a subset of breast cancers utilize ER to sustain their aberrant capabilities. Notably, genetic knockout of ER in mice is compatible with viability, but animals display abnormalities in the development of female reproductive organs (uterus, ovaries, and mammary glands) and other organ systems (e.g., diminished bone mineralization) [36]. None-theless, the tissue context-specific ER requirement for cell proliferation across adult tissues has provided a wide therapeutic window for ER modulation as a therapeutic approach in breast cancer.

Several pharmacological strategies are available to target the ER LBD to suppress its function [37]. Selective estrogen receptor modulators (SERMs), such as tamoxifen and raloxifene, directly compete with estrogen for binding to the ER LBD [38]. Other ER antagonists such as fulvestrant bind to the ER LBD at much higher affinity than SERMs and cause ER degradation [39,40]. Another route to ER inhibition is aimed at reducing the availability of estrogen by inhibiting aromatase, an enzyme that converts circulating androgens into estrogen [41]. The net effect of each of these therapies is a selective block in cell cycle progression and the induction of programmed cell death, which can lead to tumor regression *in vivo* while having an acceptable side effect profile in other tissues (Figure 4A) [37,42].
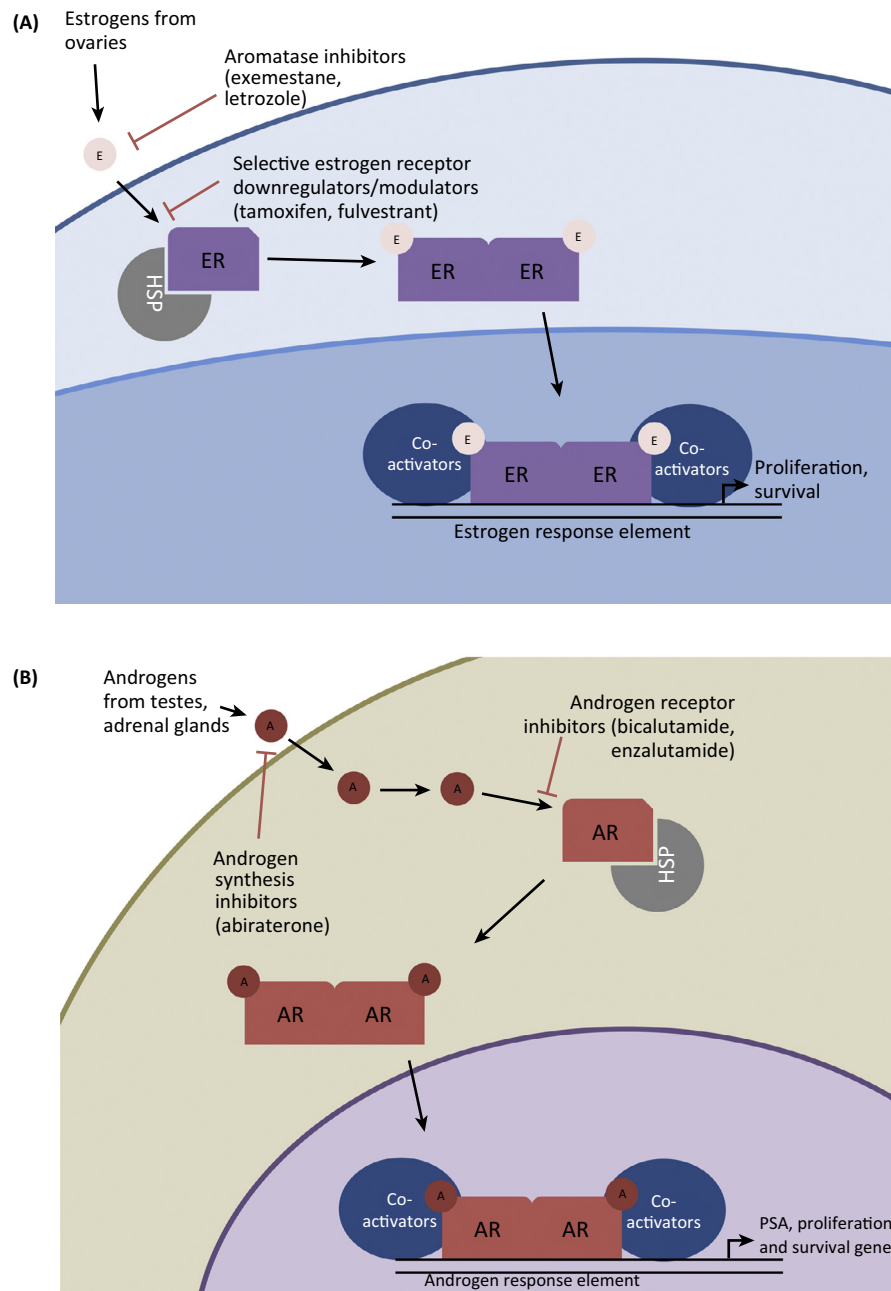
Figure 4. Targeting the Estrogen and Androgen Receptors in Breast and Prostate Cancers. (A) Estrogens (E), primarily produced in the ovaries, enter a breast epithelial cell and bind to the estrogen receptor (ER). Upon binding its ligand, ER is released from heat shock protein (HSP) chaperones, dimerizes, and enters the nucleus. Here, it binds to estrogen response elements and recruits coactivators to regulate its target genes to promote the growth, proliferation, and survival of breast cells. Anti-estrogen therapy comes in two major modes: inhibitors of estrogen synthesis, such as the aromatase inhibitors exemestane and letrozole, and inhibitors of ER ligand binding, such as tamoxifen and fulvestrant. (B) Androgens (A) enter a prostate epithelial cell, are converted from testosterone to dihydrotestosterone, and bind to the androgen receptor (AR). Upon binding its ligand, AR is released from HSP chaperones, dimerizes, and enters the nucleus. It recruits coactivator proteins to androgen response elements in the genome, including those regulating the prostate cancer biomarker prostate-specific antigen (PSA), and promotes the growth, proliferation, and survival of prostate cells. Anti-androgen therapy falls principally into two categories: androgen synthesis inhibitors, such as the CYP17A1 inhibitor abiraterone, and inhibitors of ligand binding, such as bicalutamide and enzalutamide.

One remarkable feature of ER revealed through epigenomic approaches is its capacity to rearrange its global genomic occupancy, or cistrome, in response to various stimuli [35,43]. Chromatin immunoprecipitation combined with high-throughput sequencing (ChIP-seq) analysis in primary human breast tumors has revealed a unique ER cistrome in poor- versus favorable-prognosis tumors. These ER cistromes are specified in part through the actions of the pioneer TF FOXA1 (forkhead box A1), which can render enhancers competent for ER occupancy [44,45]. Signaling cascades downstream of HER2 (epidermal growth factor receptor 2/ERBB2), an oncogene amplified in ~20% of breast cancers, can also reprogram ER cistromes and attenuate the sensitivity of breast cancer cells to tamoxifen [46,47]. Similarly, inflammation within the tumor microenvironment is associated with resistance to tamoxifen therapy and remodeling of ER occupancy at enhancers, which can be mediated by tumor necrosis factor $\propto$ (TNF$\propto$)-dependent activation of nuclear factor κb (NF-κB) [48,49]. Copy-number amplifications of ER-bound enhancers at 17q23 and 20q13 have also been associated with tamoxifen resistance, which may provide a genetic means of reprogramming ER genomic occupancy [50]. Collectively, these studies highlight how TF cistromes can be dynamically altered to dictate the transcriptional output and overall efficacy of TF-modulating therapeutics.

AR in Prostate Cancer

Androgens, such as testosterone and dihydrotestosterone, are steroid hormones that perform essential roles in the development of the male reproductive system, including a role in promoting growth of normal prostate epithelium [51]. Similar to the estrogen dependence of breast cancers, tumors derived from prostate epithelium rely on endogenous androgens for disease maintenance and progression [52]. This finding has motivated numerous strategies to deplete or block the effect of androgens as a therapeutic approach for men with advanced prostate cancer. The majority of the effects of androgens on human biology is mediated by AR. In prostate cancer cells, the interaction of androgens with the LBD of AR leads to transcriptional changes at an array of downstream target genes involved in the control of cell proliferation and survival (Figure 4B) [53,54].

Androgen production can be suppressed surgically by orchiectomy or pharmacologically by targeting the hypothalamic–pituitary axis with luteinizing hormone releasing hormone (LHRH) analogs (e.g., leuprolide) or by blocking the enzymatic activity of cytochrome P450 CYPC17 (e.g., with abiraterone) [55–57]. Another class of drugs block the effects of androgens through direct antagonism of AR function. First generation anti-androgens (e.g., flutamide and bicalutamide) and second-generation anti-androgens (enzalutamide and ARN-509) compete with endogenous androgens for binding to the AR LBD [53,58,59]. Second generation anti-androgens exhibit enhanced affinity for AR and have overcome several of the common resistance mechanisms associated with first-generation agents [53,60]. However, AR point mutations and alterations of AR splice variants have emerged as resistance mechanisms that also limit the efficacy of second-generation anti-androgens [58,61–64].

Analysis of AR genomic occupancy has yielded significant insights into mechanisms of prostate cancer progression and resistance to anti-androgen therapy [54]. One of the major determinants of AR cistromes in prostate cancer is the ETS (avian erythroblastosis virus E26 oncogene homolog) family of TFs, which are genetically altered and overexpressed in this disease [65,66]. Depending on the cellular context, ETS factors can either repress or support the output of AR signaling [65,66]. Recent evidence also suggests that the essential function of AR in advanced prostate cancer can be replaced by GR, thereby allowing a mechanism of glucocorticoid-dependent resistance to anti-androgen therapy [67]. In such tumors, it was shown that GR invades the AR cistrome to maintain a parallel transcriptional pathway that supports disease progression [67].

Targeting of TF Cofactors

The regulatory function of TFs is reliant on direct interactions with a vast assortment of transcriptional cofactors as a means of influencing RNA polymerase II activity. Hence, many TF–cofactor interaction surfaces represent compelling therapeutic targets. While historically such chemical approaches have been limited by a lack of potency, a few small-molecule or short peptide-based approaches that target cofactor interactions have been shown to suppress oncogenic TF function and exhibit promising therapeutic effects in preclinical cancer models.

NOTCH1–MAML in T cell leukemia (T-ALL)

NOTCH1 encodes a transmembrane protein that is cleaved upon binding to extracellular ligands to allow translocation of its intracellular domain (ICN1) to the nucleus, where it serves as cofactor for the TF CSL ('CBF1, suppressor of hairless, Lag-1') [68]. The ICN1–CSL interaction creates a docking site for the mastermind-like (MAML) family of coactivators, which together promote the transcriptional output to NOTCH1 signaling [68]. Notably, *NOTCH1* mutations are found in T-ALL that increase the nuclear localization of ICN1 to promote leukemia initiation [68]. As a potential treatment strategy for NOTCH1-driven leukemia, Moellering *et al.* developed a cell-permeable stabilized α-helical peptide derived from MAML1 (SAHM1), which binds to ICN1–CSL with a K_d of 120 nM to competitively block the association of endogenous MAML1 with ICN1 [69]. Treatment of *NOTCH1*-mutant T-ALL (T-acute lymphoblastic leukemia) cells with SAHM1 attenuated NOTCH1-dependent transcriptional signatures and inhibited T-ALL progression in xenograft models [69].

BCL6–SMRT in B Cell Lymphoma

BCL6 is an oncogenic zinc-finger TF that is often overexpressed in B cell lymphomas as a consequence of *BCL6* chromosomal translocations or promoter mutations [70]. BCL6 represses its downstream target genes via a BTB domain which interacts directly with a variety of corepressors, including SMRT (silencing mediator of retinoic acid and thyroid hormone receptor) [70]. To devise a means of disrupting BCL6-mediated repression, a structure-based *in silico* drug design effort led to the identification of a small molecule, 79-6, that binds to the SMRT interaction site of the BCL6 BTB domain with a K_d of 125 μM [71]. 79-6 can disrupt SMRT–BCL6 interactions in lymphoma cells and leads to upregulation of BCL6 target genes [71]. Despite the moderate affinity for BCL6, treatment of lymphoma-bearing mice with 79-6 led to diminished tumor growth *in vivo* [71].

Blockade of TF Output by Chemical Inhibition of BRD4

An example of a general TF cofactor is the bromodomain and extraterminal (BET) protein BRD4, which can interact directly with a vast array of TFs in a bromodomain-dependent or -independent manner [72]. Moreover, BRD4 bromodomains can also bind to acetylated nucleosomes that lie adjacent to TF-occupied enhancers and promoter, thus allowing BRD4 to promote TF-mediated activation even in the absence of direct TF interactions [72]. Inhibition of BET bromodomains with potent small-molecule inhibitors (e.g., JQ1 or IBET) has been shown to suppress the functional output of a vast array of oncogenic TFs, including ERG (ETS-related gene), c-Myb, c-Myc, E2F1 (E2F transcription factor 1), and NF-κB [73–77]. Moreover, several oncogenic loci exhibit massive enrichment of BRD4 at distal enhancer elements, termed super-enhancers, which may also confer cancer cell hypersensitivity to BRD4 inhibition [78]. Chemical inhibition of BET bromodomains has been shown to suppress tumor progression in a wide range of animal models while, remarkably, exhibiting minimal toxicity to normal tissues [72,76]. BET inhibitors are currently under investigation as cancer therapeutics in several early-stage clinical trials.

One of the impressive effects of BRD4 inhibition is its capacity to suppress the expression of genes encoding oncogenic TFs, including *MYC* [79,80]. If such effects can occur with a degree

of specificity, such an approach provides an attractive indirect route for TF modulation. While not a TF cofactor *per se*, the histone H3 lysine 79 (H3K79) methyltransferase DOT1L (DOT1-like) is essential to maintain expression of essential homeodomain-containing TFs (e.g., HOXA9) in AML [81]. Furthermore, small-molecule inhibitors of DOT1L suppress *HOXA9* expression and leukemia progression in animal models, which has led to the initiation of clinical trials evaluating these agents in leukemia patients [81]. Chemical inhibition of the CDK7 (cyclin-dependent kinase 7) subunit of TFIIH (transcription factor II human) has also been shown to disproportionately suppress the expression of lineage-specific TFs in various cancer models in association with therapeutic benefit [82].

Targeting TFs for Proteasome-Mediated Destruction

An alternative approach to disrupting TF–DNA and TF–cofactor interactions with small-molecules is to target TFs for proteolysis, an approach that has been associated with remarkable clinical efficacy in the examples highlighted below.

Targeting PML–RARA for Destruction with As_2O_3 and ATRA

The mechanism underlying the curative effects of As_2O_3 and ATRA in APL has been the subject of intense investigation in recent years. Despite its identification as therapeutic via an empirical evaluation, As_2O_3 has been shown to induce PML–RARA degradation by directly interacting with the PML moiety of the fusion TF [83,84]. In this context, arsenic can replace the zinc ion that normally interacts with PML [84]. This leads to oxidation of vicinal cysteine residues and enhances the oligomerization of PML–RAR, which in turn increases its interaction with the SUMO (small ubiquitin-like modifier)-conjugating enzyme UBC9 ('ubiquitin-conjugating enzyme 9') [83,84]. This results in PML–RARA sumoylation and subsequent RNF4 (ring finger protein 4)-mediated polyubiquitination, ultimately leading to destruction of the oncoprotein [83–86]. This example highlights how pharmacological TF degradation can be a highly-selective and effective therapeutic approach in treating lethal malignancies.

ATRA reverses the transcriptional repression mechanism of PML–RARA to cause APL differentiation; however, earlier work had shown that ATRA also triggers the degradation of PML–RARA [87]. The latter effect has been suggested to occur as an indirect consequence of ATRA interacting with the prolyl isomerase PIN1 (peptidylprolyl *cis/trans* isomerase 1), which in turn regulates PML–RARA stability [88]. Synthetic retinoid molecules have recently been identified that potently antagonize PML–RARA-mediated repression, but without altering PML–RARA levels [89]. Although these retinoids induce differentiation of APL cells to a comparable extent to ATRA, these compounds are much less active in eradicating leukemia in mice [89]. This suggests that differentiation is not the underlying mechanism relevant to the curative effects of ATRA in APL [89]. It now appears that PML–RARA destruction via ATRA or As_2O_3 leads to eradication of leukemia stem cells via induction of p53-mediated senescence, which leads to curative effects in this disease [90].

Targeting TFs or Cofactors for Destruction using Phthalimide-Based Drugs

Phthalimide-based drugs (thalidomide, lenalidomide, and pomalidomide) were originally withdrawn from clinical use because of their teratogenicity, but were later realized to exhibit potent therapeutic effects in multiple myeloma and myelodysplasia. The molecular target of phthalimides was recently discovered to be the cullin-RING ubiquitin ligase protein cereblon [91]. To reveal the relevant cereblon substrates whose levels are modulated by phthalimides, two independent groups carried out proteomic screens that led to the identification of Ikaros-family TFs, IKZF1 and IKZF3, as the cereblon substrates modulated by phthalimide treatment of multiple myeloma cells [92,93]. Binding of phthalimides to cereblon triggered polyubiquitylation of IKZF1/3 and subsequent proteasome-mediated degradation (Figure 5) [92,93]. Structural studies suggest that the interaction of thalidomide with cereblon may create a neomorphic
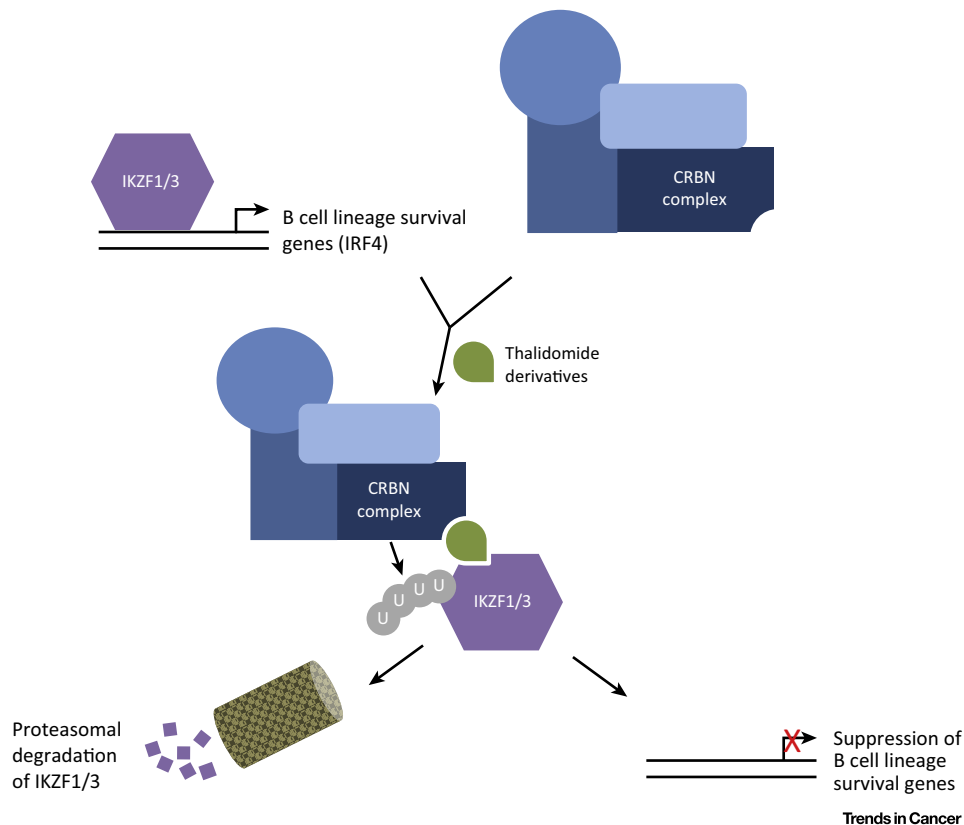
Figure 5. Targeting Ikaros TFs with Phthalimide Induces Cereblon-Mediated Proteolysis. IKZF1 and IKZF3 are TFs that regulate B cell lineage transcriptional programs. Targets of IKZF1/3 in multiple myeloma include IRF4. Cereblon (CRBN) is an E3 ubiquitin ligase in a complex. Thalidomide and its derivatives pomalidomide and lenalidomide bind to cereblon, blocking its access to its normal ubiquitylation targets. These drugs additionally bind to IKZF1/3, thus recruiting them to the CRBN complex and resulting in their ubiquitylation (U) and proteasomal degradation as a neosubstrate. Abbreviations: IKZF, Ikaros family zinc finger 1; IRF4 interferon regulatory factor 4.

interface for IKZF1/3 that enhances substrate recognition, potentially at the expense of natural cereblon substrates [94,95]. IKZF1/3 are essential TFs in the B cell lineage, and mutation of the cereblon degron motifs found on these TFs was sufficient to render myeloma cells resistant to phthalimides [92,93]. In analogy to As_2O_3 and ATRA in APL, these studies demonstrate how an empirically identified cancer therapy was subsequently realized to induce TF destruction as part of its mechanism of action.

The aforementioned successes of small-molecule-based targeting of TFs for proteolysis raises the question as to the whether such an approach can be generalized to target other intractable proteins. A recent study has now shown that various small molecules can be conjugated to the aryl ring of thalidomide to cause cereblon-mediated degradation of their interacting proteins [96]. This was shown using the BET bromodomain inhibitor JQ1, which when linked to thalidomide led to potent suppression of BET protein levels and enhanced anti-leukemia effects [96]. An independent series of thalidomide conjugates were also able to cause degradation of FKBP12 (FK506 binding protein 12) [96]. This study reveals a powerful chemical tool that could be employed for targeting oncogenic TFs or their cofactors. Traditional chemical approaches require high-affinity and high-specificity interactions with functionally-important surfaces to interfere with their targets. Phthalamide conjugation would presumably allow small molecules to suppress their protein targets without necessarily binding to functionally important surfaces, which has potential for expanding the number of targetable proteins.

Concluding Remarks

Our understanding of the clinical efficacy and current limitations of NHR modulation in cancer can greatly aid our assessment of other TF classes as candidates for drug development (see Outstanding Questions). One important lesson learned from the agents that target AR and ER is that a therapeutic window need not rely on the targeting of a genetically altered TF functionality. Targeting of ER and AR instead exploits a lineage-specific, non-oncogene dependency on these regulators that is inherited from the cell of origin. A large number of TFs are also required in discrete cell types, and hence targeting of such regulators could have an acceptable risk-to-benefit ratio, depending on the essentiality of the tissue of origin. NHR modulation has also provided fundamental insights into the modes of resistance that can emerge upon suppressing a single TF dependency, such as mutations of the TFs themselves, mutations of cofactors, and remodeling of TF cistromes.

One theme that emerges from this review is that chemical modulation of TFs can be achieved through remarkably diverse, and often empirical, strategies. The clinical success of agents such as As_2O_3 and thalidomide underscores how small molecules can target TFs for proteasome-mediated destruction in a highly-selective manner. This represents an alternative to the chemical disruption of TF–cofactor or TF–DNA interactions, which can be limited by a lack of potency [97]. High-throughput cell-based chemical screens that evaluate for TF degradation may provide a means to develop agents that suppress other elusive TF dependencies in oncology, such as c-Myc. Conversely, TFs can also be stabilized pharmacologically by blocking their destruction, as in the case of drugs that block MDM2-mediated targeting of p53 [32]. Finally, TFs can also be suppressed at the transcriptional level by targeting of general factors such as BRD4, DOT1L, and CDK7 [72,82].

Recent advances in functional genomics, such as the implementation of CRISPR (clustered regularly interspaced short palindromic repeats)-based genetic screens, will soon provide a comprehensive picture of TF dependencies across diverse forms of cancer [98–100]. The context-specific nature of many TF dependencies is likely to lead to the identification of a large number of therapeutic opportunities. However, to exploit TFs as drug targets demands a deep biochemical understanding of TF–cofactor interactions and the mechanisms that control TF protein stability. Basic research that investigates mechanisms of TF function in normal and cancer contexts will be crucial to advance this important area of translational cancer research.

Acknowledgments

References

1. Yan, C. and Higgins, P.J. (2013) Drugging the undruggable: transcription therapy for cancer. *Biochim. Biophys. Acta* 1835, 76–85
2. Lee, T.I. and Young, R.A. (2013) Transcriptional regulation and its misregulation in disease. *Cell* 152, 1237–1251
3. Darnell, J.E., Jr (2002) Transcription factors as targets for cancer therapy. *Nat. Rev. Cancer* 2, 740–749
4. Lee, E.Y. and Muller, W.J. (2010) Oncogenes and tumor suppressor genes. *Cold Spring Harb. Perspect. Biol.* 2, a003236
5. Bretones, G. *et al.* (2015) Myc and cell cycle control. *Biochim. Biophys. Acta* 1849, 506–516
6. Garraway, L.A. and Lander, E.S. (2013) Lessons from the cancer genome. *Cell* 153, 17–37
7. Rice, K.L. and de The, H. (2014) The acute promyelocytic leukaemia success story: curing leukaemia through targeted therapies. *J. Intern. Med.* 276, 61–70
8. de The, H. *et al.* (1990) The t(15;17) translocation of acute promyelocytic leukaemia fuses the retinoic acid receptor alpha gene to a novel transcribed locus. *Nature* 347, 558–561
9. Wang, Z.Y. and Chen, Z. (2008) Acute promyelocytic leukemia: from highly fatal to highly curable. *Blood* 111, 2505–2515
10. Huang, M.E. *et al.* (1988) Use of all-trans retinoic acid in the treatment of acute promyelocytic leukemia. *Blood* 72, 567–572
11. Huang, M.E. *et al.* (1987) All-trans retinoic acid with or without low dose cytosine arabinoside in acute promyelocytic leukemia. Report of 6 cases. *Chin. Med. J. (Engl.)* 100, 949–953
12. Lo-Coco, F. *et al.* (2013) Retinoic acid and arsenic trioxide for acute promyelocytic leukemia. *N. Engl. J. Med.* 369, 111–121
13. Lin, R.J. *et al.* (1998) Role of the histone deacetylase complex in acute promyelocytic leukaemia. *Nature* 391, 811–814
14. Martens, J.H. *et al.* (2010) PML–RARalpha/RXR alters the epigenetic landscape in acute promyelocytic leukemia. *Cancer Cell* 17, 173–185

Outstanding Questions

Can insights into the curative mechanisms of ATRA and As_2O_3 in APL inform how we might pursue disease-eradicating therapies in other types of cancer?

Will structural insight into TF–cofactor interaction surfaces inform the development of potent and selective small molecules that suppress oncogenic transcriptional circuits?

Why does chemical targeting of general components of the transcriptional apparatus lead to gene-specific transcriptional effects? Why are such agents selectively toxic to cancer cells relative to normal tissues?

Will oligonucleotide-based approaches (RNA interference, antisense oligonucleotides, DNA decoys) provide novel avenues to selectively target TFs in cancer?

Can cell-based screens be designed that reveal novel small molecules that convert oncogenic TFs into neosubstrates for ubiquitin conjugating enzymes?

What is the complete repertoire of essential TFs for the maintenance of each cancer type? How many TFs are required in a cancer-specific manner and would be suitable as therapeutic targets? How many TFs would lead to cancer-specific lethality if overexpressed or stabilized?

Can mapping of TF cistromes be implemented as a diagnostic test to guide the clinical management of cancer patients? Can mapping of TF dependencies in tumor specimens be performed to guide the use of TF-modulating therapeutics?

Can emerging insights into mechanisms of resistance to NHR-modulating therapies be utilized to develop combination drug regimens that improve overall survival?

15. Illendula, A. *et al.* (2015) A small-molecule inhibitor of the aberrant transcription factor CBFbeta–SMMHC delays leukemia in mice. *Science* 347, 779–784

16. de Bruijn, M.F. and Speck, N.A. (2004) Core-binding factors in hematopoiesis and immune function. *Oncogene* 23, 4238–4248

17. Lukasik, S.M. *et al.* (2002) Altered affinity of CBF beta-SMMHC for Runx1 explains its role in leukemogenesis. *Nat. Struct. Biol.* 9, 674–679

18. Nicolaides, N.C. *et al.* (2010) The human glucocorticoid receptor: molecular basis of biologic function. *Steroids* 75, 1–12

19. Inaba, H. and Pui, C.H. (2010) Glucocorticoid use in acute lymphoblastic leukaemia. *Lancet Oncol.* 11, 1096–1106

20. Pui, C.H. and Evans, W.E. (2006) Treatment of acute lympho-blastic leukemia. *N. Engl. J. Med.* 354, 166–178

21. Wang, Z. *et al.* (2003) Microarray analysis uncovers the induction of the proapoptotic BH3-only protein Bim in multiple models of glucocorticoid-induced apoptosis. *J. Biol. Chem.* 278, 23861–23867

22. Abrams, M.T. *et al.* (2004) Inhibition of glucocorticoid-induced apoptosis by targeting the major splice variants of BIM mRNA with small interfering RNA and short hairpin RNA. *J. Biol. Chem.* 279, 55809–55817

23. Jing, D. *et al.* (2015) Opposing regulation of BIM and BCL2 controls glucocorticoid-induced apoptosis of pediatric acute lymphoblastic leukemia cells. *Blood* 125, 273–283

24. Paugh, S.W. *et al.* (2015) NALP3 inflammasome upregulation and CASP1 cleavage of the glucocorticoid receptor cause glu-cocorticoid resistance in leukemia cells. *Nat. Genet.* 47, 607–614

25. Piovan, E. *et al.* (2013) Direct reversal of glucocorticoid resistance by AKT inhibition in acute lymphoblastic leukemia. *Cancer Cell* 24, 766–776

26. Mullighan, C.G. *et al.* (2011) CREBBP mutations in relapsed acute lymphoblastic leukaemia. *Nature* 471, 235–239

27. Pottier, N. *et al.* (2008) The SWI/SNF chromatin-remodeling complex and glucocorticoid resistance in acute lymphoblastic leukemia. *J. Natl. Cancer Inst.* 100, 1792–1803

28. Duffy, M.J. *et al.* (2014) p53 as a target for the treatment of cancer. *Cancer Treat. Rev.* 40, 1153–1160

29. Xue, W. *et al.* (2007) Senescence and tumour clearance is triggered by p53 restoration in murine liver carcinomas. *Nature* 445, 656–660

30. Ventura, A. *et al.* (2007) Restoration of p53 function leads to tumour regression in vivo. *Nature* 445, 661–665

31. Zhang, Q. *et al.* (2014) Targeting p53–MDM2–MDMX loop for cancer therapy. *Subcell. Biochem.* 85, 281–319

32. Vassilev, L.T. *et al.* (2004) In vivo activation of the p53 pathway by small-molecule antagonists of MDM2. *Science* 303, 844–848

33. Huang, B. *et al.* (2014) Estrogen receptors in breast carcinogen-esis and endocrine therapy. *Mol. Cell. Endocrinol.* Published online November 26, 2014. http://dx.doi.org/10.1016/j.mce.2014.11.015

34. van Kruchten, M. *et al.* (2013) PET imaging of oestrogen recep-tors in patients with breast cancer. *Lancet Oncol.* 14, e465–e475

35. Manavathi, B. *et al.* (2014) Estrogen receptor coregulators and pioneer factors: the orchestrators of mammary gland cell fate and development. *Front. Cell Dev. Biol.* 2, 34

36. Lee, H.R. *et al.* (2012) Functions and physiological roles of two types of estrogen receptors, ERalpha and ERbeta, identified by estrogen receptor knockout mouse. *Lab. Anim. Res.* 28, 71–76

37. Mehta, R.S. *et al.* (2012) Combination anastrozole and fulvestrant in metastatic breast cancer. *N. Engl. J. Med.* 367, 435–444

38. Komm, B.S. and Mirkin, S. (2014) An overview of current and emerging SERMs. *J. Steroid Biochem. Mol. Biol.* 143, 207–222

39. Howell, A. (2006) Pure oestrogen antagonists for the treatment of advanced breast cancer. *Endocr. Relat. Cancer* 13, 689–706

40. Wijayaratne, A.L. and McDonnell, D.P. (2001) The human estrogen receptor-alpha is a ubiquitinated protein whose stability is affected differentially by agonists, antagonists, and selective estrogen recep-tor modulators. *J. Biol. Chem.* 276, 35684–35692

41. Goss, P.E. *et al.* (2011) Exemestane for breast-cancer prevention in postmenopausal women. *N. Engl. J. Med.* 364, 2381–2391

42. Scherbakov, A.M. *et al.* (2013) Molecular mechanisms of hor-mone resistance of breast cancer. *Bull. Exp. Biol. Med.* 155, 384–395

43. Tang, Q. *et al.* (2011) A comprehensive view of nuclear receptor cancer cistromes. *Cancer Res.* 71, 6940–6947

44. Ross-Innes, C.S. *et al.* (2012) Differential oestrogen receptor binding is associated with clinical outcome in breast cancer. *Nature* 481, 389–393

45. Carroll, J.S. *et al.* (2005) Chromosome-wide mapping of estro-gen receptor binding reveals long-range regulation requiring the forkhead protein FoxA1. *Cell* 122, 33–43

46. Lupien, M. *et al.* (2010) Growth factor stimulation induces a distinct ER(alpha) cistrome underlying breast cancer endocrine resistance. *Genes Dev.* 24, 2219–2227

47. Ferreira, A.R. *et al.* (2015) Treatment of early-stage HER2+ breast cancer-an evolving field. *Ecancermedicalscience* 9, 523

48. Osborne, C.K. and Schiff, R. (2011) Mechanisms of endocrine resistance in breast cancer. *Annu. Rev. Med.* 62, 233–247

49. Franco, H.L. *et al.* (2015) TNFalpha signaling exposes latent estrogen receptor binding sites to alter the breast cancer cell transcriptome. *Mol. Cell* 58, 21–34

50. Hsu, P.Y. *et al.* (2013) Amplification of distant estrogen response elements deregulates target genes associated with tamoxifen resistance in breast cancer. *Cancer Cell* 24, 197–212

51. Shen, M.M. and Abate-Shen, C. (2010) Molecular genetics of prostate cancer: new prospects for old challenges. *Genes Dev.* 24, 1967–2000

52. Huggins, C. *et al.* (1941) Studies on prostatic cancer. II. The effects of castration on advanced carcinoma of the prostate gland. *Arch. Surg.* 43, 209–223

53. Carver, B.S. (2014) Strategies for targeting the androgen receptor axis in prostate cancer. *Drug Discov. Today* 19, 1493–1497

54. Sharma, N.L. *et al.* (2013) The androgen receptor induces a distinct transcriptional program in castration-resistant prostate cancer in man. *Cancer Cell* 23, 35–47

55. Moul, J.W. (2014) Utility of LHRH antagonists for advanced prostate cancer. *Can. J. Urol.* 21, 22–27

56. de Bono, J.S. *et al.* (2011) Abiraterone and increased survival in metastatic prostate cancer. *N. Engl. J. Med.* 364, 1995–2005

57. Ryan, C.J. *et al.* (2013) Abiraterone in metastatic prostate cancer without previous chemotherapy. *N. Engl. J. Med.* 368, 138–148

58. Wyatt, A.W. and Gleave, M.E. (2015) Targeting the adaptive molecular landscape of castration-resistant prostate cancer. *EMBO Mol. Med.* 20, 878–894

59. Aragon-Ching, J.B. (2014) The evolution of prostate cancer therapy: targeting the androgen receptor. *Front. Oncol.* 4, 295

60. Tran, C. *et al.* (2009) Development of a second-generation anti-androgen for treatment of advanced prostate cancer. *Science* 324, 787–790

61. Joseph, J.D. *et al.* (2013) A clinically relevant androgen recep-tor mutation confers resistance to second-generation antian-drogens enzalutamide and ARN-509. *Cancer Discov.* 3, 1020–1029

62. Korpal, M. *et al.* (2013) An F876L mutation in androgen receptor confers genetic and phenotypic resistance to MDV3100 (enza-lutamide). *Cancer Discov.* 3, 1030–1043

63. Balbas, M.D. *et al.* (2013) Overcoming mutation-based resis-tance to antiandrogens with rational drug design. *Elife* 2, e00499

64. Antonarakis, E.S. *et al.* (2014) AR-V7 and resistance to enzalu-tamide and abiraterone in prostate cancer. *N. Engl. J. Med.* 371, 1028–1038

65. Chen, Y. *et al.* (2013) ETS factors reprogram the androgen receptor cistrome and prime prostate tumorigenesis in response to PTEN loss. *Nat. Med.* 19, 1023–1029

66. Yu, J. *et al.* (2010) An integrated network of androgen receptor, polycomb, and TMPRSS2-ERG gene fusions in prostate cancer progression. *Cancer Cell* 17, 443–454

67. Arora, V.K. *et al.* (2013) Glucocorticoid receptor confers resis-tance to antiandrogens by bypassing androgen receptor block-ade. *Cell* 155, 1309–1322

68. Aster, J.C. *et al.* (2011) Notch signalling in T-cell lymphoblastic leukaemia/lymphoma and other haematological malignancies. *J. Pathol.* 223, 262–273

69. Moellering, R.E. *et al.* (2009) Direct inhibition of the NOTCH transcription factor complex. *Nature* 462, 182–188

70. Hatzi, K. and Melnick, A. (2014) Breaking bad in the germinal center: how deregulation of BCL6 contributes to lymphomagenesis. *Trends Mol. Med.* 20, 343–352

71. Cerchietti, L.C. *et al.* (2010) A small-molecule inhibitor of BCL6 kills DLBCL cells in vitro and in vivo. *Cancer Cell* 17, 400–411

72. Shi, J. and Vakoc, C.R. (2014) The mechanisms behind the therapeutic activity of BET bromodomain inhibition. *Mol. Cell* 54, 728–736

73. Roe, J.S. *et al.* (2015) BET bromodomain inhibition suppresses the function of hematopoietic transcription factors in acute myeloid leukemia. *Mol. Cell* 58, 1028–1039

74. Chapuy, B. *et al.* (2013) Discovery and characterization of super-enhancer-associated dependencies in diffuse large B cell lymphoma. *Cancer Cell* 24, 777–790

75. Asangani, I.A. *et al.* (2014) Therapeutic targeting of BET bromodomain proteins in castration-resistant prostate cancer. *Nature* 510, 278–282

76. Filippakopoulos, P. *et al.* (2010) Selective inhibition of BET bromodomains. *Nature* 468, 1067–1073

77. Nicodeme, E. *et al.* (2010) Suppression of inflammation by a synthetic histone mimic. *Nature* 468, 1119–1123

78. Loven, J. *et al.* (2013) Selective inhibition of tumor oncogenes by disruption of super-enhancers. *Cell* 153, 320–334

79. Delmore, J.E. *et al.* (2011) BET bromodomain inhibition as a therapeutic strategy to target c-Myc. *Cell* 146, 904–917

80. Zuber, J. *et al.* (2011) RNAi screen identifies Brd4 as a therapeutic target in acute myeloid leukaemia. *Nature* 478, 524–528

81. Bernt, K.M. and Armstrong, S.A. (2011) A role for DOT1L in MLL-rearranged leukemias. *Epigenomics* 3, 667–670

82. Kwiatkowski, N. *et al.* (2014) Targeting transcription regulation in cancer with a covalent CDK7 inhibitor. *Nature* 511, 616–620

83. Zhang, X.W. *et al.* (2010) Arsenic trioxide controls the fate of the PML–RARalpha oncoprotein by directly binding PML. *Science* 328, 240–243

84. Jeanne, M. *et al.* (2010) PML/RARA oxidation and arsenic binding initiate the antileukemia response of As2O3. *Cancer Cell* 18, 88–98

85. Lallemand-Breitenbach, V. *et al.* (2008) Arsenic degrades PML or PML–RARalpha through a SUMO-triggered RNF4/ubiquitin-mediated pathway. *Nat. Cell Biol.* 10, 547–555

86. Tatham, M.H. *et al.* (2008) RNF4 is a poly-SUMO-specific E3 ubiquitin ligase required for arsenic-induced PML degradation. *Nat. Cell Biol.* 10, 538–546

87. Zhu, J. *et al.* (1999) Retinoic acid induces proteasome-dependent degradation of retinoic acid receptor alpha (RARalpha) and oncogenic RARalpha fusion proteins. *Proc. Natl. Acad. Sci. U.S.A.* 96, 14807–14812

88. Wei, S. *et al.* (2015) Active Pin1 is a key target of all-trans retinoic acid in acute promyelocytic leukemia and breast cancer. *Nat. Med.* 21, 457–466

89. Ablain, J. *et al.* (2013) Uncoupling RARA transcriptional activation and degradation clarifies the bases for APL response to therapies. *J. Exp. Med.* 210, 647–653

90. Ablain, J. *et al.* (2014) Activation of a promyelocytic leukemia-tumor protein 53 axis underlies acute promyelocytic leukemia cure. *Nat. Med.* 20, 167–174

91. Ito, T. *et al.* (2010) Identification of a primary target of thalidomide teratogenicity. *Science* 327, 1345–1350

92. Kronke, J. *et al.* (2014) Lenalidomide causes selective degradation of IKZF1 and IKZF3 in multiple myeloma cells. *Science* 343, 301–305

93. Lu, G. *et al.* (2014) The myeloma drug lenalidomide promotes the cereblon-dependent destruction of Ikaros proteins. *Science* 343, 305–309

94. Fischer, E.S. *et al.* (2014) Structure of the DDB1–CRBN E3 ubiquitin ligase in complex with thalidomide. *Nature* 512, 49–53

95. Chamberlain, P.P. *et al.* (2014) Structure of the human cereblon–DDB1–lenalidomide complex reveals basis for responsiveness to thalidomide analogs. *Nat. Struct. Mol. Biol.* 21, 803–809

96. Winter, G.E. *et al.* (2015) Phthalimide conjugation as a strategy for in vivo target protein degradation. *Science* 348, 1376–1381

97. Koehler, A.N. (2010) A complex task? Direct modulation of transcription factors with small molecules. *Curr. Opin. Chem. Biol.* 14, 331–340

98. Wang, T. *et al.* (2014) Genetic screens in human cells using the CRISPR–Cas9 system. *Science* 343, 80–84

99. Shalem, O. *et al.* (2014) Genome-scale CRISPR–Cas9 knockout screening in human cells. *Science* 343, 84–87

100. Shi, J. *et al.* (2015) Discovery of cancer drug targets by CRISPR–Cas9 screening of protein domains. *Nat. Biotechnol.* 33, 661–667